Phenomic study of glucan synthesis in developing barley endosperm mutant seeds

using spectroscopy, chemometrics and spectral inspection

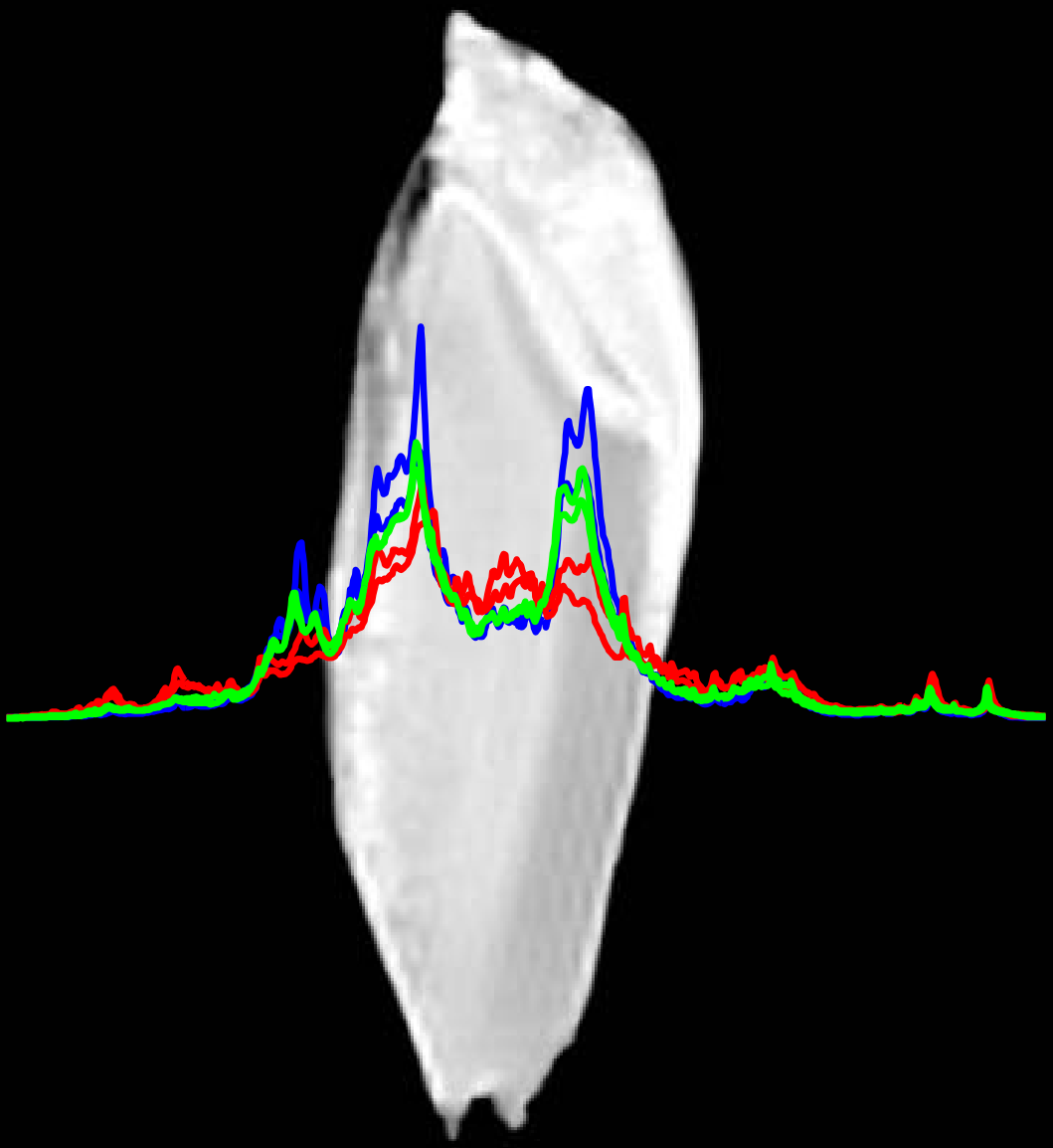

PhD Thesis

Helene Fast Seefeldt

February, 2008

University of Aarhus

University of Copenhagen

Phenomic study of glucan synthesis in developing barley endosperm mutant seeds

using spectroscopy, chemometrics and spectral inspection

PhD thesis by
Helene Fast Seefeldt
February 2008

Supervisors:
Senior Scientist Bernd Wollenweber[a]
and Professor Søren Balling Engelsen[b]

[a]University of Aarhus, Denmark
Faculty of Agricultural Sciences
Department of Genetics and Biotechnology
Research Centre Flakkebjerg
Slagelse, Denmark

[b]University of Copenhagen, Denmark
Faculty of Life Sciences
Department of Food Science
Copenhagen, Denmark

Front page: Superimposed image of MRI intensity map of soaked *lys5f* seed and NMR spectra.

Preface

This Ph.D. thesis has been submitted to fulfill the requirements for obtaining the Ph.D. degree at the Life Science Faculty (LIFE), University of Copenhagen (KU). The project was undertaken at the Faculty of Agricultural Sciences (FAS), University of Aarhus and at the Institute of Food Sciences, KU-LIFE, University of Copenhagen. The project was financed by the Competence Fund at FAS, University of Aarhus. The main supervisors were Senior Scientist Dr. Bernd Wollenweber (FAS) and Professor Søren Balling Engelsen (KU-LIFE).
Part of the experimental work was performed at the Sir Peter Mansfield Magnetic Resonance Centre, University of Nottingham, United Kingdom under the supervision of Dr. Walter Köckenberger in the period September–December 2004.
In the thesis, three papers are enclosed in appendices **A-C**, which have been published or are submitted in international peer-reviewed journals. The papers cover the subjects: barley endosperm mutants, mixed-linkage β-glucan and starch, seed development, spectroscopic fingerprinting and chemometrics. References to the papers are given as bold letters (**A-C**).

A. Seefeldt, H.F.; Blennow,A.; Jespersen, B.M.; Wollenweber, B and Engelsen, S.B. (2007). Accumulation of mixed linkage β-(1→3),(1→4)-D-glucan-D-β-glucan during grain filling in barley – A vibrational spectroscopy study. *Journal of Cereal Science, submitted.*

B. Seefeldt, H.F.; Viereck, N.; Larsen, F.H.; Wollenweber, B and Engelsen, S.B. (2008). Bulk carbohydrate grain filling of barley β-glucan mutants studied by ^{1}H HR MAS NMR. *Cereal Chemistry, submitted*

C. Seefeldt, H.F.; van der Berg, F.; Köckenberger, W.; Engelsen, S.B and Wollenweber, B. (2007). Water mobility in the endosperm of high β-glucan barley mutants as studied by Nuclear Magnetic Resonance Imaging. *Magnetic Resonance Imaging, 25, 425-432*

The thesis aims at using spectroscopic tools to evaluate seed development on a phenomic level with emphasis on starch and β-glucan and employing two barley endosperm mutants. Theory in genetics and molecular biology is combined with that of vibrational and magnetic resonance spectroscopy to evaluate mutational changes in the bulk seed glucan synthesis and their pleiotropic effects. The practical utilization of the results is discussed with regard to human nutrition and technological value of foods.

Helene Fast Seefeldt
Nyborg, February 2008

Acknowledgements

First of all a great and warm thanks to Dr. Bernd Wollenweber and professor Søren Balling Engelsen for giving me the opportunity to carry out this PhD study and to introduce me to the possibilities of spectroscopy, chemometrics and the biological pathways. I am grateful for their supervision and patience throughout the project and for keeping me on the right track through the sometimes bewildering paths of science.

My collegeues at FAS, Flakkebjerg and at KU-LIFE are greatly thanked for being always helpful, inspiring and encouraging and making this Ph.D. a good experience.

Dr. Walter Köckenberger and the people at Sir Peter Mansfield Magnetic Resonance Centre are all warmly thanked for making my stay interesting and a very good experience both academically and socially.

I am grateful to technician Betina Hansen and technician Ole Braad Hansen, University of Aarhus for their aid with the experiments in the green house and in the semifield. Moreover, technician Lisbeth Hansen, LIFE, University of Copenhagen is greatly acknowledged for her assistance and work with the chemical analysis.

Assistant Professor Nanna Viereck and associate professor Flemming Hofman Larsen are gratefully acknowledged for introducing me to NMR and appreciated for their educational skills. My appreciation to associate professor Andreas Blennow for last-minute starch analyses. Thanks to associate professor Frans van der Berg for making magic of the MRI data.

A special and warm appreciation to assistant professor Birthe Møller Jespersen for providing seed material and for always having time for encouragement, discussions and practical help. My mentor professor Lars Munck has been a major inspiration with an enthusiastic ways of sharing his experience and I am deeply thankful for his comments, discussions, encouragement and for sharing his unique barley mutant collection. Anne-Marie, Elisabeth and Svend: Thank you for your time, your comments and help with the lay-out.

Finally, I would express my deepest appreciation and love to my family and friends. Especially, my husband Philipp, and my parents for support and encouragement and not least for logistic support with the kids.

Table of contents

List of other publications

The following publications are different public disseminations of the work carried out during this Ph.D. study, but are not included in the thesis.

Viereck, N., Nielsen, M.M.H., Engelsen, S.B., and Seefeldt, H.F.(2005). HR MAS NMR-spectroskopi: En hel ny verden for fødevareforskningen. *Dansk Kemi*, 86(11). Pp.1-8

Seefeldt, H.F., Viereck, N., Wollenweber, B., and Engelsen, S.B. (2006). Metabolite profiling of developing barley seeds by single seed HR MAS NMR spectroscopy. Nutrigenomics and Health –from Vision to Food. *Scandinavia J. Food & Nutrition*. P.26.

Seefeldt, H.F., Wollenweber, B., and Engelsen, S.B. (2005). NMR imaging of drying barley seeds. Proceedings 4th European Young Cereal Scientists and Technologists Workshop, Vienna. Pp. 27-28

Seefeldt, H.F., Viereck, N., and Wollenweber, B., (2005). Impact of a high-temperature event on carbohydrate composition in barley seeds analysed by novel single seed MAS-NMR analysis. *NJF Report,* 1. p.46

Seefeldt, H.F., and Tønning, E.(2005).Videnskabsteori for ph.d.ere. *Jord og Viden*, 150(17). Pp. 12-13.

Jespersen, B.M., and Seefeldt, H.F. (2007). Funktionelle fødevarer. Kronik I *Fyens Stiftstidende*, 13. marts 2007.

List of abbreviations

ADP-glc	Adenosine 5´diphosphate glucose
AGPase	ADP-glucose pyrophosphorylase
ATR	Attenuated total reflection
β-glucan	Mixed-linkage β-(1→3),(1→4)-D-glucan
COW	Correlation optimized warping
CPMAS	Cross polarized magic angle spinning
CPMG	Carr-Purcell-Meiboom-Gill
DAF	Days after flowering
EISC	Extended inverted signal correction
FID	Free induction decay
FT	Fourier transformation
Glc-1P	Glucose-1 Phosphate
HR MAS	High resolution magic angle spinning
iECVA	interval extended canonical variate analysis
iPLS	interval partial least squares regression
IR	Infrared spectroscopy
MRI	Nuclear magnetic resonance imaging
MSC	Multiplicative signal correction
NADH	Nicotinamide adenine dinucleotide
NIR	Near-Infrared spectroscopy
NIT	Near-Infrared transmittance spectroscopy
NMR	Nuclear magnetic resonance
PC	Principal component
ppm	Parts per million
PCA	Principal component analysis
RF	Radio frequency
RMSECV	Root mean square error of cross validation
SS	Starch synthase
SSgb	Starch synthase granule bound
SBE	Starch branching enzyme
T_1	Longitudinal or spin-lattice relaxation time constant
T_2	Transverse or spin-spin relaxation time constant
UDP-glc	Uridine diphosphate glucose
UGPase	UDP glucose pyrophosphorylase

Summary

Barley is, besides its commercial value, a versatile model for both basic genetic/physiological and applied food research. New aspects of the barley model system are presented in this thesis. A new food and industrial focus on barley has emerged due to its high content in the endosperm of the hydrophilic cell wall fiber mixed linkage β-(1→3),(1→4)-D-glucan (β-glucan). In contrast to crystalline starch the amorphous β-glucan has a higher dynamic capability to take up and release water. In U.S.A a positive health claim on products containing β-glucan underpins the beneficial health potential of β-glucan partly due to the fact that β-glucan is not digested in the upper part of the intestines, and partly due to the water absorbing ability of β-glucan. This influences the lowering of cholesterol, the glycemic index and explains its prevention of colon cancer. For industrial purposes β-glucan acts as hydrocolloid retaining water in products, as texturant replacing fats and as a prebiotic growth medium. The synthesis and exact structure of β-glucan is not fully elucidated, as well as the exact physiological functions of β-glucan in the plant cell wall and in human nutrition are unknown.

Two molecularly defined endosperm mutants were selected from a collection of barley endosperm mutants established in the 1970s in a search for improved protein (lysine): 1) A structural gene mutant (*lys5f*), which is a high β-glucan content compensating starch endosperm mutant (17% dry matter (d.m) β-glucan), but 50% less starch than a control variety, and 2) a regulatory gene mutant (*lys3a*) for protein with less hordein compared to soluble proteins but low in β-glucan (4% d.m). The mutants were investigated with a commercial malt barley variety (5% d.m β-glucan) as a standard. The aim was to use spectroscopic tools to investigate the genetic expression on the phenomic level of the two mutants in relation to a drought event with focus on the bulk carbohydrates: starch and β-glucan. A two week drought event from 0 to 13 days after flowering (DAF) resulted in shorter, more yellow plants with a reduced rate of photosynthesis. Two spikes for each sample were harvested from 9 to 47 DAF at eight temporal stages. The seed material was freeze-dried and grounded except for seeds used for single-seed nuclear magnetic resonance (NMR) spectrosocpy.

Near-infrared spectroscopy (NIR) in the range 400-2500 nm and mid-infrared (IR) spectroscopy in the range 700-1800 cm^{-1} were employed. Moreover, proton high-resolution magic angle (HR MAS) NMR was employed on both single seeds and on flour. For reference purposes chemical analysis of β-

glucan (Calco-flour and enzymatic method), starch (glucose oxidation of NADH), and amylose (iodine complexing) content were measured, as well as number of seeds on the spikes, fresh seed weight and seed weight after freeze drying. All data were evaluated with multivariate chemometric data analysis: principle component analysis (PCA) for classification and partial least squares regression (PLS) for calibration of the reference analysis.

No effect of the drought treatment could be verified from any of the methods employed, and hence a compensation of the drought treatment must have occurred in the seeds, probably from relocation of nutrients from vegetative parts to the seeds. However, the spectroscopic data from the mutants and the control revealed clear temporal and genotypic differences both observed directly by spectral data inspection and by classification through PCA. All the spectroscopic data could by PLS regression predict starch and β-glucan except for single seed NMR due to immobilization of the bulk carbohydrates. In order to mobilize protons in bulk carbohydrates, a ^{1}H HR MAS NMR experiment was performed at 75^{o} C. This enabled prediction of starch. An attempt to calibrate β-glucan was unsuccessful due to an immobilization of β-glucan in the high β-glucan-content mutant *lys5f* at the late seed developmental stage at 47 DAF. It is speculated whether this immobility of the β-glucan is due to different hydration environment in *lys5f* cells. The importance of β-glucan for the water relations in the cells were demonstrated in a NMR imaging (MRI) experiment in which mature normal control barley and *lys5f* seeds were soaked for a week. The intensity maps of the protons in the seeds together with a measurement of the water uptake showed that *lys5f* contained more water than the control. Relaxation studies showed moreover, that the water in *lys5f* had a higher mobility compared to the water in the control. Finally, the MRI experiment confirmed the uneven distribution of water in the seeds and an uneven release of water during a subsequent drying with water retained at the longest in the embryo.

By analyzing water content during seed development compared to the control variety, *lys5f* showed to have an early increase at 20 DAF explained by the increase in β-glucan, whereas *lys3a* had a late gene expression demonstrated by an increase in water content at 30 days due to a higher ratio of hydrophilic proteins. The water activity in the cells is of crucial importance for all the enzymatic processes and hence, a changed water activity due to e.g. a higher content of β-glucan or hydrophilic proteins result in indeterministic and unpredictable changes in the phenotype (phenome) that can not in detail be predicted from genomic or transcriptomic data. The differential expression of water content during seed synthesis in *lys5f* and *lys3a* revealed could therefore partially explain a range of pleiotropic effects that has been described in literature for the these mutants. This includes large changes in β-glucan, higher content of fat, alterations in E-vitamin composition and in

protein composition compared to a control variety. Thus the phenome in *lys5f* and *lys3a* are altered due to the pleiotropy of single mutation events.
Barley is genetically homozygote and hence, the total response of the mutant genes *lys5f* and *lys3a* compared to the control variety could be studied on the phenomic level as unique IR and NIR patterns directly in spectra with a very high reproducibility. In this thesis, it was shown that mutant specific IR and NIR patterns are established already during early seed development and despite varying content of specific seed storage compounds, the patterns are conservative throughout seed development. Hence, IR and NIR spectroscopy indicative for patterns of chemical bonds can be used as a coarse grained overview of the phenome when validated by chemical analyses and thus used for genotypic classification. Chemometrics through PCA is useful for the identification of spectral regions in large data sets that are able to classify genotypes. However, it was shown here that spectral data inspection of the selected spectral interval must be performed in order to notice the finely tuned reproducible genotype-specific patterns that are partly destroyed by data compression such as PCA.

Resumé

Byg er en vigtig model plante indenfor anvendt fødevare forskning, genetik og fysiologi. I denne Ph.d. afhandling præsenteres nye aspekter af byg som en genetisk og fysiologisk model plante. Der er skabt ny interesse for byg på grund af kernernes høje indhold af mixed linkage β-(1→3),(1→4)-D-glucan (β-glucan), som er en hydrofil cellevægs fiber i endospermen. For nylig har man in USA tilladt positiv anprisning af fødevarer, der indeholder β-glucan, da det har kolesterol-sænkende effekt, stabilisere blodsukker indholdet og nedsætter risikoen for tyktarmskræft. I modsætning til det krystallinske stivelse har det amorfe β-glucan en dynamisk evne til at optage og frigive vand. Den vandabsorberende evne og det forhold at β-glucan ikke optages i tyndtarmen er grunden til de sundhedsmæssige fordele af β-glucan. I industrien drager man også nytte af at β-glucan virker som et hydra-kolloid, der kan tilbageholde vand i produkter. Desuden kan β-glucan virke som en strukturforbedrende ingrediens, som en fedt-erstatning og som præbiotisk vækstmedie. Syntesen og den eksakte struktur af β-glucan er ikke fuldstændig klar ligesom den fysiologiske funktion af β-glucan in cellevæggen og i human ernæring ikke er fuldt belyst.

Basis for dette studie er to endosperm mutanter, der stammer fra en samling byg mutanter, der blev lavet i 1970'erne i søgningen efter ernæringsmæssigt forbedrede bygsorter med et højere indhold af lysin. Den ene er en strukturel mutant (*lys5f*), som er en β-glucan kompenserende stivelses-mutant med et indhold af β-glucan på 18% tørvægt. Den anden er en regulatorisk protein mutant (*lys3a*) med et lavere indhold af det hydrofobe protein hordein, samt et lavt indhold af β-glucan (4% tørvægt). Som kontrol blev en kommerciel byg sort valgt med et β-glucan indhold på 6% tørvægt. Målet for dette studie er at bruge spektroskopiske metoder til at undersøge gen-ekspressionen på det fænotypiske plan for de to mutanter i relation til en stress periode i form af tørke. Fokus var stivelse og β-glucan syntesen gennem kerneudvikling.
Halvdelen af planterne blev udsat for to ugers tørke fra 0 til 13 dage efter blomstring (DEB). Dette medførte mindre og mere gule planter med en reduceret fotosyntese. Aks blev høstet otte gange fra 9 til 47 DEB. Frøene blev vejet, talt og frysetørret og vejet igen. To frø per aks blev taget fra til NMR enkelt kerne analyse. Resten blev formalet og brugt i alle yderligere analyser. Nær-infrarød (NIR) spektra i området 400-2500 nm og midt-infrarød (IR) spektra i området 700-1800 cm^{-1} blev optaget for alle prøver. Desuden blev proton high-resolution (HR) magic angle spinding (MAS) kerne magnetisk resonans (NMR) brugt på både enkelt kerner og melet. Som reference ana-

lyser blev der bestemt β-glucan-indhold vha. Calcoflour og enzymatiske metoder, stivelse (glucose oxidation af NADH) og amylose vha. Jod kompleksbinding. Alle data er blevet evalueret med multivariat kemometrisk data analysemetoderne: principal komponentanalyse (PCA) til klassifikation og partial least squares regression (PLS) til bestemmelse af kalibrering af referenceanalyserne.

Der kunne ikke genfindes nogen effekt af tørkebehandlingen i nogen af de kemiske eller spektroskopiske data, ligesom der statistisk ikke var forskel på kernevægten af de tørkebehandlede og kontrol planterne. Dette skyldes sandsynligvis en omfordeling af næringsstoffer fra de vegetative dele af planten til kernerne. Til gengæld kunne spektroskopiske data klart klassificere både genotypiske og udviklingsmæssige forskelle i prøverne både udfra en PCA og fra visuel inspektion af spektra. Alle de spektroskopiske metoder kunne via PLS prædiktere stivelse og β-glucan bortset fra enkelt kerne NMR. Dette skyldes at oplagsstofferne ikke var mobiliseret. For at mobilisere alle stofferne blev der lavet et ^{1}H HR MAS NMR eksperiment på melet hvor det foruden at blive spundet ved høj hastighed også blev varmet op til 75^{o}C. Dette muliggjorde prædiktion af stivelse ligesom tydlige genotypiske forskelle i stivelses syntesen kunne ses i spektra. Til gengæld, var det ikke muligt at lave en kalibrering til β-glucan, fordi β-glucan er NMR-immobilt i *lys5f* ved den sidste høst, 47 DEB. Dette kan skyldes et andet hydreringsmiljø i *lys5f* i forhold til kontrolsorten. Vigtigheden af β-glucan for vandforholdene i cellen blev demonstreret i et NMR imaging (MRI) eksperiment, hvor modne kerner af kontrolsorten og *lys5f* blev lagt i blød i en uge. Protonintensitetskort samt relaksationsstudier af *lys5f* viste, at den indeholdt mere vand end kontrolsorten. Relaksationsstudiet viste desuden, at vandet i *lys5f* havde en højere mobilitet i forhold til kontrollen. MRI eksperimentet bekræftede desuden den ulige fordeling af vand i kernen samt den heterogene tab af vand, der sås ved den efterfølgende tørring, hvor embryoet holdt på vandet længst.

Ved at analysere vandindholdet gennem kerneudviklingen i mutanterne i forhold til kontrolsorten blev det fundet, at *lys5f* er et tidligt gen, da et øget vandindhold blev set ved 20 DEB. Dette skyldes den samtidige akkumulering af β-glucan. I *lys3a* var der også en stigning i vandindholdet i forhold til kontrollen, men først ved 30 DEB, hvilket indikere et sent gen. I *lys3a* skyldes stigningen i vandindholdet en ændring i forholdet mellem hydrofile og hydrofobe proteiner. Vandaktiviteten I cellerne er meget vigtige for alle de enzymatiske processer. En ændring i vandaktiviteten medfører uforudsigelige ændringer i fænotypen (fænomet), som ikke kan forudsiges i detaljer med genomiske eller transcriptomiske data. Forskellene i vandindholdet gennem kernefyldningen i *lys5f* og *lys3a* kan delvis forklare de mange pleiotropiske effekter, der er beskrevet for de to mutanter i litteraturen. Dette inkluderer bl.a. store ændringer i β-glucan indholdet, et højere indhold af fedt, ændringer i E-vitaminsammensætningen samt i proteinsammensætningen. Dvs. at

fænomet i *lys5f* og *lys3a* er ændret p.g.a de pleiotropiske effekter af en enkelt mutation.

Byg er genetisk homozygot, og derfor kan den fuldstændige effekt af mutant generne *lys5f* og *lys3a* i forhold til kontrolsorten studeres på det fænotypiske plan som unikke IR and NIR mønstre direkte i spektra med en meget høj reproducerbarhed. I denne afhandling er det påvist, at mutantspecifikke IR and NIR mønster dannes allerede tidligt i kernefyldningen. Trods de store variationer i indholdet af bestemte oplagsstoffer er mønstrene meget konstante gennem hele kernefyldningen. Toppene i IR og NIR spektra repræsenterer kemiske bindinger, der kan valideres med de kemiske analyser. Derfor giver IR og NIR et, om end grovkornet, overblik over fænomet med alle de pleiotropiske effecter, der måtte være efter en enkelt mutation. Dette kan bruges til at lave sorts-bestemmelse med. Kemometri og PCA er meget velegnet til at identificere spektrale områder i store datasæt, der gør det muligt at klassificere genotyper. Det er dog vist her at spektral data inspektion af de valgte spektrale områder er nødvendig for at opdage de meget fine reproducerbare genotypiske mønstre, som delvis ødelægges i en PCA.

1 Introduction

Barley has a great advantage as a representative cereal model plant in biological and industrial research due to good climate adaptability, high potential yield, and versatile applications in food, feed and brewing industries. Furthermore, it is a diploid, self-pollinating species that facilitates detailed genetic description.

In this study, barley seeds are the object of interest due to two facts: a unique barley mutant collection with mutations in isogene lines offers the possibility to study gene-expression on the phenomic (the output of the gene-expression at a given time under defined conditions) level under various environments revealed by spectroscopy in combination with chemometrics. Secondly, barley seeds have a high content of β-glucan that holds interesting beneficial health and food-industrial potential.

This PhD study focuses on the starch α-glucans: amylose and amylopectin and the major cell wall fiber mixed-linkage β-(1→3),(1→4)-D-glucan (β-glucan). The glucans are the most abundant polymers of D-glucose residues in cereals: Starch and β-glucan comprises approx. 80% of the endosperm tissue (the storage part of the seed). The glucans are used either as energy in food, as fermentation source, health components or raw material for industrial products. The endosperm is of interest as it can be seen as a conserved physio-chemical fingerprint of the genetic and environmental influences under which the plant was grown.

Seed development and the grain filling processes are of major interest from the point of view of the establishment of the yield and the seed composition (quality) to the physiological processes involving the effect of genetic and environmental regulation of the biosyntheses. Environmental conditions such as drought are found to have profound impact on yield and starch composition in cereals. Hence, to overview the gene expression and the environmental impact on the phenotypic level relative to temporal development, drought was applied to the plants during seed development.

For breeding purposes as well as industrial processing of cereal products, it is of importance to know how the genetic variability of e.g. glucans are expressed and regulated on the phenotype (phenome) level and to interpret the complex networks of the biosynthesis-pathways during seed development. The understanding of the biosyntheses and its regulations can be ad-

dressed in many ways such as by destructive chemical methods, but should preferably be complemented with analysis of the outcome from the whole system (the phenotype) through non-invasive spectroscopy. Until recently it has been impossible to overview the outcome of gene expression from single mutations on the phenomic level. However, spectral patterns can now be elucidated by spectroscopy leading to a digitized coarse representation of the whole phenome that can be evaluated and explored by chemometrics.

Near-infrared reflectance (NIR) and mid-infrared (IR) spectroscopy have proven valuable for analysing whole systems when combined with chemometrics. NIR and IR are easy-to-perform spectroscopic methods providing information at the level of chemical bonds. Nuclear Magnetic Resonance (NMR) is in biological systems often tuned to protons, which have the highest sensitivity to NMR. NMR is a low-perturbation and non-invasive technique providing information about the amount of protons present and the cellular environment in which they are present. These three spectroscopic methods have been employed in this PhD study to study how these spectroscopic methods can follow the developmental changes of glucans in the endosperm tissue.

1.1 The aims and outline

This study is an exercise in exploring the possibilities of spectroscopy to answer biological and genetic questions during seed development. The biological kick-off for this thesis was that NIR in combination with a PCA has revealed single gene barley endosperm mutations with a primary effect on starch synthesis that resulted in unexpected secondary or pleiotropic effects such as a starch-compensating increase in β-glucan content in ripe seeds (Munck et al., 2004). Hence, two contrasting barley mutants – one structural (*lys5f*) and one regulative (*lys3a*) mutant, with pleiotropic effects on starch and β-glucan have been used for all the analyses. These mutants are isogenic and originate from the same parent Bomi, and have potential in cereal dietary foods due to their altered composition of starch, β-glucan and protein composition (lysine). The aims of the PhD study was to study how changes induced by a single mutation influence the developmental properties of the phenome and the entire seed constitution compared to conventional barley during varying environmental conditions. That is:

- To study β-glucan and other chemical variables pleiotropic to mutants as a whole during seed development by spectroscopy
- To study if the varying content of starch and β-glucan in the mutants would lead to similar response by a drought period during seed development

- To study mutants of isogenic lines during seed development in order to spectrally separate the genetic and environmental effects
- To investigate the onset of single genes on the phenomic level
- To prove the self-organising principle of barley endosperm tissue during seed development by spectroscopy in combination with chemometrics and data inspection

The choice of NIR, IR and NMR spectroscopy as tools to investigate seed development was based on the expected advantage of replacing traditional, destructive, uni-variate chemical analysis with high-throughput methods that can operate directly on the material, in this case flour and seeds, and giving unique fingerprinting data of physio-chemical relevance. In particular it was investigated if:

- Spectroscopy in combination with chemometrics can be used to study the quantity of seed glucans that are changed by a single mutation and thus to be used as a fingerprinting technique of genetic variability with a high reproducibility
- ^{1}H HR MAS NMR can be used on single seeds during seed development
- Spatially resolved water signals from NMR imaging can discriminate between high β-glucan and low β-glucan genotypes and reveal the influence of β-glucan on water holding capacity
- Data inspections of spectra could reveal more/other information than gained from chemometric evaluation

The application of the above mentioned tools on developing barley seeds resulted in three papers, covering aspects enclosed in the aims:

- Characterization and investigation of two extreme barley mutants with regard to β-glucan content during grain filling using classical reference methods as well as the spectroscopic phenome fingerprinting methods; NIR and IR
- Characterization of the timing of grain filling processes with emphasis on starch and β-glucan in the barley mutants with varying β-glucan and starch content using ^{1}H HR MAS NMR
- Visualisation of the water distribution in barley mutants with varying β-glucan content with NMR imaging and determination of relaxation times

The thesis is divided into a theoretical part (Chapters 2 and 3) and an experimental based part (Chapters 4 and 5). Chapter 2 covers barley biology and molecular genetics with regard to endosperm mutants and barley seed glucans. Chapter 3 gives the basic theory of NIR, IR and NMR including a theoretical part on the chemometric data analysis. In chapter 4 the results of

the experimental work including the application of spectroscopy in cereal sciences are presented and discussed with the current literature in the area. Chapter 5 is an introduction to the use of NIR for phenomic analysis based on the results from this study. Chapter 6 gives a perspective on the analysis of the rich data material that has been collected and how these results can be applied in breeding and food research to develop new dietary foods for health and industrial purposes. Finally, chapter 6 sums up the conclusions.

2 Barley biology

"*See the west wind moves like a lover so, upon the fields of barley…when we walked the fields of Gold*" (Sting, 1993). These 'Fields of Gold' that Sting refers to are not cherished only because of their beauty, but chiefly due to their major importance as feed and malt. This section presents the background literature on barley as an experimental system, the synthesis and regulation of glucans and the history of 'high-lysine' barley endosperm mutants.

2.1 Barley, the 'Golden crop'

Barley is the fourth most important cereal after wheat, rice and maize comprising 24,000,000 tonnes on an annually, worldwide basis (FAO, 2006). The majority (approx. 90%) of the barley production in the Western countries are used for feed and malt (FAO, 2006). Only in the Near-middle-East, North Africa region and in Japan and Korea is barley a regular food source (Jadhav et al., 1998). However, the market for barley used for food and industrial purposes is increasing in Europe (Anonymous, 2007) and a positive health claim in the U.S. associating consumption of barley products with reduction of risk of coronary heart disease (FDA, 2006) will probably further increase the commercial interest in barley for food. The health claim is related to the high content of the endosperm cell wall fiber mixed linkage β-(1→3),(1→4)-D-glucan (*β-glucan*).

2.1.1 Commercial use of barley

The high-value product of common barley is malt. A rapid germination (hydration) of seeds results in hydrolysis of starch releasing the energy for fermentation. The hydration is followed by a drying process leading to malt (Munck et al., 1981). β-glucan is undesired in the brewing industry, as it causes incomplete cell wall degradation, which in turn leads to less mobilized starch and proteins for hydrolysis (Woodward and Fincher, 1983), because β-glucan forms highly viscous aqueous solutions leading to filtration problems and thereof following hazing of the beer (Aastrup et al., 1985; Fincher and Stone, 1986), and undegraded or partially degraded β-glucan may precipitate also leading to hazing or precipitates in the final product (MacGregor and Fincher, 1993). Finally, the β-glucan can react with poly-

phenoles, proteins, and polysaccharides to form complexes leading to diminished stability of the beer during storage (MacGregor and Fincher, 1993). A small amount of β-glucan has some advantages in brewing as it gives foam stability and body to the beer. The focus on breeding varieties for malting has lead to rather low levels of β-glucan in commercial varieties ranging 2.0-5.0% w/w (MacGregor and Fincher, 1993).

Approx. 60% of the barley grown worldwide is used for feed (FAO, 2006). The nutritional value of barley for feed, compared to other cereals like wheat and maize, is due to a relative high level of essential amino acids, but the energy in husked barley is relative low due to a high amount of fiber (Munck, 1981). From a human point of view, the composition of barley grains is in accordance with many health recommendations for food: it is high in fibre content, contains beneficial antioxidants such as E-vitamin and B-complex vitamins, and is low in fat and free of cholesterol (Munck, 1981). However, whole-grain barley is not a popular eating due to the indigestible and rough husk. Hence, the commercial barley food products have been developed with removed husk (pericarp and testa) through pearling.

The health related aspects of barley is related to the starch composition (the ratio between amylose/amylopectin) and the cell wall fibres; β-glucan and arabinoxylans (Jadhav et al., 1998). The physiological response to barley as a nutrient is equal for mono-gastric animals and humans. However, depending on the point-of-view the fibers are wanted or unwanted: In general, humans and animals (Knudsen, 2001) and especially birds (McNab and Smithard, 1992) are unable to synthesize enzymes capable of hydrolysing plant cell wall polysaccharides leading to an almost undegraded fiber fraction influencing the mobility trough the alimentary tract (Fincher and Stone, 1986). In birds cereal fibers, especially β-glucan, leads to excess drinking resulting in sticky droppings (McNab and Smithard, 1992; Fincher and Stone, 1986), which causes many sanitary problems. Barley has therefore been considered a less valuable food source for chickens, as they gain less energy (Jadhav et al., 1998) and this limits growth. β-glucan is considered a *soluble dietary fiber* (Laroche and Michaud, 2007) but contain also an insoluble portion. However, ruminants can degrade the cell wall polysaccharides with the aid of microflora-and fauna (MacGregor and Fincher, 1993). In mono-gastric mammalians such as pigs, the energy engraved in the fiber fraction is not absorbed by the human/animal but rather the fiber fraction impairs the access to the stored starch. There is some degradation of β-glucan by bacteria in the colon of monogastric animals leading to production and absorption of organic acids. The problems related to β-glucan in animal husbandry are nowadays overcome by adding hydrolyzing enzymes to the fodder that works in the alimentary tract.

The high content of β-glucan in barley is the reason, why barley has gained renewed interest in the food industry, as a health factor and as a high-value product. The health aspects include reduce serum cholesterol in hypercholesterolemic individuals of rats, hamsters and humans (Kalra and Joad, 2000; Kahlon et al., 1993; Bourdon et al., 1999; Behall et al., 2005), the modulation of gluco-regulation in diabetic people (Léon et al., 2000; Wursch and Pi-Synyer, 2006) by decreasing the glycemic response due to decreased absorption of carbohydrates (Lifschitz et al., 2002), lowering the risk of colon cancer (McIntosh, 1993), and moreover, β-glucan reduces the absorption of triglycerides (Kahlon et al., 1993) as β-glucan increases emulsion droplet size (Lazaridou and Biliaderis, 2007). The improved dispersion of nutrients and mobility through the alimentary tract, the hindrance of accessing the stored energy and the prolonged satiety feeling (Knudsen, 2001) are properties of β-glucan beneficial for obese people. Finally, the gelling ability of 'Glucagel™', which is the product from a non-enzymatic extraction method for β-glucan implying a hot-water extraction followed by a freeze and thaw treatment of the extract (Morgan and Ofman, 1998), has a positive effect on the mammalian immune system such as healing processes and immunity (Lazaridou and Biliaderis, 2007).

2.1.2 The chemical composition of barley seeds

The major anatomical features in a barley seed can be seen in **Figure 2-1**. The outer parts of the seed are comprised of the husk and the pericarp (also referred to as testa). In hull less barley the husk is removed during harvesting (Jadhav et al., 1998). The aleurone layer is the outermost layer of the endosperm tissue and is together with the embryo involved in the release of enzymes during germination.

In general, the majority of the barley grain (see **Table 2-1**) on dry weight basis is made up of starch constituting 60-64% of the dry weight that consists of two polymeric components: amylose and amylopectin. Proteins makes up 8-15% and the cell wall components β-glucan (3-6%) and arabinoxylans (4-8%) are the second most abundant compounds comprising 7-14% of the dry weight. The minor constituents are lipids and fatty acids (2-3%), husk-bran (mainly consisting of cellulose, which comprises 1.5-5% of the total seed) and low molecular weight sugars besides a range of minerals (3%) and vitamins such as the vitamin B complex, and vitamin E (MacGregor and Fincher, 1993).

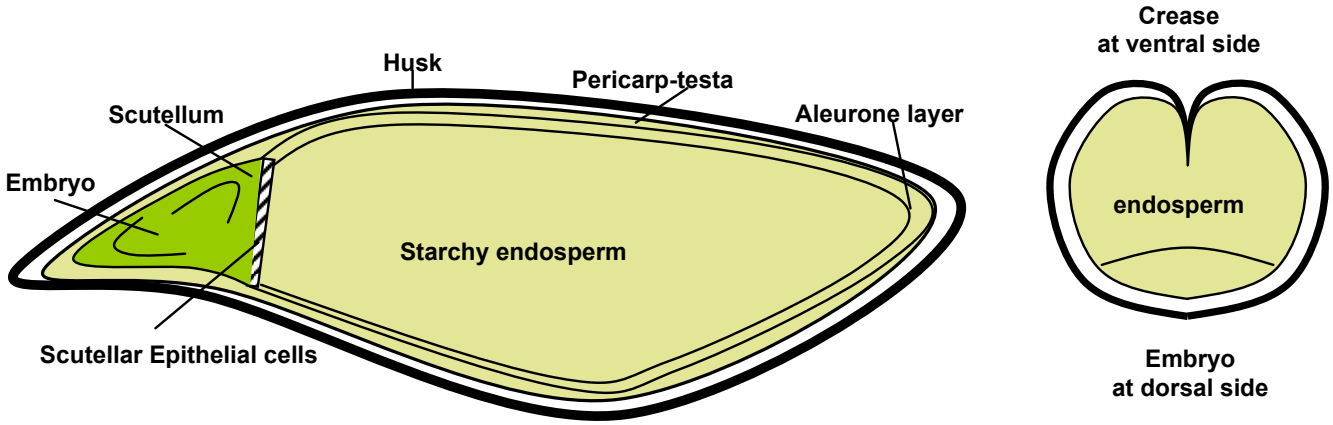

Figure 2-1. The anatomy of a barley grain. Modified from Jadhav et al. (1998) and McEntyre et al (1998).

The period from flowering to maturity is the cardinal summit for the barley plant influencing the final quantity and composition of the barley seed. During flowering, a double fertilisation occurs in which one *gamete* (the sperm cell) from pollen penetrates the egg cell to form the *zygote* (the diploid fusion of the male and female gametes) that becomes the *embryo* (the pre-structures of a new plant), while the other gamete fuses with the two united polar nuclei to form the *endosperm* (the storage tissue) and the aleurone layer (Olsen et al., 1992). The origin of a new seed starts with the fertilisation of a flower. All developmental events in this study are related to *days after flowering* (DAF) here defined as the time when 50% of the anthers are dusting.

Table 2-1. The location and general amounts of barley seed compounds. Modified from Munck (1981), Jadhav et al (1998) and MacGregor and Fincher (1993).

Grain structure	Subcompartment	Chemical compounds
Protective cover	Husk	Arabinoxylans, hemicellulose, cellulose fibres
	Pericarp/ testa	Alkane layers of waxes, phenolic compounds
Endosperm	Endosperm	Starch, protein matrix, lipids, traces of minerals (P, K, Na, Ca, Mg)
	Aleurone	Arabinoxylans (71%), β-glucan (25%), lipids, protein, phytic acids, Vitamin and minerals. Secretes enzymes into the endosperm during germination.
	Endosperm cell walls	β-glucan (75%), arabinoxylans (20%), cellulose, glucomannan and callose. Phytic acids, Proteins, Minerals.
Embryo	Embryo	Protein, Enzymes, Lipids, Vitamins
	Embryo cell walls	Uronic acids, pectin, β-glucan

Based on growth characteristics, starch accumulation and metabolic patterns three stages were determined in barley seed development by (Sreenivasulu et al., 2004), see **Figure 2-2**. The first phase from 0-5 DAF is characterized by cell divisions and lack of starch. This phase is concomitant with the cellularization stage in which a rapid phase of cell division starts after fertilization and last 4-5 days (Ellis and Marshall, 1998). During the second stage from 6-10 DAF, the initial starch accumulation occurs (Jenner et al., 1991; Weschke et al., 2000; Sreenivasulu et al., 2004) with a linear increase of storage deposition from 10-20 DAF, after which the synthesis of the storage compounds and the intermediates levels off (Sreenivasulu et al., 2004; Rolletschek et al., 2004).

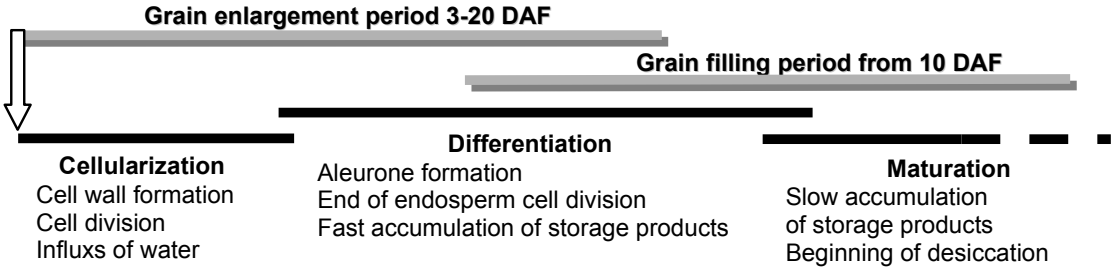

Figure 2-2. Schematic representation of the time course of cereal seed development. Arrow indicates flowering. Modified from Jenner et al., (1991), Emes et al., (2003) and Philippe et al., (2006).

In general, accumulation of starch is correlated to the curve of dry weight increase (Coles, 1979), as starch is the major contributor to grain weight.

The accumulation of β-glucan was found to increases steadily from anthesis and until 30-35% water content was achieved in spring barley by Léon et al., (2000), but the accumulation pattern is both environmentally and genetically controlled, see 2.2. In an immuno-labeling study of barley, β-glucan immunolabeling appeared in the endosperm already between 4 and 5 DAF in the cell walls (Wilson et al., 2006).

2.1.3 The barley starch and cell wall glucans

The functionality and quality of cereal starch and fibers are dependent on the ratio of the various glucan fractions, but also on the structure of the glucans. *Amylose* is a linear molecule of α-(1→4)- glucans, whereas *amylopectin* is a branched α-(1→6),(1→4)- glucan. The endosperm cell wall fiber β-glucan is a linear mixed linkage β-(1→3),(1→4)-D-glucan molecule. The primary structure of the glucans is presented in **Figure 2-3**. The majority (65-80%) of starch in normal barley consists of the highly branched amylopectin (Kang et al., 1985), (MacGregor and Fincher, 1993). Amylose winds up in a helical conformation and can form inclusion complexes with a range of small hydrophobic molecules such as lysophopspholipids and free fatty acids (Morrison

and Gadan, 1987) altering the functionality of high-amylose starches such as gelatinisation, retrogradiation, and the ability to be hydrolyzed (Anker-Nilssen et al., 2006) due to different crystallinity (MacGregor and Fincher, 1993). The amount of amylose thus influences the swelling and gelling properties of the starch during cooking TJEK TESTER 1993.

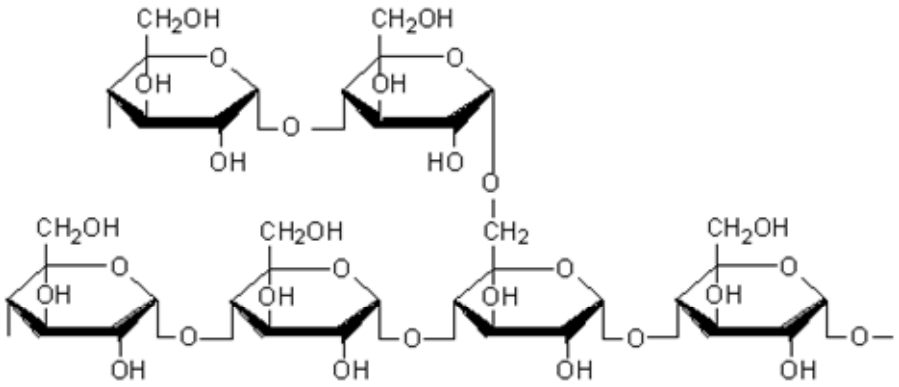

Amylopectin: α-1,4 and α-1,6 glucosidic bonds

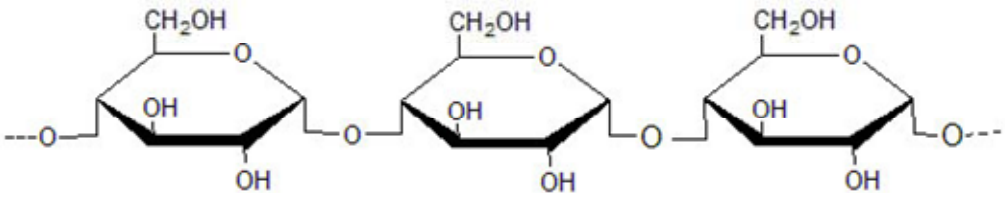

Amylose: α-1,4 glucosidic bonds

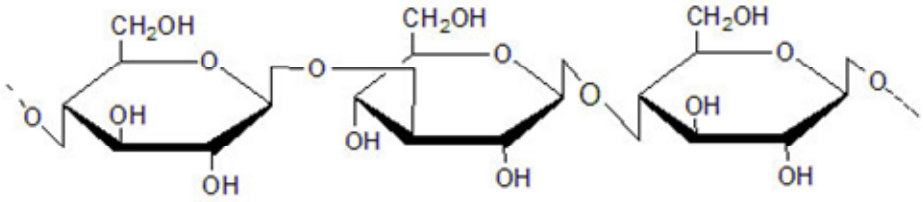

β-Glucan: mixed β-1,3 and β-1,4 glucosidic bonds

Figure 2-2. The structure of α-(1→6)glucan: the branched amylopectin (top), α-(1→4)glucan: the linear amylose (middle) and mixed linkage β-glucan (bottom).

β-glucan is the most abundant soluble fibre in barley where it constitutes 75% of all polysaccharides in the endosperm cell wall (Fincher, 1975). The water-soluble β-glucan from barley contains approx. 70% β-(1→4)-glycosyl linkages and 30% β-(1→3)-glycosyl linkages (Woodward et al., 1983), (see **Figure 2-4**). β-glucan act partly as a structural element and partly as a flexible storage material that is hydrolyzed during grain filling and germination (Buckerigde et al., 2004). β-glucan is not a strict defined polysaccharide with respect to size, solubility, and molecular structure (Woodward et al., 1983;

Hrmova and Fincher, 2001) and fine chemical structure differences occur between cereals and within a specific cereal seeds (Cui et al., 2000). β-glucan in barley endosperm cell walls is embedded in a protein matrix (Thompson and LaBerge, 1977) away from the cell surface hence being sheltered behind the cell wall pentosans impeding access to β-glucan (Bamforth and Kanauchi, 2001). This influences the isolation and extraction procedures of β-glucan (Lazaridou and Biliaderis, 2007).

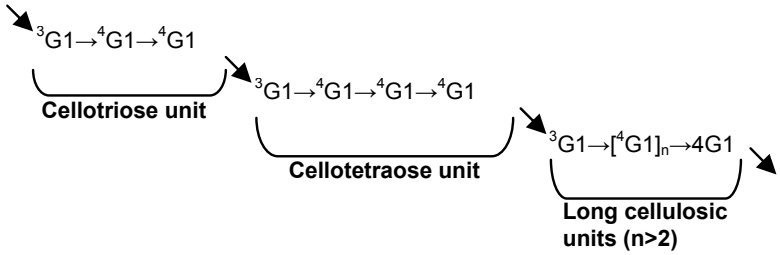

Figure 2-3. The generalised structure of cereal β-glucan.
G1: β-D-glucopyranosyl. Cellotriose (three units), cellotetraose (four units) and longer chains of cellulosic units of β-(1→4)-linked glucans. The arrows indicate β-(1→3) linkages. Modified from Lazaridou and Biliaderis (2007).

The functionality of β-glucan is dependent on the ratio of β-(1→4):β-(1→3)-linkages as it changes the ratio between cellotriose /cellotetraose and the cellulosic chains (see **Figure 2-4**). Soluble β-glucan is found to have fewer cellotriose units than insoluble β-glucan (Johansson et al., 2004; Izydorczyk et al., 1998a; Izydorczyk et al., 1998b). 25% of the total β-glucan in barley is insoluble and this fraction of β-glucan is non-covalently bound to the arabinoxylans (Johansson et al., 2004). As seen from **Figure 2-4**, repetitions of two or more succeeding β-(1→4)-linkages are often found separated by single β-(1→3)-linkages (Fincher and Stone, 1986). However, 10% of water-soluble barley β-glucan consists of blocks of up to 10 or more contiguous β-(1→4)-glycosyl residues (Wood et al., 1994) giving rise to longer cellulosic regions leading to alterations in e.g. gel ability (Johansson et al., 2004).

2.1.4 Synthesis of starch and β-glucan

The precursor for starch synthesis is the adenosine 5' diphosphate glucose (ADP-glc) produced by the enzyme ADP glucose pyrophosphorylase (AGPase, EC 2.7.7.27), see **Figure 2-5**. Once the imported sucrose has been converted to AGP-glc, it is destined to be incorporated into starch (James et al., 2003). Sucrose is generated from the photosynthetic processes in the leaves. Sucrose synthase (SS, EC: 2.4.1.21) is the first step in the conversion of sucrose to either UDP-glucose or fructose, two intermediates in the pathway to ADP-glc and hence to starch. SS in cereals is primarily associated with the endosperm cytosol, but exists also in membrane-bound forms (Emes et al., 2003; Rudi et al., 2006). Fructose is converted to glucose-1-

phosphate (Glc-1P), which can also be phosphorylated to form ADP-glc (Bewley and Black, 1983) within the plastids.

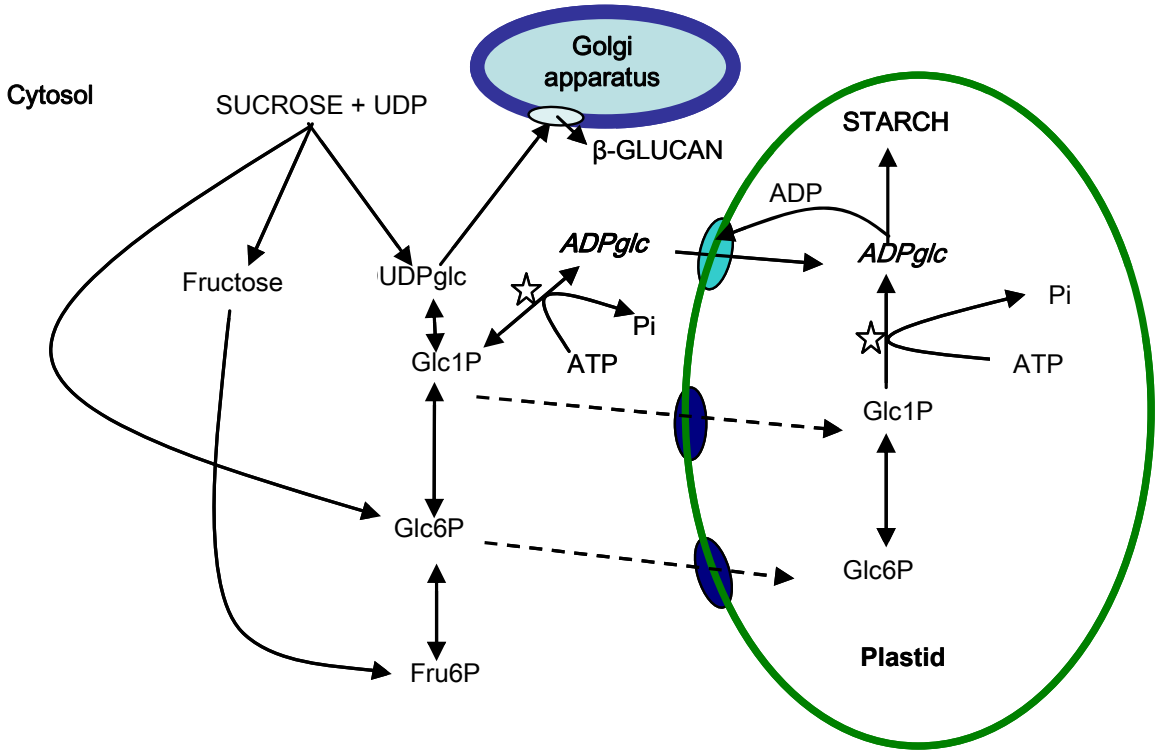

Figure 2-5. Schematic representation of starch synthesis in endosperms showing the biosynthetic pathways leading to starch production in the endosperm plastids. UDP: Uridine diphosphate, glc: glucose, Fru6P: fructose 6 phosphate, Pi: orthophosphate. Stars indicates the action of AGPase. The blue circles at the plastid membrane are the transport proteins. The light blue transport protein is dependent on counter exchange of ADP: adenosine diphosphate. Modified from Emes et al., (2003).

However, ADPglc can also be synthesized in the cytosol, and then transported into the plastids in cereal endosperm, as AGPase is primarily found in a cytosolic form in cereals (James et al., 2003; Thorbjørnsen et al., 1996). The transport of ADP-glc into plastids is depended on a counter-exhange most likely with ADP (Bowsher et al., 2007). The cytosolic form of AGPase accounts for 65-95% of the total AGPase activity (Tetlow et al., 2004) and the cytosolic localization of AGPase is important for partitioning large amounts of carbon into starch when sucrose is plentiful (Beckles et al., 2001). In the plastids, granule-bound starch synthase (SSgb) (EC 2.4.1.21) forms α-(1→4)- linkages and utilizes ADP-glc to elongate linear chains (Tetlow et al., 2004). Starch branching enzyme (SBE, EC 2.4.1.18) generates α-(1→6)-linkages leading to the branching characteristics of amylopectin (James et al., 2003).

The biosynthesis of β-glucan is despite many years investigation (Becker et al., 1995; Buckerigde et al., 2004; Tsuchiya et al., 2005) still not fully eluci-

dated. What is certain is that UDP-glc is the precursor for β-glucan, cellulose (β-(1→4)-glucan) and callose (β-(1→3)-glucan), (Buckeridge et al., 2004). Cellulose is synthesized at the plasma membrane in association with SS, whereas the β-glucan and callose are catalyzed by Golgi membranes (Becker et al., 1995). The β-(1→3),(1→4)-D-glucan-glucan synthase (No E.C number) appears to consists of two units; a cellulose-like core synthase and a distinct glycolsyl transferase (Buckerigde et al., 2004). The enzymes catalyzing the cellulose, callose and β-glucan differ in pH-activity profiles and requirements for metal cations (Becker et al., 1995). The physiological state of the membranes, the concentration of the substrate and the competition between callose, cellulose and β-glucan are important for the synthesis of β-glucan and its precise structure.

2.2 Regulation of glucan synthesis during grain filling

The ability of the seed to generate amylose, amylopectin and β-glucan is engraved in the genome (see definition in section 2.3.1). The amount and composition of the compounds found is subject to regulation by environment (Aastrup, 1979; Tester, 1997; Rudi et al., 2006).

Extreme or high temperatures compared to usual growth conditions during seed development influences the rate and duration of grain filling (Savin and Nicolas, 1999) that affects grain yield and the properties of starch (Wallwork et al., 1998a; Savin and Nicolas, 1996; Passarella et al., 2002; Anker-Nilssen et al., 2006) by altering the size of starch granules (Tester, 1997), the ratio between small and large granules (Savin et al., 1997), increasing the amylose:amylopectin ratio (Savin and Nicolas, 1999), altering the amount of lipid complexed with amylose (Morrison, 1993) and degradation of the starch granules (Wallwork et al., 1998a). The β-glucan content is negatively affected by high temperature (Passarella et al., 2002) and are being partly hydrolyzed (Wallwork et al., 1998a). The environmental influence is complex: The enzymes involved in starch synthesis are e.g. influenced negatively as well as positively by temperature, depending on timing and severity of temperature stress (Wallwork et al., 1998b).

Drought stress affects yield by reducing both sink such as number of seeds per spike, number of spikes and the source, which is the photosynthetic supply (Blum, 1996). Water stress in the sense of limited water supply induces a variety of changes in the cereal seeds such as reduced grain yield (Savin and Nicolas, 1996), increase in apparent amylose content (Savin and Nicolas, 1999), and an enhanced activity of endosperm starch synthesis enzymes due to relocated nutrients (Ahmadi and Baker, 2001; Yang and

Zhang, 2006). The effect of the drought stress relies on the timing and severity (Stone and Nicolas, 1995), and variety (Savin and Nicolas, 1996). Just as starch, β-glucan synthesis and degradation is affected by the moisture conditions (Paynter and Young, 2004). Rain was found to have a reducing effect on the level of total β-glucan found in barley grains (Aastrup, 1979; Coles, 1979) and the opposite is true for dry conditions before harvest (Jadhav et al., 1998; MacGregor and Fincher, 1993). However, a shorter-grain filing period due to warmer and drier conditions in a study of β-glucan content in barley and wild progenitors, could not confirm the increased β-glucan synthesis (Léon et al., 2000) indicating the multitude response depending on the given situation.

2.3 Barley as an experimental model for gene expression

Barley is a diploid, 99.5% self-pollinated, homozygotic research model plant well-suited for studying biosynthesis; as it allows direct phenotype screening of mutant genes. Moreover, the barley starch produced is similar to more genetically complex cereals such as the hexaploid wheat (Evers et al., 1999). Recently, a barley gene chip representing more than 21,000 genes expressed in various tissues to various developmental times have been developed (Close et al., 2004). Collections of genotype accessions registered in databases such as 'American USDA-ARS GRIN database' containing more than 30,000 barley accessions, and 'European Barley Database' give access to a wealth of experimental possibilities. Most of the barley mutants existing in the mutant collections have only been superficially exploited for their use in unravelling biosyntheses and screening for levels of desired traits. This is due to a lack of methods for over viewing the phenome but this is now possible by spectroscopy. The mutants constitute valuable genetic material for improvement/development of targeted barley varieties useful for development of novel food or value-added products.

2.3.1 The systems biology approach to study barley

Systems biology is the multidimensional representation of all the biosynthetic processes constituting an organism from the heritage material to the actual manifestation of organism sees **Figure 2-6**. In the following, the components constituting systems biology will be defined.

The genetic code of each individual is engraved in the helix-structured DNA that is made up of two sugar-nucleotide backbones on which base-pairs are attached. The *genome* is the complete genetic material carried by an individual and present in every cell. The genome is normally fixed, but can be

changed by mutations or during sexual reproduction. When executing the genetic code a *transcription* of the template DNA will be made into the mirrored RNA. Only specific sequences (the active genes) of the DNA in a specific tissue are transcribed into RNA. The transcript of the genome at a given time and under defined conditions is known as the *transcriptome*. The transcriptome is not static but varies with time, external conditions and from tissue to tissue. From the transcriptome the genes are translated as proteins. The entire protein constitution at a given time under defined conditions of a cell, a tissue or an individual is the *proteome*. While the information in the genome is one-dimensional that of the proteins is three dimensional. Hence, their structure and functional interactions between proteins and the internal cell milieu must be taken into account. Genes are not unambiguously in the sense that one gene can be translated to more than one protein due to alternative splicing or post-translational modification of the proteins (Burian, 2004). The *metabolome* is the complete set of small-molecule metabolites and non-protein products found at a given time, in a specific tissue under defined conditions. Hence, the metabolome is also dynamic. Finally, all biochemical, physiological and morphological characteristics of an organism can be described by the *phenome*. The *genotype* is the descriptor of the genome, whereas the *phenotype* is the descriptor of the phenome.

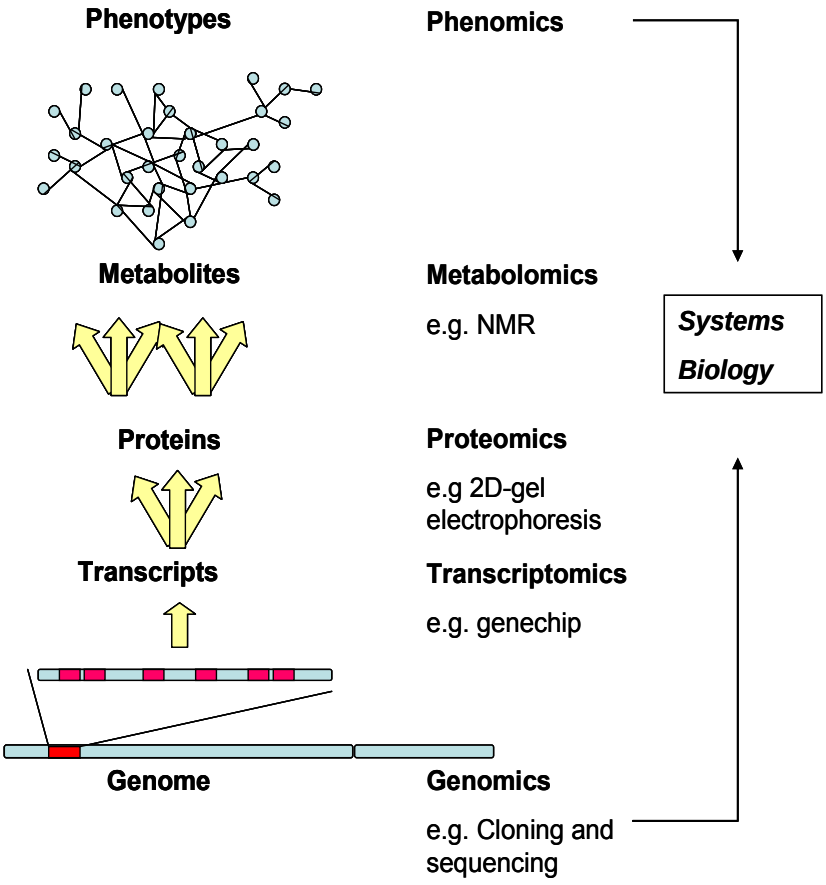

Figure 2-4. A schematic representation of systems biology. The step-wise increase in complexity from gene to phenome is indicated with the yellow arrows. The research areas involved are the 'omics'. Adapted from Tian et al., (2007)

The study of all the processes from the genome to the phenome is termed *systems biology* (see **Figure 2-6**). The 'omics' are the scientific areas involved in elucidating the different stages from genome to phenotype. It is

important to notice, that the complexity of the interaction in the system increases from bottom to the top. Until now it has been difficult to overview the phenotype as a whole and to produce digitized phenome data that could match the genome, transcriptome and proteome. This explains that phenomics not yet has gained the major headlines in scientific literature. But as shown in the following, this drawback can partly be overcome by spectroscopy. As the expression of genes is dependent on the life-stage of the tissue, the term *epigenesis* is used to describe the time-dependent expression of genes in developing tissue such as the endosperm.

It is generally accepted, that a change in a structural gene for e.g. an enzyme leads to a specific change in the corresponding enzyme activity. However, genes also affect other genes and traits, a phenomenon known as *pleiotropy*. This is to some extent described by examples in the plant breeding literature as well as cases where one gene is altering two or more phenotypic traits. *Epistasis* is the phenomenon where the alteration of one gene affects the expression of one other gene in a pair wise manner. As reported by (Munck, 2005), the Russian entomologist Sergei S. Chetverikov (1880-1959) had advanced thoughts about pleiotropy that now is relevant for the systems biology approach. He introduced the concept of the '*genetic milieu*' of a developing organism e.g. endosperm, in which *'the pleiotropic action of a gene will influence not only the specific character corresponding to it but generally speaking the entire soma'*, Hence, one can not consider the expression of one gene as an independent manifestation, but as an action on the whole genotype and related to the internal milieu in which the gene acts.

The phenotype is dependent on the expression of genes according to time and environment, and the expression of a gene-trait is dependent on the entire constitution of the genotype. Recent work has widened the definition of a gene from a structural unit embedded in the DNA influencing only one enzyme (Burian, 2004) to be supplemented by the secondary pleiotropic effects of a changed gene sequence e.g. by mutations. Also, a gene can give rise to more than one transcript by alternative splicing of the transcripts, or to equal transcripts but distinct proteins, and finally, to different transcripts leading to distinct proteins (Burian, 2004). It will in this thesis be demonstrated that both the internal cellular and external environments determine what proteins should be expressed from the genome in agreement with the statement of Chetverikov.

There are two major asexual ways of manipulating the genome: mutations and molecular genetic modification. Mutations are alterations in the base-pair constitution of the DNA. This can be either alteration to a single gene producing a different allele. An allele is another version of the same gene. In a diploid organism inclusion of two alleles are possible. If the alleles are the same, the individual is a *homozygote*. Due to self-pollination barley lines are

near-homozygotic for all genes. However, mutations can also be alterations to the structures and/or numbers of chromosomes and are often lethal. Point *mutations* can be spontaneous or introduced either by chemicals or radiation (X-rays, gamma-rays, neutrons and others) (Harten, 1998). Molecular genetic modification is the transfer of foreign genetic material or alteration of expression of existing genetic material in an asexual way of increasing gene variability and covers a range of techniques not further considered here. In mutational studies, single-gene mutations are introduced in *near-isogenic* lines. Isogenic lines are genotypes with almost 100% identical genomes except for the mutant gene. In self-pollinated plants such as barley, isogenic lines are easily obtained as no 'forreign' genetic material is introduced during pollination.

2.3.2 The 'high-lysine' barley endosperm mutants

Mutational work, whether introduced or spontaneous, has for more than a century played a role in developing agricultural plants with specific traits (Harten, 1998). In the 1960s, a spontaneous mutation in maize was found, which had elevated levels of the essential amino acids; lysine and tryptophan. This kick-started an intensive search of mutations also in barley collections for improved nutritional value (Harten, 1998). One of the results of these searches in barley collections was the discovery of the spontaneous high protein, high lysine barley mutant later known as Hiproly (Munck et al., 1970). The high-lysine character was found to be controlled by a single recessive gene termed *lys1* located on chromosome 7 (Karlsson, 1976).

The high-lysine mutants were identified as having very high dye-binding capacity in relation to nitrogen. The dye-binding method is a measurement of total basic amino acids (lysine, histidine and arginine) using acilane-orange (Mossberg, 1969; Munck et al., 1970). The x-y plot of dye-binding capacity to nitrogen content has since then proven to be useful for detecting even minor changes in the lysine content (Doll, 1983). Dye-binding screening for induced high-lysine mutants in barley at a large scale was initiated at Risø in 1969. Mutations were induced either chemically with EMS (ethyl methane sulphonate), EI (ethyleneimine) or by γ-rays. This screen revealed a number of high-lysine mutants. Two of these mutants were chosen as the basis for this study; the chemically induced mutants: Risø 1508 (*lys3a*) and Risø 13 (*lys5f*). Both were derived from the parent variety Bomi. Risø 1508 has according to the revised mutation a single, recessive mutation in gene locus *lys3a* located on chromosome 5 (Jacobsen et al., 2005), whereas Risø 13 has a mutation in a single, recessive gene locus *lys5f* located on chromosome 6 (Doll, 1983). Both mutants suffers from a reduced seed yield due to an impaired starch accumulation in the seeds (Doll, 1983). The two mutants, *lys5f* and *lys3a* have been used in all the studies founding the basis of this

thesis and in **PAPER A**, **PAPER B** and **PAPER C**. The gene-names will be used as descriptor for these mutants.

A NIR-based screening of the barley endosperm mutants, and their recombinants with normal barley varieties and normal parents were conducted 1998-2005 by Munck and co-workers (see (Munck et al., 2004) and (Munck, 2007), for review). An exploratory strategy was used where prior knowledge of the mutants was set aside in order to let the spectral NIR data reveal new independent information. The first publication on genotype specific spectra by Munck et al., (2001) surprisingly demonstrated that *lys3a* genotypes and normal genotypes could be differentiated as characteristic spectral patterns in both a field and a greenhouse environment. The patterns were physiochemically evaluated by correlations to chemical and proteomic analysis (Jacobsen et al., 2005). Genetics was mainly characterized by patterns and environment by spectral off-set. In a second publication by Munck et al., (2004), NIR spectra from 1100-2500 nm from twelve chemically defined and undefined high lysine mutants as well as sixteen normal barley varieties field- and greenhouse grown were classified as three distinct clusters in a PCA score plot, see **Figure 2-7**.

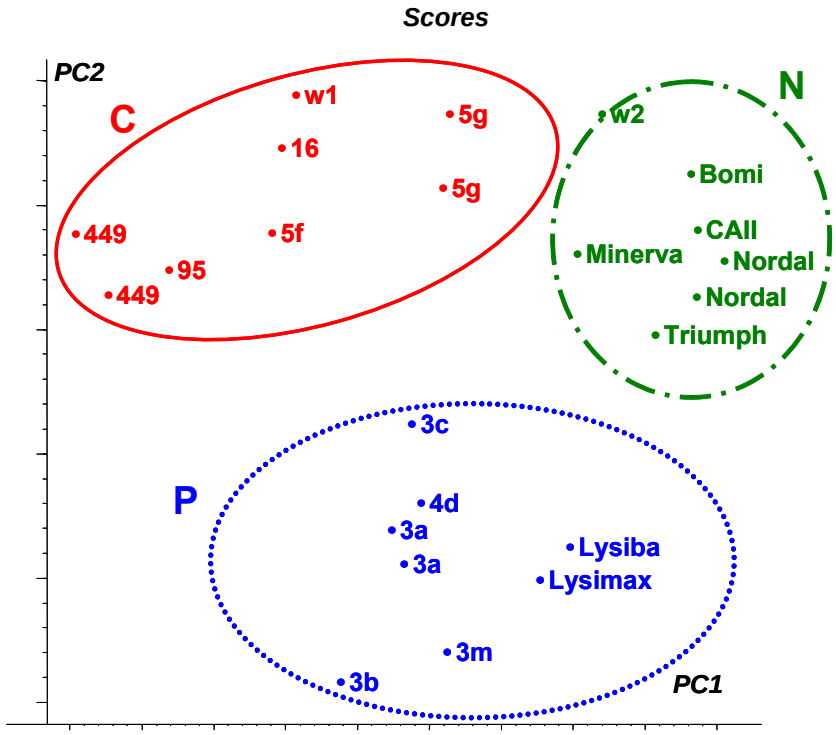

Figure 2-5 . A PCA on the 'high lysine mutants', some commercial barley varieties and some recombinants. Three clusters could be revealed. The red C-cluster contains the mutants with altered starch and β-glucan (BG) content of 12.3% compared to wildtype, the blue P cluster contains the protein mutants and commercial derivatives (BG content=3.7%). Finally, the green cluster N contains the commercial varieties with a BG content of 4.7%. From Munck, (2007).

These three clusters proved to be able to differentiate between commercial barley varieties, regulative protein-mutants with low content of β-glucan and drastically altered composition of proteins (lysine), and a well defined cluster of carbohydrate structural starch mutants with high levels of β-glucan, low content of starch and a smaller change in protein (lysine) content (Munck et al., 2004; Jacobsen et al., 2005). These groupings were later confirmed bu

spectral data inspections and chemical analysis (see **Table 2-2**). The *lys3a* gene is a regulator gene influencing a range of structural genes in other chromosomes (Munck et al., 2001). This is effected by a de-methylation process that inhibits the expression of genes of many proteins e.g. hordein in a yet unknown way. In contrast, *lys5f* is a structural gene affecting the transport of ADP-glc. The mutant *lys5f* is unable to transport ADP-glc across the plastid envelope (Patron et al., 2004). Because *lys5f* is a mutant for the transporter mechanism, more sucrose is channelled towards the β-glucan synthesis via the activated sugar UDP-glc, see **Figure 2-5**. *Lys5f* has a higher catalytic activity of UDP-glucose pyrophosphorylase (UGPase), AG-Pase and SS that are all catalyzing reversible processes (Rudi et al., 2006). The amylose content is not much affected in *lys5f* and an allelic form of *lys5*, *lys5g* are found to have normal levels of amylose (Tester et al., 1993) indicating that amylopectin levels are altered.

Lys3a has an equal dry weight per seed compared to the parent variety until 8 DAF, when starch synthesis commences but *lys3a* ends with lower final starch content than Bomi. This is also manifested in a double content of free sugars in *lys3a* endosperm (Doll, 1983) and a decreased number of the small type B-starch granules (Shewry et al., 1987) although they appear larger. The number of the large A-type starch granules per endosperm in *lys3a* is comparable to Bomi. The amylose level is close to normal but the total lipid-free amylose was well below Bomi (Tester et al., 1993). The *lys3a* has a harder seed than normal malting barley and a higher content of cellulose compared to normal barley (Jacobsen et al., 2005).

Although, *lys5f* and *lys3a* are introduced in the same genetic background of Bomi, and have only alterations in one single gene, they appear to have radically different phenomic expression (Munck, 2007). A comparison on the chemical composition of the two mutants and their parent variety Bomi are shown in **Table 2-2.**

Table 2-2. Comparison of chemical composition of two mutants and the parent variety Bomi. They were all green house grown. Modified from Jacobsen et al., (2005).

Mutant	β-glucan (%)	Starch (%)	β-glucan + Starch	Dry matter	Protein (%)	Lipids (%)	Lys (mol%)
Lys3a	3.2	51.0	51.8	90.1	14.4	3.4	5.1
Lys5f	17.8	30.0	50.5	91.8	16.0	3.7	3.6
Bomi	6.0	52.3	56.6	90.5	12.8	1.8	3.4

It is noteworthy, that *lys5f* has a triple amount of β-glucan compared to Bomi, whereas *lys3a* only has half the content compared to the parent variety. Interestingly, some alleles of *lys3* has normal levels of β-glucan suggesting that the high lysine content and low β-glucan content are controlled by adja-

cent genes (Munck et al., 2004). Another striking feature is the very low content of starch found in *lys5f* compared to the other to genotypes. Finally, an increase in the lipids is found for both mutants compared to Bomi (Jacobsen et al. 2005) due to an increase in triglycerides and polar lipids (Shewry et al., 1987).

3 Phenomic fingerprinting by spectroscopy and chemometrics

Historically, the cereal industry has been a frontier in the development of fast, spectroscopic analyses (Møller Jespersen and Munck, 2008). In this chapter, the theory of three spectroscopic methods used to follow the expression of the *lys5f* and *lys3a* mutant genes during epigenesis are described. An overview of spectroscopic methods is seen in **Figure 3-1**. The spectroscopic methods explore intrinsic features of molecules in various ways.

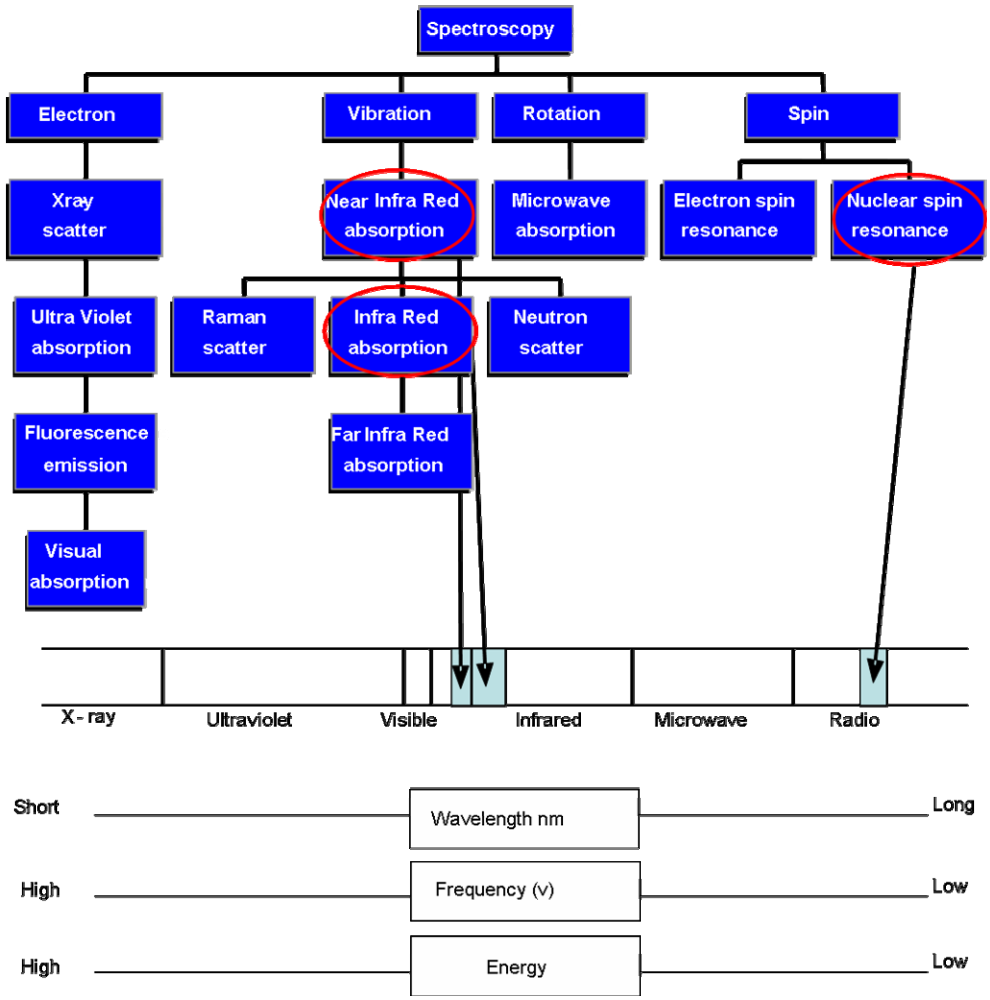

Figure 3-1. Overview of various molecular spectroscopy methods divided into electron, vibration, rotation and spin spectroscopy. The vibration and spin spectroscopy used in this thesis are marked with a circle. Modified from Engelsen (2006) and Pavia, (2000).

The three marked techniques: near-infrared (NIR), infrared (IR) and nuclear magnetic resonance (NMR) spectroscopy will be described in this and the following paragraphs as they are the fundament of the experimental work in chapter 4. The three selected methods all employ energy levels which are rather low and hence do not induce mutations or generates free radicals harmful to biological material, as the energy level is too low to break bonds in contrast to e.g. X-ray analysis. The NIR and the IR are vibrational spectroscopy methods, whereas NMR is a spin-spectroscopy. They are share a high sensitivity to protons and hence are valuable for studying biological material with a high content of water.

3.1 Near-InfraRed (NIR) and mid-InfraRed (IR) spectroscopy

The traditional way of analyzing cereals and their phenotypes relies on defined, destructive chemically analysis. In the 1960s, the use of NIR on milled wheat for prediction of protein and water was initiated by K. Norris (Williams and Norris, 1987). Since 1980s, NIR has established as a valuable analyzing method in pharmacology, agricultural industries and as an at/on-line quality control in the food and food ingredients industries (Zachariassen et al., 2005). In breeding NIR is used as a screening technique for uni-variate traits such as protein, malting quality (Osborne, 2006), baking quality (Dowell et al., 2006) and for multivariate quality traits where high quality and low quality cultivars can be used as references for variety selection (Møller Jespersen and Munck, 2008). Recently, NIR has gained attention as an *in vitro* method for feed quality e.g. determination of total dietary fibers in barley (Kays et al., 2005). As mentioned in the previous chapter, especially NIR has proven very useful in the investigation of barley mutants on the phenomic level.

NIR and IR spectroscopy measure the vibrations of molecular covalent bonds as absorbance of electromagnetic radiation corresponding to variation in the vibrational energy levels. As every specific bond has a different natural frequency of vibration depending on the environment in which it is present, each molecule has its own specific infrared spectrum. This can be used as a fingerprint for molecules. Hence, infrared spectroscopy can be used for classifications of substances by comparing fingerprints. Moreover, structural information about molecules can be obtained from infrared spectra as specific bonds e.g. N-H, have specific absorptions. For water the vibrational motions present are symmetric stretching, asymmetric stretching and bending, as seen from **Figure 3-2**.

The IR region is between 4000-200 cm^{-1} (2500-50000 nm). The IR region contains chemical information from fundamental vibration bands. Stretching

and bending are the two most common infrared active modes of vibrational motion found in IR. The absorption frequency in the IR spectrum is determined by the masses of atoms present, the bond strength and the type of molecular vibrations (stretching, bending, rocking, wagging and twisting). In IR, fundamental bands of C-H, O-H, N-H, C-O and C=O stretching bands are dominating.

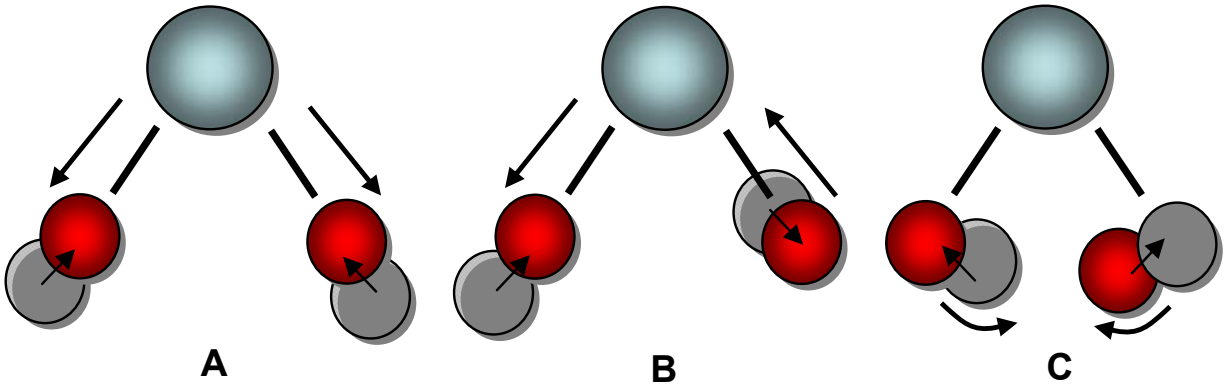

Figure 3-2. Schematic representation of the vibrational modes of water. Symmetric stretching (A), asymmetric stretching (B) and bending (C).

In NIR spectroscopy, the first, second and third overtones and the combination tones of the fundamental IR vibration bands are present almost as a hologram of the IR spectra. The overtones of O-H, C-H and N-H found in the NIR spectra of wheat flour is a mirror of the corresponding fundamental stretching vibrations found in the IR spectra, see **Figure 3-3**.

The NIR region is between 14300-4000 cm^{-1} (780 - 2500 nm). The NIR spectra show mainly absorption due to anharmonic bonds primarily bonds to hydrogen. The first and second overtones are found as bands between 800 and 1800 nm whereas the part from 1900-2500 nm covers the combination overtones, see **Figure 3-3**. Information is abundant in NIR spectra, but the peaks are broad and often overlapping hindering structural analysis.

A NIR or IR spectrum can be analyzed in terms of intensity, frequency position and form. The intensity and exact frequency position is dependent on the variation in dipole moments, which in turns is related to the functional group. The broad bands of even simple molecules observed in NIR is due to partly overlapping over-and combination tones as well as differences in local molecular environment i.e. non-bonded interactions in particular in hydrogen bonds. A thorough introduction to the theory on NIR can be found in Williams and Norris (1987).

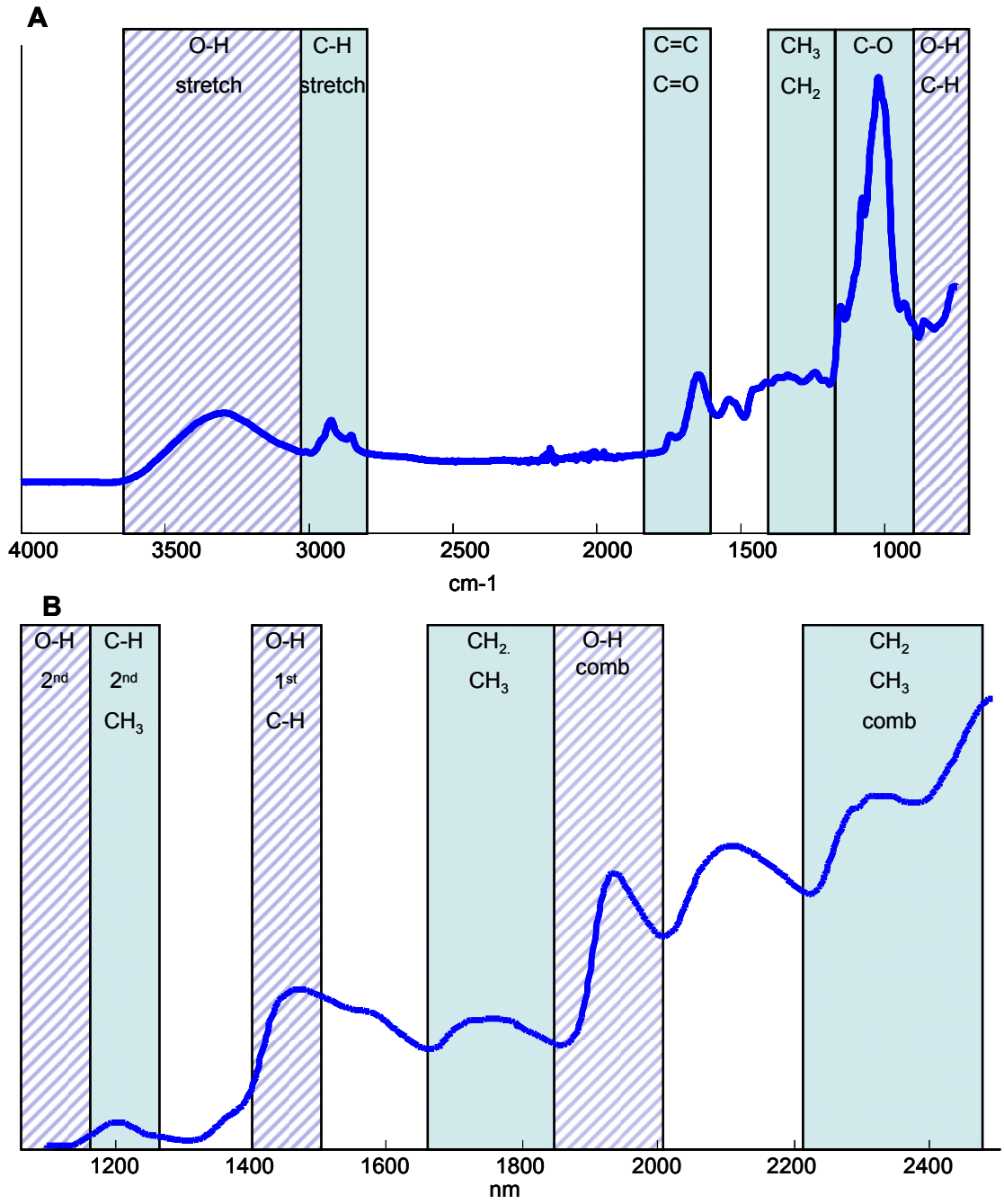

Figure 3-3. Selected absorption regions in an average barley flour spectrum. IR flour spectrum (A), The corresponding, hologramme NIR flour spectrum (B). Stretch= stretching. Comb= combination bands. 1st and 2nd refers to the first and second overtones of the fundamental vibrations. Hatched bars are water related regions. Modified from Tønning (2007).

According to Lambert-Beers law, the absorbance (A) is dependent on the absorption coefficient (α), the path length of light through a sample (l) and the concentration of the absorbing analyte (c), **Equation 1**:

$$A = \alpha * l * c \qquad (1)$$

Dispersive NIR and IR spectrometers are instruments based on the splitting of the light beam by either a prism or more common by grating. Such instruments produce spectra in the *frequency-domain*, thus the spectrum is a plot of intensity versus frequency. More modern infrared spectrometers produce an *interferogram* by employing the interference arising from the splitting of a wave. The interferogram is a plot of intensity versus time (Pavia et al., 2000). The interferogram is then Fourier transformed. *Fourier Transformation* (FT) (Griffiths and de Haseth, 1986) is a mathematical operation resulting in a plot of intensity versus frequency such as obtained from dispersive systems. FT systems have facilitated better wavelength accuracy and higher throughput than dispersive systems (Sohn et al., 2004) with a spectrum recorded in less a second.

NIR and IR can be obtained in *reflectance- or transmission* mode. NIR obtained in transmission spectroscopy mode is referred to as NIT and has been commonly used in cereal seed research and development and can be performed on seeds as well as ground material as the light can pas through the sample. NIR reflectance, on the other hand, is often recorded on ground seeds in order to obtain reflection from a relatively smooth and homogeneous surface (Kays et al., 2005). IR transmission requires special sampling, as the sample must be presented as a very thin film in the order of micrometers for the light to pass through. Hence, samples are ground with an adhesive material often the compound nujol that is a mineral oil, which is largely IR transparent or more commonly diluted in the IR transparent salt: KBr.

IR can more conveniently be used in the reflectance mode using the *attenuated total reflection* (ATR) involving the acquisition of radiation reflected from the interface between the material and a crystal. This facilitates sampling of grounded material such as flour. ATR-IR is simple, direct, flexible and a sensitive method. Diamond ATR can be used for solids, pastes and liquids. In **PAPER A**, FT-IR with ATR sampling and NIR in the reflectance mode have been applied to study barley flour during seed development. In this study NIR refers to NIR reflectance and IR to FT-IR using ATR-sampling.

3.2 Nuclear Magnetic Resonance (NMR) basics

Nuclear Magnetic Resonance (NMR) covers a family of versatile analytical techniques used in vivo, in vitro, on liquids, cell extracts, solids, semi-solids and plant material e.g. rootlets (Ratcliffe, 1996). Here just an introduction to the NMR theory will be presented. A thorough introduction to the theory of NMR applied to plant biology can be found in the literature (Kockenberger, 2001b; Ratcliffe, 1994; Ratcliffe, 1996); a similar introduction to NMR imaging have been given by (Ishida et al., 2000). A basic, physical introduction to NMR is given by (Hore, 2001).

Some nuclei with an odd atomic mass and/or atomic number possess an angular momentum and this in combination with the nuclei charge lead to a magnetic moment conceptually understood as a bar magnet spinning around its own axis (**Figure 3-4**). Hereafter, such a magnetic, nuclear spin is simply referred to as '*spin*'. The major biologically important isotopes with spins are ^{1}H, ^{13}C, ^{31}P, ^{17}O, and ^{15}N.

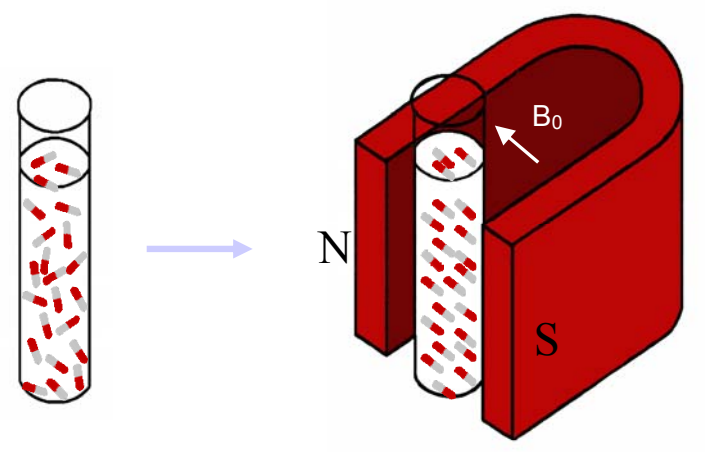

Figure 3-3. Theory of nuclei possessing a nuclear spin and their behaviour in an external magnetic field. The nuclear spins are represented by small bar magnets.

When exposed to an external, strong magnetic field, the internal bar magnets will become aligned to the external magnetic field, in a new thermal equilibrium where a majority of the spins align parallel to the external magnetic field, whereas the rest align anti parallel. There is an energy difference between the two spin states (parallel/anti parallel), where the energy difference depend on the strength of the external magnetic field. This leads to a weak net magnetization that can be manipulated by a radio-frequency pulse to obtain a signal. The net magnetization can be represented by a vector. The vector rotates in the longitudinal plane by the Larmor frequency (ω) proportional to the magnetic field acting on the nuclei ($\mathbf{B_o}$), **Equation 2**. The gyromagnetic constant (γ) is unique for each nucleus.

$$\omega = \gamma * \mathbf{B_o} \qquad \textbf{(2)}$$

In pulse NMR (as in contrast to continuous wave NMR that are not considered here), a short (µsec) radio frequency (RF) pulse of energy is applied to manipulate the system. When exactly on resonance with the Larmor frequency, the net magnetization will be shifted and rotate in the transverse plane, where it can be measured like the principle of a bike dynamo; a magnet precessing in a coil will induce a current, which can be detected as a signal. The excited spins starts to lose their excitation energy and return to their equilibrium state – they are said to relax and this is observed as a decay of the signal, called the *free-induction decay* (FID), **Figure 3-5**. The decay of the signal is dependent on the relaxation processes. Two types of relaxation occur: 1) The *spin-spin or transverse relaxation* (T_2), in which the spin system will begin to loose coherence in the transverse plane, leading to a decay of the signal. The spin-spin relaxation can be determined indirectly

using techniques like the Carr-Purcell-Meiboom-Gill (CPMG) pulse sequence (Carr and Purcell, 1954; Meiboom and Gill, 1958), which enhances the signal by creating echoes. 2) The *spin-lattice or longitudinal relaxation* (T_1) is the return of the magnetization to equilibrium along axis of the magnetic field. This can be determined either by Inversion recovery or saturation experiments. The use of the spin-spin relaxation time (T_2) was used in **PAPER C**.

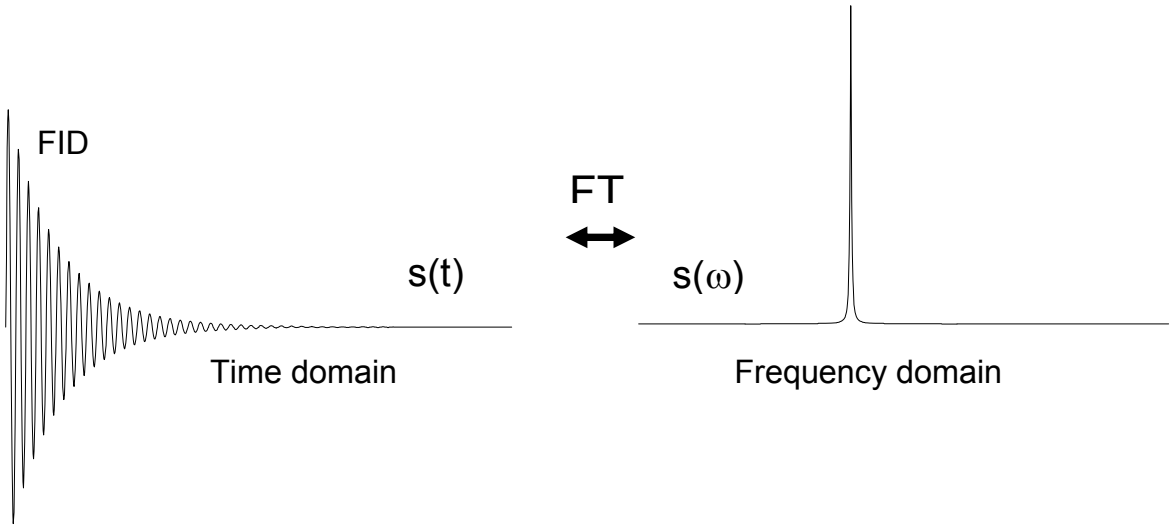

Figure 3-5. The free induction decay (FID) and the Fourier transformation (FT) reversible giving either a frequency related spectrum or a time-related spectrum.

The FID is acquired in the time-domain and directly from the FID physical information can be extracted such as the density of protons to the time zero before the relaxation occurs. Hence, information about water distribution can be extracted giving physio-chemical information such as the compartmentalization of the tissue including the size, the chemical composition of the compartments, the possible exchange of water between the compartments and determination of molecular mobility (Ratcliffe, 1994).

The water status of mobile and less mobile water molecules can be distinguished by the different relaxation rates (Ratcliffe, 1994; Ridenour et al., 1996; Krishnan et al., 2004b). The multi-exponential nature of the T_2 relaxation curves is by consensus interpreted in terms of different types of pools of water; structural water, free water or the mobility of water. In general, NMR studies on hydrated seeds suggest that long (> 10 ms) relaxation values are typical of unbound water and characterize the external- or mobile water pool whereas water with hindered mobility is characterized by shorter relaxation time constants. Water with short T_2 relaxation time constants (μs-ms) is usually associated with macromolecules or solids (Brosio et al., 1992; Ridenour et al., 1996; Krishnan et al., 2004b). However, the interpretation of NMR properties of water in compartmented systems is not always straight forward and should be done with caution (Ratcliffe, 1994). A bi-exponential fitting was used in **PAPER C**.

In order to get chemical information from the FID, a Fourier transformation (FT) is needed to obtain well resolved signals in the frequency domain. A frequency dependent spectrum can be analyzed with regard to (Ratcliffe, 1994):

- *Intensity*: related to the content of metabolites containing the spin producing the signal. The intensity is often proportional to concentration (Viereck et al., 2006). However, intensity is affected by the spin density, relaxation times and the molecular self-diffusion coefficient of mobile compounds in the tissue and thus not always directly proportional to the concentration (Horigane et al., 2001)

- *Frequency*: related to the identity of the magnetic nucleus, the strength of the magnetic field and the chemical environment of the nucleus. The small differences in frequency are measured in *parts per million* (ppm) relative to a standard, giving rise to the chemical shift. Thus, the *chemical shift* value is independent of the strength of the magnetic field. To correlate chemical shift values with values from databases it requires accurate calibration of sample temperature, solvent and pH (Leeflang et al., 2000)

- *Line shape and widths*: line broadening is depended on rigidity of the sample, uniformity of the magnetic field or material, interactions with paramagnetic ions or air bubbles, reduced molecular mobility and exchange effects. Line shape is a result of interactions between neighbouring chemical bonds (coupling interactions)

- *Relaxation times*: See above

It is possible to assign the compounds in a sample by analyzing the NMR spectrum as described above. For the assignment of heterogeneous compounds, a one-dimensional (1D) spectrum can be too rough with many overlapping signals (Fan, 1996) requiring two-dimensional NMR (2D NMR) allowing determination of molecular positions of the spins. 2D spectra are contour intensity plots as a function of frequency. There are two types of 2D experiments: The homonuclear 2D spectra are symmetrical about the diagonal with the same spin on both axes. The second type is heteronuclear spectra that are asymmetrical because the second dimension represents the chemical shift scale of a different nucleus (usually ^{13}C, ^{15}N or ^{31}P). Homo- and heteronuclear 2D NMR was used in **PAPER B**.

Solid samples have a fast decaying signal compared to liquids due to fast relaxation (μs), since the movement of the various nuclei are restricted. This is leading to very broad resonances in a FT-spectrum, in the order of kHz.

To overcome these broad resonance, spinning the samples at 54.7^{o} (the 'magic angle') with regard to the external magnetic field will average out the dipolar interactions and the susceptibility to the magnetic. This technique is known as *magic angle spinning* (MAS), **PAPER B**. A MAS acquired spectrum of a solid sample is very similar in resolution to a liquid spectrum. However, when MAS is used on living systems, care must be taken when choosing spinning rates. Spinning rates of more than 2 kHz were found to destroy germinated barley seeds (Ridenour et al., 1996). However, dry cereal seeds can withstand much higher spinning rates, probably up to 5 kHz (Ridenour et al., 1996). Another method to study solids is *^{13}C cross-polarization* (CP) MAS NMR, in which a transfer of polarization from the abundant protons to the less abundant spins such as ^{13}C and back to the protons is made (Pines et al., 1972).

3.2.1 Magnetic resonance imaging (MRI)

The Noble prize in physiology and medicine were in 2003 jointly-given to Sir Peter Mansfield and Sir Paul Lauterbur for their invention of Magnetic resonance imaging (MRI) (Lauterbur, 1973; Grannell and Mansfield, 1975). MRI obtains images non-destructively by measuring the physical conditions of a nuclear spin in a defined small picture element (*pixel*) by applying a linear magnetic gradient across the sample (Ishida et al., 2000), see **Figure 3-6**. As with NMR, a radio frequency pulse is applied to excite the system. The magnetic field gradient is superimposed on the main external magnetic field resulting in local magnetic fields giving rise to spatially encoded frequencies. Using the Fourier transformation a one-dimensional projection of the sample is obtained. For each pixel, a signal is obtained which can be analyzed equally as the NMR spectra. The spatial resolution of MRI can be from 10 µm to a few hundred µm (Kockenberger, 2001a) enabling anatomical and morphological studies of plants on a cellular level (Ishida et al., 2000). The resolution is dependent on the pixel element dimensions. In general, a pixel element has the volume size of 1/1000 compared to high resolution NMR. Therefore, only spins with very high sensitivity in NMR area can be used in MRI. Hence, most MRI maps protons in water, oils and soluble carbohydrates in biological tissues (Ishida et al., 2000). There exists a relationship between the spatial resolution, the time required for acquisition and the detection sensitivity such that an enhanced spatial resolution requires longer acquisition times (Kockenberger, 2001a).

The conventional use of MRI of biological material is measured by spin-echo 2D-FT method, in order to overcome the obstacles of heterogeneous material (Callaghan, 1991). In optical microscopy, contrast is generated by reflection in light, but in MRI contrast is generated by the concentration of spins and the relaxation processes. The images can be either T_1 or T_2-weighted. The latter emphasises regions with high water mobility, and the former low-

mobility water areas (Ishida et al., 2000). These methods are very useful for the determination of water status in cells or defined tissues and hence determination of metabolism, as metabolism is dependent on water activity. T_2 weighted images were used in **PAPER C**.

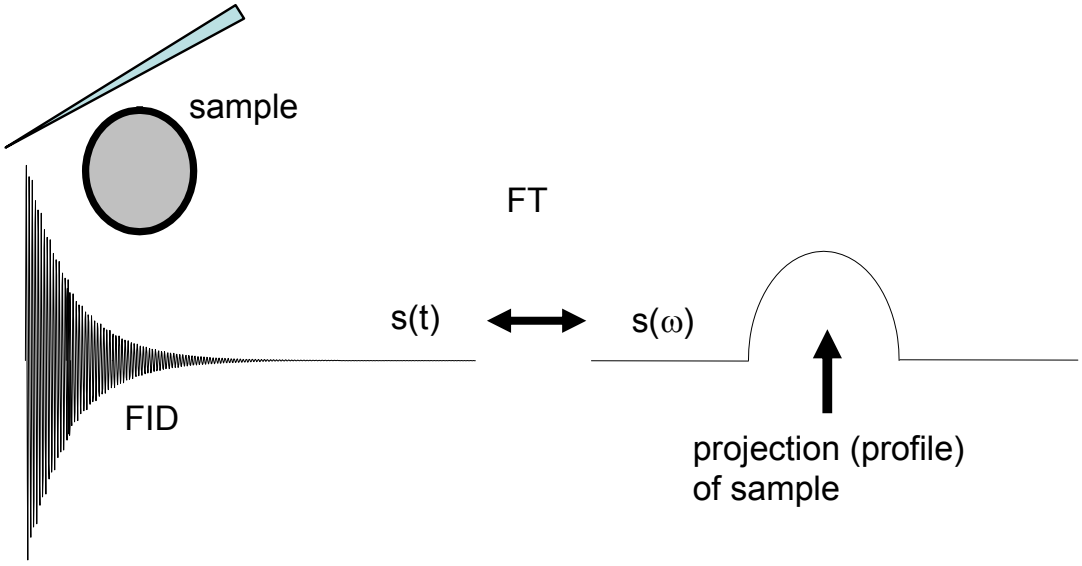

Figure 3-4. The principle of MRI. A magnetic gradient is placed across the sample in both the x,y and z direction. This induces changes in the local magnetic field, that can be resolved as a spatial dependent signal. FID= Free induction decay. FT= Fourier Transformation. Blue triangle= Magnetic gradient. Modified from Köckenberger (2004).

MRI can be used quantitatively if reference solutions of the metabolites of interest are included in the experiment (Kockenberger, 2001b). Besides the spin-echo 2D-FT MRI, specialized methods such as *chemical shift imaging* of metabolites (tuning to a metabolite frequency), *spectroscopic imaging* generating full spectrum from each pixel (3D: two spatial and one spectra dimension), *correlation peak imaging* (4D: two spatial and two spectral dimensions), imaging of diffusion measured by NMR as a self-diffusion coefficient using a gradient and fast imaging methods have been employed in plant biology (Kockenberger, 2001b; Ishida et al., 2000) but will not be described here. Contrast-agents such as paramagnetic metal ions, the use of stable isotope tracers such as ^{13}C-labelled metabolites can be used in MRI for manipulation of the signals, but is also not considered here.

3.3 Comparison of the spectroscopic methods

The comparison of the spectroscopic methods presented here is mainly based on the experiences from the work presented in **PAPER A**, **B** and **C.** The most obvious and important requirement of the three spectroscopic

methods is the lack of laborious sample preparation, lack of use of chemicals, the rapid measurements and the minute need of sample size. In NIR and IR, the raw material as is, is analyzed using a minimum of time and equally important, the material can be used for other analyses. NMR is slightly more tedious, as the sample must be placed carefully in the rotor, and a NMR-insensitive solvent and an internal chemically reference must be added often rendering the sample useless for other analysis. Another important feature of the methods, are that they all provide complex fingerprints of metabolic or genetic origin and they give physio-chemical information about the sample. They all share the ability to provide multivariate data giving the possibility to acquire information on more quality attributes simultaneously.

In the case of NIR and IR handling of the apparatus is easy and do not require specialized skills. In contrast, NMR experiments require skilled personal for proper pulse sequence selection, tuning to the spin, shimming of the magnet and definition of the experimental conditions. Sample presentation is an issue common for all of the three methods, as improper presentation can induce artifacts in the spectra. In NMR, especially, the introduction of air bubbles leads to magnetic distortion (Kockenberger, 2001b). The sample size used for ground grain in NIR spectroscopy typically requires 5-30 g, although micro cups are available for less than 1 g (Osborne, 2006). The smallest possible sample for seeds are a single seed and single-kernel NIR (SK-NIR), (Osborne, 2006; Tønning et al., 2007) and single-seed NIT (Delwiche, 1995; Pedersen et al., 2002) has been widely used. Sample size for ATR-FT-IR was minute, as it only has to cover the diamond (2 mm). Analyzing grinded samples such as flour requires careful sample presentation in order to get a representative spectrum. Hence, the sample cup used in NIR should be packed densely and without air bubbles. In the case of ATR-FT-IR, the sample should homogeneously cover the diamond.

In analyzing solid and semi-solid samples such as seeds and flour, NMR has a clear theoretical advantage to IR and NIR, as it acquires signal from the entire sample, whereas in NIR and IR the light must be able to penetrate the sample. Working with flour and small sample sizes such as grains this is not a problem for either of the methods. In the case of analyzing cereal seeds IR is not an option, as the weak IR radiation can only penetrate less than 0.1 mm. NIR gives a more effective sample penetration by the light at shorter wave-lengths compared to IR. However, IR has a more straight forward relationship between peaks and chemical bonds making it a good choice for structural analysis (Kacurakova and Wilson, 2001). Although, the NIR spectra is influenced by a range of physical and chemical phenomena such as particle size and hardness, and pH (Williams, 2001) the NIR spectra are of extraordinary high reproducibility (Møller Jespersen and Munck, 2008).

As all of the three methods in this study have in common high sensitivity to X-H bonds which in turns implies that the methods are valuable in determining water and water states. Water is not only of interest, it can also dominate the spectra making it difficult to distinguish other bands or peaks. For complex, heterogeneous biological material such as cereal seeds and flour, the NMR spectra can be rather 'crowded' due to the superposition of resonances leading to difficulties in assigning the spectra to chemical compounds. NIR, IR and NMR spectra are influenced by pH and temperature and for NIR and IR they are also influenced by the relative humidity of the samples. The spatially encoded signals from MRI enable visual determination of spatial distribution of water. Furthermore, it can be used for temporal studies elucidating development of a sample under a given condition.

The infra-red methods are both high-through-put: NIR and IR spectra are obtained within seconds for each scan. In all the methods mentioned, acquisition time influences the signal to noise ratio, but it is mainly in NMR, acquisition time is an issue and depending on the type of NMR experiment a sampling time can be everything from a few minutes to days. Where the IR and NIR instrumentation is fairly cheap to buy and run, super-conducting magnets needed for structural and metabolic/phenomic NMR analysis are very expensive. Furthermore, the running costs of the NMR magnet are high due to the need of helium and liquid nitrogen.

The production of cereal based products whether being used for human consumption, feed or highly processed cereal products calls for optimized, high-quality raw material but also for procedures to control the final output. The spectroscopic methods and especially NIR is currently used as an in- and online process analytical tool (Zachariassen et al., 2005). Attempts are being made to incorporate NMR in the process line as well, but the challenges are to keep a homogeneous magnetic field and optimal shimming for a flow of samples.

3.4 Chemometrics

The classification or calibration of spectroscopic data such as NIR that generates thousands of collinear wavelengths, can not be handled sufficiently by conventional, uni-variate statistical methods (Munck and Møller, 2005). *Chemometrics* can be defined as the use of multivariate data analysis on chemical data (Martens and Martens, 2001) designed to extract maximum chemical information from the data. This information is found as latent structures in the data. Chemometrics involve a data reduction step and a visual representation of data which enables pattern recognition. Furthermore, chemometrics in combination with spectroscopic screening methods is an inductive, hypothesis generating method not requiring specific assumptions

other than what is generated by the data as patterns (Munck et al., 1998) and that after measurements can be validated prior to knowledge. Chemometrics can be used to overview large spectral data sets and points to 'regions of interest' in the spectra that should be finally evaluated by spectral evaluation. Chemometrics reduces the laborious and tedious work of assigning every peak in a metabolite profiling NMR spectrum by identifying key metabolites, which can then be selected for further assignment.

3.4.1 Pre-processing of spectral data

Spectral data can be pre-processed to eliminate or reduce the systematic variation introduced by scatter effects, chemical interferences or variation due to the apparatus. Scatter reduction optimizes the following chemometric analysis. When applying NIR and IR spectroscopy to flour it is normally necessary to take into account the scatter effect. It is important to separate the physical effect due to seed hardness/particle size from the chemical effect when evaluating NIR spectra (Osborne et al., 1993). Scatter variation is due to particle size and shape, sample packing and sample surface. There are various methods for scatter-correction (Martens et al., 2003). In **PAPER A** the EISC (*extended inverted signal correction*) method for spectral data (Pedersen et al., 2002) was used (**Equation 3**):

(3) $$\textbf{Corrected spectra } z_i = a_i + b_i z_i + c_i z_i^2 + d_i \lambda + e_i \lambda^2$$

Where a is the additive off-set, b_i is the multiplicative slope, c_i is a quadratative factor, d_i and e_i are wavelength dependent factors, and λ is a wavelength vector. EISC separates chemical light absorbance from physical light-scattering. EISC was found to give better calibration models of wheat seeds and protein content measured by Near Infrared Transmittance (NIT) spectroscopy than models based on raw data, second derivatives, *multiplicative signal correction* (MSC) and MSC with subsequent second derivative (Pedersen et al., 2002). In **PAPER A**, NIR and IR spectra were EISC corrected before chemometric analyses.

In NMR, spectra small shifts can be introduced by e.g. pH or temperature differences (Viereck et al., 2006). These artifacts shifts can in some cases be effectively removed using co-shifting or *correlation optimized warping* (COW) (Tomasi et al., 2004). Warping or co-shifting was employed on the NMR data to align resonances in order to improve PCA classification. All NMR spectra were manually phase-and baseline corrected as well as shifted according to the internal reference or for sub-regions to the resonances of interest.

3.4.2 Principal Component Analysis (PCA)

Principal component analysis (PCA) (Hotelling, 1957; Wold et al., 1987) decomposes the data matrix X in to a structural part leaving only a residual that can not be described by the model, according to **Equation 4**:

$$\mathbf{X = T * P^T + E} \qquad \textbf{(4)}$$

The structural part can be described by some underlying latent structures known as *loadings* (P), which each has a weight termed *scores* (T). The data matrix X has the dimensions of the number of objects and the numbers of variables. PCA is an unsupervised method for reducing the number of dimensions in a dataset by defining new sets of orthogonal variables spanning the maximum variance. The first *principal component* (PC) describes the largest variation and is extracted first; the second largest variation is the second PC and so forth. In the new space spanned by PC1 and PC2, the objects get new coordinates according to their location relative to PC1 and PC2.

For spectral data, the data reduction can be exemplified as on **Figure 3-7**. The spectra of each object is subtracted the average spectrum in order to centre the data. The first loading plot explains the majority of the variance in data and is equal for each of the objects. The differences between the objects are the weight of the first loading. That is the value of the scores seen as the number in front each loading in **Figure 3-7**.

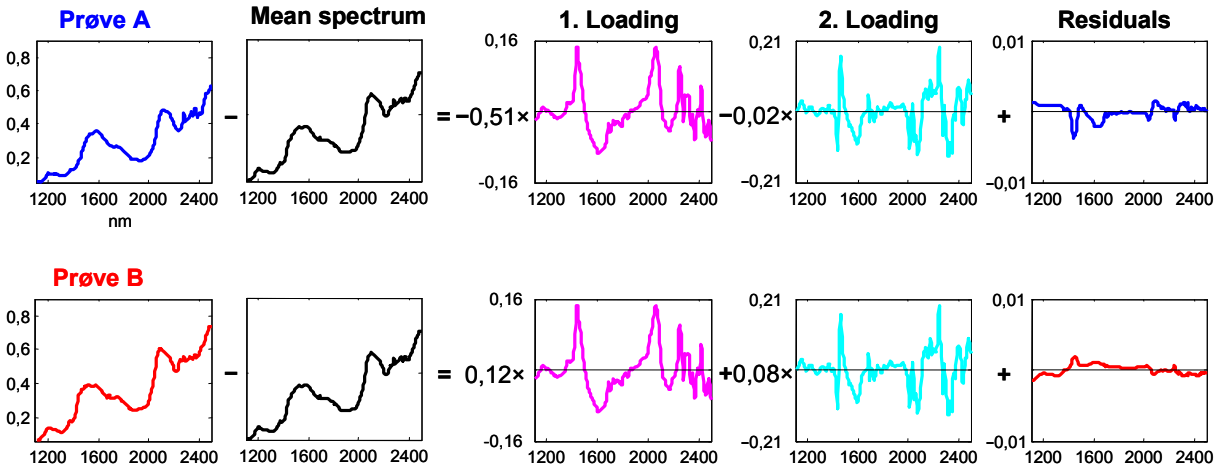

Figure 3-7. The principle of a PCA applied to NIR data. The spectral data of two samples are shown together with the mean spectra which are deducted from the sample spectra. This gives rise to a sample specific score value for each of the loadings. Modified from Engelsen and Nørgaard (1996).

The powerful *score-plot* is the display of score-values along the first and second PC. The *loading-plot* reveals the relation between the original variables and the principal components. Hence, the loading-plot is a map of 'im-

portance of the variables' in describing the variance in the data. Loading plots allow the identification of influencing variables or spectral regions visually. The reduction of dimensions in data by a PCA facilitates handling of large, multivariate datasets and is very valuable for classification, detection of clusters and outliers and for inspection of large data sets. PCA score plot was used for classification and PCA loading plots identified spectral variables influencing the PCA, **PAPERS A-C**.

3.4.3 Partial Least Squares Regression (PLS)

Partial least squares (PLS) regression (Wold et al., 1983, Martens and Næs, 1989) is often used to correlate spectroscopic data (X) with related chemical data (y). In contrast to the unsupervised decomposition of data in PCA, PLS decomposes the data matrix X (see **Equation 5**) into scores and loadings like in a PCA. However, in contrast to PCA, the identification of scores is dependent on the data (y).

(5) $$y=Xb+E$$

y is the measured reference values. X is the data matrix and E is the model error part.

An extension to PLS, is the *interval PLS* (iPLS) (Nørgaard et al., 2000) in which the variables are divided into sub-intervals of equal size and PLS is then carried out in each interval for identifying sub-models predicting better than the global model (from the entire variable dataset). A golden rule of thumb is that one PLS component needs eight samples. PLS and iPLS are used in **PAPER A**+**B**.

When making calibrations it is crucial to validate the models, either with cross-validation or preferably with an independent test set. *Cross validation* is used when the number of samples in a data set is limited and all samples are needed for the calibration. Cross validation is carried out by taking one sample (full cross validation) or a defined sub-sample out (cross validation with segments) and predicting the sample(s) with a model made on the rest of the dataset. Full cross validation or cross validation with segments have been used due to inadequate sample number for test set analysis (**PAPER A** and **B**).

The evaluation of the performance of a calibration model is measured by its prediction error; the *root mean squared error of cross validation* (RMSECV). RMSECV is based on the calibration data only. RMSECV was used in **PAPER A** and **PAPER B**.

3.4.4 Chemical reference analysis

The methods for analyzing β-glucan vary with the scope of investigation: cell wall structure and timing of synthesis such as nutritional analysis of fibres, malting quality. Quantification of high-molecular β-glucan is either based on enzymatic analysis or fluorimetry (McCleary and Glennieholmes, 1985; Munck et al., 1989). The enzymatic methods uses lichenase that is an endo-β-(1→3),(1→4)-D-glucan-β-glucan glucanase (EC 3.2.1.73) (McCleary and Mugford, 1997), specifically cleaving β-(1→4) linkage just after β-(1→3) from the non-reducing end (Yoo et al., 2007). The released glucose is determined using glucose oxidase/peroxidise assay. The problem using an enzymatic kit for β-glucan determination is precipitation due to long linear β-(1→4)-linked region, which has a low solubility (Yoo et al., 2007). This can cause underestimation of β-glucan in samples with low β-glucan content. The stilbene derivative Calcoflour is a fluorochrome forming complexes with high molecular weight (>10^4) β-glucan (Munck et al., 1989). After complexing, the intensity of the Calcoflour can be determined. This can be used histochemically in grain parts or as quantification of β-glucan in flour, wort or beer (Aastrup and Erdal, 1980). The Calcoflour dye is unstable due to photo decomposition and thus measurement should be performed in closed systems (Munck et al., 1989). Using the Calcoflour method the content of β-glucan in *lys5f, lys3a* and Cork was determined (**PAPER A** and **PAPER B)**. However, in *lys5f*, the Calcoflour values for the last four harvests deviated through development, and hence the enzymatic test was made as control and it confirmed the extreme level of β-glucan in *lys5f*.

In cereals, mainly enzymatic procedures are used for starch quantification where starch is being hydrolyzed followed by the measurement of the products (McCleary et al., 1994). It has been difficult to determine the total starch due to extraction problems and specificity of the detection methods (MacGregor and Fincher, 1993) leading to a residual fraction containing 'resistant' starch. Introducing a second hydrolysis step has circumvented the problem (McCleary et al., 1994). When measuring starch from flour it is important to 'wash' the flour with ethanol to ensure that only glucose originating from starch to be measured (**PAPER A**). The hydrolysis of the starch was in **PAPER A** measured as the production of NADH during glucose oxidation and compared to a glucose standard. When determining the content of starch it is important to ensure that the method is set up to handle the high content of starch found in seeds. In a preliminary study of starch content in the three mutants, a modified experimental procedure developed for leaf starch resulted in useless results mainly due to a high gelatinization of the starch. Due to lack of experimental material, the starch analysis were only performed on one sample for each of the three genotypes and for the eight temporal stages giving 24 samples, analyzed in triplicates.

Determination of the amylose content was performed by analysis of an iodine-binding complex of solubilised starch (Bay-Smidt et al., 1999). However, this only provides the apparent amylose content as amylose is also present in complexes with lipids these are not identified by this method (Wesley et al., 2003). Furthermore, this method cannot distinguish between the linear α-(1→4)-glucan in amylose and long linear chains in amylopectin (Delwiche et al., 1995). In **PAPER A**, the iodine-complexing method was employed on extracted starch despite the problems involved.

4 Bulk glucan synthesis in developing barley endosperm mutants

In this section the results from the experimental work of the study will be presented and discussed in context with the appropriate literature.

4.1 The effect of drought on seed carbohydrates

As described in 2.2, extreme environmental conditions influence the plant growth, the seed development and the composition of the carbohydrates in the seed. Water or drought stress is one of the most important limiting factors on crop yield world-wide (Chaves et al., 2003), (see section 2.2) and it is becoming increasingly important due to the current climate-changes (IPCC, 2007). To optimize agricultural practice, breeding strategies and crop product stability the effect of drought periods on cereals are important to understand. In order to elucidate the effect of a drought period on the seed bulk carbohydrate composition, three barley genotypes with varying content of β-glucan were exposed to drought, starting at flowering and lasting two weeks. The hypothesis was that depending on the seed carbohydrate composition, in this case the ratio between starch and β-glucan, the seeds would be affected by drought in different ways.

4.1.1 Semi-field experimental setup

In 2005, a semi-field pot-experiment was set up at Research Centre Flakkebjerg, University of Aarhus. The experimental set-up is seen from **Figure 4-1**. Three barley accessions differing in β-glucan content were used: the regulatory mutant *lys3a*, the structural *lys5f* mutant and the conventional malt barley Cork as a control variety. The control variety is comparable to the parent variety Bomi of the mutants. Commercial barley varieties such as Cork and Bomi are much less variable with regard to their chemical composition as compared to their mutant endosperm genotypes (Munck, 2008). All three genotypes were sown in 10L pots and placed in a semi-field area. After thinning three plants remained in the pots until maturity. The two spikes were harvested from the first and second tiller as determined visually.

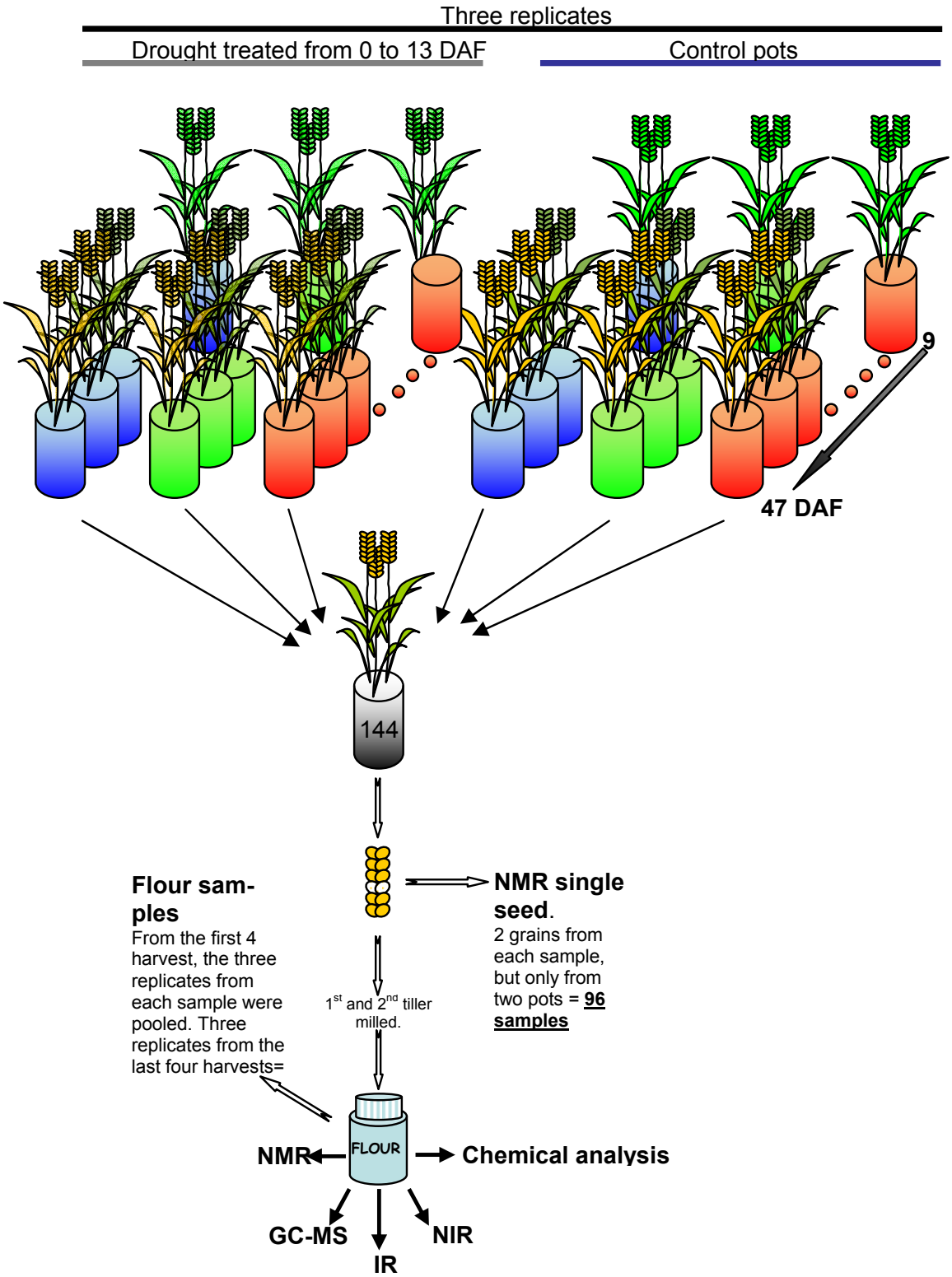

Figure 4-1. The experimental set-up of the semi-field experiment. The three genotypes are indicated by colored: blue = *lys3a*, green= control variety Cork and red= *lys5f*. Eight harvests were made from 9 DAF until 47 DAF for both control and drought treated pots and in three replicates giving a total of 144 pots. From each pot (indicated with grey and containing three plants) two spikes from the main tillers were cut, weighted and freezed and the two mid-seeds were kept for NMR analysis. The rest of the sample was grounded to flour.

Seeds on each spike were counted and weighted. On average, each spike contained 23 seeds. For each spike harvested the two mid-seeds were removed, freezed and stored for ^{1}H HR MAS NMR single seed analysis, while the rest of the seeds from the spike were freeze-dried and ground. The flour was used for all the chemical quantifications, as well as NIR, IR and ^{1}H HR MAS NMR. To obtain enough flour from the first four harvests, three replicates were pooled. Harvests were done on 9, 13, 16, 20, 23, 26, 39 and 47 DAF. At 9 DAF, the seeds were small, green, very moist and mainly consisting of husk. Between 23 and 30 DAF the seeds started to lose the green color and turn light yellow. The grains were large and round and the interior was milky-white, but still rather soft. At maturity the grains were dark yellow, very dry and mainly consisting of storage material.

Flowering was determined as the time when 50% of the anthers were dusting. When flowering time was reached, the drip water system was removed from half of the pots of each genotype for a duration of five days. Then all the pots were watered with a hose to inhibit wilting. After 13 days the drip water system was again applied to the treated pots until harvest.

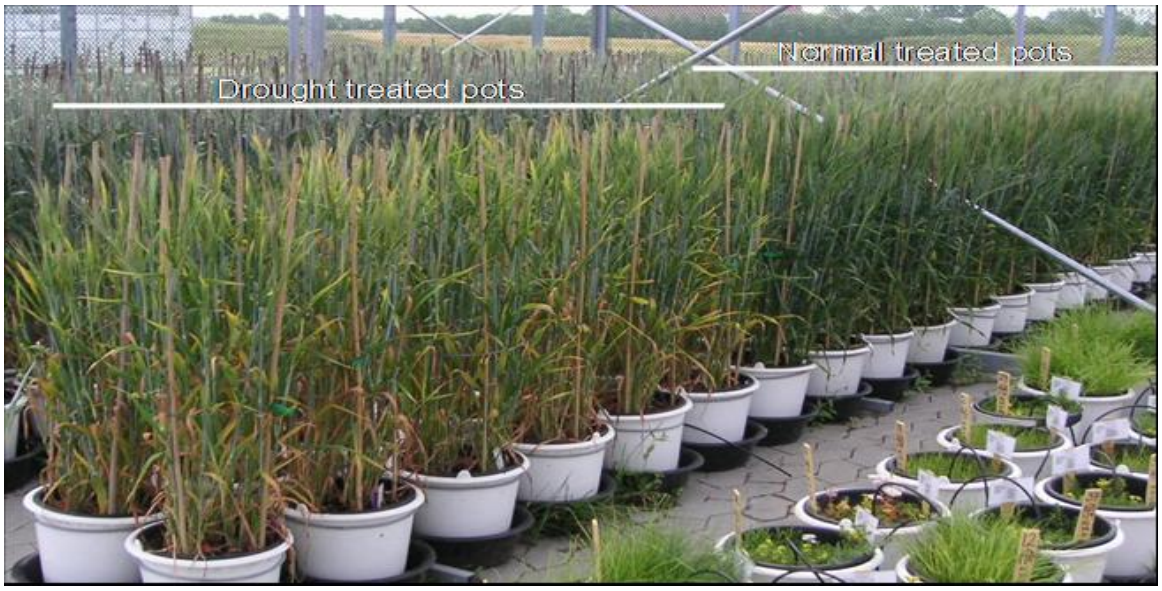

Figure 4-2. The semi-field pots. The senescenced and pale plants have been subjected to water stress. The control pots received daily drip watering. Picture taken 14 DAF.

It is obvious from **Figure 4-2** that plants experiencing drought stress were paler (early senescence) and smaller compared to the control plants. The plants were stressed until approx. -2MPa shoot water potential controlled by the *pressure bomb method* (Scholander et al., 1965) at the last day of drought stress (13 DAF) (data not shown). During the drought experiment, photosynthesis was determined by chlorophyll fluorescence using *pulse amplitude modulated* (PAM) fluorescence (White and Critchley, 1999) on the flag leaves. This resulted in light response curves measured as the photo-

synthetic *electron transport rates* (ETR) and the quantum yield of photosystem II. The measurements were performed after one week of drought (9 DAF), and at the last day of treatment corresponding to 14 DAF. These results clearly show that drought affected the photosynthetic apparatus in all of the plants, see **Figure 4-3**.

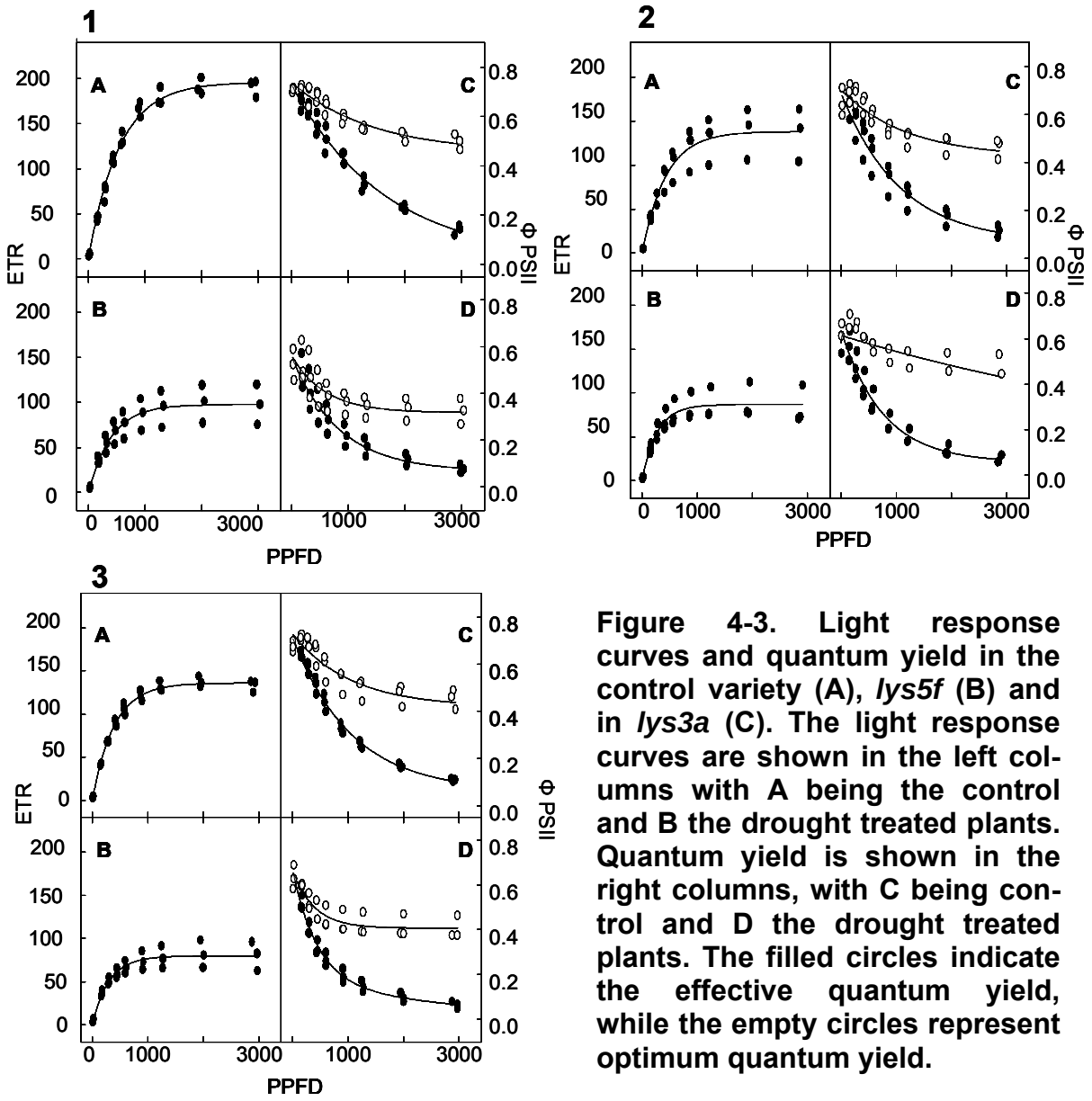

Figure 4-3. Light response curves and quantum yield in the control variety (A), *lys5f* (B) and in *lys3a* (C). The light response curves are shown in the left columns with A being the control and B the drought treated plants. Quantum yield is shown in the right columns, with C being control and D the drought treated plants. The filled circles indicate the effective quantum yield, while the empty circles represent optimum quantum yield.

In this particular study, it appears that the control variety Cork has a more efficient photosynthetic apparatus compared to the mutants under normal conditions, but after a stress period, the mutants and control variety have the same level of light response, **Figure 4-3**, **subfigure 1A**. It is very interesting that during a stress situation, the mutants appear less susceptible to water stress determined as the difference between normal and drought treated stage. From these preliminary studies it could be hypothesized that despite the mutations in *lys5f* and *lys3a* have endosperm-specific promotors, their

pleiotropic effects are not just restricted to the seed compartments but apparently the effect reaches also beyond the seeds. If the mutant endosperm genes are not expressed directly in the leaves, communication between the endosperm and the leaves could be performed by metabolite feedback such as hexoses and sucroses, which have been determined to be important signaling molecules in source-sink regulations in conjunction with other networks of hormones, phosphate, and light (Roitsch, 1999). Such a putative communication between endosperm and leaves needs further confirmation.

In literature drought is found to affect both *source*, that is the generation of photosynthesis assimilates and the *sink*, which is the photo-assimilate recipient depending on timing (Blum, 1996). In this experiment, the drought exposure was induced after the formation of tillers, spikes and flowers and hence, mainly the source was influenced. This may explain why no difference in the number of seeds between drought-treated and controls were found. The fresh seed material was weighted and number of seeds was counted (see **Appendix I**), the flour samples were analyzed by chemical analysis for starch, amylose, amylopectin chain length and β-glucan content. Furthermore, the flour samples were analyzed using NIR, IR and NMR spectroscopy (see below). In all the studies performed afterwards on seeds and on flour the chemical variables were unchanged, and there were no classification due to drought treatment in any of the PCAs conducted on NIR, IR or NMR. This was also the case when the first two harvests were analyzed separately. Inspection of NIR spectra gave similar results (see **Figure 4-11** and **Figure 4-12)**. No clear trends could be found between seeds from control pots compared to seeds from drought treated pots. Using a linear mixed model on fresh seed weight could not detect any significant effect of the treatment ($P \geq 0.13$ for treatment). One could argue that the drought response analysis should be carried out on a whole plant level due to the multiple facetted interaction of source-sink relations, hormones and the carbon pool (Blum, 1996). However, the main idea was to determine the seed response to drought under endosperm epigenesis with emphasis on the glucans. With the methods employed here no differences could be found.

It has been documented, that photosynthates from storage pools in the vegetative parts such as fructans are relocated during to the grain during grain filling (Schnyder, 1993) to compensate for reduced photosynthesis during grain filling (Yang and Zhang, 2006). Hence, an explanation for the lack of differences between the drought treated seeds and the seeds from the control plants could be the relocation of stem resources to the seeds compensating for the lack of photosynthesis. This is feasible because the plants were grown with optimal watering and fertilization before the treatment. Another explanation is that drought induces senescence, which results in increased remobilization of assimilate from vegetative part to the grain (Teulat et al., 1997) and that controlled soil drying could be favourable, as

the seeds benefits from increased remobilization. Hence, the drought treated plants and the conditions reported in the experiments were probably able to utilize their stem resources and thus counteract the reduced grain filling duration and rate. It is also worth remembering that the plants experienced optimal growth conditions before and after the stress event.

4.2 Chemical analysis of the endosperm mutants

The accumulation of β-glucan in the three genotypes determined by Calcoflour and verified by the enzymatic test is presented in **Figure 4-4a** together with the starch accumulation. See **Appendix I** for all the absolute values of the analytes measured on the seed- and flour samples. In *lys5f,* the β-glucan content reaches a maximum of 18% within the first 30 DAF with rapid increase from 13-30 DAF. On contrary, the control variety and *lys3a* showed a slow increase in β-glucan reaching a maximum of only 6% and 4% β-glucan, respectively at the late grain filling period (39 and 47 DAF). These levels of β-glucan are consistent with those found by (Munck et al., 2004). The differences in β-glucan synthesis are counteracted in the starch synthesis, where the control variety and *lys3a* show rapid increase of starch reaching maximum levels at 23 DAF of 49% and 46% starch respectively, compared to the more slow increase observed in *lys5f* reaching a maximum of only 23% at 39 DAF, **Figure 4-4b**. The onset of the β-glucan synthesis in *lys5f* is slightly later (five days) than the synthesis of starch in the control and *lys3a*.

The amylose content (% of starch) partially reflects the starch pattern with the control variety having the largest content of amylose, whereas *lys3a* and *lys5f* have approx. 10% less amylose at 47 DAF, **Figure 4-5**. In general, *lys3a* and *lys5f* have the same amylose accumulation pattern and a concomitant rapid increase of amylose equal to that of Cork until 20 DAF. Hereafter, the accumulation of amylose levels off in *lys3a* and *lys5f*. As *lys3a* has a much higher content of starch compared to *lys5f*, the decrease in amylose observed in *lys3a* must be ascribed an increased content of amylopectin. The chain length composition of amylopectin was tested, and no changes could be retrieved between the genotypes (**PAPER A**).

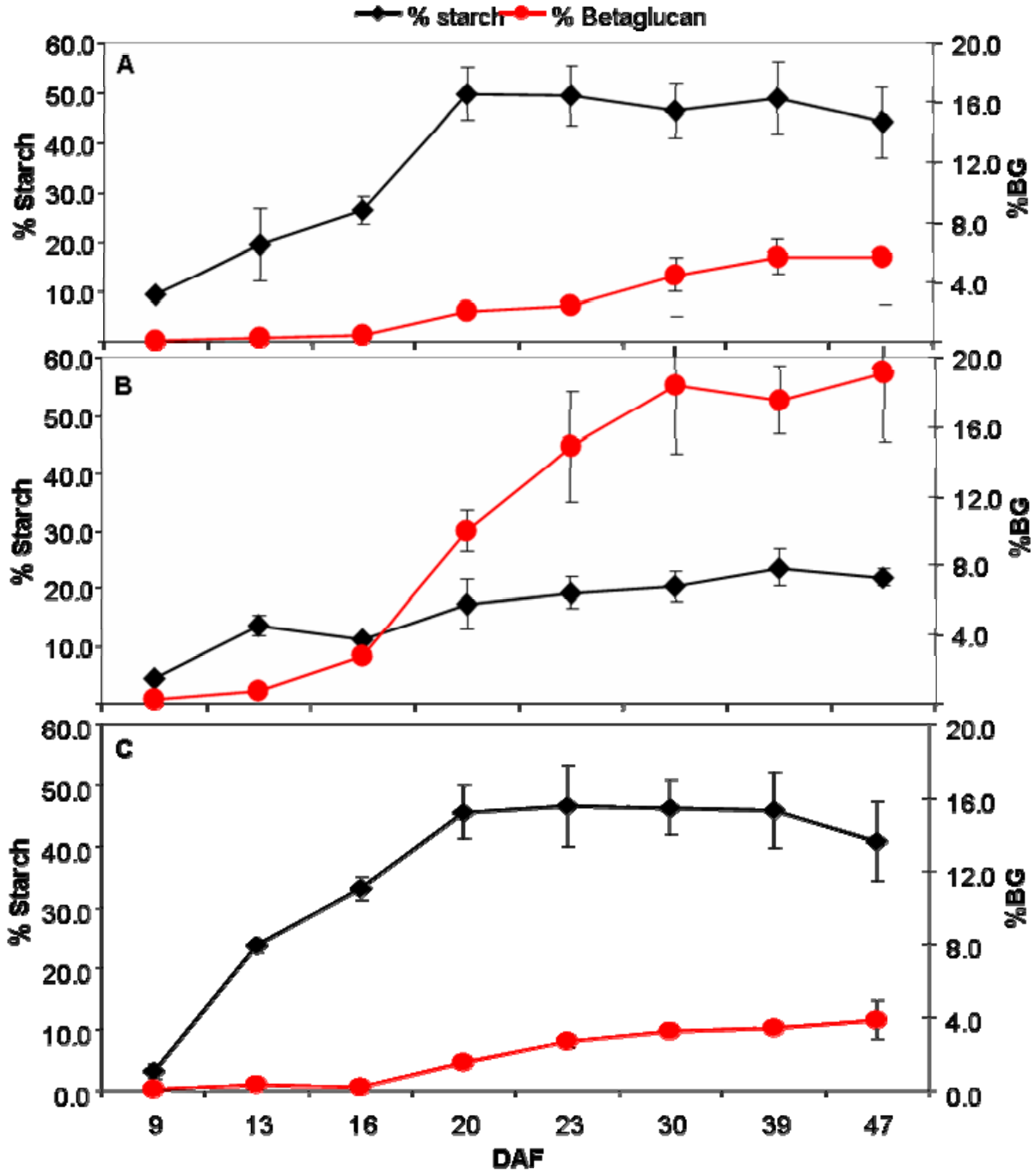

Figure 4-4. The starch accumulation pattern (black rhombs) and β-glucan accumulation (red circles) in the three genotypes during seed development: the control variety Cork (A), *lys5f* (B) and *lys3a* (C). BG= β-glucan.

The level of starch content is also represented in the dry weight of the seeds, **Figure 4-5b**. Interestingly, *lys3a* has a markedly lower level of seed freeze-dry matter weight compared to its only slightly reduced amount of starch to Cork. This can be explained by the smaller seeds found in the mutants. The increase of fresh weight follows the three phase pattern usually observed during cereal grain filling, **Figure 4-5c**: A rapid increase in fresh weight until 20 DAF where after a slower accumulation is observed before

the fresh weight decreases as a consequence of drying during maturation. The rapid increase in fresh weight corresponds to the grain enlargement period depicted in **Figure 2-2**.

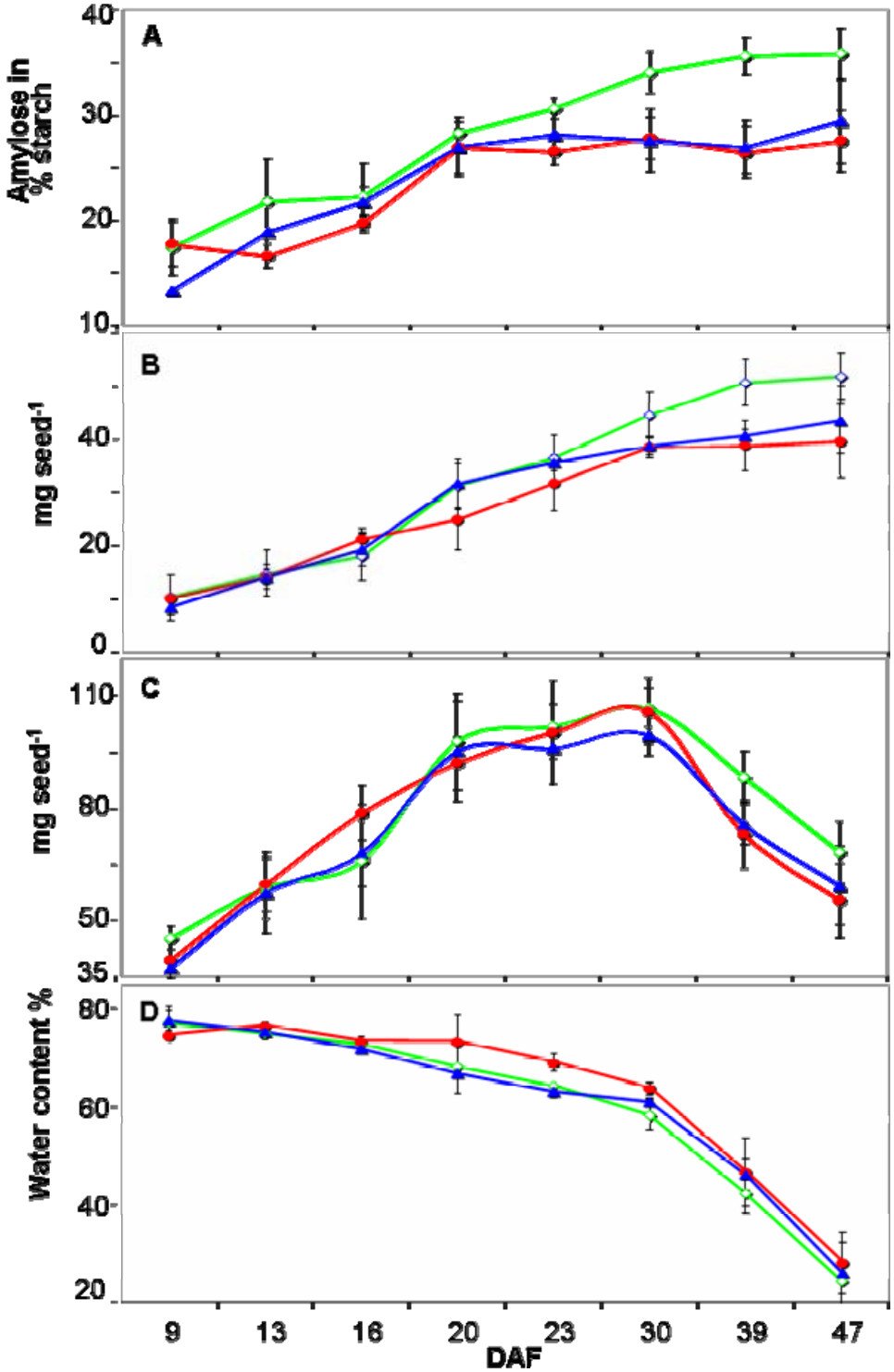

Figure 4-5. The accumulation of amylose (A), freeze-dry matter (B), fresh weight (C), and the water content (D) in seeds during grain filling. Blue= lys3a, Red= lys5f and green= Cork.

This three phase pattern of fresh weight has also been shown in developing wheat grains (Jennings and Morton, 1962; Gergely and Salgo, 2003).The

water content is initially high during early seed development and then decrease as the metabolic processes slow down and the seed enters the maturity phase from 39 DAF and onwards, **Figure 4-5d**.

Simple correlations (r) between selected chemical parameters are presented in **Table 4-1**. It was expected that water would be correlated to the hygroscopic β-glucan. However, at early seed development (9-16 DAF) β-glucan and amylose show negative correlation to water, whereas β-glucan and amylose show positive although low correlation. In this period very low levels of β-glucan are found in all three genotypes (max 2.75% in *lys5f*), the maximum content of water (approx. 75% mg seed^{-1}) and already half the content of amylose. The negative correlation between β-glucan and water is hence not surprising, and amylose as a part of the crystalline starch does not have the same affinity for water. The correlations at 23 and 47 DAF show the same patterns: β-glucan and water are now positively correlated as expected although with a rather low correlation. Amylose and water continuously negatively correlated. A simple correlation plot (**Figure 4-16**) between these chemical parameters and the NIR spectra proved analog patterns to the correlations between the chemical parameters, see 4.3.4.

Table 4-1. The simple correlation (r) between the three chemical variables at three temporal stages: an early seed developmental stage covering 9, 13 and 16 DAF, a mid-developmental stage at 23 DAF and a late temporal stage at 47 DAF. A negative value means a negative correlation.

Temporal stage		β-glucan	Amylose	Water
9-16 DAF	β-glucan	1		
	Amylose	0.17	1	
	Water	-0.22	-0.60	1
23 DAF	β-glucan	1		
	Amylose	-0.58	1	
	Water	0.50	-0.19	1
47 DAF	β-glucan	1		
	Amylose	-0.50	1	
	Water	0.47	-0.31	1

When comparing mutants grown under same conditions against a control variety, as in this case Cork, genetic differences can be revealed. A PCA analysis on the mean chemical values is presented in **Figure 4-6**. When lines are drawn between the time points (called trajectories) (Gergely and Salgo, 2003) unique patterns are found for each of the mutants. In a similar PCA/trajectories analysis on six anti-microbial proteins in the endosperm mutant analysis proved that *lys5g* (allelic to *lys5f*) was a gene with early onset, whereas *lys3a* was a gene with a late onset in seed development (Jacobsen et al., 2005).

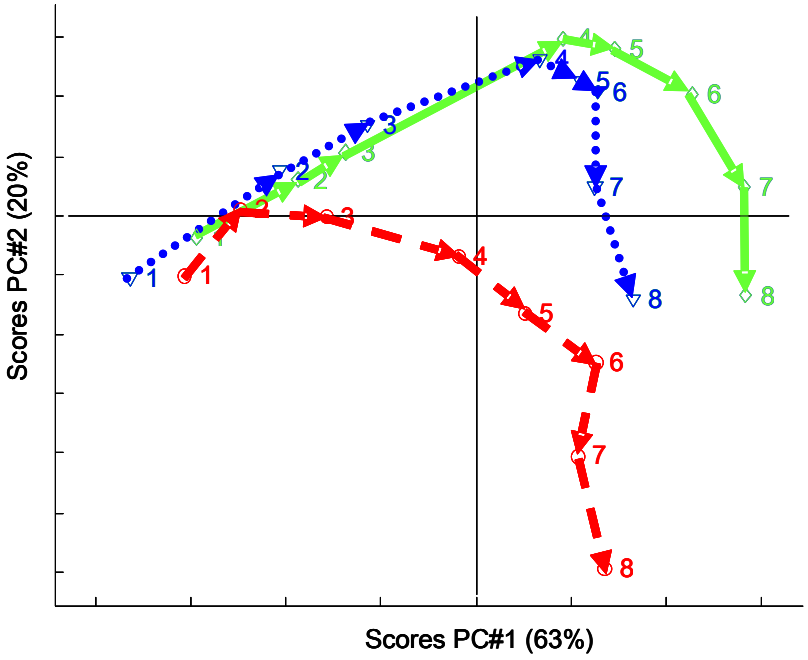

Figure 4-6. PCA of the chemical reference analyses. PCA scoreplot colored according to temporal changes in the three genotypes. The arrows follow the development from first harvest (9 DAF) to the last harvest: 8 corresponding to 47 DAF. The red line=*lys5f*, the blue, dotted line=*lys3a* and green line=Cork.

It is clear from **Figure 4-6** that *lys5f* has a different pattern compared to Cork and *lys3a*. Mutant *lys5f* follows a different pattern already from 13 DAF concomitant with the onset of β-glucan synthesis. The mutant *lys3a* on the other hand deviates from the control at the 4th harvest, which equals 20 DAF. However, the patterns are too complex to reveal exact differences in the temporal onset on genes. In this respect one should differentiate between: 1) the early developmental stage at which the gene presence could be detected either by chemistry or by spectroscopy, 2) the stage of main onset of the gene where an exponential change in gross chemical composition is taken place.

In **Figure 4-7a** the relative changes of starch and β-glucan content in the mutants compared to the normal variety is shown. The mutant gene *lys5f* and *lys3a* probably affect the onset of starch synthesis already at 9 DAF having about sixty % reduction in starch compared to the barley reference at this very low initial level. The starch content in *lys3a* reaches faster a higher level of starch (actual starch content of 23.8% by 13 DAF, **Appendix I**) compared to the normal variety (actual value of 19.5% starch by 13 DAF), and *lys3a* has a high level of starch until 16 DAF after which starch synthesis in the normal barley catches up and remains at a higher level throughout the grain filling period. *Lys5f* follows the same pattern of starch accumulation of starch as *lys3a* just with approx. 40-60% less starch than the normal barley.

The major difference between *lys5f* and Cork is seen to appear around 13-16 DAF, whereas in *lys3a* the major difference appear between 16-20 DAF. The accumulation of β-glucan gives a totally different pattern from that of starch (**Figure 4-7b**), in which the *lys5f* shows a very high increase in β-glucan content between 13 and 16 DAF, whereas the accumulation of β-glucan in normal and *lys3a* seems to follow the same pattern of accumulation with just a very low content of β-glucan compared to *lys5f*. It is evident from these comparative studies that the *lys5f* gene has an early appearance in seed development, whereas *lys3a* has a later appearance of approximately ten days. The study confirms the temporal onset of the early *lys5g* allelic to *lys5f* found by Jacobsen et al., (2005).

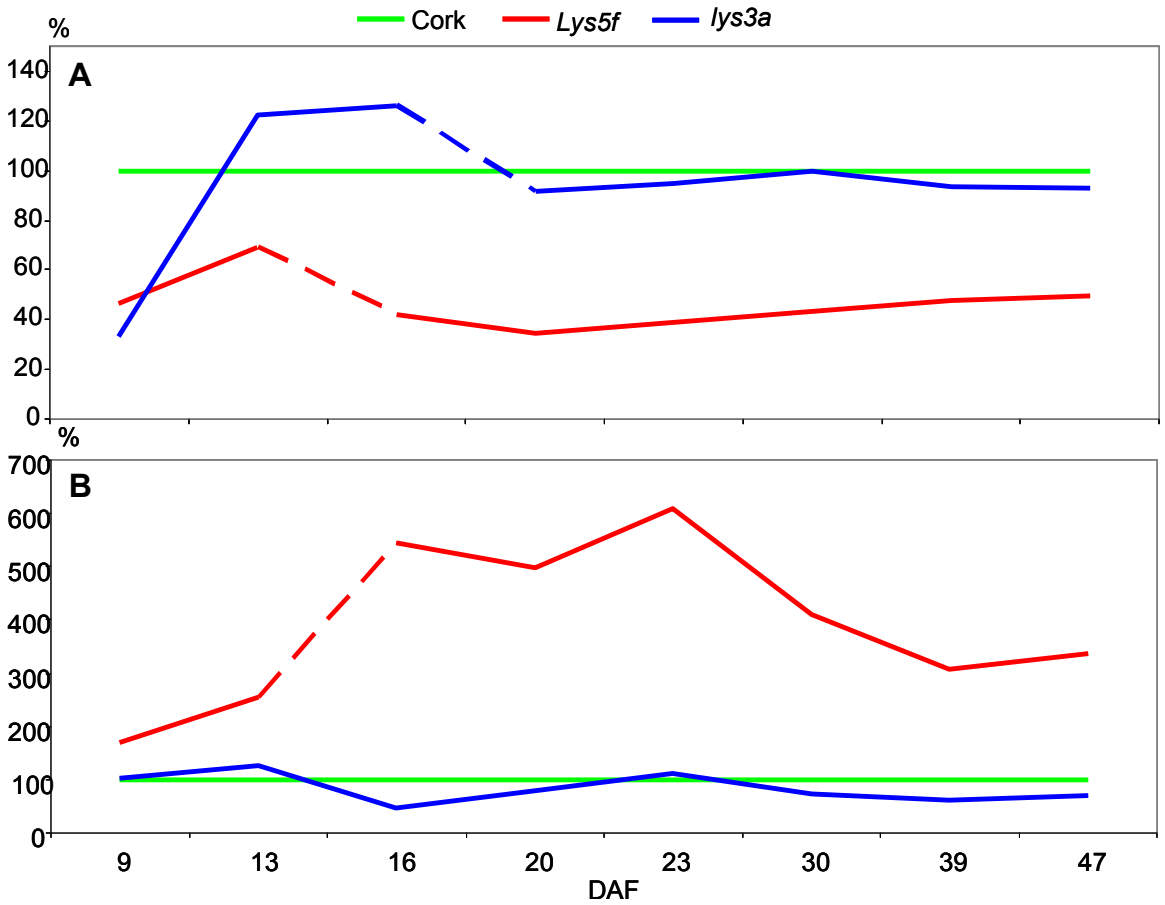

Figure 4-7. The relative content of starch and beta-glucan in *lys5f* (red lines) and *lys3a* (blue lines) compared to the normal barley Cork (green lines) during grain filling.

In conclusion: There was an indication already at 9 DAF that starch synthesis was reduced in both mutants. Specific genotypic differences between the mutants and the normal barley were found for the accumulation of starch and β-glucan, but also for amylose. The chemical analysis confirmed the β-glucan compensating mode in the starch-deficient mutant *lys5f* and revealed the onset of β-glucan accumulation to be 13 DAF. The onset of β-glucan accumulation was together with the difference in relative starch indicative of

a major early gene onset for *lys5f*. In this investigation there was no protein analysis that could detect the onset of the protein (lysine) mutant *lys3a* during development. The normal barley and the *lys3a* mutant showed rapid increase of starch to normal levels, whereas the β-glucan accumulation was only 1/3 of that of *lys5f*. In chapter five the onset of genes will be discussed in context of water content.

4.3 Spectroscopy of the endosperm mutants

The two vibrational spectroscopic methods NIR and IR described in 3.2, and the NMR spectroscopy and MRI, described in 3.3 were employed in the study of the barley endosperm mutants as described below. The experimental design depicted in **Figure 4-1** yielded a total of 96 samples (3 genotypes × 4 (1-4 harvests) × 2 replicates + 3 genotypes × 4 (5-8 harvests) × 6 replicates). Due to a minor errors in the experiment, three replicates of *lys3a* from harvests 1, 5 and 7, and two replicates of Cork harvest 5 and *lys5f* harvest 5 were lost. Hence a total of 91 samples were used for NIR and IR spectroscopy.

4.3.1 NIR and IR analysis of developing barley mutants flour

In barley, NIR calibrations exists among others to moisture (Downey, 1985), protein (Donhauser et al., 1983), starch (Szczodrak et al., 1992), amino acids (Williams et al., 1984), hot water extract (malting quality parameter) and to β-glucan (Szczodrak et al., 1992; Czuchajowska et al., 1992; De Sa and Palmer, 2006) although the predictions for β-glucan did not exceed r^2=0.76, see 4.3.4. Where NIR is mainly used for predictions of bulk components by PLS correlations and predictions, FT-IR and FT-IR micro-spectroscopy have mainly been used for structural and functional analysis especially in the study of cell wall properties (Robert et al., 2005; Barron et al., 2005; Philippe et al., 2006). Structural analysis covers orientation studies of functional groups attached to the polymer chain (Kacurakova and Wilson, 2001), and the substitution of the cell wall component xylose in wheat (Robert et al., 2005). Even though FT-IR is useful for the structural analysis of polysaccharides only few reports on structural analysis of cereal β-glucan are found: (Johansson et al., 2004) used FT-IR to study the fiber fraction of oats and barley and found that insoluble and soluble β-glucan had almost identical FT-IR spectra.

The combined use of chemometrics and spectroscopy has proven very valuable in exploring genetic variability on the phenomic level giving rise to the concept of the digitized, spectral phenome (Munck, 2007) found in the highly reproducible NIR spectra. Using this approach, it is possible to overview the outcome of gene-expression in various genotypes on the phenomic level.

4.3.2 Temporal analysis of NIR and IR spectra

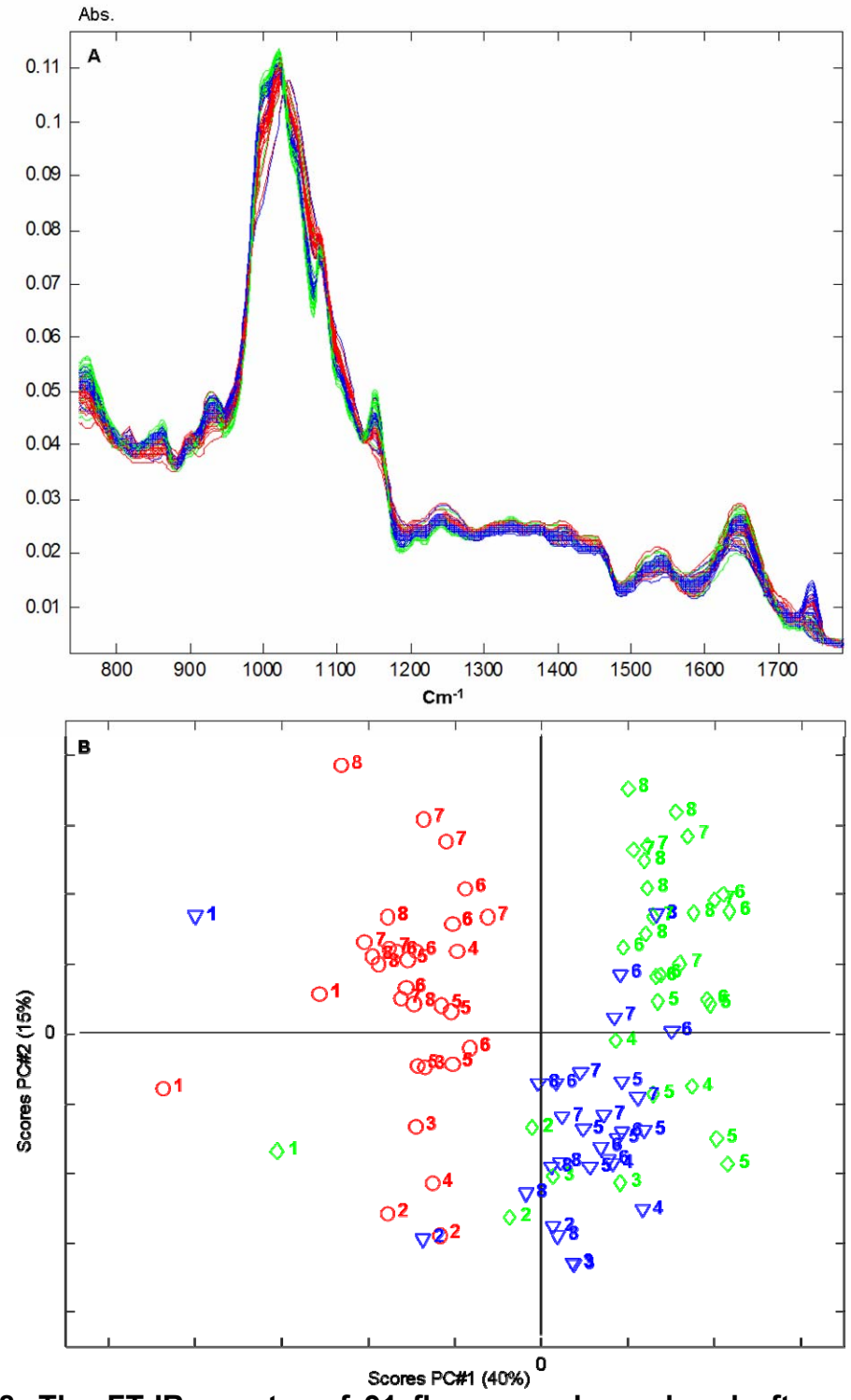

Figure 4-8. The FT-IR spectra of 91 flour samples colored after genotypes; red= *lys5f*, blue=*lys3a*, and green line= control variety (A). The corresponding PCA (B), on full cross validated data in the region 750-1800 cm^{-1}. The numbers refer to the harvest time. Control variety= green, rhombs, *lys5f*=red circles, and *lys3a*=blue, triangles.

The barley endosperm IR flour spectra were analyzed for temporal and genotypic variance by visual inspection as well as by PCA classification. An overview of the IR flour spectra is seen in (**Figure 4-8a**).

The IR spectra resemble that of other flour analysis (Philippe et al., 2006) with a characteristic peak from 1100-950 cm^{-1}. The PCA score plot of the IR spectra shown in **Figure 4-8b** shows a clear temporal development along PC1 with the three samples from 9 DAF (=1 in **Figure 4-8b**) separating away from all other samples. From the score plot a clear separation of *lys5f* (red circles) from *lys3a* (blue triangles) and the control variety (green rhombs) is also seen. Close-ups of two IR-regions are shown in **Figure 4-9**. The clustering of the early (9 DAF) samples found in the score plot are seen as 'outlier' spectral lines marked with arrows. From 9 DAF to the later temporal stages, a temporal shift from 1036 cm^{-1} towards 1021 cm^{-1} is observed in the spectra (marked with double arrows in **Figure 4-9a**). This shift must be related to the changes in water, as the shift occurs before the accumulation of bulk carbohydrates is initiated, although this region covers C-O vibrations.

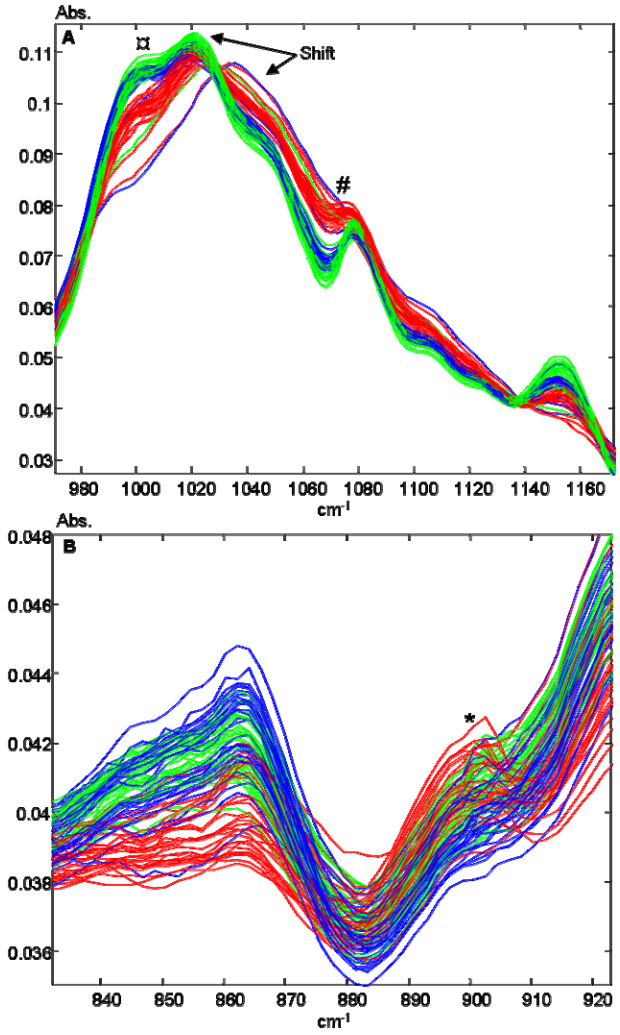

Figure 4-9. Close-up of two regions in the FT-IR spectra of the 88 flour samples in the region 970-1170 cm^{-1} (A) and the region 830 to 970 cm^{-1} (B) The arrows indicates the shift from 9 DAF to the later developmental stages. The ¤ indicates the shoulder at 1002 cm^{-1} and the # the loading found lys5f specific region. The star in (B) is a lys5f specific peak. Control variety= blue, rhombs, lys5f= red circles, and lys3a= green triangles.

It is also clear from the PCA that the *lys5f* samples separates in a cluster of its own. Hence, the IR facilitates the separating of genotypic differences better compared to the NIR spectra, see below. By inspection of the corresponding loading plot (data not shown), the separation of *lys5f* in the IR spectra is mainly due to the resonances around 1065 cm^{-1}, and at 1002 cm^{-1} the *lys5f* has a different intensity compared to the control and *lys3a.* At 1070 cm^{-1} *lys5f* has a lower

intensity of the shoulder whereas lys3a and the control have well-defined peaks at 1078 cm^{-1}.

The anomer-specific peaks in the range from 950 to 750 cm^{-1} contain information about β-glucan as well as other polysaccharide cell wall components (Philippe et al., 2006) and hence this region is most frequently used in carbohydrate analysis (Kacurakova and Wilson, 2001). In this region, pure barley β-glucan shows a peak at 895 cm-1. This cannot be found in the average flour spectra shown in **Figure 4-14** and **PAPER A**. However, the close-up of the region 840-960 cm^{-1} show that *lys5f* spectra show a minor peak at 900 cm^{-1} presumably due to β-glucan, not found in *lys3a* or the control variety.

The NIR spectra also reveal genotypic and temporal differences. A full spectrum from 400-2500 nm was acquired for each sample, see **Figure 4-10a**. In the region from 1400-1900 nm the pattern of the early temporal stages (9-16 DAF) has a distinct pattern compared to later stages. Compared to **Figure 4-4**, it is not surprising that a temporal separation occurs between 16 and 20 DAF as the accumulation of either starch or β-glucan occurs rapidly from 16 DAF and onwards concomitantly with the fresh weight increase. A corresponding PCA to the NIR spectra from 400-2500 nm was conducted on 87 samples, as four samples were identified as spectral outliers, **Figure 4-10b**. A clear separation of the temporal stages is found and much more predominant than found in the IR spectra. On the other hand, a separation of genotypic clusters is not feasible. Not even within the temporal clusters.

One could argue that the distinct chlorophyll peak at 672 nm related to the color of the seeds and the flour influences the pattern too heavily. However, a PCA conducted on the NIR region 1100-2500 nm (figure not shown) reveal only two clusters: the same clustering of the first three harvests (9-13 DAF) and then one cluster of the remaining five harvest from 16-47 DAF, but still no clear separation of the genotypes. Below, PCAs of two specific NIR regions will be considered that show a tendency of genotypic clustering. In all further studies, only the true NIR region from 1100-2500 nm is considered, as the chlorophyll peak at 672 nm dominates the spectra and is in this context not of direct interest.

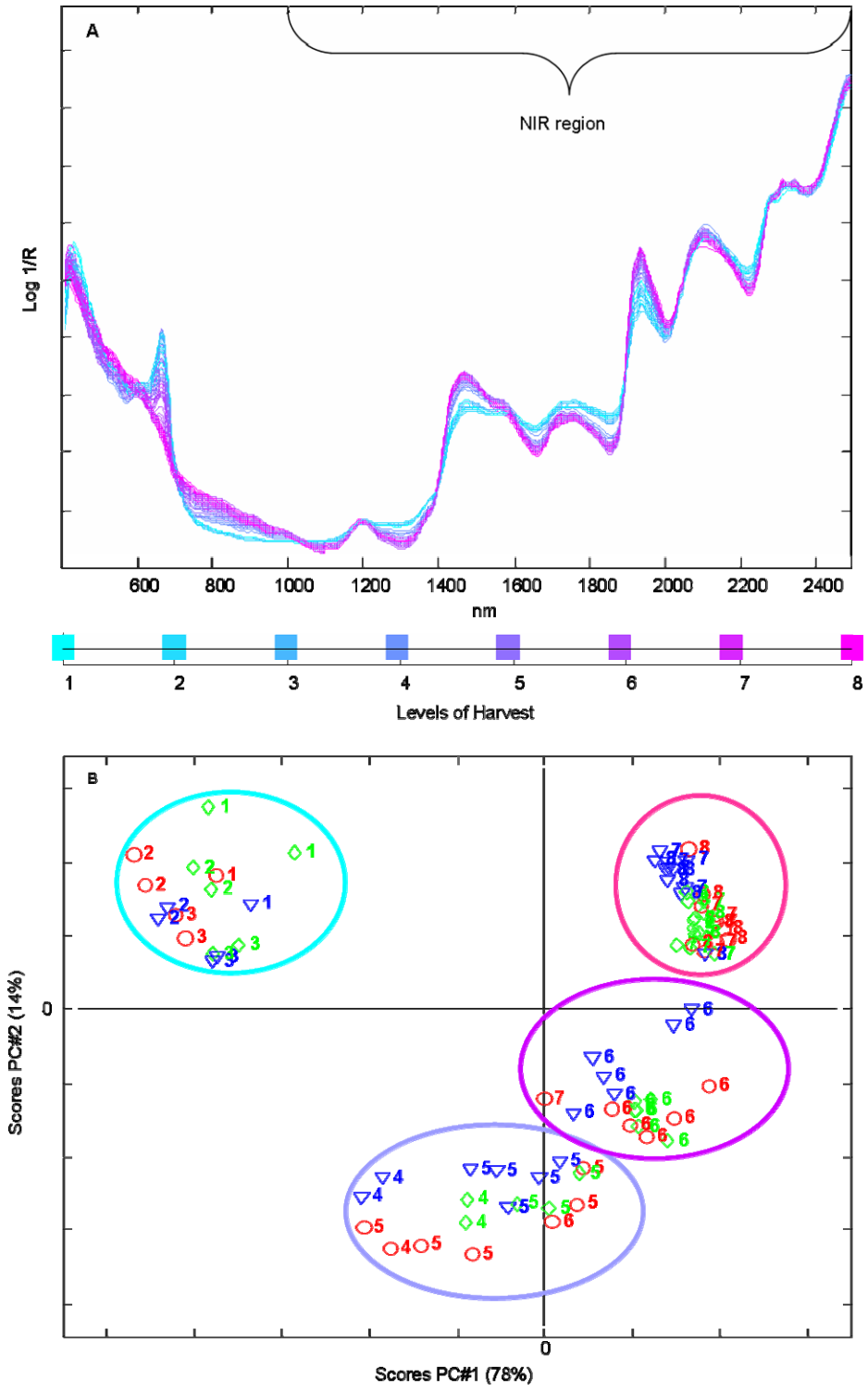

Figure 4-10. The full NIR spectra of 87 flour samples colored after temporal stage (A). The corresponding PCA colored after genotype (B). The color bar reflects the temporal changes: light blue corresponds to early seed filling, whereas the cyan represents the late part of the seed development. The numbers in B refers to the harvest times, in which 1 corresponds to 9 DAF, and 8 to 47 DAF.

4.3.3 Spectral inspection of NIR spectra

The development of physio-chemical patterns of the genotypic different endosperms is seen from **Figure 4-11** and **Figure 4-12** in two NIR regions. The two regions were firstly selected based on visual inspection (coloring after genotype) of the spectra showing clear genotypic differences in these regions. The regions were earlier confirmed by *interval extended canonical variate analysis* (iECVA) (Nørgaard et al., 2006) and were associated mainly with vibrations of C-H bonds (Møller Jespersen and Munck, 2008). The region 1680-1820 was found to contain information about water during seed development (Gergely and Salgo, 2003).

At 9 DAF in the region 1680-1810 nm the spectral form of the three genotypes is difficult to distinguish from each other and the spectra are mainly dominated by base-line off-set probably resulting from sampling difficulties. When studying the mean spectra of 9 DAF (not shown here) it was seen especially at 2260-2380nm that the contours of the mutant gene specific patterns are already established at 9 DAF. From 13 DAF, specific patterns are seen for each of the genotypes in both spectral regions, with *lys5f* having a more distinct profile than Cork and *lys3a.* When 9 DAF is compared with the following temporal stages, the genotypic trend is also recognizable.

During seed development each genotypic pattern becomes more and more distinct and the genotypic pattern is highly reproducible even from early seed development. The off-sets between repetitions seen in e.g. **Figure 4-11c** is probably due to sampling error (Møller Jespersen and Munck, 2008) that occurs when samples of about 50 seeds are taken from a total number of up to 100 seeds from each plants. Furthermore, the second and third spikes are not clearly defined in this experiment. Despite the off-set, the genotypic patterns are consistent.

Figure 4-11. The next page. NIR spectra from 9, 13 16 and 20 DAF in two regions: 1680-1820 nm and 2260-2380 nm. The blue color = lys3a, red color = lys5f, and green color= Cork. From 9 to 20 DAF only six replicates (two of each genotype) exists. From 23 DAF to 47 DAF 18 replicates (six of each genotype) are found.

Figure 4-12. The following page. NIR spectra from 23, 29, 39 and 47 DAF in two regions: 1680-1820 nm and 2260-2380 nm. The blue color = lys3a, red color = lys5f, and green color= Cork.

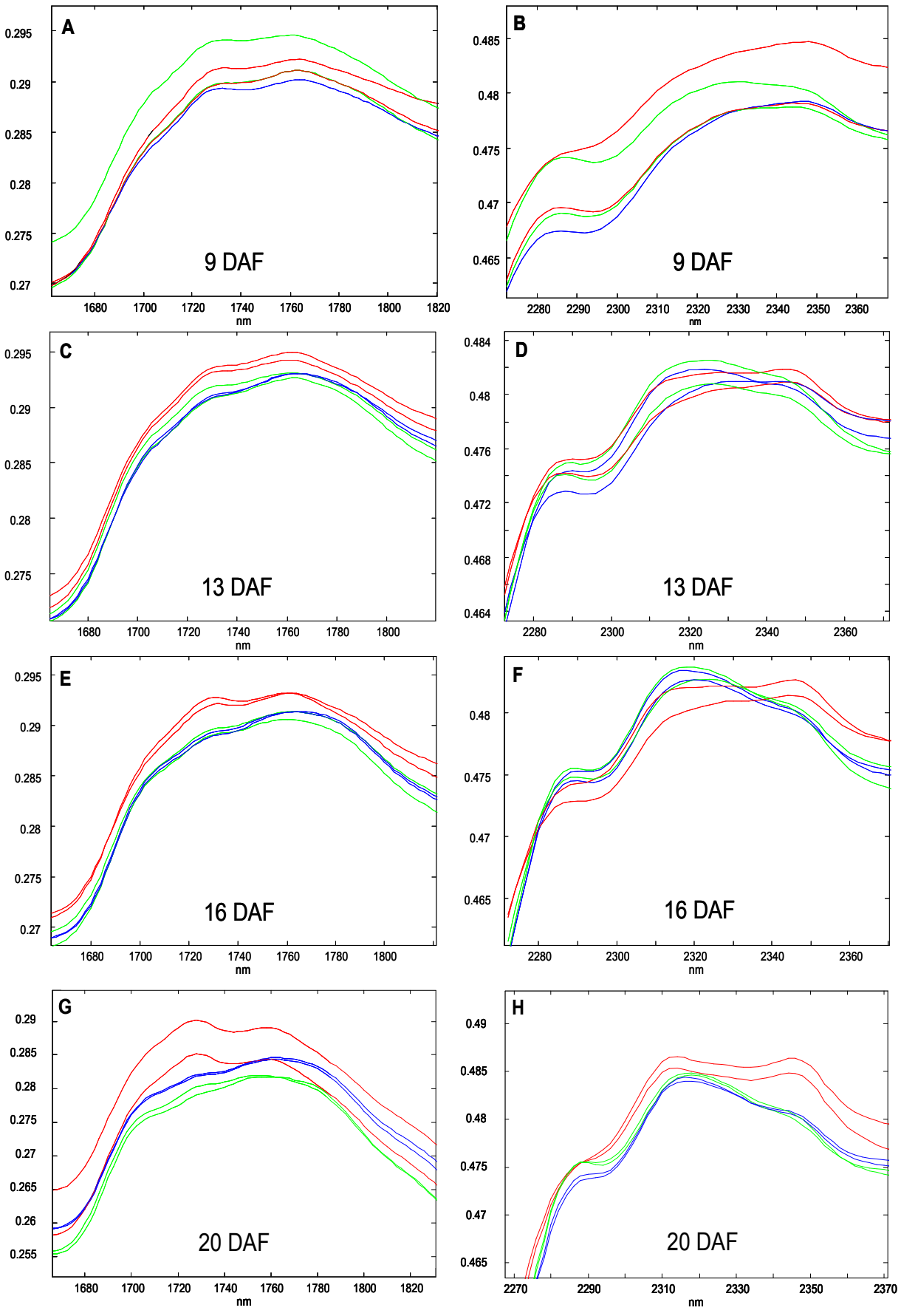
A
9 DAF
B
9 DAF
C
13 DAF
D
13 DAF
E
16 DAF
F
16 DAF
G
20 DAF
H
20 DAF
nm

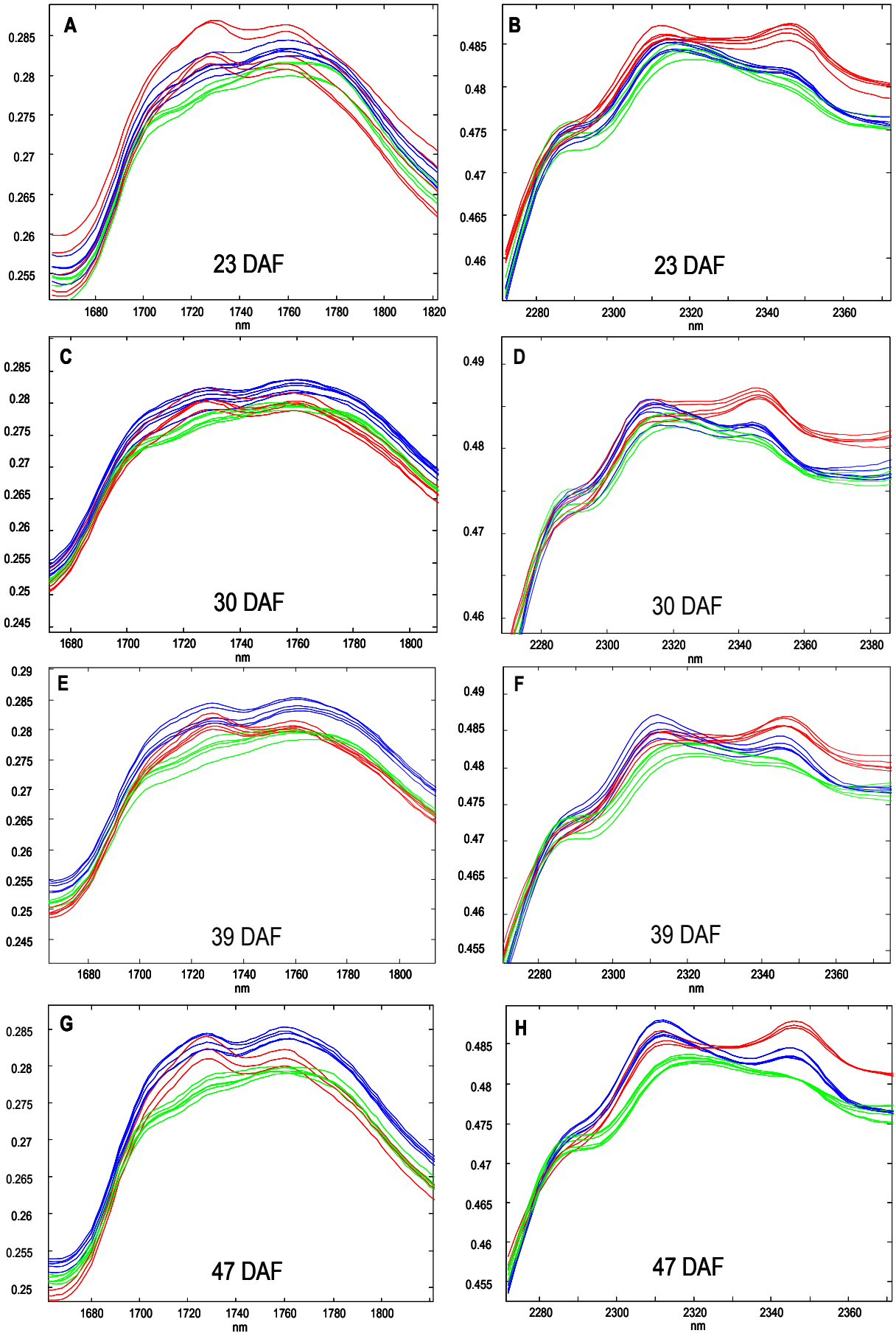
A
23 DAF
0.285
0.28
0.275
0.27
0.265
0.26
0.255
1680 1700 1720 1740 1760 1780 1800 1820
nm
B
23 DAF
0.485
0.48
0.475
0.47
0.465
0.46
2280 2300 2320 2340 2360
nm
C
30 DAF
0.285
0.28
0.275
0.27
0.265
0.26
0.255
0.25
0.245
1680 1700 1720 1740 1760 1780 1800
nm
D
30 DAF
0.49
0.48
0.47
0.46
2280 2300 2320 2340 2360 2380
nm
E
39 DAF
0.29
0.285
0.28
0.275
0.27
0.265
0.26
0.255
0.25
0.245
1680 1700 1720 1740 1760 1780 1800
nm
F
39 DAF
0.49
0.485
0.48
0.475
0.47
0.465
0.46
0.455
2280 2300 2320 2340 2360
nm
G
47 DAF
0.285
0.28
0.275
0.27
0.265
0.26
0.255
0.25
1680 1700 1720 1740 1760 1780 1800
nm
H
47 DAF
0.485
0.48
0.475
0.47
0.465
0.46
0.455
2280 2300 2320 2340 2360
nm

In the region 1680-1820nm, *lys5f* (red lines) are seen to have to characteristic shoulders at 1725 and 1760nm that are also present in *lys3a* (blue lines) although less marked. These peaks corresponds well to the oil signals at 1724 and 1762nm (Møller Jespersen and Munck, 2008) and the higher lipid content found in the mutants compared to normal barley **Table 2-2**.

In the region 2260-2380nm three major shoulders are found for *lys5f* and *lys3a* at 2285, 2310 and 2346 nm. The first shoulder is also present in Cork and is seen already at 9 DAF. The latter peak at 2346 nm corresponds to fat, and thus fits the higher lipid content in the mutants. The NIR spectral pattern at maturity in this investigation fits with the patterns found for the mutants *lys5f* (Munck et al., 2004) and *lys3a* (Munck et al., 2001). In the latter paper, a high reproducibility of the genotypic patterns in mature barley seeds was also proved although an environmental impact was observed between the field-grown and the green-house grown seeds mainly as an off-set. In this developmental study, all samples were grown under equal conditions in the semi-field allowing a very clear-cut representation of the phenome as genotype specific spectral patterns that can be physio-chemical validated, see 4.3.4.

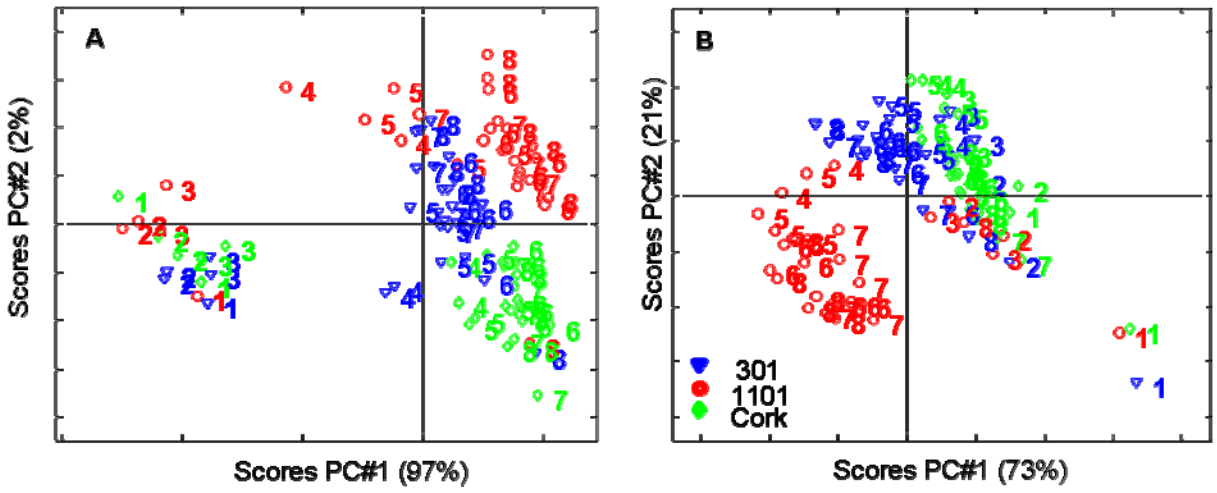

Figure 4-13. PCA conducted on the 1680-1820 nm (A) and 2260-2380 nm (B) comparable to Figures 4-10 and 4-11. The numbers corresponds to the temporal stages, where 1 equals 9 DAF, 2 equals= 13 DAF and so forth until 8 equals 47 DAF.

A PCA was performed on each of the two intervals 1680-1820 nm and 2260-2380 nm and shown in **Figure 4-13**. In the region 1680-1820 the samples from 9 to 16 DAF are in a distinct cluster of their own, whereas the samples from 4 to 8 (20 to 47 DAF) separates in a cluster of their own like seen in the score plot of the full NIR spectra discussed above. A tendency of genotype separation is also seen. However, the recognizable, distinct genotypic pattern seen in the spectra is not revealed in the PCA. As no genotypic difference can be found within the cluster of the stages 9-16 DAF, it appears that

the three genotypes are more or less similar. However, when consulting the spectra in **Figure 4-11** and **Figure 4-12**, the genotypic patterns are manifested in the spectra already from 9 DAF. The same considerations are valid for the region 2260-2380 nm.

In conclusion, a PCA score plot does not comprise the fine genotypic structures representing the entire phenome and observed in the highly reproducible spectra. To study mutant phenotypes including many pleiotropic effects (see chapter 5), careful data inspection is required as further emphasized by Munck, (2007).

4.3.4 Calibration of NIR and IR analysis to bulk carbohydrates

Differences between the mutants can be explored by differential spectra preferably in iso-genic backgrounds and interpreted by consulting the spectroscopic literature with regard to assigned chemical bonds and by chemometrics through iPLS regression to confirm the chemical analysis data (Munck, 2007). For interpretation K. Norris, as demonstrated by Munck, (2007) showed that comparative spectral inspection is essential to visually identify the response of specific spectral bands identified from the literature.

The identification of spectral regions assigned to various carbohydrates has involved comparison of NIR spectra of starches with various compositions and origin, with that of pure compound spectra (Czuchajowska et al., 1992). Pure spectra of wheat amylose, wheat starch, purified cellulose, and purified β-glucan were acquired for both IR and NIR. An average IR flour spectrum (green line in **Figure 4-14b**) tends to follow partly that of pure β-glucan and partly that of pure starch. The average NIR flour spectrum in **Figure 4-14a** tends to follow the starch/amylose spectra throughout the spectra, but in the region 2260-2400 nm major differences are found. Using visual inspection of NIR spectra from flour and spectra of pure carbohydrates, Czuchajowska et al., (1992) identified regions describing the carbohydrates in the flour and made predictions to β-glucan (r^2 = 0.85) in a flour set with a β-glucan range of 5.8-6.4%. Predictions of β-glucan to a more heterogeneous sample set with a range of β-glucan from 3-9.5%(Szczodrak et al., 1992) gave poor predicitions of r^2=0.76. A similar approach utilizing mixtures of starch and β-glucan in defined ratios was used to identify a region between 1600 and 1800 nm for giving the best correlation to β-glucan by Henry, (1985), however with a poor prediction (r^2= 0.69).

All the flour samples originate from seeds that were freeze-dried. Freeze-drying was performed at once for the whole material under the same conditions. As the NIR and IR are performed on freeze-dried material, the calibrations that are made to water do not longer directly represent water in the

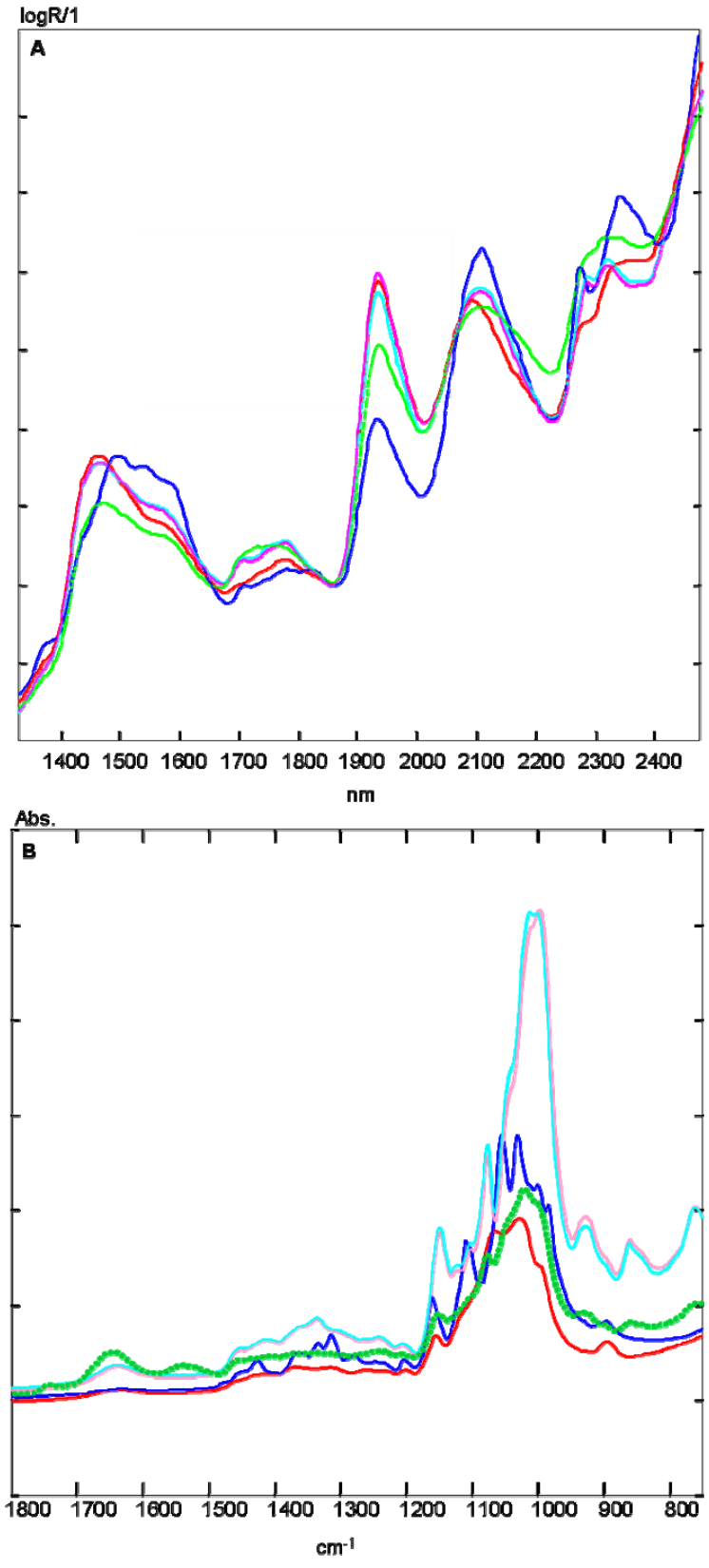

Figure 4-14. NIR (A) and FT-IR (B) spectra of the pure substances β-glucan (red line), cellulose (blue line), wheat starch (pink line) and wheat amylose (turquoise line) compared to an average seed flour spectrum (green line).

samples but is a measurement of the evaporated water. Thus, the correlations given in the following are between spectral data and evaporated water (water content % of freeze-dry matter). The calibrations can be influenced both by putative water not removed by freeze-drying or by structural changes in the β-glucan polymers where the evaporated water was present. It awaits more experiments to determine if the water removed by freeze- drying is correlated to the water removed by conventional oven-drying for dry matter determination of the flour. In this experiment there has been no material left after the chemical analysis to measure bound water left after freeze-drying.

Evaporated water content was in general poorly predicted by the full IR spectra (r^2=0.52) and was less well predicted compared to NIR, which predicted evaporated water with r^2=0.83, see **Table 4-2** and **4-3**. That it is possible to do a fair prediction of water in the NIR spectra indicates that the freeze-dried seed material has molecular structures, which has a certain potential for water holding and uptake. The flour samples could have

taken up water after the freeze drying event. In the present study, more water is present in *lys5f* (see **Figure 5-1**). This can be explained by the fact that the amorphic β-glucan in its dry state is able to dynamically take up or release moisture more readily compared to crystalline starch.

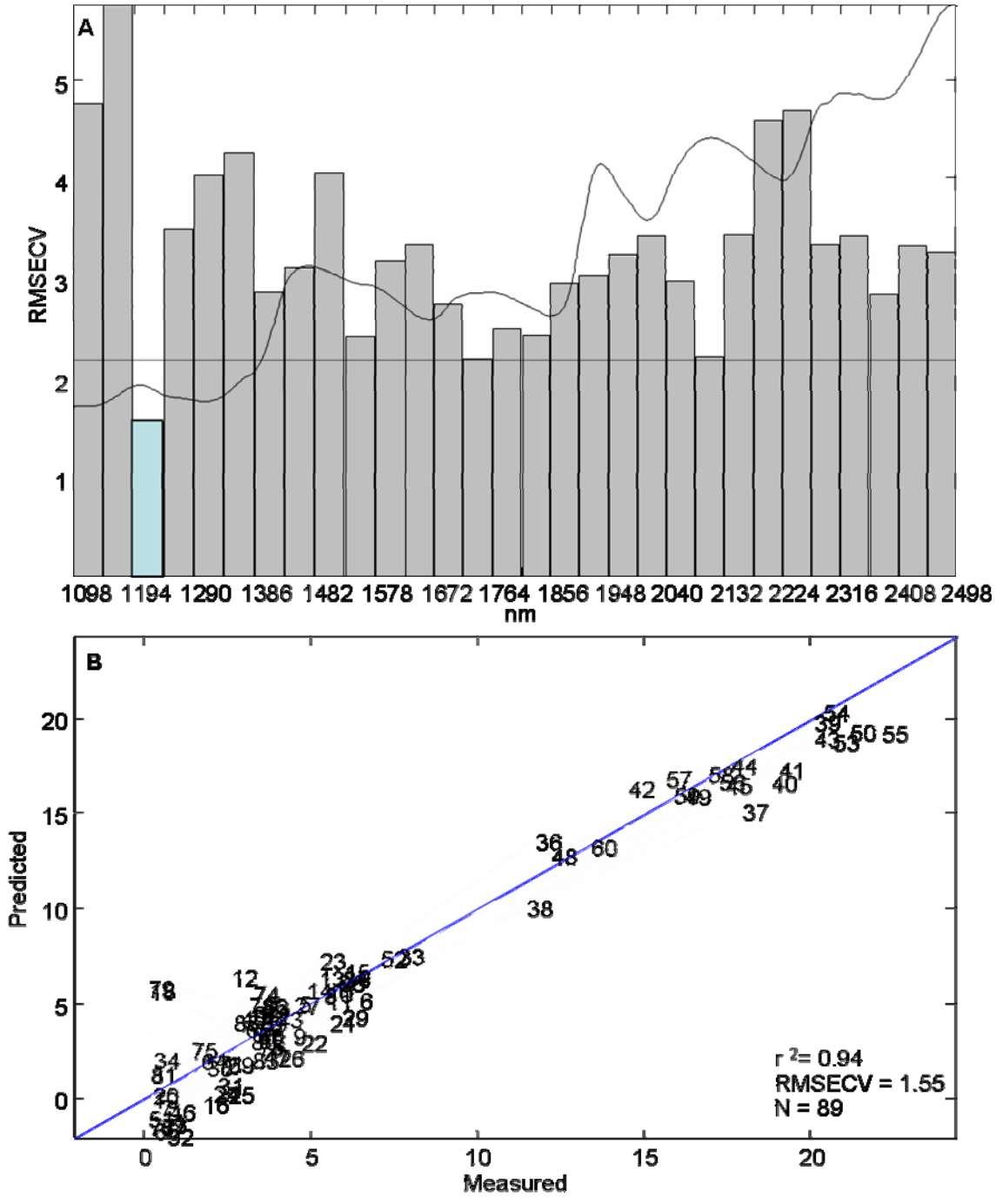

Figure 4-15. iPLS of the 1100-2500nm NIR region to beta-glucan (A). Two spectral outliers were removed. The global model and all sub-intervals were modeled with 4 PLS components and full cross validation. The global model had r=0.94 and RMSECV= 2.16. The interval from 1194-1240nm (marked with light blue) performed better than the global model (B).

An iPLS was performed to facilitate interpretation and to reveal sub-regions in the IR and NIR spectra giving the best prediction of β-glucan, starch and amylose. In **Figure 4-15a**, a NIR spectrum with the 30 intervals are shown together with the interval performing the best. Only one interval performed better than the global model (RMSECV value for the global model is indicated with a broken line. The calibration of this interval is shown in **Figure 4-15b**.

NIR and IR were calibrated to β-glucan, **Table 4-2** and **Table 4-3**. A few samples of *lys5f* were detected as outliers in the prediction plot and were also found to have deviating values for β-glucan. These samples were removed before modeling.

Table 4-2. The prediction of the chemical parameters β-glucan, amylose and evaporated water content by NIR determined by iPLS.

Spectra range	N	Y-ref	Opt. PLS	Calibration range	r	r^2	RMSECV
1100-2500 nm	89*	β-glucan	2	Global	0.94	0.89	2.16
	89*	β-glucan	4	1194-1240	0.97	0.94	1.55
	89*	β-glucan	4	1718-1760	0.95	0.90	2.04
	89*	β-glucan	5	2086-2130	0.95	0.91	1.96
1100-2500 nm	91	Amylose	8	Global	0.92	0.85	2.26
1100-2498 nm	88#	Evaporated Water	6	Global	0.91	0.83	7.39

* Outliers removed: two *lys5f* replicates from 20 and 30 DAF. # Two replicates of the control variety from 9 and 23 DAF, and one *lys5f* replicate from 39 DAF. N is the number of samples. Opt.PLS is the number of components needed by the model. Data were mean centered and full cross validation was employed. 30 intervals were tested. Only for β-glucan, intervals were found that better predicted β-glucan compared to the global model. Three out of 30 intervals performed better.

Table 4-3. The prediction of the chemical parameters β-glucan, amylose and evaporated water content by IR determined by iPLS.

Spectra range	N	Y-ref	Opt. PLS	Calibration range	r	R^2	RMSECV
750-1300 cm^{-1}	91	β-glucan	6	Global	0.93	0.86	2.33
	89*	β-glucan	8	Global	0.98	0.96	1.30
750-1300 cm^{-1}	91	Amylose	2	Global	0.90	0.81	2.46
750-1300 cm^{-1}	91	Evp. water	2	Global	0.72	0.52	12.68
	91	Evp. water	6	1097-1133	0.80	0.64	10.87
	91	Evp. water	2	1135-1172	0.73	0.53	12.40
	91	Evp. water	4	1212-1249	0.76	0.57	11.95

* Outliers removed: two lys5f replicates from 20 and 30 AF. Only for evaporated water, three intervals were found that better predicted water content compared to the global model. Model performed like for NIR.

A calibration r^2 = 0.89 for β-glucan to the entire NIR spectra was found for 89 samples, but one interval of the 30 performed significantly better than the global model: the region 1194-1240 nm performed extremely well (r^2 = 0.94), **Figure 4-15b**. This high correlation obtained in the present investigation is remarkable as it covers a range of β-glucan content from 3 to 17%. In **PAPER A** less good calibrations were made, as the β-glucan data used for *lys5f* was taken from one measurement of β-glucan that had very large deviations. In the calibrations made here, the best values from three, independent β-glucan measurements were chosen. The best values were checked to be real in an enzymatic test. As with the NIR spectra, two *lys5f* samples were detected as outliers and removed in the IR spectra. A very high calibration to β-glucan across the IR spectra in the region 750-1300 cm^{-1} was found for the 89 samples (r^2 = 0.96) and no sub-regions performed better than the full spectrum.

A PLS performed to starch (n=24) gave poor predictions to the full NIR spectrum (r^2=0.75), but the region 1680-1810 nm gave relatively high calibrations to starch (r^2=0.91) with the use of 3 PLS components and RMSECV of 4.60. Czuchajowska et al., (1992) also found wavelengths in this region containing principal bands of starch. This particular region contains C-H, $C-H_2$ and $C-H_3$ stretching vibrations. Amylose was better predicted by the full region than by sub-regions of the spectra. Amylose was predicted with an r^2 = 0.85, which is less than prediction found in rice (r^2 = 0.95) (Delwiche et al., 1995). The differences could be due to varying complexing of the amylose with lipids (Morrison and Gadan, 1987) between barley and rice, leading to varying reference values. A better prediction to amylose was found for the full IR region than by sub-regions of the spectra. Amylose was predicted with an r^2 = 0.81, which is less than found for NIR, **PAPER A**. The literature on IR and cereal carbohydrates are related to structural analysis rather than calibrations (Séné et al., 1994; Kacurakova and Wilson, 2001)

The spectral assignments of NIR spectra can be found in the literature (Osborne et al., 1993; Williams, 2001). These are approximations based on measurements of purified preparations of chemical compounds. In Jacobsen et al., (2005), a PCA analysis of 27 chemical parameters and NIR spectra of the endosperm mutants gave comparable gene classifications. Moreover, the mutants *lys5f* and *lys3a* that have the double amount of lipids compared to the control, have distinct peaks in the NIR spectra at 1724, 1762 and 2347 nm that are indicative of lipids (Møller Jespersen and Munck, 2008). A simple correlation plot between NIR and mature barley seeds by Møller Jespersen and Munck, (2008) to starch, β-glucan, amid and protein proved the specificity of chemical information in the NIR spectra. A similar plot is presented in **Figure 4-16**. The chemical values for amylose, β-glucan and evaporated water are correlated to every second wavelength in the NIR spectra.

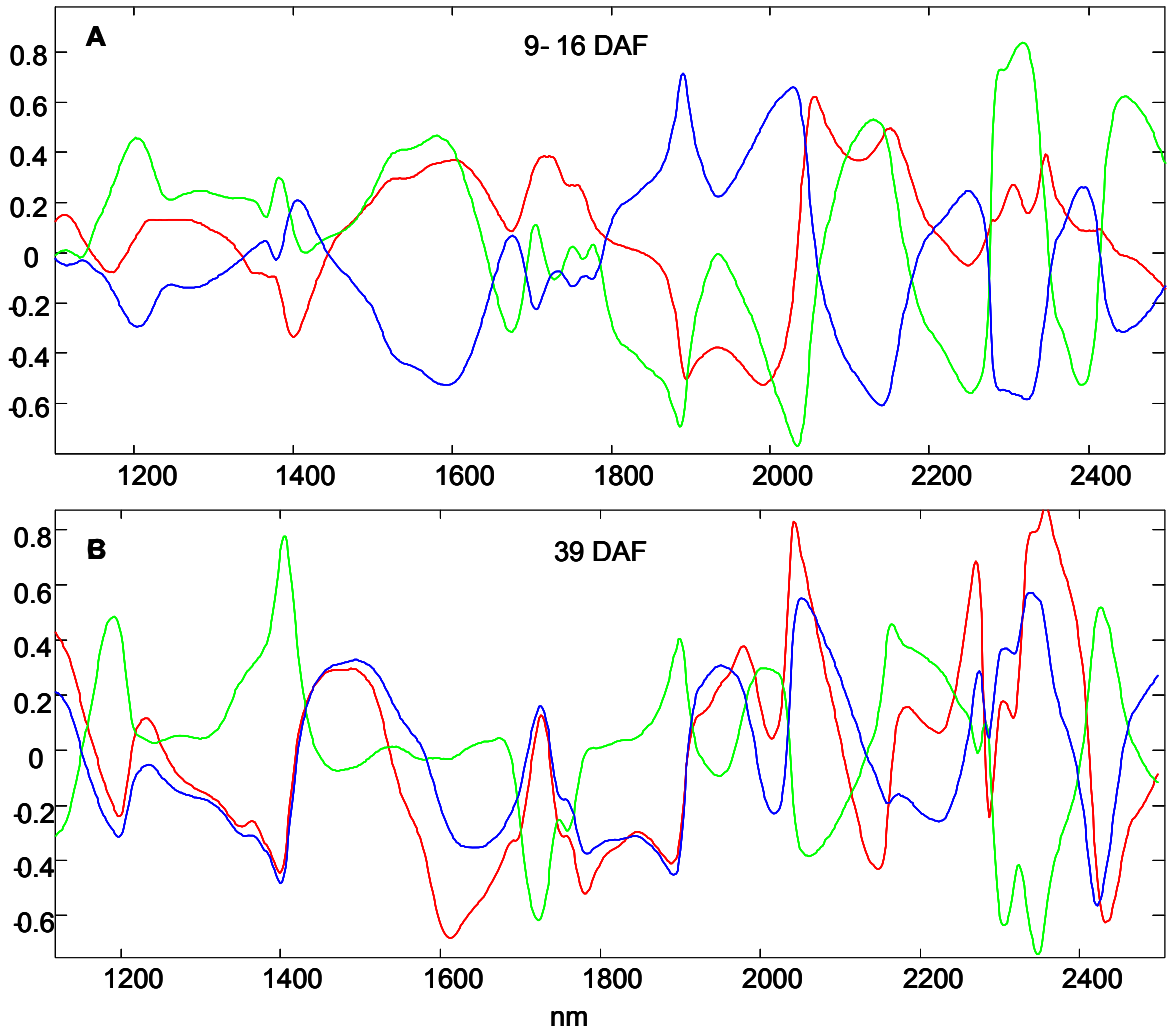

Figure 4-5. Simple correlation coefficients (r) between every second NIR wavelength from 1100-2500 nm for 91 samples, and β-glucan (red), amylose (green) and water content (blue) for early grain filling 9-16 DAF (A) and at late grain filling 39 DAF (B).

The correlation patterns found by Møller Jespersen and Munck, (2008) could also be found for correlations to β-glucan and amylose in this study for mature seeds, where β-glucan has an opposite correlation to that of amylose. The amylose reference (N=89) was used instead of starch reference (N=24). Interestingly, the correlations to spectra from 9-16 DAF are quite different from the correlations from 23 DAF and onwards. β-glucan and amylose followed the same pattern with regard to positive and negative correlation and discussed with **Table 4-1**. β-glucan has high correlation to especially the region from 2300-2400 nm, overlapping the genotype specific region in 2260-2380 nm. The genotype specific region from 1680-1820 nm show high correlation to amylose, and hence to starch. These correlations are consistent with what was found in **Table 4-1**. Thus, the NIR spectra can be regarded a pattern of physio-chemical information and hence the NIR spectra overviews the phenome based on the chemical constitution of the seed.

4.3.5 Single seed ^{1}H HR MAS NMR

Single seeds can be characterized as solids with liquid domains (Bardet et al., 2001). This special feature is a challenge for the NMR spectroscopist, as the experimental design used for solids and liquids differ significantly. Usually, ^{13}C CP MAS NMR is used to study solids, and has been used in studies of protein and starch in various types of seeds (O'Donnell et al., 1981), triacyl-glycerols (Bardet et al., 2001) and cell wall properties (Jarvis and McCann, 2000; Tang et al., 2000). Very few reports exist on seeds studied with ^{1}H HR MAS NMR and none has been found on developing cereal seeds. The rather rare use of ^{1}H HR MAS NMR study of single seeds is due to the water sensitivity and problems of mobilizing more crystalline parts of the seed. However, liquid-state ^{1}H high resolution (HR) MAS NMR is faster and more sensitive than ^{13}C CPMAS solid state NMR, because of ^{1}H's higher sensitivity. ^{1}H HR MAS NMR of wheat flour was used in combination with chemometrics as a fingerprinting technique allowing for classification of Italian durum wheat according to geographical origin (Sacco et al., 1998) and to varietal origin (Brescia et al., 2002).

When using MAS on biological material considerations about possible destruction of the material must be done, (see 3.3). Hence, a preliminary experiment was conducted in order to optimize signal with a minimum of seed destruction. A spinning rate of 2000 Hz gave optimum signal with elimination of water spin side bands in the region of interest (0-6 ppm) concomitant with minimum destruction of grain, as determined by visual inspection. Another question addressed in preliminary studies was the use of solvent and exposure time to solvent. Deuterated water (D_2O) was chosen as it resulted in a minimum of seed damage and equals the most the natural environment. The use of DMSO gave glassy, fragile seeds. A steady state of water exchange was found after 2 hours, after which no further change of spectra could be observed. Therefore, all samples were left for a minimum of 2 hours before sampling. Except for the very early seeds, the seeds were too thick to be in the rotor, hence the seeds were halved along the crease (see insert in **Figure 4-17**).

As seen from **Figure 4-17**, the ^{1}H HR MAS NMR experiments on single seeds lead to informative spectra. At maturity, the seed is almost a solid with a very rigid, crystalline matrix leading to fewer, broader but more distinct resonances. At the early grain filling stages (9 DAF) the spectra are characterized by many, small mobile metabolites seen as multiplets. The spectra are characterized by four major sub-regions: The α-anomeric region (**Figure 4-17, A**) including a strong signal from unsaturated lipids, the β-anomeric region (**Figure 4-17, B**), the carbohydrate region 3-6 ppm (**Figure 4-17, C**) which contain signals from the pyranoses, unsaturated lipids, the H_α and H_β from the amino acids. The last regions is the 'lipid' region from 0.5-3 ppm

(**Figure 4-17, D**) which contain low-intensity signals from the protons in the aliphatic side chains of amino acids and proteins, but is mainly dominated by lipids in mature flour spectra.

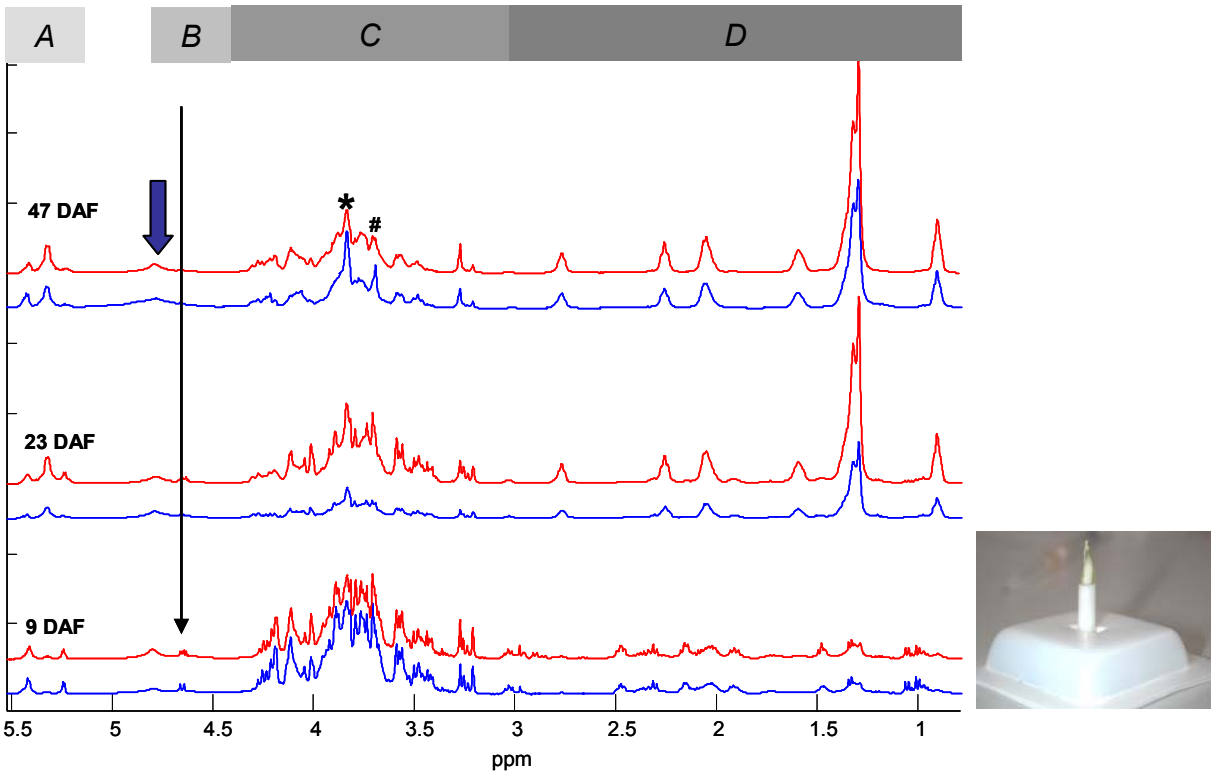

Figure 4-17. ^{1}H HR MAS NMR spectra of Cork (blue) and lys5f (red) at 9 (bottom), 23 (middle) and 47 DAF (top) on single seeds. The overall regions A-D indicate the major resonances found in this region: A) α-anomers and unsaturated lipids B) β-amomers, C) pyranoses and D) lipids. The fat blue arrow indicates the reminiscence of the water peak. The * and the # indicates two interesting carbohydrate peaks discussed in the text. The inserted picture is half an immature seed in the 4-mm rotor.

It is puzzling that the lipids dominate the spectra as heavily as they do, since fat and lipids only constitutes around 3% in the mature seed (see **Table 2-1**). However, it indicates the higher level of fat and lipids found in *lys5f* compared to the control (Munck et al., 2004), and even more that lipid-protons are more mobile and hence more ^{1}H NMR-sensitive than the protons found in rigid molecules like e.g. starch. In a study of durum wheat flour the same high levels of lipids were found (Sacco et al., 1998) but not commented on. In order to pursue this lipid indication, a determination of the fatty acids was conducted. However, these results will be dealt with in a subsequent paper and are not the scope of this thesis.

The β-glucose at 4.64 ppm (region B) is present at 9 DAF but absent at 47 DAF indicating that β-glucose is no longer present or no longer mobile and hence, NMR insensitive at 47 DAF. It must be noted that the β-(1→3) anomer at 4.75 ppm and β-(1→4) anomer at 4.54 ppm could not be retrieved in

the spectra partly due to the broad, neighboring water peak at 4.78 ppm and partly due to immobility (see section 4.3.3), wherefore the quantification of compounds such as both β-glucan and rigid structures such as starch was not possible. The α-anomeric triplet peaks (region A) from 4.98-5.36 ppm increase during grain filling mirroring mainly the accumulation of starch and partly the unsaturated lipids: a part of the lipid signal from unsaturated lipids is also found at 5.32 ppm interfering with the α-(1→4) peak at 5.36 ppm. Within region C especially two peaks at 3.83 ppm (denoted with a star in **Figure 4-17**) and a peak at 3.69 ppm (denoted with the cross in the figure) show different accumulation patterns between *lys5f* and the control, and the peaks have higher intensity in the control than *lys5f* at 47 DAF. These peaks also appear in loading plots related to a PCA performed on the last five harvests (from 23 DAF and onwards), see below for further discussion. No calibrations were performed on the single seed NMR spectra, as the compounds of interest (the carbohydrates) were not fully mobilized. Mobilization was enhanced in the following experiment by heating the samples.

4.3.6 ^{1}H HR MAS NMR on flour

In order to mobilize all of the crystalline compounds (especially starch), a ^{1}H HR MAS NMR experiment was performed on flour samples from 9, 13, 23 and 47 DAF. The experiment was conducted at 75^{o}C to ensure full gelatinization of starch. Furthermore, the samples were exposed to a spinning rate of 7 kHz. Flour spectra of the three accessions during early, middle and late grain filling for the region 3-6 ppm are shown in **Figure 4-18**. Compared to the seed spectra, the flour spectra showed higher intensity and better resolution as expected. The recorded barley flour spectra appear quite similar to wheat flour spectra spun at 5 kHz in a phosphate buffer (Amato et al., 2004) and could hence be regarded as a typical cereal flour spectra, **PAPER B**.

4.3.7 Temporal analysis of NMR flour data

The overall picture is the same for seed and flour spectra: At 9 DAF peaks are present, which are no longer seen at 47 DAF especially in the region 3.3 to 4.3 ppm. These peaks are probably related to small mono- and disaccharides, as well as other small non-carbohydrate metabolites.

The intensity of the peaks at 3.83 and 3.69 ppm are very different for the control barley and *lys5f*. The peak at 3.69 ppm is also inferior in intensity in *lys5f* in the flour at 47 DAF as it was for seeds. A closer view of the β-glucose region shows the same features found for seeds just better resolved: the control variety Cork has the highest intensity of β-glucose, β-(1→3) and β-(1→4) at 47 DAF and also higher than *lys5f*.

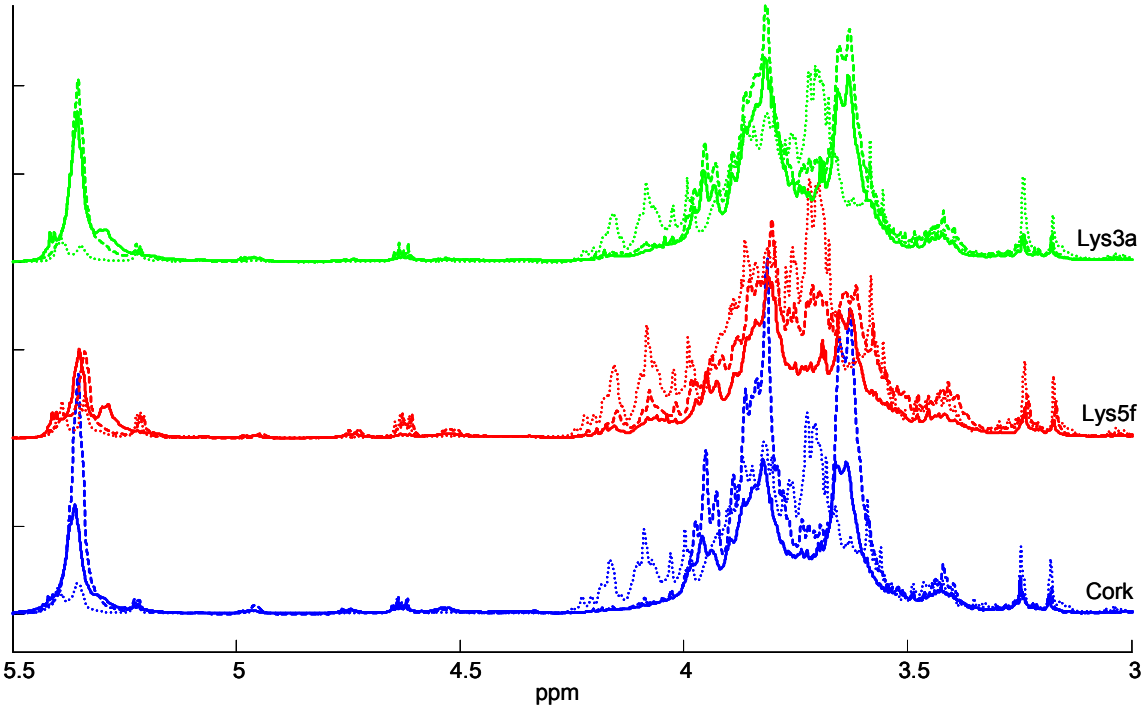

Figure 4-18. The NMR region 5.5-3 ppm covering the anomeric and the carbohydrate region in flour from 9 DAF (dotted line), 23 DAF (broken line) and 47 DAF (full line).

In general, the intensities for the three β-anomers are highest at 23 DAF concomitant with the highest content of β-glucan found in *lys5f*. The poor visual quantification of β-glucan from the spectra was retrieved as very poor PLS-calibrations made to β-glucan and the NMR region between 3-6 ppm (see 4.3.7 below). On the contrary, a fair iPLS calibration to starch was made and revealed two intervals 5.2-5.4 ppm corresponding to the α-anomeric peaks, and an interval covering 3.87-3.65 ppm and hence the two resonances described above. These resonances are indicative of starch (Nilsson et al., 1996).

A PCA (full cross validated) in the region 6-3 ppm could less clearly classify the three accessions compared to the same region for seeds **Figure 4-19**, in which *lys5f* could be separated from the control and *lys3a*. However, a temporal separation in the seed and the flour PCA along PC1 can be identified. In the seed samples, the early seed development stages 9-16 DAF form a distinct group. This fits well with the chemical analysis showing that the differences in gross accumulation of storage compounds takes place from 20 DAF and onwards.

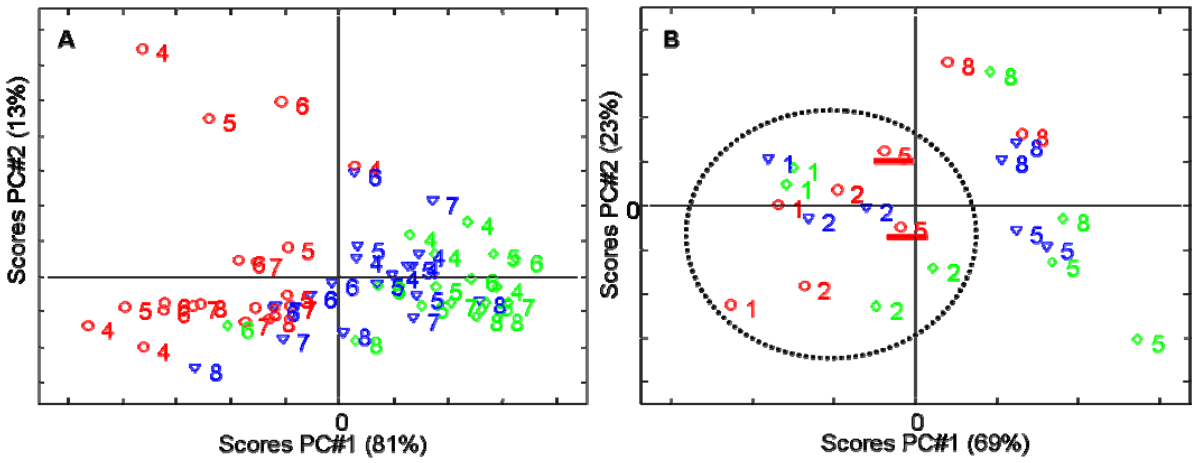

Figure 4-19. PCA analysis of 1H HR MAS NMR spectra of single seed (A) and of flour (B). The single seed PCA is based only on the samples from 23 DAF ('5') and until 47 DAF ('8'). Red circles= lys5f, blue triangles=lys3a and green rhombs = the control variety 'Cork'. The circles encompass the early part of grain filling, 9-13 DAF ('1' and '2') and in the case of *lys5f* also 23 DAF ('5').

Hence, only from 20 DAF ('4' in **Figure 4-19a**) to 47 DAF ('8' in **Figure 4-19a**) are used for the PCA analysis. Interestingly, in the flour spectra the *lys5f* samples from 23 DAF ('5' in **Figure 4-19b**) groups together with the early samples. This could be explained by the loading plots of the flour spectra (not shown): The loadings revealing that the positive part of PC1 equal to the late grain filling was determined by peaks at 5.36 (α-(1→4)) and 3.64 ppm and hence, are starch related, **PAPER B**.

It is not possible to assign every resonance in the ^{1}H HR MAS NMR spectra due to the overlapping of signals especially in the carbohydrate region. The assignments done were based on literature (Nilsson et al., 1996; Petersen et al., 2000; Amato et al., 2004) and confirmed by 2D COSY, TOCSY and HSQC spectra. 2D spectra enable assignment of peaks although the complexity of heterogeneous systems such as barley flour hinders total assignment as seen in the region 3-4 ppm where the resonances are like a smear (**Figure 4-20b**). The 2D spectra were acquired for *lys5f* at 9 DAF and 47 DAF. The α-(1→4) peak is clearly seen in the ^{13}C-HSQC spectra at 5.36 ppm for both ^{1}H and 102.1 ppm for ^{13}C at both early and late grain filling. The β-(1→3) and β-(1→4) peaks are only present at 47 DAF (blue spots in **Figure 4-20a**).

Unfortunately, no 2D spectra were acquired at 23 DAF, although this is the time point with maximum intensity in the carbohydrate region and the onset of β-glucan synthesis appears.

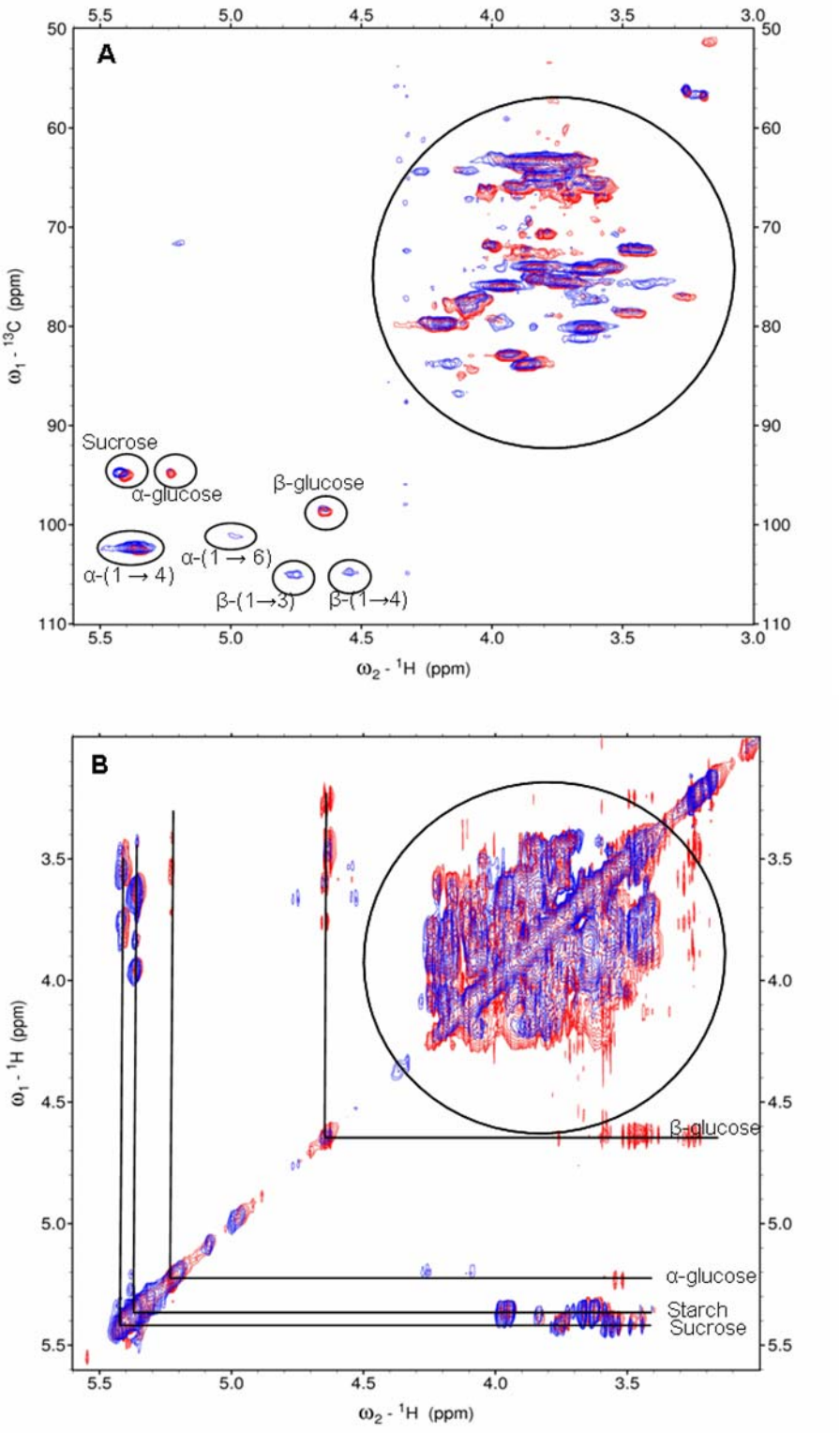

Figure 4-20. 2D experiments of *lys5f* barley flour from 9 DAF (red) and 47 DAF (blue). ^{13}C-HSQC spectra (A). The corresponding TOCSY spectra (B). Only sites with proton chemical shifts in the region 3-5.6 ppm are shown as these are the regions carrying information about the carbohydrates.

It could have been of interest to more closely follow the grain filling using 2D experiments and also to see whether the β-(1→3) and β-(1→4) would have been present at 9 DAF in the control variety Cork as seen from the 1D ex-

periment. Unfortunately, the 2D experiments are quite time consuming as acquisition time for one experiment was 17 hours thus, restricting the numbers of experiments possible to perform.

4.3.8 Calibration of NMR flour analysis to bulk carbohydrates

Calibrations to the NMR flour spectra confirmed the visual inspections of the spectra: The starch iPLS for the spectral region 3-6 ppm revealed four NMR spectral regions performing better than the global model (r^2=0.85 and RMSECV= 6.48). In particular, the iPLS models for the α-anomeric region between 5.29-5.40 ppm (r^2=0.86, RMSECV= 5.9), and the carbohydrate region 3.56-3.67 ppm (r^2=0.86 and RMSECV= 5.6) confirming these regions are related to starch (Nilsson et al., 1996).

In contrast, the global iPLS model of the spectral region 3-6 ppm for β-glucan performed markedly worse than the starch calibration (r^2=0.45, RMSECV= 4.57) even when using 4 PLS components. The best iPLS model used the region 3.39-3.56 ppm (r^2=0.56 and RMSECV= 4.08). However, in all the plots the high β-glucan values of *lys5f* were seen as outliers. Hence, a calibration to only Cork and *lys3a* was performed. This resulted in a much improved global model for the spectral region 3-6 ppm (r^2=0.81, RMSECV= 0.84) using 2 PLS components and 16 samples. Two intervals performed better: 2.98-3.09 ppm and 3.44-3.55 ppm with equal r^2=0.87, RMSECV= 0.71). However, none of the iPLS models to β-glucan selected the region between 4.5 and 4.8 ppm, which contain the most obvious choices of resonances indicative of β-glucan. For some yet unknown reason, the β-glucan in *lys5f* is NMR 'invisible' at seed maturity, **PAPER B**.

This NMR-'invisibility' could be due to differences in the structural composition of β-glucan in the mutants compared to the normal barley such as long consecutive sections of β-(1→3) or β-(1→4) linked glucans that cannot be detected by ^{1}H NMR (Pelosi et al., 2006). It is also possible that the 'invisible' β-glucan in *lys5f* is related to the cell wall conformation, which probably is of thicker nature than seen in Cork and *lys3a*. Interestingly, tt was possible to extract the β-glucan from *lys5f, lys3a* and Cork using the Gluca-gel™ procedure (Morgan and Ofman, 1998), but ^{1}H NMR spectra of the extracts could not reveal any differences between the genotypes. It is difficult to relate solubility to NMR sensitivity: liquid state ^{1}H NMR and solid-state ^{13}C NMR proved that soluble and insoluble spectra of purified barley β-glucan were essentially the same (Johansson et al., 2004). Another explanation of the NMR invisibility of β-glucan in the mature *lys5f* could be the location of β-glucan in the cell wall and the rigidity of the structure between β-glucan, the protein matrix and the pentosans (see 2.1.3). The location of β-glucan in the cell wall and cell wall environment could thus be different in *lys5f* compared to the Cork barley genotype. This might affect the NMR sensitivity of the β-

glucan in *lys5f.* It awaits further analysis to determine whether this 'invisibility' is genotypic dependent or related to the very high content of β-glucan leading to different structural and conformational behavior of the β-glucan.

Other types of NMR spectroscopy has proved efficient in revealing structural information about β-glucans: structural analysis of soluble oat β-glucans (Westerlund et al., 1993) was studied using ^{13}C and ^{1}H NMR of isolated β-glucan, 2D-liquid ^{13}C NMR of isolated β-glucan of oat bran proved that the glucose units were joined only by (1→3) and (1→4) linkages (Johansson et al., 2000), and Wood et al., (1994) found using liquid ^{13}C that in general, the β-glucan of barley, rye and oat were similar with only minor differences in the ratio of cellotriose:cellotetraose units. It was not possible to find literature in which NMR has been used for the quantification of β-glucan in heterogeneous samples such as seeds or flour.

4.3.9 NMR imaging (MRI) of mature barley seeds

There is a vast amount of literature on the use of MRI and various seeds mainly involving hydration patterns: moisture distribution studies in developing seeds, such as rice (Horigane et al., 2001), wheat (Jenner et al., 1988) and barley (Glidewell, 2006). These studies showed that water flow in seeds occurs in localized regions of the grain and is not homogenously distributed in the seed.

It was unfortunately not possible to do MRI on the developing barley seeds, because of lack of growing plant material. Instead, the mature seeds of Cork and *lys5f* were studied with the aim of analyzing the relaxation times in the contrasting genotypes in different parts of the seed, **PAPER C**. In order to be able to acquire signal from the barley seeds, they were hydrated for a week and their water uptake were weighted. In contrast to Cork, *lys5f* took up much more water, due to the hygroscopic nature of β-glucan. Hydration and desiccation studies of seeds monitored by MRI are plentiful: a non-uniform distribution of water and water mobility was found in barley and soybean seeds (Kano et al., 1990), and in developing barley seeds, where a bright core indicated different water mobility compared to the rest of the seed (Glidewell, 2006).

The intensity of proton signals from Cork and *lys5f* after six days of hydration is seen from **Figure 4-21**. The mutant *lys5f* has a markedly higher intensity and this is in accordance with a higher water uptake measured by weight (data not shown).

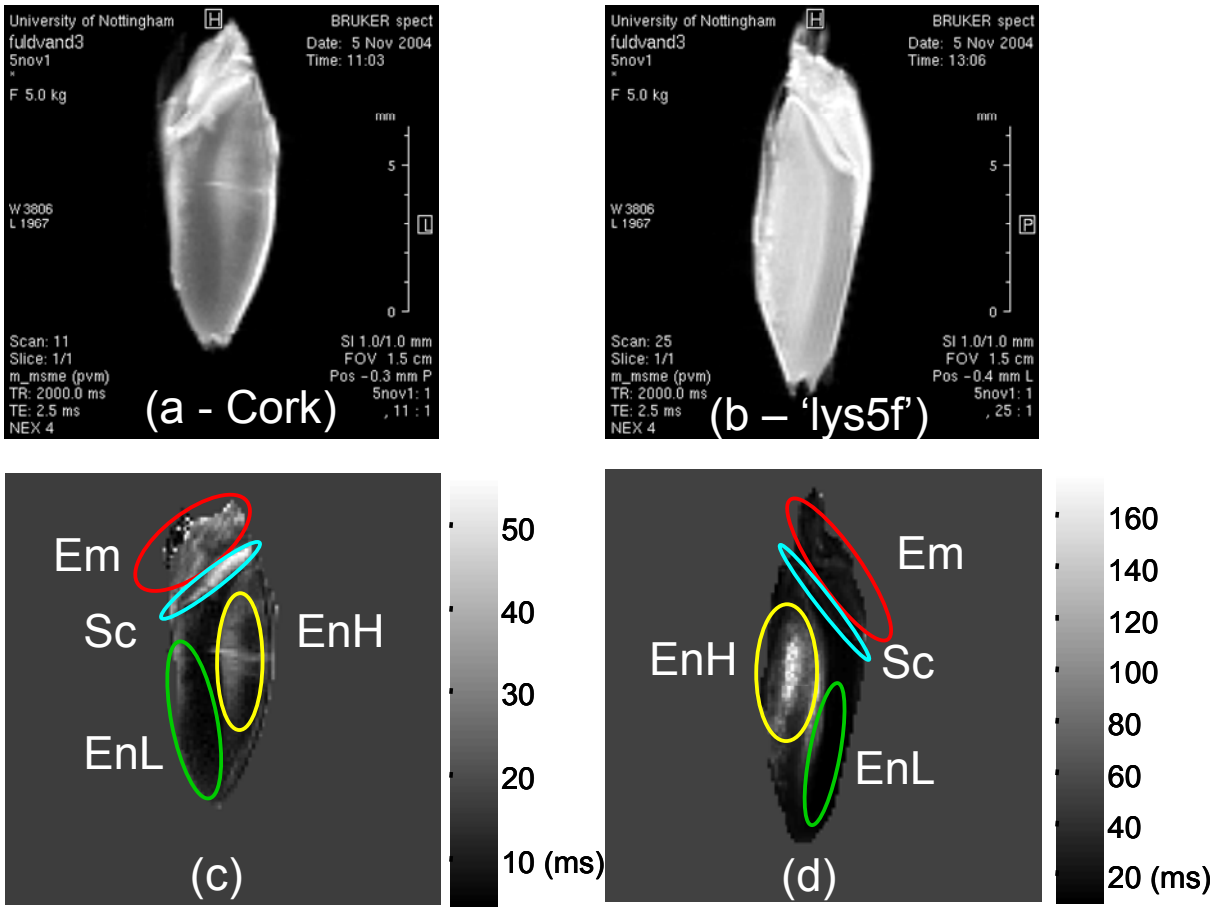

Figure 4-21. Proton intensity in a Cork (a) and a lys5f (b) seed. The four regions defined in the Cork seed (c) and the lys5f seed (d). Em= embryo, Sc=scutellum, EnH= endosperm high intensity, and EnL=endosperm, low intensity. Images from Seefeldt et al., (2007).

Relaxations studies like this, in which water mobility is related to a various parameters are very common: correlations between relaxation times and water content (Dinola et al., 1988), coat texture (Marconi et al., 1993), viability (Krishnan et al., 2004b; Krishnan et al., 2004a; Agosti et al., 1991) and chemical stress (Miedziejko, 1997) in seeds. The relaxation studies have be used to describe different states of water. In lettuce seeds the differences in water status was described by a three state water model corresponding to bound, solid and free water (Dinola et al., 1988) and in wheat with a two-phase model (Gruwel et al., 2001), and a two-phase model in dry wheat seeds, whereas germinating and non-germinating seeds showed a tri-phasic model of T_2 relaxations (Krishnan et al., 2004b). The relaxation data from hydrated Cork and *lys5f* seeds revealed two-state water model. Furthermore, differences in relaxation times were found within the various parts of the seed, **Figure 4-21**; with the embryo having the highest water mobility, and the endosperm the lowest water mobility, see **Table 4-4**. Genotypic differences of water mobility were also found within the different parts of the seed. *Lys5f* had higher water mobility throughout the entire seed compared to Cork

except for the scutellum. Especially, in the bright core, *lys5f* had very high water mobility as determined by very long T_2 relaxation times (>100 ms). (Oscarsson et al., 1997) stained barley endosperms differing in cell wall size with Acid fuchsin and Calcoflour White and found that accessions with high content of β-glucan had thicker cell walls especially around the ventral crease. The high water mobility in *lys5f* could hence be accounted for by thicker cell walls, **PAPER C**.

Table 4-4. Relaxation times estimated in four different regions of the seed in Cork and lys5f. Data from Seefeldt et al., (2007).

Compartment	Decay Rate (Standard Deviation)	
	Cork (Fig. 1a)	***'1101' (Fig. 1b)***
Embryo (Em)	22.2ms (2.9)	25.8ms (6.9)
Scutellum (Sc)	50.9ms (5.4)	28.2ms (9.2)
Endosperm Low intensity (EnL)	6.9ms (0.8)	9.5ms (0.6)
Endosperm High intensity (EnH)	25.7ms (3.8)	152.4ms (27.4)

MRI was also used to analyze the water holding capacity of the seeds during a desiccation process. The hydrated seeds were placed in the magnet together with silica gel. Each six hours the seeds were scanned in a total of 36 hours in order to follow the desiccation processes, **Figure 4-22**. Desiccation studies have revealed that moisture distribution in wheat seeds are not uniformly distributed at an equilibrium (Ghosh et al., 2004), since the embryo contained most of the mobile water. The reduction of water was also found to be evacuated non-uniformly from rice during drying (Ishida et al., 2004).

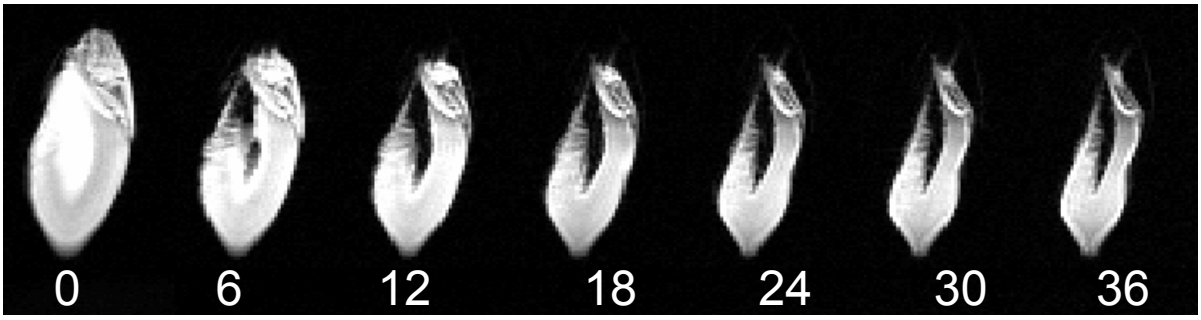

Figure 4-22. Seven time-points during desiccation of *lys5*f seed. The numbers refer to hours of drying. Images from Seefeldt et al., (2007).

The barley seeds from the control variety and *lys5f* also showed a non-uniform distribution of water as well as a non-uniform loss of water, in which the endosperm looses water fastest, whereas the embryo retains water the longest, **Figure 4-22**. The desiccation process appears thus to be a two-step process where most of the water is lost at a fast rate until a certain point at which the water is so immobile that further desiccations occurs very slowly.

This is also observed in castor bean (Morris et al., 1990) and in barley (Ishida et al., 2004). The mode of drying appears to be non-uniform across the seed since the embryo has a high signal even after 36 h of drying.

Table 4-5. Average decay rate and standard deviation (in parentheses) for the wet (0 h after drying) and dry (36 h after drying) seeds based on ten randomly, selected pixels from each of the four marked compartments as indicated on Figure 4-21. Data from Seefeldt et al., (2007).

Seed	Condition	Embryo (ms)	Scutellum (ms)	Endosperm Low intensity (ms)	Endosperm High intensity (ms)
Lys5f	Wet, (0h)	24.5 (8.3)	22.5 (5.6)	11.1 (1.1)	35.5 (8.1)
Lys5f	Dry, (36h)	17.2 (6.4)	23.4 (7.1)	7.1 (1.3)	6.7 (1.0)
Cork	Wet, (0h)	21.2 (5.9)	18.1 (1.6)	6.6 (1.2)	15.8 (1.7)
Cork	Dry, (36h)	20.1 (7.0)	21.1 (2.8)	*)	5.4 (2.7)

*) Signal strength for this region of the image is insufficient for accurate fitting.

It is verified that the embryo and scutellum is less affected than the endosperm, **Table 4-5**. Especially the high intensity region in the endosperm around the ventral crease shows a marked decrease in relaxation rate between the wet and dry seed. The mobility of the water in the high intensity region of *lys5f* is decreased more predominantly than in Cork during drying, probably because the water in the standard barley Cork was much less mobile even in the wet seeds, **PAPER C**. The endosperm loses water in a non-uniform way from top to bottom instead of from outside in. In conclusion, genotypic differences in hydration pattern and in the desiccation processes were found, as well as non-uniform distribution of water within the seed.

4.4 Conclusions on endosperm mutant analysis

It was not in the present experiment possible to retrieve an effect of the drought treatment on the seed weight, in any of chemical values recorded by analysis or by spectroscopy, although it was demonstrated that the drought period had an effect on photosynthesis during the treatment. The mutants were less affected in photosynthesis response to the drought compared to the control variety Cork. Further experiments are needed to verify the hypothetic possibilities previously discussed that an adaptive stress response is another pleiotropic effect of the mutations. The lack of impact of the drought event on the seed composition and seed weight could be explained by early onset of senescence in the treatments. During senescence nutrients are relocated to the seed. The drought period induced senescence and hence

increased the remobilization of assimilates to the grain, counteracting the reduced grain filling rate and duration normally connected with temperature and drought stresses. In order to investigate the full response of the drought treatment, the entire biomass of the plants as well as the total yield of the plants should ideally have been measured.

The analysis of β-glucan synthesis in the mutants clearly demonstrated that *lys5f* had a much higher rate of β-glucan synthesis in an early stage of grain filling compared to the control and *lys3a*. However, the high rate of β-glucan was on the cost of starch synthesis, which was much lower for *lys5f* compared to the other two genotypes. The mutants were also impaired in their freeze-dry matter weight compared to normal barley mainly due to lack of starch and smaller grain size. The starch in *lys5f* and *lys3a* contained less amylose in % compared to the control variety. The early onset of the major effect of *lys5f* gene and the late onset of the *lys3a* gene were confirmed by studying relative β-glucan accumulation, starch accumulation and freeze-dried evaporated water content compared to the control barley during seed development.

It is seen that in *lys5f* β-glucan accumulation takes place from 13 DAF, and is opposite the starch accumulation. The increase in β-glucan content is mirrored by the increase in water content relative to the control variety as will be discussed in the next chapter and in **Figure 5-1**. Apparently, *lys3a* has from 9-13 DAF a faster starch accumulation rate compared to the control as seen in the relative increase.

The NIR and IR spectra facilitated in distinguishing genotypic temporal changes during seed development. Both spectral types showed that the sample spectra from 9-16 DAF have a different appearance compared to the later seed samples. This could also be retrieved in the score plot of the PCA analysis, showing a distinct cluster of the 9-16 DAF samples in both types of spectra. In the IR region between 1200-700 cm^{-1} the spectral form of *lys5* is different from that of *lys3a* and normal barley. A probable β-glucan peak at 900 cm^{-1} was identified only in *lys5f* and not in the control or *lys3a* genotypes.

Two regions in the NIR spectra show very clear genotypic separation: 1680-1820 nm and 2260-2380 nm. From 9 DAF the features of the genotypic patterns were outlined and from 13 DAF the genotypic spectral patterns were manifested. The NIR spectra were highly reproducible and finely tuned for each genotype. Such finely tuned patterns require gentle, spectral data inspection in order to reveal the detailed, genotypic patterns. This confirms the observation by (Munck, 2007) studying the NIR spectra of ripe seeds of the same mutants. PCA analysis on the NIR spectra in the two regions could not retrieve the same finely tuned genotypic differences. Correlations to β-

glucan, amylose and water proved that NIR and IR spectra gave high correlations to β-glucan (r^2=0.94 for the region 1194-1240 nm) and r^2=0.96 for the entire IR spectra. NIR gave the better predictions to evaporated water and amylose compared to IR.

^{1}H HR MAS NMR on single seeds and on flour gave very informative spectra with many peaks. Only the carbohydrate and anomeric spectral regions have been considered in **PAPER B**. Visual inspection of the seed NMR spectra showed that less intensity in the region 3-6 ppm and the intensity of the β-glucose related peaks were higher in Cork than in *lys5f* in the single seed spectra. Mobilizing the complex endosperm compounds using higher temperature and elevated spinning rates increased the resolution of the spectral region between 3-6 ppm. However, the intensity of the β-(1→3) or β-(1→4) peaks still proved to be higher in the control variety at maturity compared to *lys5f*. Hence, poor calibration to β-glucan was found. On the other hand, a good resolution of the carbohydrate region and anomeric region resulted in good correlations to starch.

2D experiments showed distinct profiles for 9 DAF and 47 DAF and assignment of the α- and β-glucose as well as starch and carbohydrate residues in β-glucan could be made. The complexity of the spectra makes ^{1}H HR MAS NMR suited for fingerprinting analysis. It is worth remembering that cereal seeds or cereal flour is not a simple, chemical model system, but a highly heterogeneous material and thus NMR reveal trends and fingerprints rather than specific assignment due to overlapping and broad signals. ^{1}H HR MAS NMR on single seeds lacked robustness in quantifying β-glucan and starch. But single seed NMR was very useful for classification of the mutants and to distinguish the temporal differences during grain filling. Although the classification is guided by the differences in starch, the pleiotropic effects are seen throughout the entire NMR spectrum and separating all three of the accession in a PCA score plot.

5 Introducing spectroscopy as a tool for observation of the barley phenome

'Science in its purest form is the reduction of the behavior of a system to a set of mathematical rules that define it' (Sweetlove et al., 2003). This is a much erroneous conclusion. Science needs the holistic approach to study systems in order to fully understand the complexity and beauty of a system – in this study exemplified by the barley spectral endosperm model.

The work of Munck et al. (2001), (2004) and (2005) demonstrated for the first time the significance of visual spectral inspection to overview the whole pleiotropic effect of single mutant genes on the phenomic level. These genotypic spectral signatures were shown to be based on physio-chemical patterns expressed by molecular vibrations of the chemical bonds and could be visualized by chemometrics. From this work, a hypothesis evolved that the phenotype is a physio-chemical imprint of a self-organizing network in the cereal seed endosperm (Munck et al., 2001; Munck, 2003; Munck, 2005; Møller Jespersen and Munck, 2008). The remarkably high reproducibility of the NIR spectra of *lys5f*, *lys3a* and the control variety during seed development demonstrates the biological self-organizing principle that was interpreted by Munck and Møller (2005) and by Munck (2007) as the system consisting of enzymes and cellular compartments that executes the codes from DNA depending on developmental stage and environment. The outcome of the system is probabilistic but can be observed as a barcode of chemical bonds in the NIR spectra. The biological system acts in a probabilistic way determined by chemical affinity, but the outcome appears to be deterministic as interpreted from the high reproducibility seen in the NIR spectra (Munck, 2007). The self-organizing and probabilistic seed endosperm is mediated by water. Water is the essence of life (*Aqua vitae*) as every enzymatic process is dependent on water activity and the dipolar effect of water that facilitates the self-organizing and irreversible chemical reactions that builds up a biological cell. The activity of the enzymes results in changes in the metabolome that is transferred to the phenome. Turning to the genotypes in this study, some very interesting features on water is observed.

The control variety Cork has a higher fresh seed weight compared to *lys5f* and *lys3a* (See **Appendix I**), but the water content is markedly higher in

lys5f and *lys3a* compared to the control, **Figure 5-1**. The high content of water in the mutants are due to two different features: *lys5f* is dominated by a high content of β-glucan that readily takes up and releases water, in *lys3a* it is due to a high content of water soluble proteins on the cost of the hydrophobic protein hordein (Jacobsen et al., 2005). As seen from **Figure 5-1**, the water content in *lys5f* relative to the control variety increases dramatically from 16 DAF concomitant with the major accumulation of β-glucan (**Figure 4-4**, **Appendix I** and **II**), whereas *lys3a* first increases in water at 23 DAF. This is probably concomitant with the accumulation of water soluble proteins on the expense of hordeins (Jacobsen et al., 2005) that was not determined in the present study. In agreement with the findings of the major effects of gene onset in chapter 4 (**Figure 4-6** and **Figure 4-7**), *lys5f* has an early gene onset, whereas *lys3a* has a late gene onset during grain filling.

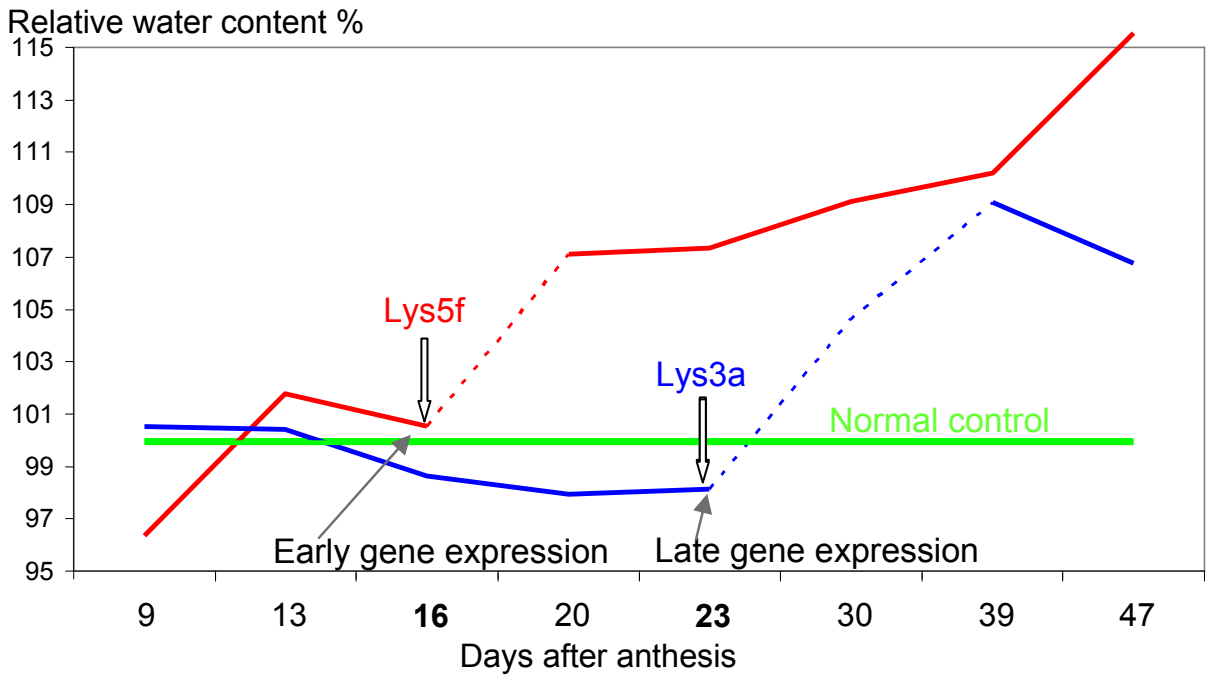

Figure 5-1. The relative water content of the mutant genotypes compared to Cork. The timing of the manifestation of water differences is marked with arrows.

The water holding/releasing ability of *lys5f* was also demonstrated in the MRI hydration/desiccation experiment in which more intense images were observed in *lys5f* compared to Cork, but also a faster loss of water during desiccation. The differences in proton intensity in the MRI experiment are speculated to reflect different types of water (**PAPER C**). However, one should be careful to equal higher intensity with higher concentration, when no internal reference is used. In the hydration experiment, *lys5f* was found to take up 42% more water during germination than Cork, measured by weight increase (**PAPER C**), indicating that a higher water content was in fact reflected by the higher magnetization intensity. Hence, the MRI experiment of soaked

lys5f seeds in water showed that the high content of β-glucan leads to more water and more mobile water indicative of a higher water activity and thus different enzymatic conditions compared to the control variety.

.

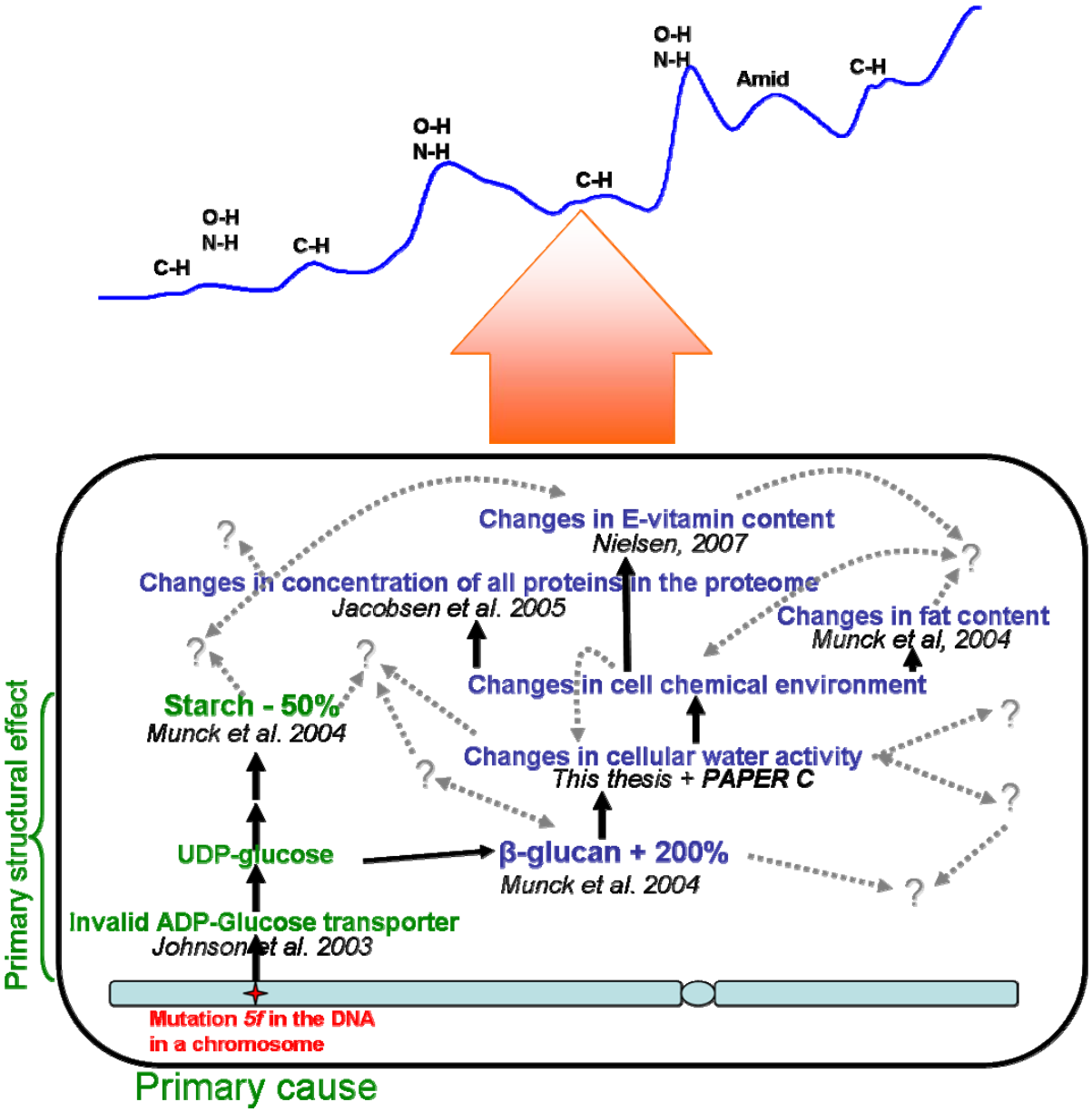

Figure 5-2. The primary and secondary effects induced by a single mutation in *lys5f* endosperm. The green path symbolizes the primary structural effect of the gene disruption. However, as described in the text above, unexpected pleiotropic effects of the mutation were found in various compounds of the endosperm. The broken arrows indicate some of all the yet unknown interactions there might possible be, and most likely many more broken arrows could have been drawn. The entire phenome can be overviewed using NIR as a pattern of chemical bonds. Modified after Møller Jespersen and Munck (2008).

The MRI results together with the analysis of the gene onset in **Figure 5-1** have now confirmed that water content is an important part of the physiochemical fingerprint of the intact developing seed: the effect of the water

content is mediated through changes in water activity that influences physiological changes of the enzyme activities in the internal cell milieu of the endosperm tissue. Chetverikovs statement in 2.3.1 that a gene effects by pleiotropy the entire soma, now fits perfectly well: Differences in water concentration and water mobility may lead to very different cellular environments. Hence, the mutations in *lys5f* and *lys3a* indirectly lead to changes in water activity. This in turn has an impact on the enzymatic processes as well as the energy levels in the compartments. A change in cellular water content, and more important in water mobility change the entire constitution of the cell (Møller Jespersen and Munck, 2008), (Munck, 2007) and hence the entire outcome of the mutation! This self-inflicting system is depicted in **Figure 5-2**. The original structural mutant *lys5f* and the regulatory mutant *lys3a* are isogenic lines of Bomi, but the single-gene alterations lead to a range of unpredictable changes that are not easily identified by classical biochemical analysis and molecular path-modeling: this includes the extreme levels of β-glucan, changed water content and activity, changed protein composition, and changed fat and composition of E-vitamin (Møller Jespersen and Munck, 2008), **Figure 5-2**.

It follows from the above discussion that it is too simple to refer to a mutant based on one phenotypic trait such as shrunken endosperm, when the same mutant can be identified as high lysine, as low in carbohydrates or having an opaque appearance all reflecting the pleotropic effects mutations can cause (Jacobsen et al., 2005). Such major pleiotropic effects have also been studied in potato; a manipulation of carbohydrate metabolism in potato led to other morphological phenotypes such as altered flowering, abnormal organ development, and early senescence (Lytovchenko et al., 2007). The many pleiotropic effects observed from single mutations suggests that the starch metabolic enzymes operate in complexes (Tetlow et al., 2004) and thus it is impossible to foresee in detail what phenomic changes even single mutations will induce especially when considering different gene backgrounds. This explains why the attempt to improve yield by changing traits related to yield at a low level of organization often has ended in failure. It is often not possible to identify a linear chain of events progressing from the plant biochemistry or cell physiology to the final crop yield (Slafer, 2003). So far the paradigm has been: 'The complexity of the plant metabolic network is such that it is not yet possible to construct predictive models of metabolic performance that allow rational metabolic engineering of plant genomes' (Sweetlove et al., 2003). However, the simple technique of NIR has proven effective in obtaining a coarse overview of the entire outcome of the genome in interaction with environment as a digitized, spectral phenome (Munck, 2007). This is seen as a pattern based on the physio-chemical constitution of the genotype and identified as molecular vibrations in the NIR spectra.

When working with introducing alteration in a genome whether it is through mutations or transgenomics, this discussion has now pointed to an approach to overview the outcome of the gene alteration on the phenomic level. Firstly, it must be realized that the biological system is self-organizing and contains some indeterminacy that cannot be foreseen. Thus, in order to handle the many pleiotropic effects together with the indeterminacy of the self-organizing system, a complementary top-down approach to study the outcome must be used (Munck, 2007). This involves spectroscopic fingerprinting methods that can be focused on by using chemometrics. Gene classification based on vibrational spectra (Munck et al., 2004) to reveal the molecular state could be the first step in a procedure revealing new pathways of synthesis and gene regulation, like the one identifying β-glucan-compensating starch mutant *lys5f*. This can then be followed by a bottom-up strategy like more tedious methods of transcriptomics and proteomics (Jacobsen et al., 2005), like the approach that detected the invalid AGPase transporter in *lys5f* (Patron et al., 2004). Such a combined strategy is useful for both basic research as well as for plant breeding purposes.

The variation of single endosperm analytes such as protein (N x 6.25) is found to be very large (e.g. from 6 to 16 %) between single seeds of the same homozygotic wheat genotype grown in a field trial (Nielsen et al., 2001) and major variations in β-glucan content is found within seed positions in barley spikes (Zhang et al., 2002). This large variation between single seeds can explain some of the off-set between replicates seen in **Figure 4-11** and **Figure 4-12**. Each sample in the figures consists of approx. 50 seeds from two spikes. Sampling errors are found to be greatly underestimated introducing more error than the following analytical and data-analysis steps (Tønning et al., 2006). This theory of sampling (TOS) leads to the requirement of very careful sampling methods. This is certainly valid for univariate parameters. However, complex parameters or food functionality such as malting and baking quality can now be defined by NIR spectroscopy and sorted for in industrial scale on single seed basis (Löfqvist and Nielsen, 2004). A large variation in baking quality was shown even between single seed batches originating from the same homozygotic wheat variety grown in the same environment (Munck, 2008). However, when looking at the multivariate fingerprint that signifies the whole seed genotype as represented by spectral phenome using NIR, seed sampling is no longer an issue as the NIR spectra of single genetic homozygotic seeds from the same field contain information about the total composition of genetic and environmental impact as a reproducible pattern that is largely independent of sampling (Møller Jespersen and Munck, 2008). The NIR spectra from a population of homozygotic seeds on the same field are so to speak a sum of the genetics, all the biosynthetic processes and their interactions unique for each genotype grown in a specific environment.

6 Perspectives and conclusion

The semifield experiment facilitated a controlled environment with regards to precipitation, and compared to greenhouse experiments it ensured good plant health and comparable growth conditions to that of plants in the field. Drought stress appears to be a very complex mechanism in plants and this study showed that the barley has a large compensating ability to overcome drought stress, when growth conditions are optimal before and after the stress. When studying the effect of climate changes more than one factor should ideally be studied: drought is often related to high temperatures and solar radiation also plays a role on the growth of plants. Hence, the experimental set-up in this study was too simple to investigate the impact of climate changes with regards to water stress.

The use of vibrational spectroscopy in the agriculture and food industries is already widely used but mainly for the detection of single analytes (Møller Jespersen and Munck, 2008). However, as described in this thesis, the use of e.g. NIR has much further applications. In every case of complex trait analysis in foods or more specific in cereals, spectroscopy in combination with chemometrics can aid in classification or in identifying few, relevant parameters that are correlated to more complex traits. So far the use of IR and NMR has mainly celebrated successes within the structural analysis of compounds. However, using the spectral outcome as fingerprint methods enables also IR and NMR to be used for classifications. New, easy sample handling like the IR ATR-sampling opens for a more widespread use of IR. NMR is still not widely used due to the requirement of highly skilled operating personal, but the first in-and online NMR prototypes for the industry have been developed (Dyrby, 2004). NMR relaxations rates are widely used for determination of fat and water content in food (Pedersen et al., 2001). Principally, spectroscopic fingerprinting techniques in combination with chemometrics can be used for all sorts of authentication of products or varieties such as oil (Mannina et al., 2003), flour (Brescia et al., 2002) and for detection of growth conditions (Munck et al., 2001), to test if products contain the declared ingredients and no xenophobic material e.g it can be used to check for gene-modified material, and for comparison of wildtype and altered genetic material through the pattern recognition found in a score plot (see 2.3.2).

The increasing demand for plant-based products for bio-ethanol in combination with failed crop productions world-wide have resulted in sky-rocketing

prizes on cereals. Higher prizes on cereals open possibilities for niche productions to be rentable. Value-added sorting instead of bulk harvest leading to lots with specific composition is now feasible. A new cereal sorting machine based on NIR/NIT spectroscopy is able to do single seed sorting of ten tonnes per hour for e.g. baking quality in wheat (Löfqvist and Nielsen, 2004; Møller Jespersen and Munck, 2008). Other such spectroscopy based sorting/authentication apparatus will probably emerge and could also involve the dietary fiber issue such as β-glucan.

Optimizing cereal raw-materials for value-added products could include alteration of the composition of carbohydrates. Alterations can be introduced using gene transformation technology, genetically alteration of enzymes, introduction of mutations or by means of classical breeding. Genetic engineering is a highly cherished method of improving plant productivity and changing plant chemical composition: Introducing altered composition of carbohydrates with potential functionality in industrial applications has been achieved using gene transfer of e.g. dextran in potato from *Leuconostoc sp*. or α-glucan in maize from *Streptococcus sp*. (Lytovchenko et al., 2007). However, gene manipulated products are being perceived skeptically in Europe and ethical discussions on the use of xenogenetic material are well-known. Furthermore, as described above, gene alterations have profound effect on the total outcome of a cereal phenotype that has to be seriously considered. The variation found between genotypes in the content of β-glucan shows that there is a large potential in exploiting this variation also in conventional breeding programmes.

The *lys5f* has potential industrial interest due to the high content of β-glucan. There is a major industrial interest in β-glucan that is mirrored in the increasing number of publications and patents involving functions of β-glucan (Laroche and Michaud, 2007). The use of β-glucan as a hydrocolloid is based on its rheological and physio-chemical characteristics such as gelling capacity, swelling ability, ability to increase the viscosity of aqueous solutions, water-holding capacity, and susceptibility /resistance to bacterial degradation and fermentation (Cui et al., 2000; Lazaridou and Biliaderis, 2007). The functionality of β-glucan can among others be used for prolonging shelf-life of bread (Holtekjolen et al., 2006) as a prebiotic agent promoting gut microflora (Laroche and Michaud, 2007), as a stabilizer and thickening component in food (Burkus and Temelli, 2000; Laroche and Michaud, 2007) and thus be used as a fat-replacer (Burkus and Temelli, 2000; Morgan and Ofman, 1998) and for improving sensory mouth feeling (Lazaridou and Biliaderis, 2007). As described in chapter 2, β-glucan also provides many health benefits. Hence, there is a market for barley cultivars with high levels of β-glucan. In contrast to many years of breeding towards less β-glucan in malting barley, breeders now respond to the industrial needs and breed for high β-glucan barley varieties. However, much needs to be learned before fully exploring the fea-

tures of β-glucan: from the regulation of the β-glucan in the seed, the location of β-glucan in the cell wall and whether it differs between genotypes, the structural differences of β-glucan and how they are conserved (or not) during extraction and through the processing of the product. The yield of the new improved lines is also an important issue. A research programme 'BEST' at KU-LIFE aims at answering some of the questions regarding the stability and structure of β-glucan during processing.

6.1.1 Conclusions and future work

It should be obvious from the previous chapters that the cross-field (see **Figure 6-1**) between barley mutants, spectroscopy and chemometrics is a source of highly relevant data with a great potential in food research, plant breeding and molecular research. The vast amount of information hidden in the spectral data of the three genotypes in this investigation has only been slightly revealed, and much more information is to be extracted and published at a later stage.

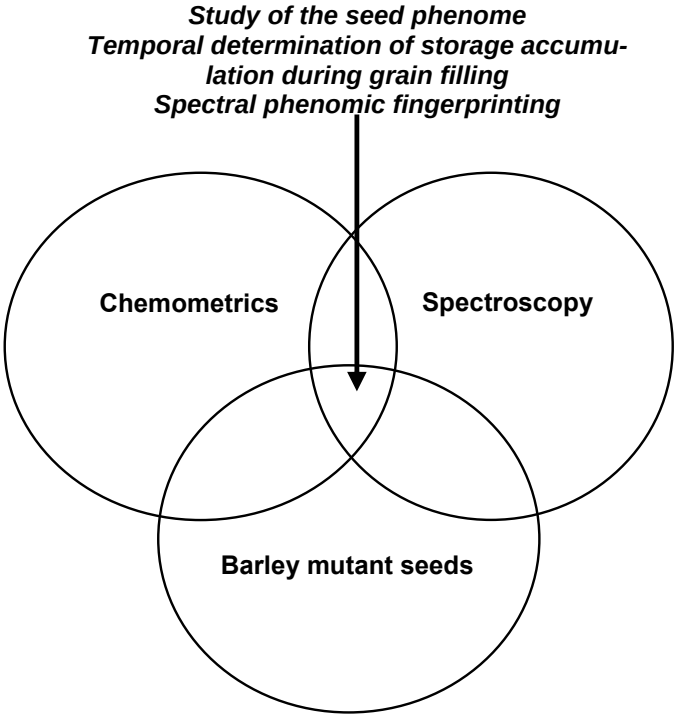

Figure 6-1. Illustration of the cross-fields on which this PhD study is based: spectroscopy, biology and chemometrics. These three fields have made it possible to overview the spectral phenome.

The aims of this study was to '*study how changes induced by a single mutation influence the developmental properties of the phenome and the entire constitution compared to conventional barley at varying environmental conditions*', see 1.1. In summary, these are the conclusions on the results:

1) The methods chosen in this study could not reveal any differences between seed material grown normally or under drought treatment during early seed development
2) The mutants were less affected by drought stress in the leaves compared to the normal barley
3) Both the chemical and spectroscopic methods reproduced the genetic differences in the seed material, as well as the temporal changes. Moreover, the spectroscopic methods proved able to distinguish the genotypic differences with very high reproducibility.
4) The vibrational spectroscopic methods were able to quantify the bulk storage compounds in the seeds.
5) ^{1}H HR MAS NMR could quantify only the mobilized compounds in the flour samples. Hence, only starch could be quantified. For yet unknown reasons the ^{1}H HR MAS NMR could not retrieve the high content of β-glucan found in *lys5f* at maturity.
6) MRI revealed that water in *lys5f* has a higher mobility than water in normal barley. This is ascribed the high content of β-glucan found in *lys5f* and reflects a higher water activity. The water activity especially in *lys5f* was found to be highest in a well-defined region along the crease
7) A non-uniform distribution of water during hydration and desiccation was confirmed throughout the seed
8) From single chemical analysis it was possible to identify and confirm the early onset of the major effects of *lys5f* gene and the late corresponding onset of the *lys3a* gene.
9) Accumulation of water and β-glucan was concomitant with the onset of the mutant genes. This, together with the many pleiotropic effects found in *lys5f* illustrated well the concept of the self-organising principle of barley endosperm tissue during seed development.

The conclusions of this study lead to more questions that await investigations:

Ad 1) Analysis of the composition of starch granules and proteins in control and drought treated seeds could be interesting, as this composition in the literature have been found to change during stress.

Ad 2) Analysis of differences in senescence pattern, the total plant yield or the photosynthesis between the mutants and the normal barley mutants during a drought stress could be valuable for determining whether the differences in stress response in the leaves found in the current study to be pleiotropic effects. Mutant endosperm genes could in this respect give interesting information as anticipated in this study

Ad 3) A thorough full data analysis of the spectral pattern in IR and NMR still awaits to define whether they show the same finely tuned reproducibility and representation of genetic information seen in NIR

Ad 4) Further analyses on the structure and solubility of β-glucan in the mutants and during seed development and desiccation are needed using solid state NMR to define the denaturation of the β-glucan complex *in situ*

Ad 5) Further investigations are needed to elucidate whether the immobility of β-glucan is due to structural changes of β-glucan, to genotypic differences in cell wall location or to a different water environment in the cells.

Ad 6) It would be useful to do MRI on developing mutant seeds in order to follow the water mobility concomitantly with the accumulation of bulk seed carbohydrates in order to further confirm the self-organizing principle

Ad 7) An IR-microscopy investigation of the *lys5f* seeds should be done to verify that the well defined internal structure seen in the MRI experiments are due to thicker cell walls composed by β-glucan or to determine if more β-glucan also is present in the interior endosperm cell from which it is produced

Ad 8) the onset of different proteins in the mutants should be investigated to identify those that are correlated to the onset of the mutant genes

Another semi-field experiment with *lys3a*, *lys5f* and Bomi as control variety could give the answers to many of the questions above. A semifield set-up is useful as the plants experience close-to field conditions, but it is possible to give all samples exact same conditions reducing the effect of variation in e.g. soil composition. Still it is possible to apply water-related stresses. Answers to the above questions could be valuable for both breeders and basic researchers within molecular biology and food research.

"What lies behind us and what lies before us are tiny matters compared to what lies within us"

O.W. Holme

s

7 Appendix I

Table of the absolute values measured on the seed and flour by traditional methods. The values in italics are the standard deviations.

ID	Fresh mg seed^{-1}		Watercontent % mg seed^{-1}		DM mg seed^{-1}		Betaglucan % dm		Starch % dm		Amylose % starch	
Cork9	45.3	*3.05*	77.17	*3.23*	10.31	*1.45*	0.14	*0.06*	9.52	*0.32*	17.46	*2.63*
Cork13	58.9	*8.45*	74.96	*0.98*	14.74	*2.18*	0.28	*0.03*	19.50	*7.25*	21.81	*3.98*
Cork16	65.8	*15.18*	72.80	*1.43*	17.94	*4.55*	0.50	*0.32*	26.27	*2.77*	22.29	*3.07*
Cork20	97.9	*12.94*	68.20	*5.65*	31.14	*4.60*	1.99	*0.32*	49.72	*5.30*	28.30	*0.41*
Cork23	102.0	*5.93*	64.25	*0.49*	36.43	*1.89*	2.44	*0.27*	49.37	*5.99*	30.66	*1.04*
Cork30	106.9	*5.05*	58.29	*3.10*	44.59	*4.04*	4.48	*0.32*	46.45	*5.59*	34.07	*2.00*
Cork39	88.3	*6.96*	42.32	*3.94*	50.74	*2.20*	5.69	*0.30*	48.95	*7.30*	35.66	*1.74*
Cork47	68.3	*8.35*	24.44	*4.27*	51.90	*4.33*	5.66	*0.41*	44.06	*7.16*	35.84	*2.46*
Lys59	39.3	*2.96*	74.36	*0.27*	9.99	*0.74*	0.23	*0.11*	4.42	*0.85*	17.73	*2.07*
Lys513	59.7	*6.94*	76.28	*1.05*	14.14	*1.54*	0.72	*0.02*	13.45	*1.72*	16.64	*0.07*
Lys516	78.7	*7.24*	73.17	*0.71*	21.12	*2.05*	2.75	*1.21*	11.07	*0.39*	19.71	*0.79*
Lys520	92.0	*7.06*	73.05	*5.65*	24.82	*5.82*	9.93	*3.23*	17.11	*4.32*	26.94	*2.43*
Lys523	100.3	*13.78*	68.98	*1.68*	31.62	*5.29*	14.85	*2.38*	19.14	*2.86*	26.54	*1.28*
Lys530	106.0	*8.88*	63.61	*1.25*	38.49	*2.12*	18.38	*1.56*	20.19	*2.72*	27.79	*1.92*
Lys539	73.1	*9.12*	46.63	*6.85*	38.74	*4.81*	17.55	*3.97*	23.39	*3.27*	26.48	*2.46*
Lys547	55.5	*10.07*	28.24	*6.35*	39.62	*7.09*	19.10	*1.86*	21.72	*1.58*	27.55	*2.86*
Lys39	37.3	*2.51*	77.59	*2.14*	8.43	*1.50*	0.14	*0.00*	3.20	*1.25*	13.35	*0.00*
Lys313	57.5	*10.83*	75.29	*1.44*	14.12	*2.22*	0.36	*0.20*	23.86	*0.99*	18.85	*3.30*
Lys316	67.9	*8.76*	71.80	*1.17*	19.20	*2.97*	0.24	*0.09*	33.16	*1.84*	21.78	*1.45*
Lys320	95.2	*13.49*	66.80	*0.50*	31.62	*4.65*	1.59	*0.19*	45.54	*4.36*	27.01	*2.82*
Lys323	96.1	*2.95*	63.05	*1.39*	35.52	*1.57*	2.73	*0.39*	46.69	*6.68*	28.13	*2.04*
Lys330	99.5	*5.24*	61.00	*0.79*	38.80	*1.65*	3.28	*0.14*	46.34	*4.47*	27.57	*3.00*
Lys339	75.7	*5.47*	46.17	*3.31*	40.62	*1.16*	3.49	*0.13*	45.89	*6.22*	26.96	*2.52*
Lys347	59.4	*10.57*	26.09	*6.12*	43.58	*6.33*	3.91	*1.05*	40.85	*6.59*	29.48	*4.08*

8 Appendix II

Table of the relative values of the parameters compared to the values of the control variety Cork.

Sample	*% Fresh weight*	*% Water content*	*% Dry weight mg*	*% Betaglu-can*	*% Starch*	*% Amy-lose*
Cork9	100	100	100	100	100	100
Cork13	100	100	100	100	100	100
Cork16	100	100	100	100	100	100
Cork20	100	100	100	100	100	100
Cork23	100	100	100	100	100	100
Cork30	100	100	100	100	100	100
Cork39	100	100	100	100	100	100
Cork47	100	100	100	100	100	100
Lys59	87	96	97	169	46	102
Lys513	101	102	96	256	69	76
Lys516	120	101	118	546	42	88
Lys520	94	107	80	498	34	95
Lys523	98	107	87	608	39	87
Lys530	99	109	86	410	43	82
Lys539	83	110	76	308	48	74
Lys547	81	116	76	338	49	77
Lys39	82	101	82	102	34	76
Lys313	98	100	96	127	122	86
Lys316	103	99	107	48	126	98
Lys320	97	98	102	80	92	95
Lys323	94	98	97	112	95	92
Lys330	93	105	87	73	100	81
Lys339	86	109	80	61	94	76
Lys347	87	107	84	69	93	82

9 References

1. Aastrup,S. 1979. Effect of rain on beta-glucan content in barley grains. Carlsberg Research Communications 44:381-393.

2. Aastrup,S., and K.Erdal. 1980. Quantitative-Determination of Endosperm Modification and Its Relationship to the Content of 1,3-1,4-Beta-Glucans During Malting of Barley. Carlsberg Research Communications 45:369-379.

3. Aastrup,S., K.Erdal, and L.Munck. 1985. Low beta-glucan barley mutants and their malting behaviour. Journal of the Institute of Brewing 91:130.

4. Agosti,R.D., R.Lenk, and H.Greppin. 1991. Nuclear-magnetic resonance study of the germination of a cereal. Archives des Sciences 44:235-243.

5. Ahmadi,A., and D.A.Baker. 2001. The effect of water stress on the activities of key regulatory enzymes of the sucrose to starch pathway in wheat. Plant Growth Regulation 35:81-91.

6. Amato,M.E., G.Ansanelli, S.Fisichella, R.Lamanna, G.Scarlata, A.P.Sobolev, and A.Segre. 2004. Wheat flour enzymatic amylolysis monitored by in situ 1H NMR spectroscopy. Journal of Agricultural and Food Chemistry 52:823-831.

7. Anker-Nilssen,K., E.M.Færgestad, S.Sahlstrom, and A.K.Uhlen. 2006. Interaction between barley cultivars and growth temperature on starch degradation properties measured *in vitro*. Animal Feed Science and Technology 130:3-22.

8. Anonymous. 2007. Supply balances (4.1.4.2) for 2000-2003. European Commision, Eurostat and Agriculture and Rural Development. Available: http://epp.eurostat.ec.europa.eu (October 10, 2007).

9. Bamforth,C.W., and M.Kanauchi. 2001. A simple model for the cell wall of the starchy endosperm in barley. Journal of the Institute of Brewing 107:235-240.

10. Bardet,M., M.F.Foray, J.Bourguignon, and P.Krajewski. 2001. Investigation of seeds with high-resolution solid-state 13-C NMR. Magnetic Resonance in Chemistry 39:733-738.

11. Barron,C., M.L.Parker, E.N.C.Mills, X.Rouau, and R.H.Wilson. 2005. FTIR imaging of wheat endosperm cell walls in situ reveals compositional and architectural heterogeneity related to grain hardness. Planta 220:667-677.

12. Bay-Smidt,A.M., A.Blennow, M.Bojko, and B.L.Møller. 1999. The effect of the phosphate and amylopectin molecular size on peak viscosity of starch pastes. Annual Transactual Nordic Rheology Society 7:31-38.

13. Becker,M., C.Vincent, and J.S.G.Reid. 1995. Biosynthesis of (1,3)(1,4) beta-glucan and (1,3) beta-glucan in barley (*Hordeum vulgare* L.). Planta 195:331-338.

14. Beckles,D.M., A.M.Smith, and T.ap Rees. 2001. A cytosolic ADP-glucose pyrophosphorylase is a feature of graminaceous endosperms, but not of other starch-storing organs. Plant Physiology 125:818-827.

15. Behall,K.M., D.J.Scholfield, and J.Hallfrisch. 2005. Comparison of hormone and glucose responses of overweight women to barley and oats. Journal of the American College of Nutrition 24:182-188.

16. Bewley,J.D., and M.Black. 1983. Physiology and biochemistry of seeds -in relation to germination. Springer-Verlag, New York.

17. Blum,A. 1996. Crop response to drought and the interpretation of adaptation. Plant Growth Regulation 20:135-148.

18. Bourdon,I., W.Yokoyama, P.Davis, C.Hudson, R.Backus, D.Richter, B.Knuckles, and B.O.Schneeman. 1999. Postprandial lipid, glucose, insulin, and cholecystokinin responses in men fed barley pasta enriched with beta-glucan. American Journal of Clinical Nutrition 69:55-63.

19. Bowsher,C.G., E.F.A.L.Scrase-Field, S.Esposito, M.J.Emes, and I.J.Tetlow. 2007. Characterization of ADP-glucose transport across

the cereal endosperm amyloplast envelope. Journal of Experimental Botany 58:1321-1332.

20. Brescia,M.A., G.D.Martino, C.Fares, N.D.Fonzo, C.Platani, S.Ghelli, F.Reniero, and A.Sacco. 2002. Characterization of Italian durum wheat semolina by means of chemical analytical and spectroscopic determinations. Cereal Chemistry 79:238-242.

21. Brosio,E., A.A.Dinola, M.Fracassi, E.Carnovale, and E.Marconi. 1992. NMR study of seed hydration: The role of the seed anatomical structures in water uptake of soaked cowpeas. Cellular and Molecular Biology 38:693-697.

22. Buckerigde,M.S., C.Rayon, B.Urbanowicz, M.A.S.Tiné, and N.C.Carpita. 2004. Mixed linkage (1-3),(1-4)-Beta-D-Glucans of grasses. Cereal Chemistry 81:115-127.

23. Burian,R.M. 2004. Molecular epigenesis, molecular pleiotropy, and molecular gene definitions. History and philosophy of the life sciences 26:53-80.

24. Burkus,Z., and F.Temelli. 2000. Stabilization of emulsions and foams using barley beta-glucan. Food Research International 33:27-33.

25. Callaghan,P.T. 1991. Principles of nuclear magnetic resonance microscopy. Clarendon Press, Oxford.

26. Carr,H.Y., and E.M.Purcell. 1954. Effects of diffusion on free precession in nuclear magnetic resonance experiments. Physical Review 94:630-638.

27. Chaves,M.M., J.P.Maroco, and J.S.Pereira. 2003. Understanding plant responses to drought - from genes to the whole plant. Functional Plant Biology 30:239-264.

28. Close,T.J., S.I.Wanamaker, R.A.Caldo, S.M.Turner, D.A.Ashlock, J.A.Dickerson, R.A.Wing, G.J.Muehlbauer, A.Kleinhofs, and R.P.Wise. 2004. A new resource for cereal genomics: 22K barley GeneChip comes of age. Plant Physiology 134:960-968.

29. Coles,G. 1979. Relationship of mixed-link beta-glucan accumulation to accumulation of free sugars and other glucans in the developing barley endosperm. Carlsberg Research Communications 44:439-453.

30. Cui,W., P.J.Wood, B.Blackwell, and J.Nikiforuk. 2000. Physico-chemical properties and structural characterization by two-dimensional NMR spectroscopy of wheat beta-D-glucan - comparison with other cereal beta-D-glucans. Carbohydrate Polymers 41:249-258.

31. Czuchajowska,Z., J.Szczodrak, and Y.Pomeranz. 1992. Characterization and estimation of barley polysaccharides by Near-Infrared spectroscopy.1.Barleys, starches, and beta-D-glucans. Cereal Chemistry 69:413-418.

32. De Sa,R.M., andG.H.Palmer. 2006. Analysis of beta-glucan in single grains of barley and malt using NIR-spectroscopy. Journal of the Institute of Brewing 112:9-16.

33. Delwiche,S.R. 1995. Single wheat kernel analysis by Near-Infrared transmittance: Protein Content. Analytical Techniques and Instrumentation 72:11-16.

34. Delwiche,S.R., M.M.Bean, R.E.Miller, B.D.Webb, and P.C.Williams. 1995. Apparent amylose content of milled rice by near-infrared reflectance spectrophotometry. Analytical Techniques and Instrumentation 72:182-187.

35. Dinola,A.A., E.Brosio, M.Delfini, F.Manes, and S.Quattrocchi. 1988. Hydration mechanism study in lettuce seeds by proton NMR relaxation. Cellular and Molecular Biology 34:639-648.

36. Doll,H. 1983. Barley seed proteins and possibilities for their improvement. p. 207-223. *In* W.Gottschalk, and H.P.Muller (ed.) Seed proteins. Martinus Nijhoff.

37. Donhauser,E.G., O.linsenmann, and E.Faltermeier. 1983. Evaluation of near infrared spectrophotometry in the malting and brewery laboratory. Monatsschrift für Brauwelt 36:474-478.

38. Dowell,F.E., E.B.Maghirang, G.L.Lookhart, R.O.Pierce, B.W.Seabourn, S.R.Bean, J.D.Wilson, and O.K.Chung. 2006. Predicting wheat quality characteristics and functionality using near-infrared spectroscopy. Cereal Chemistry 83:529-536.

39. Downey,G. 1985. Estimation of moisture in undried wheat and barley by near infrared reflectance. Journal of Science in Food and Agriculture 36:951-953.

40. Dyrby,M. 2004. Multivariate analysis of high-field NMR data in food and medicine. Ph.D. thesis, The Royal Veterinary and Agricultural University, Copenhagen, Denmark.

41. Ellis,R.H., and B.Marshall. 1998. Growth, yield and grain quality of barley (*Hordeum vulgare* L.) in response to nitrogen uptake. Journal of Experimental Botany 49:1021-1029.

42. Emes,M.J., C.G.Bowsher, C.Hedley, M.M.Burrell, E.S.F.Scrase-Field, and I.J.Tetlow. 2003. Starch synthesis and carbon partitioning in developing endosperm. Journal of Experimental Botany 54:569-575.

43. Engelsen, S.B. 2006. Lecture notes 'Quantitative food spectroscopy'. University of Copenhagen, Faculty of Life Sciences.

44. Engelsen,S.B., and L.Norgaard. 1996. Comparative vibrational spectroscopy for determination of quality parameters in amidated pectins as evaluated by chemometrics. Carbohydrate Polymers 30:9-24.

45. Evers,A.D., A.B.Blakeney, and L.O'Brien. 1999. Cereal structure and composition. Australian Journal of Agricultural Research 50:629-650.

46. Fan,W.M.T. 1996. Metabolite profiling by one- and two-dimensional NMR analysis of complex mixtures. Progress in Nuclear Magnetic Resonance Spectroscopy 28:161-219.

47. FAO. 2006. Statistical yearbook 2005/2006. The Food and Agricultural Organization of the United Nations. Available from http://www.fao.org/es/ESS/yearbook, (October 10, 2007).

48. FDA. 2006. FDA Finalizes Health Claim Associating Consumption of Barley Products with Reduction of Risk of Coronary Heart Disease. U.S. Food and Drog Administration (FDA).19 May 2006. Publication no. P06-70. Available from: http://www.fda.gov/bbs/topics/NEWS/2006/NEW01375.html (February 10, 2008).

49. Fincher,G.B. 1975. Morphology and chemical composition of barley endosperm cell walls. Journal Institute of Brewing **81**:116-122.

50. Fincher,G.B., and B.A.Stone. 1986. Cell walls and their components in cereal grain technology. p. 207-295. *In* Y.Pomeranz (ed.) Ad-

vances in cereal science and technology. American Association of Cereal Chemists.

51. Gergely,S., and A.Salgo. 2003. Changes in moisture content during wheat maturation - what is measured by near infrared spectroscopy? Journal of Near Infrared Spectroscopy 11:17-26.

52. Ghosh, P. K., Jayas, D. S., Gruwel, M. L. H, and White, N. D. G. Magnetic resonance image analysis ot explain moisture movement in wheat drying. 2004. ASAE/CSAE meeting paper no 043118. St.Joseph, Michigan, U.S.

53. Glidewell,S.M. 2006. NMR imaging of developing barley grains. Journal of Cereal Science 43:70-78.

54. Grannell,P.K., and P.Mansfield. 1975. Microscopy Invivo by Nuclear Magnetic-Resonance. Physics in Medicine and Biology 20:477-482.

55. Griffiths,P.R., and J.A.de Haseth. 1986. Infrared spectrometry. John Wiley and Sons, New York.

56. Gruwel,M.L.H., B.Chatson, X.S.Yin, and S.Abrams. 2001. A magnetic resonance study of water uptake in whole barley kernels. International Journal of Food Science and Technology 36:161-168.

57. Harten,A.M.v. 1998. Mutation breeding: theory and practical applications. Cambridge University Press.

58. Henry,R.J. 1985. Near-Infrared reflectance analysis of carbohydrates and its application to the determination of (1-3)(1-4)-beta-D-glucan in barley. Carbohydrate Research 141:13-19.

59. Holtekjolen,A.K., A.K.Uhlen, E.Brathen, S.Sahlstrom, and S.H.Knutsen. 2006. Contents of starch and non-starch polysaccharides in barley varieties of different origin. Food Chemistry 94:348-358.

60. Hore,P.J. 2001. Nuclear magnetic resonance. Oxford science publications.

61. Horigane,A.K., W.M.H.G.Engelaar, M.Yoshida, A.Okubo, and T.Nagata. 2001. Visualisation of moisture distribution during development of rice caryopses (*Oryza sativa* L.) by nuclear magnetic resonance microimaging. Journal of Cereal Science 33:105-114.

62. Hotelling,H. 1957. Analysis of a complex of statistical variables into principal components. Journal of Educational Psycology 24:417-520.

63. Hrmova,M., and G.B.Fincher. 2001. Structure-function relationships of beta-D-glucan endo-and exohydrolases from higher plants. Plant Molecular Biology 47:73-91.

64. IPCC. Climate change 2007: synthesis report. 4, 1-23. 2007. Intergovenmental Panel on Climate Change.

65. Ishida,N., M.Koizumi, and H.Kano. 2000. The NMR microscope: a unique and promising tool for plant science. Annals of Botany 86:259-278.

66. Ishida,N., S.Naito, and H.Kano. 2004. Loss of moisture from harvested rice seeds on MRI. Magnetic Resonance Imaging 22:871-875.

67. Izydorczyk,M.S., L.J.Macri, and A.W.MacGregor. 1998a. Structure and physicochemical properties of barley non-starch polysaccharides. I. Water-extractable beta-glucans and arabinoxylans. Carbohydrate Polymers 35:249-258.

68. Izydorczyk,M.S., L.J.Macri, and A.W.MacGregor. 1998b. Structure and physicochemical properties of barley non-starch polysaccharides. II. Alkali-extractable beta-glucans and arbinoxylans. Carbohydrate Polymers 35:259-269.

69. Jacobsen,S., I.Søndergaard, B.Møller, T.Desler, and L.Munck. 2005. A chemometric evaluation of the underlying physical and chemical patterns that support near infrared spectroscopy of barley seeds as a tool for explorative classification of endosperm genes and gene combinations. Journal of Cereal Science 42:281-299.

70. Jadhav,S.J., S.E.Lutz, V.M.Ghorpade, and D.K.Salunkhe. 1998. Barley: Chemistry and value-added processing. Critical Reviews in Food Scienc 38:123-171.

71. James,M.G., K.Denyer, and A.M.Myers. 2003. Starch synthesis in the cereal endosperm. Current Opinion in Plant Biology 6:215-222.

72. Jarvis,M.C., and M.C.McCann. 2000. Macromolecular biophysics of the plant cell wall: Concepts and methodology. Plant Physiology and Biochemistry 38:1-13.

73. Jenner,C.F., T.D.Ugalde, and D.Aspinall. 1991. The physiology of starch and protein deposition in the endosperm of wheat. Australian Journal of Plant Physiology 18:211-226.

74. Jenner,C.F., Y.Xia, C.D.Eccles, and P.T.Callaghan. 1988. Circulation of water within wheat-grain revealed by nuclear magnetic resonance micro-imaging. Nature 336:399-402.

75. Jennings,A.C., and R.K.Morton. 1962. Changes in carbohydrate, protein and non-protein nitrogenous compounds of developing wheat grain. Australian Journal of Biological Sciences 16:318-331.

76. Johansson,L., L.Virkki, S.Maunu, M.Lehto, P.Ekholm, and P.Varo. 2000. Structural characterization of water soluble beta-glucan of oat bran. Carbohydrate Polymers 42:143-148.

77. Johansson,L., P.Tuomainen, M.Ylinen, P.Ekholm, and L.Virkki. 2004. Structural analysis of water-soluble and -insoluble beta-glucans of whole-grain oats and barley. Carbohydrate Polymers 58:267-274.

78. Kacurakova,M., and R.H.Wilson. 2001. Developments in mid-infrared FT-IR spectroscopy of selected carbohydrates. Carbohydrate Polymers 44:291-303.

79. Kahlon,T.S., F.I.Chow, B.E.Knuckles, and M.M.Chiu. 1993. Cholesterol-lowering effects in hamsters of beta-glucan-enriched barley fraction, dehulled whole barley, rice bran, and oat bran and their combinations. Cereal Chemistry 70:435-440.

80. Kalra,S., and S.Joad. 2000. Effect of dietary barley beta-glucan on cholesterol and lipoprotein fractions in rats. Journal of Cereal Science 31:141-145.

81. Kang,M.U., Y.Sugimoto, S.Sakamoto, and H.Fuwa. 1985. Developmental changes in the amylose content of endosperm starch of barley (*Hordeum vulgare L*) during the grain filling period after anthesis. Agricultural and Biological Chemistry 49:3463-3466.

82. Kano,H., N.Ishida, T.Kobayashi, and M.Koizumi. 1990. H1-NMR imaging analysis of changes of free-water distribution in barley and soybean seeds during maturation. Japanese Journal of Crop Science 59:503-509.

83. Karlsson,K.E. 1976. Linkage studies on the *lys* gene in relation to some marker genes and translocations. p. 536-541. *In* H.Gaul (ed.) Barley Genetics III. Verlag Karl Thiemig.

84. Kays,S.E., N.Shimizu, F.E.Barton II, and K.Ohtsubo. 2005. Near-Infrared transmission and reflectance spectroscopy for the determination of dietary fiber in barley cultivars. Crop Science 45:2307-2311.

85. Knudsen,K.E.B. 2001. The nutritional significance of 'dietary fibre' analysis. Animal Feed Science and Technology 90:3-20.

86. Kockenberger,W. 2001a. Functional imaging of plants by magnetic resonance experiments. Trends in Plant Science 6:286-292.

87. Kockenberger,W. 2001b. Nuclear magnetic resonance micro-imaging in the investigation of plant cell metabolism. Journal of Experimental Botany 52:641-652.

88. Kockenberger,W. 2004. Lecture notes 'NMR microscopy in Plant Physiology'. University of Nottingham. Magnetic Resonance Centre.

89. Krishnan,P., D.K.Joshi, M.Maheswari, S.Nagarajan, and A.V.Moharir. 2004a. Characterisation of soybean and wheat seeds by nuclear magnetic resonance spectroscopy. Biologia Plantarum 48:117-120.

90. Krishnan,P., D.K.Joshi, S.Nagarajan, and A.V.Moharir. 2004b. Characterization of germinating and non-germinating wheat seeds by nuclear magnetic resonance (NMR) spectroscopy. European Biophysics Journal 33:76-82.

91. Laroche,C., and P.Michaud. 2007. New developments and prospective applications for beta(1,3) glucans. Recent Patents on Biotechnology 1:59-73.

92. Lauterbur,P.C. 1973. Image formation by induced local interactions: examples employing nuclear magnetic resonance. Nature 242:190-191.

93. Lazaridou,A., and C.G.Biliaderis. 2007. Molecular aspects of cereal beta-glucan functionality: Physical properties, technological applications and physiological effects. Journal of Cereal Science 46:101-118.

94. Leeflang,B.R., E.J.Faber, P.Erbel, and J.F.G.Vliegenthart. 2000. Structure elucidation of glycoprotein glycans and of polysaccharides by NMR spectroscopy. Journal of Biotechnology 77:115-122.

95. Léon,J., S.Silz, and H.J.Harloff. 2000. Beta-D-glucan content during grain filling in spring barley and its wild progenitor *H.vulgare* ssp. *spontaneum*. Journal of Agronomy & Crop Science 185:1-8.

96. Lifschitz,C.H., M.A.Grusak, and N.F.Butte. 2002. Carbohydrate digestion in humans from a beta-glucan-enriched barley is reduced. Journal of Nutrition 132:2593-2596.

97. Lytovchenko,A., U.Sonnewald, and A.R.Fernie. 2007. The complex network of non-cellulosic carbohydrate metabolism. Current Opinion in Plant Biology 10:227-235.

98. Löfqvist, B. and Nielsen, J. P. Method and device for sorting objects. [WO 2004/060585 A1]. 2004.

99. MacGregor,A.W., and G.B.Fincher. 1993. Carbohydrates of the barley grain. p. 73-130. *In* A.W.MacGregor, and R.S.Bhatty (ed.) Barley: Chemistry and Technology. American Associated Cereal Chemists.

100. Mannina,L., A.P.Sobolev, and A.Segre. 2003. Olive oil as seen by NMR and spectroscopy. Spectroscopy Europe 15:6-14.

101. Marconi,E., E.Carnovale, A.A.Dinola, and E.Brosio. 1993. NMR assesment of water uptake in different Vigna Ssp seeds. International Journal of Food Science and Technology 28:25-33.

102. Martens,H., and T.Næs. 1989. Multivariate calibration. John Wiley and Sons, Chichester, UK.

103. Martens,H and M.Martens. 2001. Multivariate analysis of quality.-An introduction. John Wiley and Sons. 1-466

104. Martens,H., J.P.Nielsen, and S.B.Engelsen. 2003. Light scattering and light absorbance separated by extended multiplicative signal correction. Application to near-infrared transmission analysis of powder mixtures. Analytical Chemistry 75:394-404.

105. McCleary,B.V., and M.Glennieholmes. 1985. Enzymic quantification of (1-]3) (1-]4)-Beta-D-glucan in barley and malt. Journal of the Institute of Brewing 91:285-295.

106. McCleary,B.V., V.Solah, and T.S.Gibson. 1994. Quantitative measurement of total starch in cereal flour and products. Journal of Cereal Science 20:51-58.

107. McCleary,B.V., and D.C.Mugford. 1997. Determination of beta-glucan in barley and oats by streamlined enzymatic method: Summary of collaborative study. Journal of AOAC International 80:580-583.

108. McEntyre,E., R.Ruan, and R.G.Fulcher (1998). Comparison of water absorption patterns in two barley cultivars, using magnetic resonance imaging. Cereal Chemistry 75:792-795

109. McIntosh,G.H. 1993. Colon cancer: Dietary modifications required for a balanced protective diet. Preventive Medicine 22:767-774.

110. McNab,J.M., and R.R.Smithard. 1992. Barley Beta-glucan: An antinutritional factor in poultry feeding. Nutrition Research Reviews 5:45-60.

111. Meiboom,S., and D.Gill. 1958. Modified spin-echo method for measuring nuclear relaxation times. The Review of Scientific Instruments 29:688-691.

112. Miedziejko,E.M. 1997. Impact of chemical stimuli and temperature on water transport and mobility in germinating rape seeds by pulsed ^{1}H NMR spectroscopy. Magnetic Resonance in Chemistry 35:S68.

113. Morgan,K.R., and D.J.Ofman. 1998. Glucagel, a gelling beta-glucan from barley. Cereal Chemistry 75:879-881.

114. Morris,P.G., H.E.Darceuil, A.Jasinski, A.K.Jha, D.J.O.McIntyre, and D.H.Northcote. 1990. NMR spectroscopy of the germinating castor bean. Phil. Trans. R. Soc. London. A 333:487-493.

115. Morrison,W.R. 1993. Cereal starch granule development and composition. p. 176-209. *In* P.R.Shewry, and K.Stobart (ed.) Proceedings of the phytochemical society of Europe. Clarendon Press.

116. Morrison,W.R., and H.Gadan. 1987. The amylose and lipid contents of starch granules in developing wheat endosperm. Journal of Cereal Science 5:263-275.

117. Mossberg,R. 1969. Evaluation of protein quality and quantity by dye-binding capacity: a tool in plant breeding. p. 151-160. *In* IAEA (ed.) New approaches to breeding for improved plant protein.

118. Munck,L. 1981. Barley for food, feed and industry. p. 427-459. Cereals: A Renewable Resource. Theory and Practice. The American Association of Cereal Chemists.

119. Munck,L. 2003. Detecting diversity- a new holistic, exploratory approach bridging phenotype and genotype. p. 227-245. *In* R.Bothmer, T.van Hintum, H.Knupffer, and K.Sato (ed.) Diversity in barley (Hordeum vulgare). Elsevier Science B V,

120. Munck,L. 2005. The revolutionary aspect of chemometric technology. The universe and biological cells as computers.

121. Munck,L. 2007. A new holistic exploratory approach to systems biology by near infrared spectroscopy evaluated by chemometrics and data inspection. Journal of Chemometrics 21.

122. Munck,L. 2008. Breeding for quality traits in cereals- a revised outlook on old and new tools for integrated breeding. *In* M.J.Carena (ed.) Cereals. Springer.

123. Munck,L., K.E.Karlsson, A.Hagberg, and B.O.Eggum. 1970. Gene for improved nutritional value in barley seed protein. Science 168:985-987.

124. Munck, L., Gibbons, G, and Aastrup, S. 1981. Chemical and structural changes during malting. 1. EBC Congress 1981.

125. Munck,L., K.G.Jørgensen, J.Ruudhansen, and K.T.Hansen. 1989. The EBC methods for determination of high molecular-weight betaglucan in barley, malt, wort and beer. Journal of the Institute of Brewing 95:79-82.

126. Munck,L., L.Nørgaard, S.B.Engelsen, R.Bro, and C.A.Andersson. 1998. Chemometrics in food science - a demonstration of the feasibility of a highly exploratory, inductive evaluation strategy of fundamental scientific significance. Chemometrics and Intelligent Laboratory Systems 44:31-60.

127. Munck,L., J.P.Nielsen, B.Møller, S.Jacobsen, I.Søndergaard, S.B.Engelsen, L.Nørgaard, and R.Bro. 2001. Exploring the phenotypic expression of a regulatory proteome- altering gene by spectroscopy and chemometrics. Analytica Chimica Acta 446:171-186.

128. Munck,L., B.Møller, S.Jacobsen, and I.Søndergaard. 2004. Near infrared spectra indicate specific mutant endosperm genes and reveal

a new mechanism for substituting starch with (1-3,1-4) betaglucan in barley. Journal of Cereal Science 40:213-222.

129. Munck,L., and B.Møller. 2005. Principal component analysis of near infrared spectra as a tool of endosperm mutant characterisation and in barley breeding for quality. Czech Journal of Genetics and Plant Breeding 41:89-95.

130. Møller Jespersen,B., and L.Munck. 2008. Cereal and cereal products. From prediction of simple analytes to classification of complex genotypes and functional factors for quality. *In* D.-W.Sun (ed.) IR spectroscopy in foods. Elsevier.

131. Møller,B. 2004. Near infrared transmission spectra of barley of malting grade represent a physical-chemical fingerprint of the sample that is able to predict germinative vigour in a multivariate data evaluation model. Journal Institute of Brewing 110:18-33.

132. Nielsen,J.P., D.Bertrand, E.Micklander, P.Courcoux, and L.Munck. 2001. Study of NIR spectra, particle size distributions and chemical parameters of wheat flours: a multiway approach. Journal of Infrared Spectroscopy 9:275-285.

133. Nilsson,G.S., K.-E.Bergquist, U.Nilsson, and Gorton.L. 1996. Determination of the degree of branching in normal and amylopectin type potato starch with 1H-NMR spectroscopy. - Improved resolution and two-dimensional spectroscopy. Starch-Starke 10:352-357.

134. Nørgaard,L., A.Saudland, J.Wagner, J.P.Nielsen, L.Munck, and S.B.Engelsen. 2000. Interval partial least-squares regression (iPLS). A comparative chemometric study with an example from near-infrared spectroscopy. Applied Spectroscopy 54:413-419.

135. Nørgaard,L., R.Bro, F.Westad, and S.B.Engelsen. 2006. A modification of canonical variates analysis to handle highly collinear multivariate data. Journal of Chemometrics 20:425-435.

136. O'Donnell,D.J., J.J.H.Ackerman, and G.E.Maciel. 1981. Comparative study of whole seed protein and starch content via cross polarization-magic angle spinning carbon 13 nuclear magnetic resonance spectroscopy. Journal of Agricultural and Food Chemistry 29:514-518.

137. Olsen,O.A., R.H.Potter, and R.Kalla. 1992. Histo-differentation and molecular biology of developing cereal endosperm. Seed Science Research 2:117-131.

138. Osborne,B.G., T.Fearn, and P.H.Hindle. 1993. Theory of near infrared spectrophotometry. p. 13-35. *In* B.G.Osborne, T.Fearn, and P.H.Hindle (ed.) Practical NIR spectroscopy with applications in food and beverage analysis. Longman.

139. Osborne,B.G. 2006. Applications of near infrared spectroscopy in quality screening of early-generation material in cereal breeding programmes. Journal of Infrared Spectroscopy 14:93-101.

140. Oscarsson,M., T.Parkkonen, K.Autio, and P.Aman. 1997. Composition and microstructure of waxy, normal and high amylose barley samples. Journal of Cereal Science 26:259-264.

141. Passarella,V.S., R.Savin, and G.A.Slafer. 2002. Grain weight and malting quality in barley as affected by brief periods of increased spike temperature under field conditions. Australian Journal of Agricultural Research 53:1219-1227.

142. Patron,N.J., B.Greber, B.F.Fahy, D.A.Laurie, M.L.Parker, and K.Denyer. 2004. The *lys5* mutations of barley reveal the nature and importance of plastidial ADP-Glc transporters for starch synthesis in cereal endosperm. Plant Physiology 135:2088-2097.

143. Pavia,D.L., G.M.Lampman, and G.S.Kriz. 2000. Infrared spectroscopy. p. 13-29. Introduction to spectroscopy - a guide for students of organic chemistry. Harcourt College.

144. Paynter,B.H., and K.J.Young. 2004. Grain and malting quality in two-row spring barley are influenced by grain filling moisture. Australian Journal of Agricultural Research 55:539-550.

145. Pedersen,D.K., H.Martens, J.P.Nielsen, and S.B.Engelsen. 2002. Near-infrared absorption and scattering separated by extended inverted signal correction (EISC): Analysis of near-infrared transmittance spectra of single wheat seeds. Applied Spectroscopy 56:1206-1214.

146. Pedersen,H.T., H.Berg, F.Lundby, and S.B.Engelsen. 2001. The multivariate advantage in fat determination in meat by bench-top NMR. Innovative Food Science & Emerging Technologies 2:87-94.

147. Pelosi,L., L.Heux, and V.Bulore. 2006. Polymorphism of curdlan and (1-3)-beta-D-glucan synthesized in vitro: A 13C CP-MAS and X-ray diffraction analysis. Carbohydrate Polymers 66:207.

148. Petersen,B.O., M.Krah, J.O.Duus, and K.K.Thomsen. 2000. A transglycosylating 1,3(4)-beta-glucanase from *Rhodothermus marinus*. -NMR analysis of enzyme reactions. European Journal of Biochemistry 267:361-369.

149. Philippe,S., P.Robert, C.Barron, L.Saulnier, and F.Guillon. 2006. Deposition of cell wall polysaccharides in wheat endosperm during grain development: Fourier Transform-Infrared microspectroscopy study. Journal of Agricultural and Food Chemistry 54:2303-2308.

150. Pines,A., M.G.Gibby, and J.S.Waugh. 1972. Proton-enhanced nuclear induction spectroscopy: A method for high resolution NMR of dilue spins in solids. The Journal of Chemical Physics 56:1776-1777.

151. Ratcliffe,R.G. 1994. In-vivo NMR-studies of higher-plants and algae. Advances in Botanical Research, Vol 20 20:43-123.

152. Ratcliffe,R.G. 1996. In vivo NMR spectroscopy: Biochemical and physiological applications to plants. p. 1-26. *In* Y.Shachar-Hill, and P.E.Pfeffer (ed.) Nuclear magnetic resonance in plant biology. American Society of Plant Physiologists.

153. Ridenour,C.F., J.Xiong, and G.E.Maciel. 1996. Investigation of germination and aging in Moravian III barley grain by nuclear magnetic resonance. Biophysical Journal 70:511-531.

154. Robert,P., M.Marquis, C.Barron, F.Guillon, and L.Saulnier. 2005. FT-IR investigation of cell wall polysaccharides from cereal grains. Arabinoxylan infrared assignment. Journal of Agricultural and Food Chemistry 53:7014-7018.

155. Roitsch,T. 1999. Source-sink regulation by sugar and stress. Current Opinion in Plant Biology 2:198-206.

156. Rolletschek,H., W.Weschke, H.Weber, U.Wobus, and L.Borisjuk. 2004. Energy state and its control on seed development: starch accumulation is associated with high ATP and steep oxygen gradients within barley grains. Journal of Experimental Botany 55:1351-1359.

157. Rudi,H., A.K.Uhlen, O.M.Harstad, and L.Munck. 2006. Genetic variability in cereal carbohydrate composition and potentials for improving nutritional value. Animal Feed Science and Technology 130:55-65.

158. Sacco,A., I.N.Bolsi, R.Massini, M.Spraul, E.Humpfer, and S.Ghelli. 1998. Preliminary investigation on the characterization of durum wheat flours coming from some areas of south italy by means of 1H high-resolution magic angle spinning nuclear magnetic resonance. Journal of Agricultural and Food Chemistry **46**:4242-4249.

159. Savin,R., and M.E.Nicolas. 1996. Effects of short periods of drought and high temperature on grain growth and starch accumulation of two malting barley cultivars. Australian Journal of Plant Physiology 23:201-210.

160. Savin,R., and M.E.Nicolas. 1999. Effects of timing of heat stress and drought on growth and quality of barley grains. Australian Journal of Agricultural Research 50:357-364.

161. Savin,R., P.J.Stone, M.E.Nicolas, and I.F.Wardlaw. 1997. Grain growth and malting quality of barley .1. Effects of heat stress and moderately high temperature. Australian Journal of Agricultural Research 48:615-624.

162. Schnyder,H. 1993. The role of carbohydrate storage and redistribution in the source-sink relations of wheat and barley during grain filling - a review. New Phytologist 123:233-245.

163. Scholander,P.F., H.T.Hammel, E.D.Bradstreet, and E.A.Hemmingsen. 1965. SAP pressure in vascular plants. Science 148:339-46.

164. Seefeldt,H.F., F.van der Berg, W.Köckenberger, S.B.Engelsen, and B.Wollenweber. 2007. Water mobility in the endosperm of high beta-glucan barley mutants as studied by Nuclear Magnetic Resonance Imaging. Magnetic Resonance Imaging 25:425-432.

165. Séné, F.B., M.C.McCann, R.H.Wilson, and R.Grinter. 1994. Fourier-transform Raman and Fourier-transfom infrared spectroscopy. An investigation of five higher plant cell walls and their components. Plant Physiology 106:1623-1631.

166. Shewry,P.R., M.S.Williamson, and M.Kreis. 1987. Effects of mutant genes on the synthesis of storage components in developing barley endosperms. p. 95-117. *In* H.Thomas, and D.Grierson (ed.) Developmental mutants in higher plants. Cambridge University Press.

167. Slafer,G.A. 2003. Genetic basis of yield as viewed from a crop physiologist's perspective. Annals of applied Biology 142:117-128.

168. Sohn,M., D.S.Himmelsbach, and F.E.Barton. 2004. A comparative study of Fourier transform Raman and NIR spectroscopic methods for assessment of protein and apparent amylose in rice. Cereal Chemistry 81:429-433.

169. Sreenivasulu,N., L.Altschmied, R.Radchuk, S.Gubatz, U.Wobus, and W.Weschke. 2004. Transcript profiles and deduced changes of metabolic pathways in maternal and filial tissues of developing barley grains. The Plant Journal 37:539-553.

170. Stone,P.J., and M.E.Nicolas. 1995. Effect of timing of heat stress during grain filling on two wheat varieties differing in heat tolerance .1. Grain growth. Australian Journal of Plant Physiology 22:927-934.

171. Sweetlove,L.J., R.L.Last, and A.R.Fernie. 2003. Predictive metabolic engineering: A goal for systems biology. Plant Physiology 132:420-425.

172. Szczodrak,J., Z.Czuchajowska, and Y.Pomeranz. 1992. Characterization and estimation of barley polysaccharides by Near-infrared spectroscopy.2. Estimation of total beta-D-glucans. Cereal Chemistry 69:419-423.

173. Tang,H., Y.-L.Wang, and P.Belton. 2000. 13C CPMAS studies of plant cell wall materials and model systems using proton relaxation-induced spectral editing techniques. Solid State Nuclear Magnetic Resonance 15:239-248.

174. Tester,R.F. 1997. Influence of growth conditions on barley starch properties. International Journal of Biological Macromolecules 21:37-45.

175. Tester,R.F., W.R.Morrison, and A.H.Schulman. 1993. Swelling and Gelatinization of Cereal Starches .5. Riso Mutants of Bomi and Carlsberg-Ii Barley Cultivars. Journal of Cereal Science 17:1-9.

176. Tetlow,I.J., M.K.Morell, and M.J.Emes. 2004. Recent developments in understanding the regulation of starch metabolism in higher plants. Journal of Experimental Botany 55:2131-2145.

177. Teulat,B., P.Monneveaux, J.Wery, C.Borries, I.Souyris, A.Charrier, and D.This. 1997. Relationships between relative water content and growth parameters under water stress in barley: a QTL study. New Phytologist 137:99-107.

178. Thompson,R.G., and D.E.LaBerge. 1977. Barley endosperm cell walls: a review of cell wall polysaccharides and cell-wall degrading enzymes. Technical Quaterly MBAA 14:238-243.

179. Thorbjørnsen,T., P.Villand, K.Denyer, O.A.Olsen, and A.M.Smith. 1996. Distinct isoforms of ADPglucose pyrophosphorylase occur inside and outside the amyloplasts in barley endosperm. The Plant Journal 10:243-250.

180. Tian,C., E.Chikayama, Y.Tsuboi, T.Kuromori, K.Shinozaki, J.Kikuchi, and T.Hirayama. 2007. Top-down phenomics of *Arabidopsis thaliana*: Metabolic profiling by one-and two-dimensional nuclear magnetic resonance spectroscopy and transcriptome analysis of albino mutants. The Journal of Biological Chemistry 282:18532-18541.

181. Tomasi,G., F.van der Berg, and C.Andersson. 2004. Correlation optimized warping and dynamic time warping as preprocessing methods for chromatographic data. Journal of Chemometrics 18:231-241.

182. Tønning,E. 2007. Wheat baking quality in a process analytical perspective. Sampling, diversification, prediction and chemometric method development. PhD thesis, University of Copenhagen.

183. Tønning,E., L.Nørgaard, S.B.Engelsen, L.Pedersen, and K.H.Esbensen. 2006. Protein heterogeneity in wheat lots using single-seed NIT - A Theory of Sampling (TOS) breakdown of all sampling and analytical errors. Chemometrics and Intelligent Laboratory Systems 84:142-152.

184. Tønning,E., A.K.Thybo, L.Pedersen, L.Munck, Å.Hansen, S.B.Engelsen, and L.Nørgaard. 2007. Bulk quality diversification of organic wheat by single-kernel near-infrared (SK-NIR) sorting. Journal of Cereal Science, submitted.

185. Tsuchiya,K., T.Urahara, T.Konishi, T.Kotake, T.Tohno-oka, K.Komae, N.Kawada, and Y.Tsumuraya. 2005. Biosynthesis of (1-3,(1-4)-beta-glucan in developing endosperms of barley (*Hordeum vulgare*). Physiologia Plantarium 125:181-191.

186. Viereck,N., L.Nørgaard, R.Bro, and S.B.Engelsen. 2006. Chemometric analysis of NMR data. p. 1811-1821. *In* G.A.Webb (ed.) Modern Magnetic Resonance. Springer.

187. Wallwork,M.A.B., C.F.Jenner, S.J.Logue, and M.Sedgley. 1998a. Effect of high temperature during grain-filling on the structure of developing and malted barley grains. Annals of Botany 82:587-599.

188. Wallwork,M.A.B., S.J.Logue, L.C.MacLeod, and C.F.Jenner. 1998b. Effect of high temperature during grain filling on starch synthesis in the developing barley grain. Australian Journal of Plant Physiology 25:173-181.

189. Weschke,W., R.Panitz, N.Sauer, Q.Wang, B.Neubohn, H.Weber, and U.Wobus. 2000. Sucrose transport into barley seeds: molecular characterization of two transporters and implications for seed development and starch accumulation. Plant Journal 21:455-467.

190. Wesley,I.J., B.G.Osborne, R.S.Anderssen, S.R.Delwiche, and R.A.Graybosch. 2003. Chemometric localization approach to NIR measurement of apparent amylose content of ground wheat. Cereal Chemistry 80:462-467.

191. Westerlund,E., R.Andersson, and P.Aman. 1993. Isolation and Chemical Characterization of Water-Soluble Mixed-Linked Beta-Glucans and Arabinoxylans in Oat Milling Fractions. Carbohydrate Polymers 20:115-123.

192. White,A.J., and C.Critchley. 1999. Rapid light curves: A new fluorescence method to assess the state of the photosynthetic apparatus. Photosynthesis Research 59:63-72.

193. Williams,P.C. 2001. Implementation of near infrared technology. p. 145-170. *In* P.C.Williams, and K.H.Norris (ed.) Near infrared technology in the agricultural and food industries. American Association of Cereal Chemists.

194. Williams,P.C., and K.H.Norris. 1987. Near Infrared technology in agricultural and food industries. American Association of Cereal Chemists, St Paul, Minnesota, USA.

195. Williams,P.C., K.R.Preston, K.H.Norris, and P.M.Starkey. 1984. Determination of amino acids in wheat and barley by near-infrared reflectance spectroscopy. Journal of Food Science 49:17-22.

196. Wilson,S.M., R.A.Burton, M.S.Doblin, B.A.Stone, E.J.Newbigin, G.B.Fincher, and A.Bacic. 2006. Temporal and spatial appearance of wall polysaccharides during cellularization of barley (Hordeum vulgare) endosperm. Planta 224:655-667.

197. Wold,S., K.H.Esbensen, and P.Geladi. 1987. Principal component analysis. Chemometrics and Intelligent Laboratory Systems 2:37-52.

198. Wold,S., H.Martens, and H.Wold. 1983. The multivariate calibration-problem in chemistry solved by the PLS method. Lecture Notes in Mathematics 973:286-293.

199. Wood,P.J., J.Weisz, and B.A.Blackwell. 1994. Structural studies of (1->3),(1->4)-Beta-D-glucans by C(13)-nuclear magnetic resonance spectroscopy and by rapid analysis of cellulose like regions using high-performance anion-exchange chromatography of oligosaccharides released by lichenase. Cereal Chemistry 71:301-307.

200. Woodward,J.R., and G.B.Fincher. 1983. Water-soluble barley beta-glucans. Fine structure, solution behaviour and organization in the cell wall. Brewers Digestive 58:28-32.

201. Woodward,J.R., G.B.Fincher, and B.A.Stone. 1983. Water soluble (1->3, 1->4)-beta-D-glucans from barley (*Hordeum vulgare*) endosperm. II. Fine structure. Carbohydrate Polymers 3:207-225.

202. Wursch,P., and F.X.Pi-Synyer. 2006. The role of viscous soluble fiber in the metabolic control of diabetes. A review with special emphasis on cereals rich in beta-glucan. Diabetes Care 20:1774-1780.

203. Yang,J.C., and J.H.Zhang. 2006. Grain filling of cereals under soil drying. New Phytologist 169:223-236.

204. Yoo,D.H., B.H.Lee, P.S.Chang, H.G.Lee, and S.H.Yoo. 2007. Improved quantitative analysis of oligosaccharides from lichenase-hydrolyzed water-soluble barley beta-glucans by high-performance anion-exchange chromatography. Journal of Agricultural and Food Chemistry 55:1656-1662.

205. Zachariassen,C.B., J.Larsen, F.van den Berg, and S.B.Engelsen. 2005. Use of NIR spectroscopy and chemometrics for on-line process monitoring of ammonia in Low Methoxylated Amidated pectin production. Chemometrics and Intelligent Laboratory Systems 76:149-161.

206. Zhang,G., J.Chen, and J.Wang. 2002. Variation in barley endosperm beta-glucan content in three barley cultivars as a function of spike number and within-spike position. Journal of Cereal Science 35:99-101.

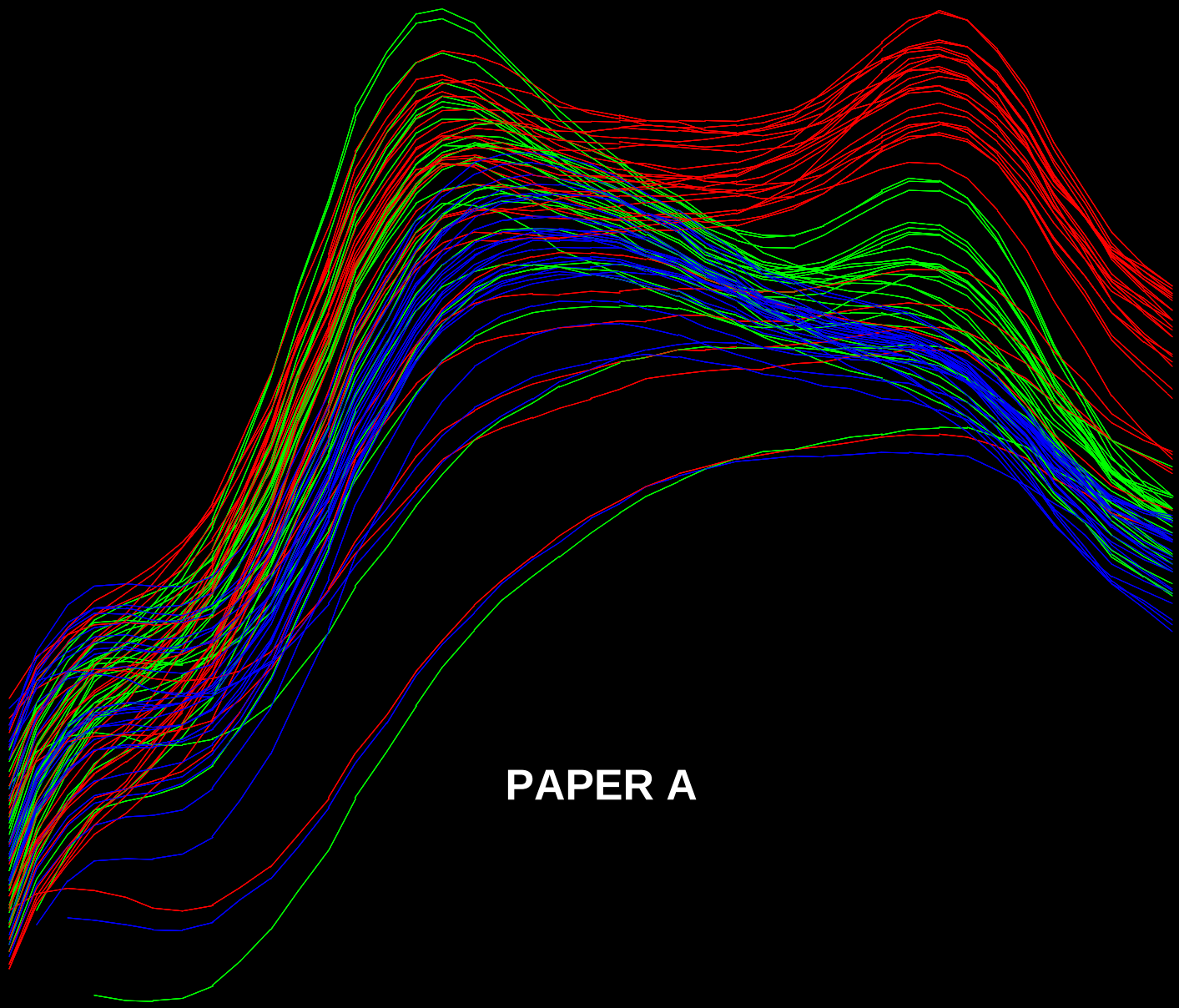

PAPER A

Accumulation of mixed linkage (1→3)(1→4)-D-β-glucan during grain filling in barley – A vibrational spectroscopy study

Helene Fast Seefeldt, Andreas Blennow, Birthe Møller Jespersen, Bernd Wollenweber and Søren Balling Engelsen

Journal of Cereal Science, submitted

Research paper

Accumulation of mixed linkage (1→3)(1→4)-D-β-glucan during grain filling in barley – A vibrational spectroscopy study

Helene Fast Seefeldt[ab], Andreas Blennow[c], Birthe Møller Jespersen[b], Bernd Wollenweber[a] and Søren Balling Engelsen[b*]

a) University of Aarhus, Faculty of Agricultural Sciences, Dept. of Genetics and Biotechnology, Forsøgsvej 1, 4200 Slagelse, Denmark

b) University of Copenhagen, Faculty of Life Sciences, Dept. of Food Science, Quality & Technology, 1958 Frederiksberg C, Denmark

c) University of Copenhagen, Faculty of Life Sciences, Dept. of Plant Biology, Centre for Molecular Plant Physiology, 1958 Frederiksberg C, Denmark

*) Corresponding author: Søren Balling Engelsen, University of Copenhagen, Faculty of Life Sciences, Dept. of Food Science, Quality & Technology, 1958 Frederiksberg C, Denmark. Tel: +45-3533-3205, Fax: +45-3533-3245, *E-mail*: se@life.ku.dk

Abbreviations:

ADP-glucose: Adenosine 5´diphosphate glucose
ATR: Attenuated total reflection
BG: Mixed linkage (1→3)(1→4)-D-β-glucan
DAF: Days after flowering
EISC: Extended inverted signal correction
FT-IR: Fourier Transformed Infrared
iPLS: Interval partial least squares regression
MSC: Multiple scatter correction
NIR: Near-infrared reflectance
PC: Principal component
PCA: Principal component analysis
PLS: Partial least squares regression
RMSECV: Root Mean Square Error of Cross Validation
SECV: Standard Error of Cross Validation
SEE: Standard Error of Estimate
VIS: Visual part of the NIR spectra

Keywords: Infrared, IR, Near-infrared, NIR, (1→3)(1→4)-D-β-glucan, grain filling

Abstract

The accumulation of mixed linkage barley (1→3)(1→4)-D-β-glucan (BG) during grain filling at eight stages was studied using standard reference methods and infrared spectroscopy. Two mutant barley genotypes having higher (starch mutant *lys5f*) and lower (high lysine mutant *lys3a*) BG content than the normal control Cork were studied. The Cork and *lys3a* genotypes showed a linear BG accumulation throughout the grain filling to reach a maximum of approx. 6 and 4% BG (w/w) dry matter, respectively. However, *lys5f* mutant exhibited exponential increase in BG synthesis to a maximum of approx. 18% BG (w/w) dry matter already 30 days after flowering (DAF), seemingly compensating for a decreased synthesis of starch.

The spectral information of the barley flour was compared to pure BG spectra and partial least squares regression (PLS) models were constructed for calibration to BG content. Informative regions in the near-infrared (NIR) and the infrared (IR) spectra were identified for separation of temporal and genetic differences. Interval PLS of *lys5f* yielded good calibration models to BG (R^2 = 0.92 for IR in the region 1440-1470 cm^{-1} and R^2 = 0.94 for NIR in the region 2280-2360 nm).

1. Introduction

In the quest for optimising cereals for soluble fibres and other health-promoting components there is a great interest in studying the metabolic changes during grain filling, such as the cell wall fibre development in barley mutants differing in mixed linkage (1→3)(1→4)-D-β-glucan (BG) using high-throughput methods. Inexpensive, spectroscopic methods based on vibrational spectroscopy offer the possibility of fast and flexible analysis of a large number of genotypes (Osborne, 2006). Near-infrared (NIR) and infrared (IR) spectroscopy measure the vibrations of molecular covalent bonds. The NIR region 14300 - 4000 cm^{-1} (780 - 2500 nm) mainly gives information about overtones and combination tones (stretching and bending) involving anharmonic bonds primarily to hydrogen, whereas the IR region 4000 - 200 cm^{-1} (2500-50000 nm) gives information about the fundamental vibrations. NIR spectroscopy is already well established for at/on-line quality control in the food and food ingredients industries (Zachariassen et al., 2005) and is able to provide information about chemical parameters such as water, protein and starch content as well as about physical parameters such as particle size and temperature. In cereals, NIR spectra of single seeds have proven very informative for the determination of different quality traits such as protein and fat content with high accuracy (Delwiche, 1995; Pedersen et al., 2002). In fact, a new high capacity single-seed TriQ NIR sorting system (Bomill AB, Lund, Sweden)(Munck, 2007) has been developed utilising NIR spectra to diversify heterogeneous bulk lots of wheat with regards to multivariate complex quality traits such as dough performance and baking value (Munck, 2007; Tønning et al., 2007). Furthermore, NIR can be used to evaluate quality traits such as the fibre fraction of cereal cell walls (Blakeney and Flinn, 2005) and genetics (Jacobsen et al., 2005; Munck et al., 2004).

While NIR spectroscopy has primarily been used in quantitative analysis of bulk components (in spite of its documented ability to predict complex qualitative traits like baking and malting quality (Munck, 2007)), IR spectroscopy has mainly been used to study well defined components such as plant cell wall polysaccharides (Chen et al., 1998; Kacurakova and Wilson, 2001; McCann et al., 1992; Robert et al., 2005; Séné et al., 1994). Recently, micro Fourier transformed infrared spectroscopy (FT-IR) was used to study the deposition of cell wall polysaccharides in wheat endosperm during grain development with emphasis on BG and arabinoxylans (Philippe et al., 2006). Also, NIR spectroscopy has proven valuable in monitoring plant physiological

processes such as carbohydrate accumulation during grain filling (Gergely and Salgo, 2005). NIR screenings of normal barley and mutants have resulted in the discovery of genotypes with a strongly increased content of soluble BG fibres (Munck et al., 2004). The high-BG barley mutant line *lys5f* is a structural (enzyme functional) low-starch mutant (Munck et al., 2004; Munck and Møller, 2005) unable to transport ADP-glucose across the plastid envelope due to an inactive ADP-glucose transporter (Patron et al., 2004). *Lys5f* is thus disabled in efficient synthesis of starch, but compensates via an extremely high content (approx. 17 % d.m.) of soluble and insoluble BG (Munck et al., 2004). The *lys3a* mutant is a regulatory mutant (Jacobsen et al., 2005) that primarily inhibits the synthesis of the hordein, but increases the soluble proteins. It has approx. 2-3 % BG compared to 3-4% in normal barley like Cork when grown in green houses (Munck et al., 2004).

The aim of this study is thus to characterise and investigate two extreme recessive barley mutants with respect to BG and starch content during grain filling using classical reference methods as well as spectroscopic fingerprinting methods. The carbohydrate mutant *lys5f* with high BG content and the protein *lys3a* with the low BG content are compared to the variety 'Cork' that has a normal content of BG.

2. Experimental

2.1 Plant material

Three genotypes of barley were included in the study: A malt barley (*Hordeum vulgare* cv. Cork) and a barley mutant *lys3a* with alterations in the *lys3* locus on chromosome five tightly linked to adjacent BG synthesis suppressing genes (Munck et al., 2004). The mutant *lys5f* has a mutation in chromosome six. A 'semifield' pot experiment (72 pots, 16.5 cm diameter, 13 cm height) was carried out from April to August 2005 at the University of Aarhus, Research Centre Flakkebjerg, Denmark. Each pot was filled with 10 litres of sphagnum with 15% Perlite (Perlite, Denmark) added. Ten seeds of each genotype were sown on April 20th and thinned to three seedlings per pot on May 31st. All pots were drip-watered throughout the experiment and standard pest control was performed against mildew and aphids when needed. Flowering was judged visually when 50% of the spikes showed clear pollen release which occurred between the 26th and 27th of June. Spikes were harvested at eight time points during grain filling: 9, 13, 16, 20, 23, 30, 39 and 47 days after flowering (DAF).

2.2 Plant analysis

The spike on the main tiller and the first spike of the side tillers were cut and immediately frozen in liquid nitrogen. After freezing the kernels were detached from the spike, counted and weighed. Kernels were transferred to $^{-}80^{o}$ C and freeze-dried within 3 weeks after harvest. One sample consisted of the seeds from two spikes. The freeze-dried grains were milled (0.5 mm, Cyclotec 1093, Foss Tecator AB, Högenas, Sweden). A total of 91 samples were analysed (Cork: 31, *lys5f*: 31 and *lys3a*: 29). The total sample set consisted of 3 genotypes at 8 temporal harvest points - two replicate spectra of each genotype from harvests 1-4 and six replicate spectra of each genotype from harvests 5-8 were analysed. This experimental design yielded a total of 96 samples (3 genotypes × 4 (1-4 harvests) × 2 replicates + 3 genotypes × 4 (5-8 harvests) × 6 replicates). Due to a minor flaw in the experiment, three replicates of *lys3a* from harvests 1, 5 and 7, and two replicates of Cork harvest 5 and *lys5f* harvest 5 were lost. The ground material was stored in sealed plastic bottles at room temperature until analysis.

2.3 Chemical analysis

The content of soluble BG was analysed by fluorimetry (Calcoflour reagent type II, Scandinavian Brewery Laboratory, Frederiksberg, Denmark) (Munck et al., 1989). The values from the last four time points in *lys5f* were checked with an enzymatic kit (Megazyme, Wicklow, Ireland) specific for mixed-linkage BG. The total content of starch was analysed as follows: Freeze dried flour (10 mg) was washed 3 times with 1 ml aliquots 80% ethanol in screw-cap Eppendorf tubes. Starch in the washed flour was gelatinised by the addition of KOH (400 µl, 0.2 M) and incubation at 95°C for 1 hour. After cooling, 140 µl 1M acetic acid was added, the samples mixed and diluted 20-fold with water. The diluted sample (10 µl) was mixed with an equal volume of amyloglucosidase (10 U/ml, Fluka) solubilised in 50 mM Na acetate pH 5.0 and starch was hydrolysed by incubation at 37°C for 2 hours. A 2 10 µl aliquot of 50 mM Mops/KOH pH 7,3, 5 mM MgCl2, 1 mM EDTA, 1 mM ATP, 1 mM NAD and 4 U/ml hexokinase was added and absorbance at 340 nm was registered. 1 µl of 500 U/ml Glucose-6-phosphate dehydrogenase was added and the production of NADH was followed until steady as the absorbance at 340 nm. Starch content in

the original flour was calculated using glucose as standard. Amylose in the flour was determined by iodine complexation, as described by Bay-Smidt et al., (1999). The amylopectin chain length distribution of the starch was analysed by high performance anionic exchange chromatography with pulsed amperometric detection (HPAEC-PAD) as described by Blennow et al., (1998).

FT-IR and NIR spectra were obtained from the pure substances: Cellulose (9004—34-6, Sigma-Aldrich Chemie, Steinheim, Germany), BG (Barley – Medium Viscosity, Megazyme, Wicklow, Ireland) and wheat starch with normal and high content of amylose (Ritmo, Sejet Plantbreeding, Horsens, Denmark). The starches were purified according to Blennow et al., (1998).

2.4 FT-IR measurements

All FT-IR spectra were acquired at room temperature using the Arid-Zone MB100 FT-IR spectrometer (ABB Bomen Inc., Quebec, PQ, Canada). The sampling was performed using an Attenuated Total Reflection (ATR) device with a diamond crystal (ZnSe, TR-plate, ARK 0055-603, Spectra-Tech Inc. CT, USA) operating in the range 4000-750 cm^{-1}. Measurements were obtained using 64 scans at 4 cm^{-1} resolution. Background scans were obtained using 128 scans. The scans were averaged and rationed against a single-beam spectrum of the clean ATR crystal and converted into absorbance units.

2.5 NIR measurements

A near-infrared instrument (Foss NIRSystems 6500, USA) was used in reflectance mode in the range of 400-2500 nm. All measurements were acquired at room temperature. For each measurement a sample cup containing approximately 0.5 g of flour was measured. The spectra were recorded in 2 nm steps using a spinning sample module. Each sample was registered using 32 scans, and the internal scanning was performed with 16 scans. The results were averaged as a log 1/*R* spectrum.

2.6 Data analysis

The spectra were analysed using the chemometric software LatentiX 1.0 (www.latentix.com, Latent5, Copenhagen, Denmark) both for visual inspection of the spectra and calculation of Principal Component Analysis (PCA) (Wold et al., 1987)

and Partial Least Squares (PLS) regressions. The PCA was performed to visualise systematic spectral variation. Calibrations and predictions of BG and amylose based on the spectral information were made using PLS. Interval Partial Least Squares Regression (iPLS) (Nørgaard et al., 2000) was performed in order to reveal the most important spectral interval correlated to the calibration parameters. Prior to analysis, the spectral data was scatter-corrected using the Extended Inverted Signal Correction (EISC) (Martens et al., 2003; Pedersen et al., 2002) and all models are mean-centred. The iPLS was carried out using the iTOOLBOX (www.models.life.ku.dk) as a routine for MATLAB 6.0 (The Mathworks Inc., Natick, USA). All reported models are validated using cross validation in segments containing the variety and, in the case of single variety calibration, full cross validation.

3. Results and discussion

The first harvest was performed nine days after flowering (DAF). At 9 DAF the seeds were small, green, very moist and mainly consisting of husk. Between 23 and 30 DAF the seeds started to lose the green colour and turn light yellow. The grains were large and round and the interior was milky-white, but still rather soft. At maturity the grains were dark yellow, very dry and mainly consisting of storage material.

Three distinct stages of the grain filling process could be determined by analysis of the fresh grain weight (Fig.1a). Until 20 DAF a rapid increase in grain weight occurred, followed by a lag phase with stable grain weight. After 30 DAF the grain weight decreased due to the drying and maturation of the seed. The first phase is characterised by a rapid influx of water and cell enlargement and continues until 10-15 DAF. During the second phase the seeds take up nutrients and start to synthesize starch and protein (Jenner et al., 1991). In the third phase the fresh weight decreases due to loss of water as indicated in Fig. 1b. Fresh weight in developing wheat grains have shown similar patterns (Gergely and Salgo, 2003; Jennings and Morton, 1962).

3.1 Accumulation of BG during grain filling - Chemical analysis

Fig. 1c shows the development of BG synthesis between genotypes during grain filling. The analysis of the BG content of the three barley genotypes (Fig. 1c) revealed that *lys5f* from 16 to 30 DAF exhibited an anomalous strong increase in BG accumulation to reach an extreme maximum BG content of approx. 18% at 30 DAF. During the same period *lys3a* and Cork exhibited slow linear accumulation of BG,

which continues throughout the grain filling period until maturity at 47 DAF. The mutant *lys3a* had lower BG content as compared to both Cork and *lys5f* reaching only approx. 4% at harvest. Cork displayed a normal content of BG reaching a maximum level of approx. 6% BG at maturity. During grain filling, Cork and *lys3a* did not start to accumulate BG until 16-20 DAF, whereas *lys5f* already started to accumulate BG between 9 and 13 DAF (Fig. 1c).

In a previous study of three normal barley varieties (Coles, 1979) a large increase in accumulation of BG starting at 19 DAF was found. In wheat the cell walls mainly consist of arabinoxylans, whereas BG constitutes only 25%, but BG was accumulating from early grain filling until 10 DAF after which arabinoxylans were dominating (Philippe et al., 2006). These observations led to the hypothesis that BG could function as a structural element of growing cell walls as well as storage material that could be hydrolysed during germination of the grain (Philippe et al., 2006).

The starch synthesis in Cork and *lys3a* (Fig. 1d) followed the same pattern having a rapid increase from 9 DAF until 20 DAF and reaching a maximum of approx. 47% starch remaining at this level until 39 DAF. For all of the genotypes a minor decrease in starch content of approx. 10% was observed. The mutant *lys5f* displayed a much slower increase throughout the entire grain filling period until 39 DAF to reach a maximum at 23% starch. A low final level of starch in *lys5f* was previously reported (Munck et al., 2004). The high content of BG in *lys5f* can hence be interpreted as a new mechanism for substituting starch synthesis with BG synthesis. Interestingly, the total accumulation of starch and BG reveals three similar patterns for the genotypes with just an offset in total accumulation. Thus, the rapid accumulation rate of BG in *lys5f* corresponds largely to the rapid accumulation of starch in the non-starch genotypes *lys3a* and Cork. This confirms the observation of the starch and BG levels found in mature seed described by Munck et al., (2004). The higher starch content found in Cork was followed by a high dry matter weight (Fig. 1e). The *lys5f* mutant had a markedly lower ratio of amylose/amylopectin (Fig. 1f) which is interesting from a starch functionality view (Tester et al., 2004). The chain length of amylopectin did, however, not differ between the three genotypes and it did not differ markedly over the developmental stages (Data not shown).

A PCA model was generated based on the chemical data, i.e. fresh weight, dry matter, water content, BG, starch and amylose in starch for every developmental stage for

each genotype (Fig. 2). A clear separation of the three genotypes is found along PC2, whereas PC1 describes the temporal variation. BG is highly correlated to the high BG-mutant *lys5f* whereas Cork is correlated to a high dry weight, but also starch content and amylose content are correlated to Cork. The early part of grain filling (*Lys5* 1-3, *lys3* 1-3 and Cork 1-3 in Fig. 2) is found to be correlated with a high content of water, whereas the late part of grain filling is negatively correlated to water content, but has a high correlation to dry weight. The time-dependent trajectories shown in Fig. 2 reveal that between the third and fourth harvest point (16 and 20 DAF) major accumulation occurs concomitant with a rapid BG accumulation in *lys5f* and a rapid starch synthesis in Cork and *lys3a*. However, the genotypes all show the same time dependent pattern.

3.2 Near-infrared analysis of the barley grain filling

The EISC pre-processed VIS/NIR spectra (400-2498 nm) of the 91 barley flour samples are displayed in Fig. 3a. The first three harvests (9-16 DAF) represented by the light blue colours clearly differ in their NIR spectral profiles from the rest of the harvests (20-47 DAF, shown as dark red colours). The first three harvests are less intensive in the first overtone region from 1400–1850 nm and the O-H combination tone centred at 1940 nm. In general, the temporal differences influenced the offset in the spectra, while the genetic differences influenced the shape of the spectra. In the visible part of the spectrum, the grain filling is clearly evidenced by the changes in the chlorophyll peak at 672 nm (Fig. 3b). As previously mentioned, the barley grains were visibly green until 30 DAF (the sixth harvest). Fig. 3c displays a score plot from a PCA of the 91 NIR spectra of the barley flour, explaining 92% of the variance. In the score plot the temporal variation is separated into four well-defined groups. The first three harvests (9-16 DAF) are markedly different from the later harvests and located in the upper left corner of the PCA. The fourth and the fifth harvests (20 and 23 DAF), in which also the BG primarily is synthesized (Fig. 1c), are clustered with the lowest scores in the score plot, the sixth harvest (30 DAF) located in lower right-part of the spectra and the last two harvests (39-47 DAF) in the upper right corner of the PCA. By inspection of the loadings, the primary reason for the clear separation of the temporal grain fillings was found to be due to the chlorophyll peak at 672 nm (Table 1). As observed in Fig. 3c**,** the actual time of flowing is difficult to determine -

in the figure a few samples reside in their previous group (marked with stars in Fig. 3c), presumably due to the inaccuracy in the DAF determination.

Munck et al. (2004) found that the combination tone region 2280–2360 nm contains unique information about the *lys3* mutants and Szczodrak et al. (1992) found that two wavelengths in the region between 2260-2380 nm correlate the best to BG. Fig. 3d shows that the NIR spectra of *lys5f* have a peak in the NIR spectra around 2345 nm (the second bold arrow). This peak is also present in the spectra of *lys3a*, but as a shoulder, whereas the spectra of Cork only have a very weak shoulder. On the other hand, the spectra of Cork have a characteristic shoulder at 2280 nm, indicating starch (first bold arrow in Fig. 3d), according to Munck (2007). This shoulder is absent in the mutants *lys5f* and *lys3a*. As Cork and *lys3a* have almost identical starch content, it could be questioned whether this peak corresponds to starch only.

From the lines indicated in Fig. 3d it can be observed that the three genotypes exhibit similar spectral properties during the first harvest (9 DAF) as well as during the second and third harvests. In order to avoid the dominance of the chlorophyll information the visual part of the spectra was discarded and the NIR region 1100-2498 nm was examined separately (data not shown). The three genotypes are clustered together until 16 DAF. From the fourth harvest (20 DAF) and onwards the three genotypes are separated into three distinct clusters. This is in excellent agreement with the rapid increase in the BG synthesis from 16 DAF to 23 DAF for *lys5f* (Fig. 1c) and the concomitant rapid increase in starch seen for *lys3a* and Cork. The loadings associated with the PCA reveal that the first PC is mainly spanned by information from moisture and starch (O-H stretching vibrations, 1440 nm and 1940 nm) (Table 1), which is in good accordance with the separation of grain filling time points along PC1. The third PC separates the genotypes into a Cork/*lys3a* cluster and a *lys5f* cluster. The corresponding loadings are starch-related peaks (Munck et al., 2004; Szczodrak et al., 1992), which manifest the different syntheses in the three genotypes.

3.3 Infrared investigation of the barley grain filling

The EISC-treated FT-IR spectra (1900-750 cm^{-1}) of the 91 barley flour samples are shown in Fig. 4a. As was the case for the NIR spectra, a clear temporal dependence is observed in the spectra (data not shown), but the difference between genotypes appears more pronounced than in the NIR spectra.

The barley flour spectra represent typical broad absorption bands of polysaccharides in the region 1200-750 cm^{-1} (Kacurakova et al., 2001) with a maximum absorption around 1021 cm^{-1}. The glycosidic absorption band at 1160 cm^{-1} reported by Robert et al (2005) and at 1150 cm^{-1} (Philippe et al., 2006) is found at 1152 cm^{-1} in our samples. Fig. 4c (raw spectra) shows the enlargement of the maximum absorption region in which a clear difference between the three genotypes is observed. At 1002 cm^{-1} the high BG mutant *lys5f* has a different intensity compared to Cork and *lys3a.* Moreover, *lys5f* has a lower intensity of the shoulder around 1070 cm^{-1}, whereas *lys3a* and Cork have well-defined peaks at 1078 cm^{-1}. With regard to the temporal changes, a shift from 1036 cm^{-1} for 9 DAF towards 1021 cm^{-1} for the end of the grain filling is observed in the spectra (Fig. 4c). The anomer-specific peaks in the range from 800 to 950 cm^{-1} contain information about BG as well as other polysaccharide cell wall components (Philippe et al., 2006). Fig. 4d displays an enlargement of this region as second derivative spectra which reveal that *lys5f* has less intensive peaks compared to Cork and *lys3a*. Cork and *lys3a* display a relatively strong α-anomer band at 855 cm^{-1}, whereas the high BG *lys5f* and the early stages of the grain filling show a much weaker α-glucan peak. This is in good accordance with the starch levels in Cork and *lys3a* compared to *lys5f.* In case of the β-anomer sensitive peak normally present at approximately 890 cm^{-1} (Fig. 4d), we only observed higher background intensity in *lys5f* than in the other two genotypes. From approx. 23 DAF the intensity is the highest corresponding to the highest level of BG. Pure barley BG shows a peak at 895 cm^{-1}, not present in the average grain spectra (see Fig. 5).

A PCA was applied to the full second-derivative IR spectra (Fig. 4b) and the first PC explains 97% of the variance. Both the first and the second PC separate the genotypes. The corresponding loading plot (Table 1) revealed that PC1 is mainly spanned by the peak at 1010 cm^{-1} and PC2 at 1049 cm^{-1}, which are the dominating peaks of starch in the second-derivative spectra of the pure substances (not shown). Thus BG seems to play a less pivotal role in discriminating the genotypes compared to starch.

3.4 Relationships between the chemical and spectroscopic methods

In order to study the relationships between the spectral data and the grain filling a range of calibration models were investigated. Global models based on the entire data set as well as local models based on either genotypes or grain filling periods were

generated to predict content of BG. Only a few studies have attempted to construct a NIR calibration to BG content. The quality of the predictions has varied greatly. Correlation coefficient=0.69 and RMSE=0.557% was achieved in the BG range 5.8-8.4% (Czuchajowska et al., 1992). In another study, an 1-VR value that is a determination for cross validation and measure of goodness of fit was found to be 0.92 and a SECV=0.45 in the BG range 0.09-5.12 % (Blakeney et al., 2005). One major problem has been the limited BG range for the calibrations. However, Szczodrak et al. (1992) succeeded in developing calibration models to BG with a correlation coefficient of 0.871 and a SEE (standard error of estimate) of 0.677 using the calibration range 2.7 - 9.5%. In this study the BG variation (calibration range) was further expanded in order to establish a quantitative model between the NIR spectra and the BG content. The global model NIR predicts BG very weakly with a squared correlation coefficient of 0.11 and a RMSECV of 6.2, indicating that the low-BG varieties Cork and *lys3a* did not support the model. The PLS model based solely on the high-BG *lys5f* predicts BG with a R^2 of 0.91 and a RMSECV of 1.9 (corresponding to the horizontal line in Fig. 5a). In order to study the influence of specific spectral regions on the calibrations, interval PLS (iPLS) was applied to the NIR spectra of *lys5f*. Six intervals were able to significantly improve the calibration performance from the global model. The best prediction of BG was not surprisingly made in the NIR region 2280-2360 nm with a R^2 of 0.94 and RMSECV of 1.5 % using 3 PLS components.

PLS calibrations to the FT-IR region and BG were also studied. As with NIR, the global FT-IR models predicted BG very weakly with a squared correlation coefficient of 0.04 and a RMSECV value of 7.37. The extreme *lys5f* bias the calibration, so a PLS model based solely on the high BG *lys5f* was performed. Using this calibration, BG was predicted with a R^2 of 0.77 and a RMSECV of 3.4 (corresponding to the horizontal line in Fig. 5b) for the entire FT-IR region. An iPLS was applied to the IR spectra of *lys5f* and seven intervals were able to significantly improve the calibration performance from the global model. The best interval was in the region 1410-1470 cm^{-1} with a R^2 of 0.92 and RMSECV of 1.9 % using 3 PLS components. This region primarily covers C-H bending vibrations.

4. Conclusions

A rapid increase in grain fresh weight during grain filling is concomitant with the increase of starch and BG. The high BG mutant *lys5f* shows an exponential increase of BG until 23 DAF and reaches a final content of 18%. This is in contrast to the low-BG mutant *lys3a* and the conventional malting barley Cork having linear phases of BG deposition and reaching maxima of only 4% and 6%, respectively. Starch deposition in these latter genotypes was exponential, reaching maxima of 47% compared to a linear increase in *lys5f* leading to a maximum of 23% starch.

The NIR and FT-IR spectra are complete chemical fingerprints of the grain and thus more complex to resolve than single chemical analysis of grains. Data extraction relies on the use of chemometrics to reveal hidden information. In the case of NIR, the genetic variation as well as the BG variation was mainly resolved from the spectral region between 2260-2380 nm. Moreover, the NIR spectra showed mostly temporal differences primarily due to complex changes in moisture. The region 2260-2380 nm for *lys5f* proved very sensitive to calibration to BG. In this region all the barley flour spectra differed and the average grain spectrum was influenced by both the starch/amylose and the BG contents, which underline the importance of this NIR region for breeding purposes. Although less sensitive, the FT-IR in the 1410-1470 cm^{-1} region contained valuable information related to BG.

Fast and non-destructive spectroscopic fingerprinting is obviously advantageous for studying physiological processes such as grain filling as the techniques are non-destructive, fast and sensitive and it is possible to do real-time analysis.

Acknowledgements

The DIAS Competence Fund and the Ministry of Food Agriculture and Fisheries are greatly acknowledged for financial support to the project (FFS05-9: Build Your Food). Betina Sørensen (University of Aarhus) and Lisbeth T. Hansen and Louise Nancke (Faculty of Life Sciences, University of Copenhagen) are acknowledged for technical support of semi-field experiments and chemical analysis. Gilda Kischinovsky is acknowledged for proofreading. The authors wish to thank Lars Munck for valuable comments and for sharing his unique barley mutant collection.

References

Bay-Smidt, A. M., Blennow, A., Bojko, M., Møller. B. L., 1999. The effect of phosphate and amylopectin molecular size on peak viscosity of starch pastes. Annual Transactual of Nordic Rheology Society 7, 31-38.

Blakeney A. B., Flinn P. C., 2005. Determination of non-starch polysaccharides in cereal grains with near-infrared reflectance spectroscopy. Molecular and Nutritional Food Research 49, 546-550.

Blennow A., Bay-Smidt A. M., Wischmann B., Olsen C. E., Møller B. L., 1998. The degree of starch phosphorylation is related to the chain lenght distribution of the neutral and the phosphorylated chains of amylopectin. Carbohydrate Research 307, 45-54.

Chen L., Carpita N. C., Reiter W.-D., Wilson R. H., Jeffries C.,McCann M. C., 1998. A rapid method to screen for cell-wall mutants using discriminant analysis of Fourier transform infrared spectra. The Plant Journal 16, 385-392.

Coles G., 1979. Relationship of mixed-link beta-glucan accumulation to accumulation of free sugars and other glucans in the developing barley endosperm. Carlsberg Research Communications 44, 439-453.

Czuchajowska Z., Szczodrak J., Pomeranz Y., 1992. Characterization and estimation of barley polysaccharides by Near-Infrared spectroscopy.1.Barleys, starches, and beta-D-glucans. Cereal Chemistry 69, 413-418.

Delwiche S. R., 1995. Single wheat kernel analysis by Near-Infrared transmittance: Protein Content. Analytical Techniques and Instrumentation 72, 11-16.

Gergely S., Salgo A., 2003. Changes in moisture content during wheat maturation-what is measured by near infrared spectroscopy? Journal of Near Infrared Spectroscopy 11, 17-26.

Gergely S., Salgo A., 2005. Changes in carbohydrate content during wheat maturation - what is measured by near infrared spectroscopy? Journal of Near Infrared Spectroscopy 13, 9-17.

Jacobsen S., Søndergaard I., Møller B., Desler T., Munck L., 2005. A chemometric evaluation of the underlying physical and chemical patterns that support near infrared spectroscopy of barley seeds as a tool for explorative classification of endoperm genes and gene combinations. Journal of Cereal Science 42, 281-299.

Jenner C. F., Ugalde T. D., Aspinall, D., 1991. The physiology of starch and protein deposition in the endosperm of wheat. Australian Journal of Plant Physiology 18, 211-226.

Jennings A. C., Morton R. K., 1962. Changes in carbohydrate, protein and non-protein nitrogenous compounds of developing wheat grain. Australian Journal of Biological Sciences 16, 318-331.

Kacurakova M., Wilson R. H., 2001. Developments in mid-infrared FT-IR spectroscopy of selected carbohydrates. Carbohydrate Polymers 44, 291-303.

Martens H., Nielsen J. P., Engelsen S. B., 2003. Light scattering and light absorbance separated by extended multiplicative signal correction. Application to near-infrared transmission analysis of powder mixtures. Analytical Chemistry 75, 394-404.

McCann M. C., Hammouri M., Wilson R., Belton P., Roberts K., 1992. Fourier Transform Infrared microspectroscopy is a new way to look at plant cell walls. Plant Physiology 100, 1940-1947.

Munck L., 2007. Breeding for quality traits in cereals - a revised outlook on old and new tools for integrated breeding. Cereals. New York, Springer Verlag. In press

Munck L., Jørgensen K. G., Ruudhansen J., Hansen K. T., 1989. The EBC methods for determination of high molecular-weight beta-glucan in barley, malt, wort and beer. Journal of the Institute of Brewing 95, 79-82.

Munck L., Møller B., 2005. Principal component analysis of near infrared spectra as a tool of endosperm mutant characterisation and in barley breeding for quality. Czech Journal of Genetics and Plant Breeding 41, 89-95.

Munck L., Møller B., Jacobsen S., Søndergaard I., 2004. Near infrared spectra indicate specific mutant endosperm genes and reveal a new mechanism for substituting starch with (1-3,1-4) betaglucan in barley. Journal of Cereal Science 40, 213-222.

Nørgaard L., Saudland A., Wagner J., Nielsen J. P., Munck L., Engelsen S. B., 2000. Interval partial least-squares regression (iPLS). A comparative chemometric study with an example from near-infrared spectroscopy. Applied Spectroscopy 54, 413-419.

Osborne B. G., 2006. Applications of near infrared spectroscopy in quality screening of early-generation material in cereal breeding programmes. Journal of Infrared Spectroscopy 14, 93-101.

Osborne B. G., Fearn T., Hindle P. H., 1993. Theory of near infrared spectrophotometry. Practical NIR spectroscopy with applications in food and beverage analysis. 2, 13-35.

Patron N. J., Greber B., Fahy B. F., Laurie D. A., Parker M. L., Denyer K., 2004. The *lys5* mutations of barley reveal the nature and importance of plastidial ADP-Glc transporters for starch synthesis in cereal endosperm. Plant Physiology 135, 2088-2097.

Pedersen D. K., Martens H., Nielsen J. P., Engelsen S. B., 2002. Near-infrared absorption and scattering separated by extended inverted signal correction (EISC): Analysis of near-infrared transmittance spectra of single wheat seeds. Applied Spectroscopy 56, 1206-1214.

Philippe S., Robert P., Barron C., Saulnier L., Guillon F., 2006. Deposition of cell wall polysaccharides in wheat endosperm during grain development: Fourier Transform-Infrared microspectroscopy study. Journal of Agricultural and Food Chemistry 54, 2303-2308.

Robert P., Marquis M., Barron C., Guillon F., Saulnier L., 2005. FT-IR investigation of cell wall polysaccharides from cereal grains. Arabinoxylan infrared assignment. Journal of Agricultural and Food Chemistry 53, 7014-7018.

Séné C. F. B., McCann M. C., Wilson R. H., Grinter R., 1994. Fourier-Transform raman and Fourier-Transform infrared spectroscopy -an investigation of five higher plant cell walls and their components. Plant Physiology 106, 1623-1631.

Szczodrak J., Czuchajowska Z., Pomeranz Y., 1992. Characterization and estimation of barley polysaccharides by Near-infrared spectroscopy.2. Estimation of total beta-D-glucans. Cereal Chemistry 69, 419-423.

Tester, R. F., Karkalas J., Qi X., 2004. Starch - composition, fine structure and architecture. Journal of Cereal Science 39, 151-165.

Tønning E., Thybo A. K., Pedersen L., Munck L., Hansen Å., Engelsen S. B., Nørgaard L., 2007. Bulk quality diversification of organic wheat by single-kernel near-infrared (SK-NIR) sorting. Journal of Cereal Science, submitted.

Wold S., Esbensen K. H., Geladi P., 1987. Principal component analysis. Chemometrics and Intelligent Laboratory Systems 2, 37-52.

Zachariassen C. B., Larsen J., van den Berg F., Engelsen S. B., 2005. Use of NIR spectroscopy and chemometrics for on-line process monitoring of ammonia in Low Methoxylated Amidated pectin production. Chemometrics and Intelligent Laboratory Systems 76, 149-161.

Tables and Figures

Table 1. The most informative peaks and their putative alignments as determined from loading plots corresponding to PCA's made on the defined regions. The peaks with the highest intensity are listed first. + indicates a positive loading, while – indicates a negative loading.

Method	Region	PC	1.peak	2.peak	3.peak	4.peak	Alignment
NIR	500-750nm	1	-672	+400	+1440	+1930	672: Chlorophyll a, 1440: C-H, O-H in starch,1940 H_2O
	500-750nm	2	-672	-400	+500	+560	
	1100-2498nm	1	+1444	-1856	+1930	-1670	1440 O-H starch, H_2O, 1940 H_2O
	1100-2498nm	3	+2250	-2477	+2355	+2384	2252, 2461 O-H starch, 2353 C-H cellulose, 2380: R-OH
	2280-2360nm	1	-2308	-2348			2310 CH_2, 2347 $HC{=}CHCH_2$
	2280-2360nm	2	+2288	+2314	-2360		2280: CH_3, 2310 C-H CH_2 , 2352: C-H cellulose,
IR	1900-750 cm-1	1	+1010	-960			900-990: aromatic, 1000-1260: C-O alcohol,
							1002 ring stretching (arabinoxylans[A]), 1160-1210:C-C(O)-C
	1900-750 cm-1	2	-1049	+1147	+1002	+1094	ester

***A* from (Philippe et al. 2006). All other alignments from (Osborne et al. 1993).**

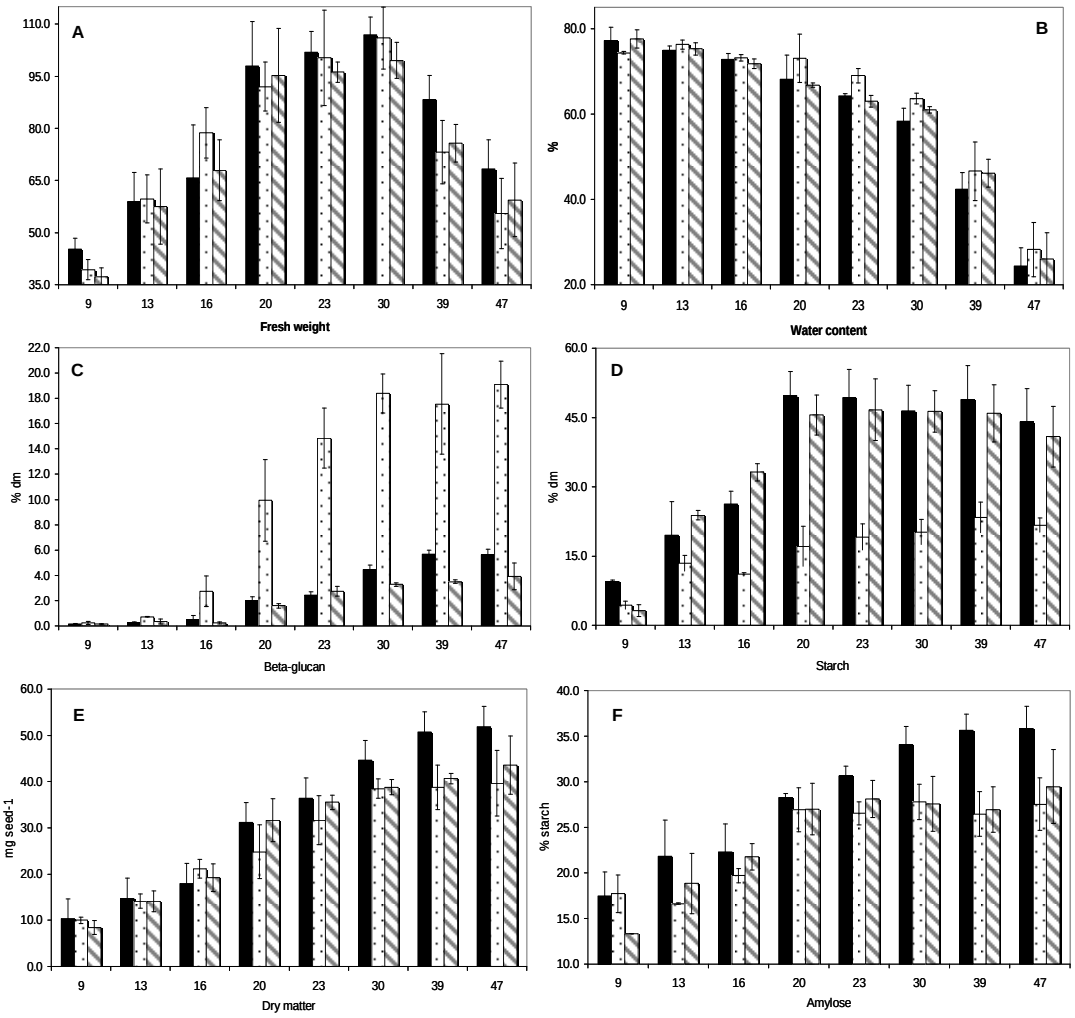

Fig. 1. A. Fresh seed weight (mg) B. Water content (%). C. BG content % (dm). D. Starch content (% dm). E. Seed dry weight (mg). F. Amylose (% in starch). All values are denoted in relation to DAF (days after flowering). Solid: Cork, dotted: *lys5f* , broken: *lys3a*.

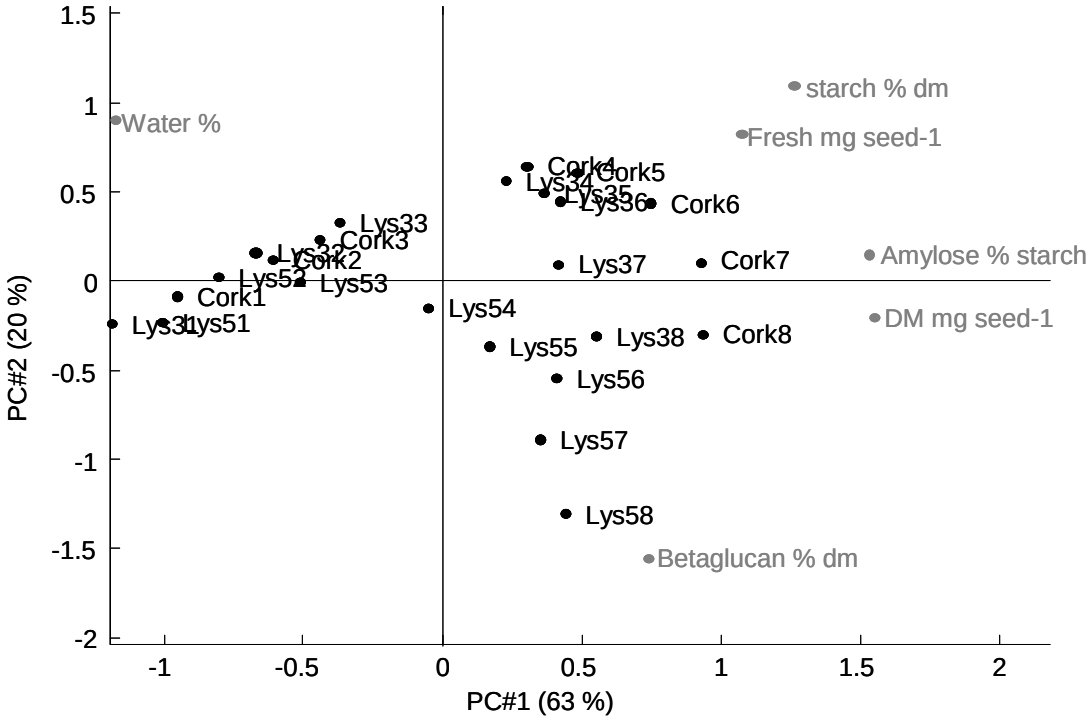

Fig. 2. PCA based on chemical data depicted as a biplot indicating both samples and variables. Time-dependent trajectories are drawn as arrows. Bold: Cork, broken: *lys5f* and grey: *lys3a*.

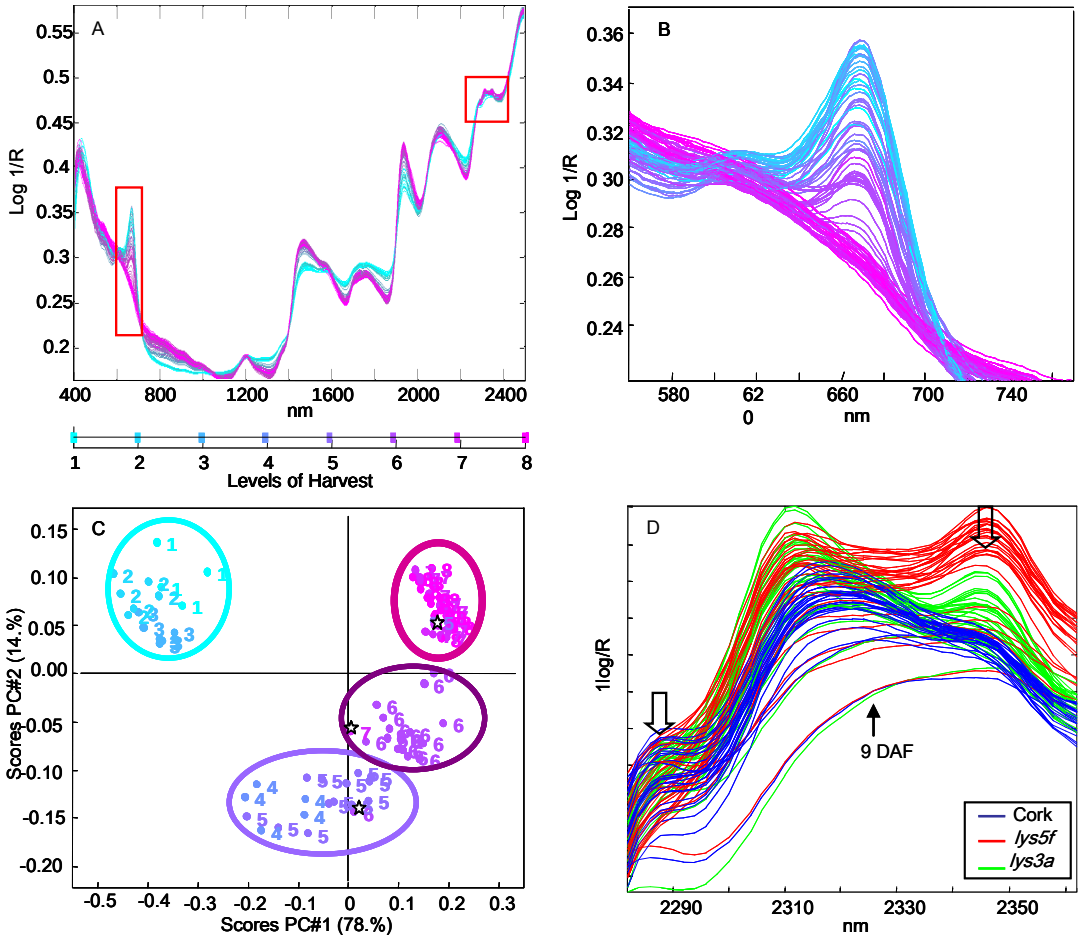

Fig. 3. The complete NIR spectra (400 – 2498 nm) of the three genotypes and eight harvest times. A) The full, EISC-treated spectra. Squares indicate enlargements shown in B and D. B) Magnification of the chlorophyll peak (672 nm) C). PCA model of the full NIR region. Blue: first three harvests, Purple: fourth and fifth harvests, Cerise: sixth harvest, Pink: seventh and eighth harvests. D) The region 2280-2360 nm. Open arrows indicate spectral features of interest. Black arrow indicates spectra of 9 DAF.

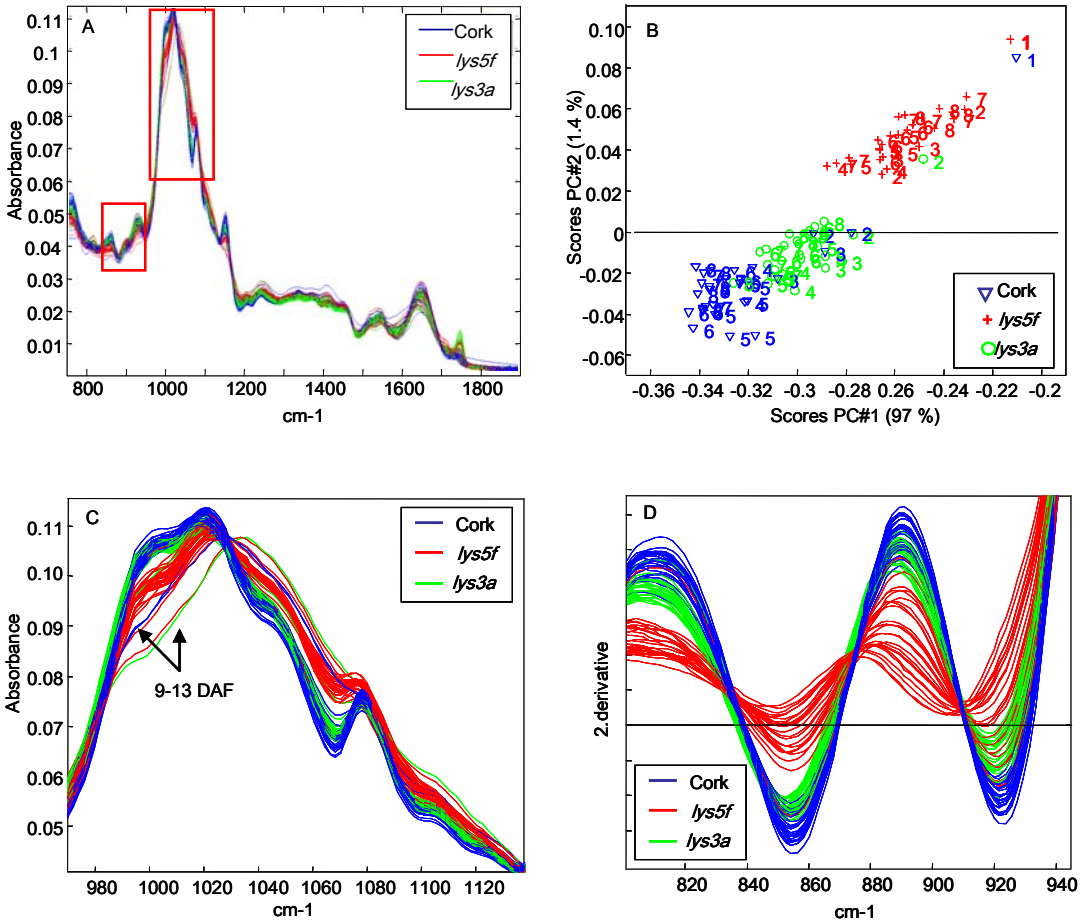

Fig. 4. FT-IR spectra of the region 750-1900 cm^{-1}. A) EISC-treated spectra. Squares are indicated magnified in C and D. B) PCA of the second derivative of the spectra (not mean-centred). C) EISC-pre-processed spectra of the region of maximum absorption. Arrows indicate 9 and 13 DAF. D) The second-derivative spectra of the region from 800-940 cm^{-1}.

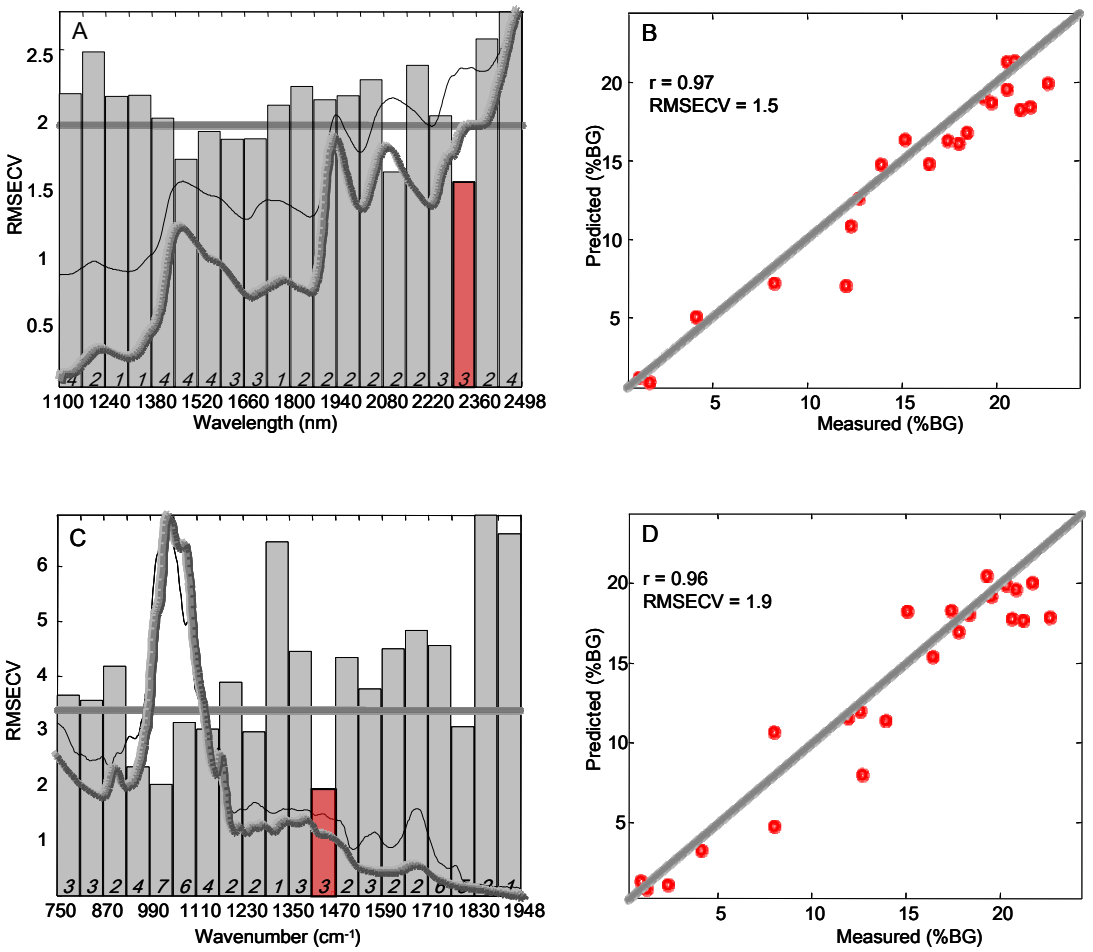

Fig. 5. RMSECV correlation coefficients of iPLS models from *lys5f* of NIR and FT-IR spectra. A) The average NIR grain spectra and a pure NIR BG spectrum (shaded line) superimposed on 20 intervals. Six intervals are better calibrators (smaller RMSECV values) for BG than the global model. Numbers on bars indicate PLS components used. The red marked interval 2280-2360 nm is the best calibrator. B) Measured versus predicted plot of *lys5f* in the interval 2280-2360 nm. C) The average IR grain spectra and a pure IR BG spectrum (shaded line) superimposed on 20 intervals. Seven intervals are better calibrators for BG than the global model. Numbers on bars and red bar as in A. D) The measured versus predicted plot of *lys5f* in the interval 1410-1470 cm^{-1}.

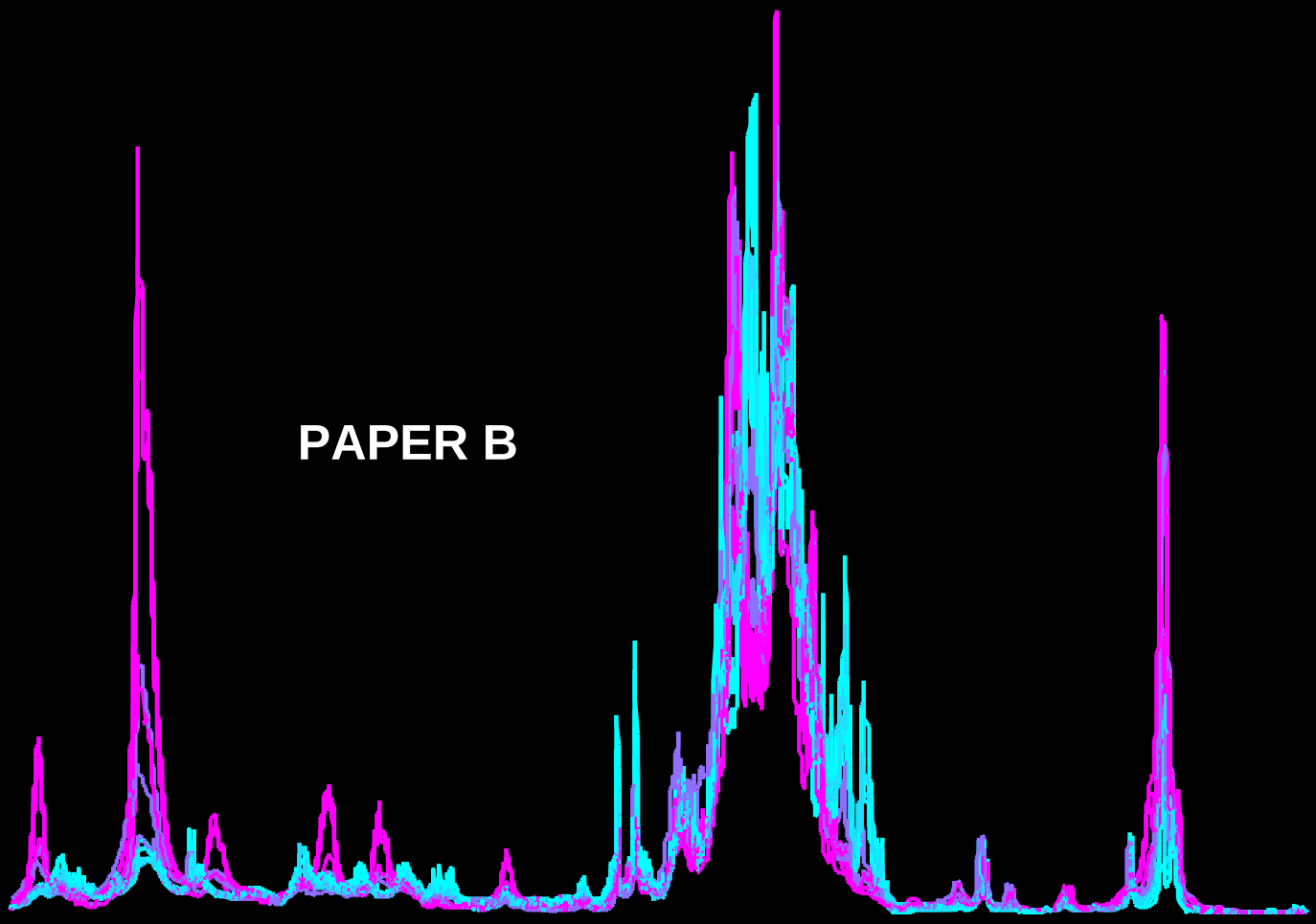

PAPER B

Bulk carbohydrate grain filling of barley β-glucan mutants studied by ^{1}H HR MAS NMR

Helene Fast Seefeldt, Nanna Viereck, Flemming Hofman Larsen, Bernd Wollenweber, Søren Balling Engelsen

Cereal Chemistry, submitted

Research paper

Bulk carbohydrate grain filling of barley β-glucan mutants studied by ^{1}H HR MAS NMR

Helene Fast Seefeldt[ab], Flemming Hofmann Larsen[b], Nanna Viereck[b], Bernd Wollenweber[a], Søren Balling Engelsen[b*]

a) University of Aarhus, Faculty of Agricultural Sciences, Dept. of Genetics and Biotechnology, Forsøgsvej 1, 4200 Slagelse, Denmark

b) University of Copenhagen, Faculty of Life Sciences, Dept. of Food Science, Quality & Technology, Rolighedsvej 30, 1958 Frederiksberg C, Denmark

*) Corresponding author: Søren Balling Engelsen, University of Copenhagen, Faculty of Life Sciences, Dept. of Food Science, Quality & Technology, Rolighedsvej 30, 1958 Frederiksberg C, Denmark, Tel: +45 3533 3205, Fax: +45 3533 3245, *E-mail*: se@life.ku.dk

ABSTRACT

The temporal and genotypic differences in bulk carbohydrate accumulation in three barley genotypes differing in their content of mixed linkage β-(1→3),(1→4)-D-glucan (β-glucan) and starch were investigated using proton high resolution magic angle spinning nuclear magnetic resonance (^{1}H HR MAS NMR) during grain filling. For the first time, ^{1}H HR MAS NMR spectra of flour from immature barley seeds are analyzed. Spectral assignments are made using two-dimensional (2D) NMR methods. Both α- and β-glucan biosynthesis were characterized by inspection of the spectra as well as by calibration to the reference methods for starch and β-glucan content. Starch was quantified with very good calibrations to the α-(1→4) peak (5.29-5.40 ppm) and the region 3.67-3.83 ppm covering starch glycopyranosidic protons from H5 and H6. In contrast, the spectral inspection of the β-anomeric region 4.45-4.85 ppm showed unexpected lack of intensity in the high β-glucan mutant '*lys5f*' at seed maturity, resulting in poor calibration to reference β-glucan content. We hypothesize that the lack of β-glucan signal in '*lys5f*' indicates partial immobilization of the β-glucan that appears to be either genotypic dependent or water/β-glucan ratio dependent.

INTRODUCTION

The functionality of cereals for food and industrial purposes is mainly determined by the composition of starch and fibers, the architecture of starch (Tester et al 2004) and the content and structure of cell wall fibers (Lazaridou and Biliaderis 2007). In particular, barley seeds contain high amounts of the cell wall fiber β-glucan (mixed linkage β-(1→3),(1→4)-D-glucan) that has attracted much attention due to its physical and biological properties (Lazaridou and Biliaderis 2007; Tsuchiya et al 2005; Storsley et al 2003; Queenan et al 2007). β-glucan is a two-face substance, on one hand causing problems in brewing and animal feed industries, and on the other hand having beneficial influence on human health. As an example, β-glucan has been shown to be able to reduce serum cholesterol in hyper-cholesterolemic individuals (Kalra and Joad 2000) and to modulate gluco-regulation in diabetics (Léon et al 2000). In contrast, β-glucan is unwanted in the brewing industry, as it forms a viscous gel which leads to hazing, (Fincher and Stone 1986). Furthermore, barley is considered a less valuable food source for chickens and pigs, as they gain less energy due to the viscous properties of β-glucan which reduce colon emptying (Knudsen 2001). A renewed interest in β-glucan arises from its functionality in food processing due to its water-binding capacity (Holtekjolen et al 2006), stabilizing and thickening ability. Hence it can be used, for example, as a fat-replacer (Burkus and Temelli 2000).

The barley seed endosperm cell walls consists of approx. 75% of β-glucan (Fincher and Stone 1986). β-glucan acts partly as a structural element and partly as a flexible storage material hydrolyzed during grain filling and germination (Buckerigde et al 2004). β-glucan is not a strictly defined polysaccharide and structure differences occur between cereals and within cereal grains (Johansson et al 2004; Zhang et al 2002).

The water-soluble β-glucan from barley contains approx. 70% β-(1→4)-glycosyl linkages and 30% β-(1→3)-glycosyl linkages. Often repetitions of two or more successive β-(1→4)-linkages are found separated by single β-(1→3)-linkages (Fincher and Stone 1986). Insoluble barley β-glucan contains a higher ratio of β-(1→4):β-(1→3)-linkages (Johansson et al 2004). The insoluble fiber fraction appears to be non-covalently bound to arabinoxylans and therefore remains insoluble even in small molar masses (Johansson et al 2004).

The content of β-glucan in barley seeds varies from 3% to 18-20% (dry matter) β-glucan (Seefeldt et al 2007) depending on genotype (Aastrup and Munck 1985; Munck et al 2004) and environmental factors (Aastrup 1979; Fincher and Stone 1986).

Besides the cell walls fibers, three major constituents are accumulated in barley during grain filling: starch, lipids and proteins. Starch constitutes approximately 61 % of the mature grain dry weight in barley (MacGregor and Fincher 1993). Cereals contain different kinds of lipids: membrane-bound oil droplets in the aleurone layer, scutellum and embryo and lipids found in the endosperm (Morrison 1978). Lipids constitute 1-3% of the cereal grain depending on genetic constitution (Jacobsen et al 2005). The lipids in the endosperm are lysophospholipids complexed with amylose (Morrison 1993). In barley, proteins account for 8-13 % dry weight, the majority being storage proteins surrounding the starch. The protein content and composition are also genetically dependent (Jacobsen et al 2005).

It would be valuable to correlate spectral fingerprints (unique identification of genotypes) with starch or β-glucan in plant breeding screening programs, and recently a spectral near-infrared (NIR) region was found giving good correlation to β-glucan (Seefeldt et al 2007). Nuclear magnetic resonance (NMR) spectroscopy is a versatile

technique that provides chemical as well as quantitative information (Kuchenbrod et al 1995) and has recently attracted much attention in plant biology studies (e.g. (Baker et al 2006; Bardet et al 2001; Fan 1996; Glidewell 2006)), as it can provide detailed information of the plant metabolome (Krishnan et al 2005).

Cereals consist mainly of semi-crystalline compounds and the standard NMR technique to detect signals from rigid, solid-state material is by ^{13}C cross polarization (CP) magic angle spinning (MAS) NMR (Pines et al 1972), by which the resonances from the protonated carbons belonging to the rigid domains are enhanced. ^{13}C CP-MAS NMR has e.g. been used to study protein and starch in various types of seeds (O'Donnell et al 1981), triacylglycerols (Bardet et al 2001) and cell wall properties (Jarvis and McCann 2000; Tang et al 2000). Liquid-state ^{1}H high-resolution (HR) MAS NMR is faster and more sensitive than ^{13}C CPMAS solid state NMR, because of ^{1}H's higher sensitivity. ^{1}H HR MAS NMR spectroscopy in combination with chemometrics has previously been used for analysis of durum wheat flour for the discrimination of varietal and geographical origin (Brescia et al 2002). Similarly, liquid-state ^{1}H NMR and chemometrics has been used for authenticity testing of orange juice (Vogels et al 1996) and olive oil (Mannina et al 2003).

The aim of this study was to explore the physiological changes in barley during grain filling by using the combination of ^{1}H HR MAS NMR and multivariate data analysis. Emphasis was on the synthesis of β-glucan and starch in barley genotypes varying from extremely low content (4% dry matter (dm)) to extremely high (18% dm) content of β-glucan, and from low starch content (24 % dm) to normal content of starch (48% dm).

MATERIALS AND METHODS

Plant material

Three genotypes of barley were used (Table I): The barley mutant line ‘*lys5f*’ is a low-starch mutant (Munck and Møller 2005;Munck et al 2004) unable to transport ADP-glucose across the plastid envelope due to an inactive ADP-glucose transporter (Patron et al 2004), but it compensates for this by a high content of soluble β-glucan (Munck et al 2004). The second mutant ‘*lys3a*’ is a protein mutant with high levels of the water-soluble proteins albumins, but low in hordeins (Jacobsen et al 2005). It has reduced starch content and low β-glucan content (Munck et al 2004). Furthermore, *‘lys3a’* has extremely high levels of lysine, histidine, arginine, asparagine, glycine and alanine compared to normal barley, but extremely low levels of glutamine, proline and phenylalanine (Jacobsen et al 2005). The third genotype is a reference malt barley (*Hordeum vulgare* cv. ‘Cork’) with normal levels of starch and β-glucan. Experimental conditions for plant growth are according to (Seefeldt et al 2007). Harvesting occasions took place 8 times during grain filling at 9, 13, 16, 20, 23, 30, 39 and 47 days after flowering (DAF).

Plant analysis

Spikes were harvested and immediately frozen in liquid nitrogen. Afterwards, the seeds were freeze-dried for two days. The freeze-dried grains were milled (0.5 mm, Cyclotec 1093, Foss Tecator AB, Högenas, Sweden). The ground flour material was stored in sealed plastic bottles at room temperature until analysis. A sample unit consisted of the seeds from two spikes. A total of 23 flour samples were analyzed, covering 9 (first harvest), 13 (second harvest), 23 (fifth harvest) and 47 (eight harvest)

DAF out of a total of eight harvests. Two replicates of all three genotypes (4 × 2 × 3) were analyzed. One sample from *'lys3a'* , 9 DAF was missing.

Chemical analysis

The content of soluble β-glucan was analyzed by fluorimetry (Calcoflour reagent type II, Scandinavian Brewery Laboratory, Frederiksberg, Denmark) (Munck et al 1989). The starch content was determined as described in (Seefeldt et al 2007).

^{1}H HR MAS NMR measurements

The flour was suspended in D_2O (14.0-14.3 mg flour + 50 µl D_2O containing 5.8 mM TSP-d_4) and spectra were acquired using a composition-pulse experiment with water suppression (Bax 1985). A Bruker AVANCE 400 NMR spectrometer (Bruker BioSpin, Rheinstetten, Germany) operating at 400.13 MHz for protons using a HR-MAS probe with a 4-mm (o.d) rotors for all experiments. ^{1}H NMR spectra were recorded at 75^{o}C using a spinning rate of 7 kHz. A total of 64 scans were acquired with a recycle delay of 4 seconds, resulting in a total acquisition time of approximately 7 minutes. A total of 32 K complex data points were acquired and zero-filled to 64 K points prior to Fourier Transform.

Furthermore, 2D spectra of '*lys5f*' from 9 and 47 DAF were acquired. 2D ^{1}H-^{1}H COSY, ^{1}H -^{1}H TOCSY and ^{1}H-^{13}C HSQC spectra were acquired at 75^{o}C using the Bruker pulse sequences; *cosygpmfgf*, *mlewphpr* and *hsqcgpph*, respectively (Bax 1985; Ancian et al 1997). The 2D spectra were assigned using the non-commercial Sparky software (www.cgl.ucsf.edu/home/sparky). All spectra were referenced to TSP-d_4 at 0.0 ppm prior to data analysis.

The spectra were analyzed using the chemometric software LatentiX 1.0 (www.latentix.com, Latent5, Copenhagen, Denmark) for inspection of the spectra as well as for calculation of Principal Component Analysis (PCA) (Wold et al 1987). The PCA was calculated on mean-centered spectra. Interval Partial Least Squares (iPLS) regression (Nørgaard et al 2000) was performed to relate the spectra to starch and β-glucan content. All reported results were validated using full-cross validation and 30 intervals.

RESULTS AND DISCUSSION

The ^{1}H HR MAS NMR spectra of the barley flour from the soft, immature seeds at 9 DAF as well as flour from the solid, mature seeds from 47 DAF were well resolved, and lipids, carbohydrates and proteins were observed (Fig. 1A). The recorded barley flour spectra are quite similar to previously recorded wheat flour spectra spun at 5 kHz in a phosphate buffer (Amato et al 2004). In the literature, most ^{1}H NMR spectra of starch are measured in DMSO (Nilsson et al 1996). However, in order to keep the flour system as close as possible to its biological environment, D_2O was chosen as solvent in this study.

The assignments of the resonances listed in Table II were obtained from 2D COSY, TOCSY and ^{13}C-HSQC spectra and confirmed by literature data (Petersen et al 2000; Amato et al 2004; Nilsson et al 1996). A more comprehensive assignment is hampered by the significantly overlapping resonances, especially in the region 3-4.5 ppm.

The barley spectra from three harvest times (9, 23 and 47 DAF) can roughly be divided into three regions: region 1 (6.0-8.5 ppm) (Fig. 1A, R1) that contains

resonances with very low intensity from e.g. aromatic protons in primarily amino acids, and proteins. Region 2 (3.0-6.0 ppm) (Fig. 1A, R2) contains resonances from the carbohydrates, unsaturated lipids as well as H_α and H_β from the amino acids. Furthermore, region 3 (0.5-3.0 ppm) (Fig. 1A, R3) contains low-intensity signals from the protons in the aliphatic side chains of amino acids and proteins, but is mainly dominated by lipids in mature flour spectra. Overall, the most intense resonances are observed from the carbohydrates in the region 3.0-5.5 ppm, whereas the intensity of the lipid resonances increases throughout the grain filling from 9 DAF to 47 DAF. It is particular pronounced for the methylene $(CH_2)_n$ resonances at 1.29 ppm. The region 0.5-3.0 ppm (Fig. 1A, R3) is at 9 DAF dominated by many multiplets with a narrow line width from side chains of free amino acids. At 47 DAF the same region is dominated by six broad lipid resonances at 0.88, 1.27, 1.58, 2.03, 2.24 and 2.75 ppm (Table II). The fact that the lipid region shows very high intensity, although barley seeds only contain fat and lipids of approx. 3%, is related to the ^{1}H HR MAS method: only mobile protons are detected by ^{1}H HR-MAS NMR and the lipids contain large amounts of protons that are highly mobile at the measurement temperature. At all three time points the intensity of the lipid peaks are highest for *'lys3a',* whereas *'lys5f'* and 'Cork' show very similar patterns. As indicated by Table I**,** *'lys5f'* and *'lys3a'* contains almost equal amounts of fat and almost twice the amount of fat compared to the normal barley.

Region 2 in the NMR spectra displayed in Fig. 1A, R2 consists of a sub-part from 3.0-4.5 ppm with broad overlapping signals, many of which are related to the ring-protons in carbohydrates (Fig. 1B). The less shielded anomeric ring protons are found in the 4.5-5.5 ppm region. Especially the anomeric α-(1→4) starch proton at 5.36 ppm is clearly observed from 23 DAF onwards. However, this signal overlaps partly with

resonances from unsaturated lipids at 5.32 ppm. 'Cork' and *'lys3a'* both have higher intensity of the anomeric α-(1→4) peak compared to *'lys5f'* from 23 DAF. This is due to the higher levels of starch in 'Cork' and *'lys3a'* compared to *'lys5f'* (Fig. 2, Table I). The anomeric resonance of the reducing α-glucose at 5.23 ppm is most clearly observed after 9 and 23 DAF and almost disappeared at 47 DAF. The same is true for the α-(1→6) resonance at 4.98 ppm which obtains a maximum intensity at 23 DAF. This indicates that a maximum number of branch points in amylopectin are present at this time.

The dry matter content of β-glucan and starch were also determined by the Calcoflour method and the production of NADH, respectively, as shown in Fig. 2. The high β-glucan-mutant *'lys5f'* displays an exponential increase in β-glucan content from 16 DAF to 30 DAF where it reaches a maximum of 19% β-glucan. In contrast, 'Cork' and *''lys3a''* display a much slower and linear increase in β-glucan content from 16 DAF until the end of grain filling where maxima of approximately 6% and 4%, respectively, are reached. In contrast, 'Cork' and *'lys3a'* exhibit a rapid increase in the content of starch from 9 to 20 DAF where levels of approx. 49% and 46%, respectively, were obtained. *'lys5f'* display a totally different starch accumulation pattern with a slow linear increase of starch synthesis throughout the grain filling period reaching a maximum of approx. 23% in the mature seed.

The NMR spectra recorded of flour from 9 DAF differ significantly from spectra of flour from the later stages of grain filling by containing many narrow multiplet resonances from a mixture of smaller, very mobile molecules. This is consistent with the continuous biosynthesis of small peptides, simple oligosaccharides and fatty acids which are incorporated into larger molecules, which in turn adopt more rigid structures at later stages of the grain filling.

Already at 23 DAF, the characteristic genotypic differences related to starch and β-glucan are established (Fig. 2) and confirmed as spectral differences seen in the close-up of the region R2 in Fig. 1B. At 23 DAF, *'lys5f'* maintains a high intensity in the region 3.68-3.78 ppm compared to 'Cork' and *'lys3a'* probably due to glucosidic monomers that cannot effectively be incorporated into starch. Starch synthesis is impaired in *'lys5f'* due to an invalid adenosine 5´diphosphate glucose pyrophosphorylase (AGPase) transporter, resulting in *'lys5f'* being unable to transport ADP-glucose across the plastid envelope (Patron et al 2004). However, after 47 DAF, *'lys5f'* has the same spectral pattern in the carbohydrate region as 'Cork' and *'lys3a'*, and differs only by having a lower intensity. It was not possible to assign the region 3.68-3.78 due to broad, overlapping resonances. The most significant changes between *'lys5f'* and 'Cork' and *'lys3a'* are the two proton signals evolving at 3.63 and 3.83 ppm which dominate this part of the spectrum at 47 DAF (Fig. 1B). Assignment of the starch peak in the glucosidic pyranose region indicated that these peaks are related to starch (Nilsson et al 1996). Interestingly, at 23 DAF, *'lys5f'* displays a lack of intensity of the peak at 3.63 ppm compared to *'lys3a'* and 'Cork', but at 47 DAF it has gained approximately the same intensity as *'lys3a'* and 'Cork'. This possibly reflects the competing biosynthesis of β-glucan and starch found in *'lys5f'* (Munck et al 2004). An intermediate peak is observed for 'lys3a' and 'Cork' at 3.97 ppm which reaches a maximum intensity at 23 DAF from where it decreases in intensity to 47 DAF. In potato starch the 5^{th} H has a chemical shift of 3.94 ppm, and this indicates that the peak found at 3.97 could be related to starch as well (Nilsson et al 1996). These differences in bulk carbohydrate accumulation patterns are reflected in the PCA of the NMR spectra (Fig. 3)**,** revealing that the major spectral variation is due to temporal grain filling along PC1, whereas the genotypic information is less obvious

(Fig. 3A). However, it is worth noting that *lys5a* has a different pattern compared to 'Cork' and *'lys3a'* and only samples from 47 DAF are represented by positive PC1 values, whereas 'Cork' and *'lys3a'* also have values from 23 DAF represented in the positive part of PC1. The corresponding loading plot (Fig. 3B) shows that the positive part of PC1 is dominated by the resonances at 5.35 ppm (overlap of α-(1→4) and an unsaturated lipid signal, see Table I), and the peak 3.65 ppm In addition a range of resonances from lipids contribute significantly to the loading between 0.5 and 3.0 ppm. The score plot from Fig. 3A was colored according to content of starch, and as seen from Fig. 3C shows a clear increase in starch content along PC1. In contrast, a colouring according to β-glucan content does not reveal any consistent patterns. Hence, the separation in temporal as well as in the genotypic separation seen in Fig. 3A could be explained by differences in starch accumulation.

As this NMR study concerns two extreme β-glucan mutants (Table II), the anomeric region from 4.45 to 4.85 ppm was of special interest, because it includes the β-(1→4), (1→3) peak at 4.75 ppm, the β-(1→4),(1→4) and β-(1→3) (1→4) peaks at 4.53 ppm and the β-glucose peak at 4.64 ppm (Fig. 4). The β-(1→4),(1→3) and the β-(1→4),(1→4) peaks are observed from 23 DAF to maturity, whereas the β-glucose peak is present from 9 DAF until maturity with highest intensity at 23 DAF. It is very intriguing that *'lys5f',* which has a significantly higher content of soluble β-glucan (Fig 4A), has the same and even a slightly lower intensity of the three β-glucose and glucan peaks compared to 'Cork' (Fig. 4C). Apparently, long consecutive chains of either β-(1→3) or β-(1→4) are not observable in an ^{1}H HR MAS NMR spectrum (Pelosi et al 2006). It is speculated that the β–glucan in *'lys5f'* may have a different composition and structure with long intersections of β-(1→3) or β-(1→4)-glucans affecting the solubility of β-glucan (Johansson et al 2004) or that parts of the β-glucan

in *'lys5f'* have become immobilized for structural or physiological reasons such as degradation. Using a non-enzymatic extraction method for β-glucan called 'Gluca-gel', implying a hot-water extraction followed by a freeze and thaw treatment of the extract (Morgan and Ofman 1998) resulted in similar extractions products of all three genotypes (Data not shown) and ^{1}H NMR analysis of the extracted material could not reveal any spectral differences (data not shown). No spectral differences could be observed for extracted soluble and insoluble β-glucan from barley neither in ^{1}H NMR nor ^{13}CP MAS spectra (Johansson et al 2004). Hence, the immobilization of β-glucan is probably not related to solubility, but must be ascribed other structural or cell wall location features.

Starch and β-glucan regression analysis

Attempts to perform regression between the NMR spectra and the reference measurements of starch, and β-glucan were made using interval partial least square regressions (iPLS). The starch iPLS for the spectral region 3.0-6.0 ppm revealed that two NMR spectral regions perform better than the global model for the 23 samples (3 PLS components, r=0.92 and RMSECV= 6.1) (Fig. 5A). In particular, the iPLS models for the α-anomeric region between 5.53-5.65 ppm (r=0.92, RMSECV= 5.9) and the carbohydrate region 3.56-3.68 ppm (r=0.93 and RMSECV=5.6, Fig. 5B) perform quantitatively very well. The last interval selected by iPLS for optimal starch correlations contained relevant signals, whereas the former interval are an indirect correlation to starch.

In contrast, the global iPLS model of the spectral region 3.0-6.0 ppm for β-glucan performed markedly worse than the starch calibration, even when using 4 PLS components and resulting in r=0.67 with a RMSECV of 4.6. By applying iPLS, it was

possible to find intervals that performed better than the global model. The best iPLS model used the region 3.39-3.56 ppm (r=0.75 and RMSECV= 4.1). This spectral region contains H2 of all the β-glucans as well as H4 and H5 of β-(1→4) (Petersen et al 2000). No significant resonances from starch should appear in this region. However, in all the plots the high β-glucan values of '*lys5f*' were seen as outliers. Hence, a calibration to only 'Cork' and '*lys3a'* was performed. This resulted in a much improved global model for the spectral region 3.0-6.0 ppm of r=0.9 and RMSECV using 2 PLS components and 16 samples (Fig. 6A). The interval 4.25-4.42 ppm gave very good prediction for β-glucan with r=0.97 and RMSECV of 0.5, however using 4 PLS components (thus with the risk of overfitting). When splitting the spectral region 3.0-6.0 ppm into 30 intervals, three regions performed well for 'Cork' and '*lys3a'* and β-glucan: the region 2.98-3.09 ppm (r=0.93 and RMSECV=0.7), the region 3.45-3.57 ppm (r=0.93 and RMSECV= 0.7, Fig. 6B) and 4.26-4.38 ppm (r=0.94 and RMSECV= 0.7). Interestingly, none of the iPLS models to β-glucan selected the region between 4.5 and 4.8 ppm, which contains the anomeric signals from β-glucan. We have found no previous quantifications of seed starch or β-glucan using NMR in the literature.

4. CONCLUSIONS

^{1}H HR MAS NMR gave very well-resolved spectra of barley flour, with clear differences between early, middle and late grain filling of the three barley genotypes. The high β-glucan mutant '*lys5f*' showed a distinct carbohydrate pattern compared to the control 'Cork' and the low-β-glucan mutant '*lys3a'*, especially with regard to the resonances at 3.83 and 3.69 ppm. For all three genotypes, clear temporal differences

between 9 DAF and 47 DAF were observed, especially in the spectral region 3.0-6.0 ppm and in particular for the anomeric α-(1→4) resonance of starch at 5.36 ppm.

Good calibrations could be made to starch for all three genotypes, whereas PLS models to β-glucan only yielded good calibrations to genotypes with low content of β-glucan ('Cork' and *'lys3a'*). For some yet unknown reason the β-glucan in the *'lys5f'* mutant is immobilized and not detectable by ^{1}H HR MAS NMR. In fact, the 'Cork' reference barley has higher intensity in the β-glucan region from 4.45-4.85 ppm than *'lys5f'*, despite the three-fold content of β-glucan found in *'lys5f'* compared to 'Cork'. It is hypothesized that the immobilization of β-glucan in the high-β-glucan mutant is either genotypic-dependent or caused by an altered hydration environment as a result of a strongly increased β-glucan to water ratio.

ACKNOWLEDGMENTS

The authors are grateful to assistant professor Birthe Møller Jespersen and Professor Lars Munck, LIFE, Copenhagen University, Denmark for providing the unique seed material and to the support from the project FFS05-9: Build your Food sponsored by the Danish Ministry of Food, Agriculture and Fisheries. The DIAS Competence Fund, Denmark is acknowledged for financial support. Betina Sørensen (University of Aarhus) and Lisbeth T. Hansen (LIFE, University of Copenhagen) are acknowledged for technical support during the semifield experiment and the chemical analysis. Gilda Kischinovsky is acknowledged for proofreading of this manuscript.

LITERATURE CITED

Aastrup, S. 1979. Effect of rain on beta-glucan content in barley grains. Carlsberg Res Comm. 44: 381-393.

Aastrup, S. and L. Munck. 1985. A beta-glucan mutant in barley with thin cell walls. Pages: 291-296 in: New Approaches to Research on Cereal Carbohydrates. R. D. Hill and L. Munck, eds. Elsevier Science Publishers B.V: Amsterdam.

Amato, M. E., G. Ansanelli, S. Fisichella, R. Lamanna, G. Scarlata, A. P. Sobolev, and A. Segre. 2004. Wheat flour enzymatic amylolysis monitored by in situ 1H NMR spectroscopy. J Agric Food Chem. 52: 823-831.

Ancian, B., I. Bourgeois, J.-F. Dauphin, and A. A. Shaw. 1997. Artifact-free pure absorption PFG-enhanced DQF-COSY spectra including a gradient pulse in the evolution period. J Magn Reson. 125: 348-354.

Bardet, M., M. F. Foray, J. Bourguignon, and P. Krajewski. 2001. Investigation of seeds with high-resolution solid-state 13-C NMR. Magn Reson Chem. 39: 733-738.

Bax, A. 1985. A spatially selective composite 90^{o} radiofrequency pulse. J Magn Reson. 65: 142-145.

Brescia, M. A., G. D. Martino, C. Fares, N. D. Fonzo, C. Platani, S. Ghelli, F. Reniero, and A. Sacco. 2002. Characterization of Italian durum wheat semolina by means of chemical analytical and spectroscopic determinations. Cereal Chem. 79: 238-242.

Buckerigde, M. S., C. Rayon, B. Urbanowicz, M. A. S. Tiné, and N. C. Carpita. 2004. Mixed linkage (1-3),(1-4)-Beta-D-Glucans of grasses. Cereal Chem. 81: 115-127.

Burkus, Z. and F. Temelli. 2000. Stabilization of emulsions and foams using barley beta-glucan. Food Res Int. 33: 27-33.

Fan, T. W. M. 1996. Recent advances in profiling plant metabolites by multi-nuclear & multi-dimensional NMR. Pages: 181-254 in: Nuclear Magnetic Resonance in Plant Biology. Y. Shachar-Hill and P. E. Pfeffer, eds. American Society of Plant Physiologists: Rockville, Maryland, U.S.A.

Fincher, G. B. and B. A. Stone. 1986. Cell walls and their components in cereal grain technology. In Y. Pomeranz, ed. Advances in cereal science and technology. St.Paul, Minnesota, USA: American Association of cereal chemists. 207-295.

Glidewell, S. M. 2006. NMR imaging of developing barley grains. J Cereal Sci. 43: 70-78.

Holtekjolen, A. K., A. K. Uhlen, E. Brathen, S. Sahlstrom, and S. H. Knutsen. 2006. Contents of starch and non-starch polysaccharides in barley varieties of different origin. Food Chem. 94: 348-358.

Jacobsen, S., I. Søndergaard, B. Møller, T. Desler, and L. Munck. 2005. A chemometric evaluation of the underlying physical and chemical patterns that support near infrared spectroscopy of barley seeds as a tool for explorative classification of endosperm genes and gene combinations. J Cereal Sci. 42: 281-299.

Jarvis, M. C. and M. C. McCann. 2000. Macromolecular biophysics of the plant cell wall: Concepts and methodology. Plant Physiol Biochem 38: 1-13.

Johansson, L., P. Tuomainen, M. Ylinen, P. Ekholm, and L. Virkki. 2004. Structural analysis of water-soluble and -insoluble beta-glucans of whole-grain oats and barley. Carbohydr Pol. 58: 267-274.

Kalra, S. and S. Joad. 2000. Effect of dietary barley beta-glucan on cholesterol and lipoprotein fractions in rats. J Cereal Sci. 31: 141-145.

Knudsen, K. E. B. 2001. The nutritional significance of 'dietary fibre' analysis. Animal Feed Sci Technol 90: 3-20.

Krishnan, P., N. J. Kruger, and R. G. Ratcliffe. 2005. Metabolite fingerprinting and profiling in plants using NMR. J Exp Bot. 56: 255-265.

Kuchenbrod, E., A. Haase, R. Benkert, H. Schneider, and U. Zimmermann. 1995. Quantitative NMR spectroscopy on intact plants. Magn Reson Imaging 13: 447-455.

Lazaridou, A. and C. G. Biliaderis. 2007. Molecular aspects of cereal beta-glucan functionality: Physical properties, technological applications and physiological effects. J Cereal Sci. 46: 101-118.

Léon, J., S. Silz, and H. J. Harloff. 2000. Beta-D-glucan content during grain filling in spring barley and its wild progenitor *H.vulgare* ssp. *spontaneum*. J Agron Crop Sci. 185: 1-8.

MacGregor, A. W. and G. B. Fincher. 1993. Carbohydrates of the barley grain. In A. W. MacGregor and R. S. Bhatty, eds. Barley: Chemistry and Technology. St.Paul, MN: American Associated Cereal Chemists. 73-130.

Mannina, L., A. P. Sobolev, and A. Segre. 2003. Olive oil as seen by NMR and spectroscopy. Spectrosc Eur. 15: 6-14.

Morgan, K. R. and D. J. Ofman. 1998. Glucagel, a gelling beta-glucan from barley. Cereal Chem. 75: 879-881.

Morrison, W. R. 1978. Wheat lipid composition. Cereal Chem. 55: 548-558.

Morrison, W. R. 1993. Cereal starch granule development and composition. Pages: 176-209 in: Proceedings of the phytochemical society of Europe. P. R. Shewry and K. Stobart, eds. Clarendon Press: Oxford.

Munck, L., K. G. Jørgensen, J. Ruudhansen, and K. T. Hansen. 1989. The EBC methods for determination of high molecular-weight beta-glucan in barley, malt, wort and beer. J Inst Brewing 95: 79-82.

Munck, L. and B. Møller. 2005. Principal component analysis of near infrared spectra as a tool of endosperm mutant characterisation and in barley breeding for quality. Czech J Genet Plant Breed. 41: 89-95.

Munck, L., B. Møller, S. Jacobsen, and I. Søndergaard. 2004. Near infrared spectra indicate specific mutant endosperm genes and reveal a new mechanism for substituting starch with (1-3,1-4) betaglucan in barley. J Cereal Sci. 40: 213-222.

Nilsson, G. S., K.-E. Bergquist, U. Nilsson, and Gorton.L. 1996. Determination of the degree of branching in normal and amylopectin type potato starch with 1H-NMR spectroscopy. - Improved resolution and two-dimensional spectroscopy. Starch-Starke 10: 352-357.

Nørgaard, L., A. Saudland, J. Wagner, J. P. Nielsen, L. Munck, and S. B. Engelsen. 2000. Interval partial least-squares regression (iPLS). A comparative chemometric study with an example from near-infrared spectroscopy. Appl Spectrosc. 54: 413-419.

O'Donnell, D. J., J. J. H. Ackerman, and G. E. Maciel. 1981. Comparative study of whole seed protein and starch content via cross polarization-magic angle spinning carbon 13 nuclear magnetic resonance spectroscopy. J Agric Food Chem. 29: 514-518.

Patron, N. J., B. Greber, B. F. Fahy, D. A. Laurie, M. L. Parker, and K. Denyer. 2004. The *lys5* mutations of barley reveal the nature and importance of plastidial ADP-Glc transporters for starch synthesis in cereal endosperm. Plant Physiol. 135: 2088-2097.

Pelosi, L., L. Heux, and V. Bulore. 2006. Polymorphism of curdlan and (1-3)-beta-D-glucan synthesized in vitro: A 13C CP-MAS and X-ray diffraction analysis. Carbohydr Pol. 66: 207.

Petersen, B. O., M. Krah, J. O. Duus, and K. K. Thomsen. 2000. A transglycosylating 1,3(4)-beta-glucanase from *Rhodothermus marinus*. -NMR analysis of enzyme reactions. Eur J Biochem. 267: 361-369.

Pines, A., M. G. Gibby, and J. S. Waugh. 1972. Proton-enhanced nuclear induction spectroscopy: A method for high resolution NMR of dilue spins in solids. J Chem Phys. 56: 1776-1777.

Queenan, K. M., M. L. Stewart, K. N. Smith, W. Thomas, R. G. Fulcher, and J. L. Slavin. 2007. Concentrated oat beta-glucan, a fermentable fiber, lower serum cholesterol in hypercholesterolic adults in a randomized controlled trial. Nutrition J. 6: 1-8.

Sacco, A., I. N. Bolsi, R. Massini, M. Spraul, E. Humpfer, and S. Ghelli. 1998. Preliminary investigation on the characterization of durum wheat flours coming from some areas of south italy by means of 1H high-resolution magic angle spinning nuclear magnetic resonance. J Agric Food Chem. 46: 4242-4249.

Seefeldt, H. F., A. Blennow, B. M. Jespersen, B. Wollenweber, and S. B. Engelsen. 2007. Accumulation of mixed linkage (1-3)(1-4)-D-beta-glucan during grain filling in barley - a vibrational spectroscopy study. J Cereal Sci. submitted.

Storsley, J. M., M. S. Izydorczyk, S. You, C. G. Biliaderis, and B. Rossnagel. 2003. Structure and physicochemical properties of beta-glucans and arabinoxylans isolated from hull-less barley. Food Hydrocolloids 17: 831-844.

Tang, H., Y.-L. Wang, and P. Belton. 2000. 13C CPMAS studies of plant cell wall materials and model systems using proton relaxation-induced spectral editing techniques. Solid State Nucl Magn Reson. 15: 239-248.

Tester, R. F., J. Karkalas, and X. Qi. 2004. Starch - composition, fine structure and architecture. J Cereal Sci. 39: 151-165.

Tsuchiya, K., T. Urahara, T. Konishi, T. Kotake, T. Tohno-oka, K. Komae, N. Kawada, and Y. Tsumuraya. 2005. Biosynthesis of (1-3,(1-4)-beta-glucan in developing endosperms of barley (*Hordeum vulgare*). Physiol Plant. 125: 181-191.

Vogels, J. T. W. E., L. Terwel, A. C. Tas, F. vandenBerg, F. Dukel, and J. vanderGreef. 1996. Detection of adulteration in orange juices by a new screening method using proton NMR spectroscopy in combination with pattern recognition techniques. J Agric Food Chem. 44: 175-180.

Wold, S., K. H. Esbensen, and P. Geladi. 1987. Principal component analysis. Chemom Intell Lab Syst. 2: 37-52.

Zhang, G., J. Chen, and J. Wang. 2002. Variation in barley endosperm beta-glucan content in three barley cultivars as a function of spike number and within-spike position. J Cereal Sci. 35: 99-101.

Tables and Figures

Table I. Comparison of chemical composition of two mutants and the normal barley 'Cork'. From: Seefeldt et al (Seefeldt et al 2007) marked with a * from 39 DAF. Protein, fat and lysine values are from Jacobsen et al (Jacobsen et al 2005).

Mutant	β-glucan (%)*	Starch (%)*	Amylose (% starch)*	Dry matter mg seed^{-1}*	Protein (%)	Fat (%)	Lys (mol%)
'*lys3a*'	3.5±0.1	45.9±6.2	27.0±2.5	40.6±1.6	14.4±2.0	3.4±0.6	5.1±0.3
'*lys5f*'	17.6±4	23.4±3.3	26.5±2.5	38.7±4.8	16.0±0.7	3.7±0.1	3.6±0.3
'Cork'	5.7±0.3	49.0±7.3	35.7±1.7	50.7±2.2	12.8±2.5#	1.8±0.1#	3.4±0.2#

#The protein, fat and lysine values are measured in Bomi, the parental line of the mutants and representing the normal barley.

Table II. Major resonances identified in the flour spectra using 2D ^{1}H-^{1}H COSY, ^{1}H -^{1}H TOCSY and ^{1}H-^{13}C HSQC of flour from 'lys5f' from 9 and 47 DAF, and confirmed by the literature (Amato et al 2004),(Nilsson et al 1996),(Petersen et al 2000) and (Sacco et al 1998).

Ppm	Compound	Temporal appearance
5.41	Sucrose	9 and 47 DAF
5.36	Starch	9 and 47 DAF
5.32	(-C**H**=C**H**-)	9 and 47 DAF
5.23	α-glucose	9 and 47 DAF
4.98	α-(1→6)	47 DAF
4.75	β-(1→4),(1→3)	47 DAF
4.64	β-glucose β-(1→4),(1→4)	9 and 47 DAF
4.54	β-(1→3),(1→4)	47 DAF
3.0-4.3	Glycosidic pyranose ring protons	Changes
2.75	-CH=CH-C**H**$_2$-CH=CH-	47 DAF
2.24	(-CH$_2$-C**H**$_2$-CO-O)	47 DAF
2.03	(-C**H**$_2$-CH=CH-)	47 DAF
1.58	(-C**H**$_2$-CH$_2$-CO-O-)	47 DAF
1.27	Backbone methylene groups	9 and 47 DAF
0.88	Terminal CH$_3$	9

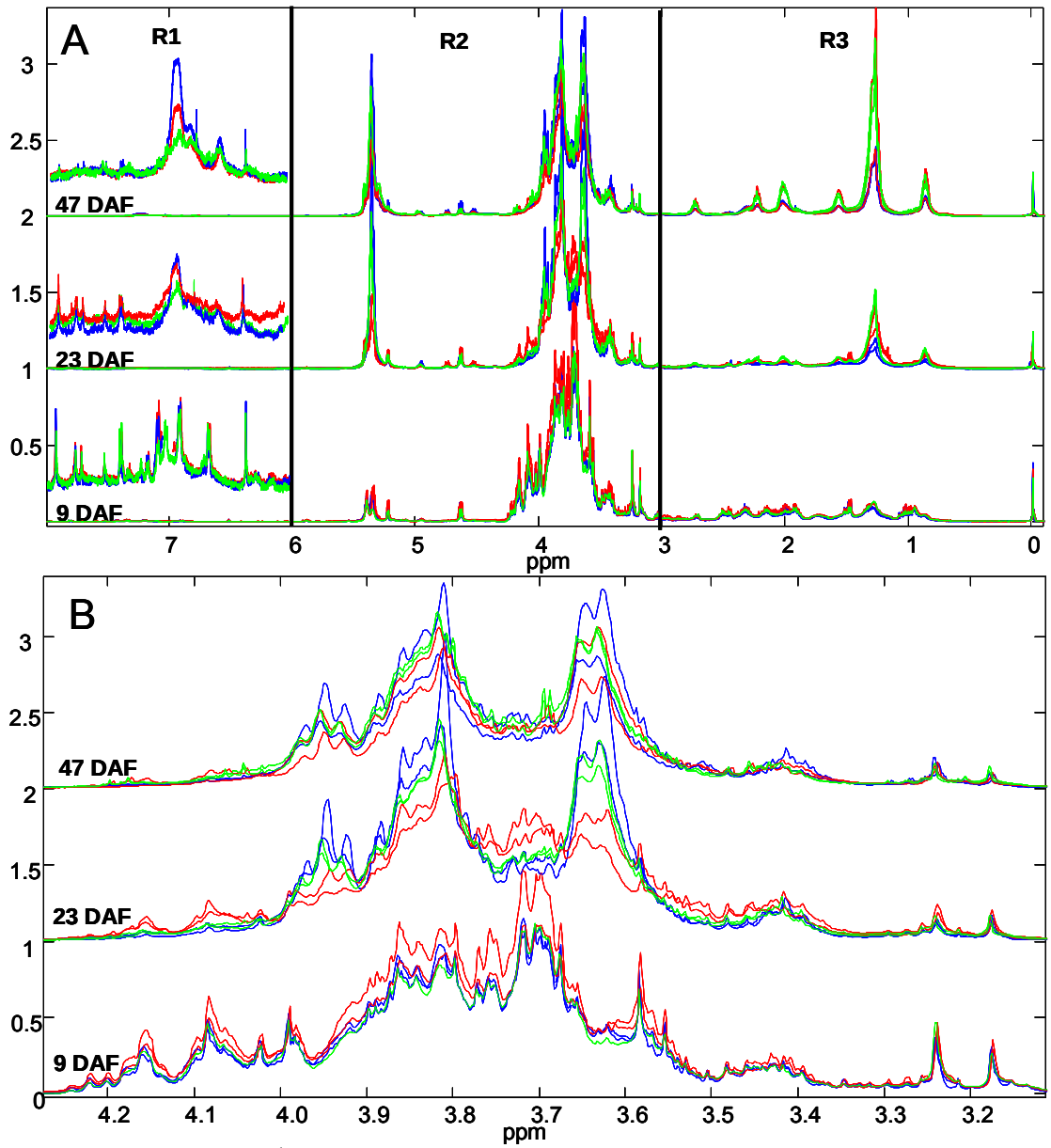

Fig. 1. Superimposed ^{1}H HR MAS NMR spectra of barley flour for three genotypes at early (9 DAF), middle (23 DAF) and late grain filling (47 DAF). The flour spectra were acquired at 348 K. In R1 an enlargement of 6.0-8.5 ppm is seen in order to identify the low intensity resonances. Vertical scaling by a factor of 300. A close-up of the region 3.0-4.5 ppm during time is seen in (B). Red lines = '*lys5f*', blue lines = 'Cork' and green lines = '*lys3a*'

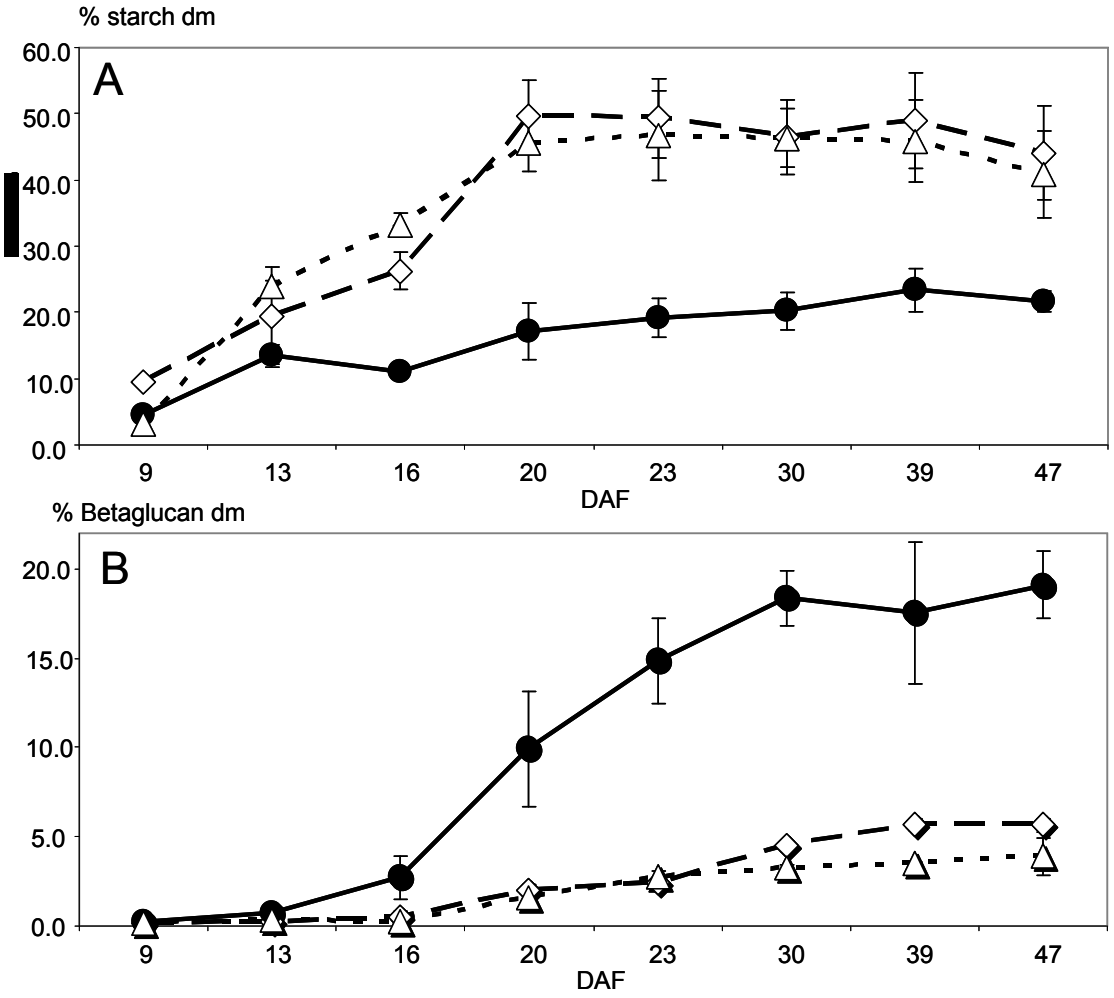

Fig. 2. The dry matter content of β-glucan and starch in three genotypes during grain filling determined by the Calcoflour method and the production of NADH, respectively. Starch content as a function of DAF (A). β-glucan content as a function of DAF (B). The bold line with circles=‘*lys5f*’, the hatched line with open rhombs= ‘Cork’, and the dotted line with open triangles = ‘*lys3a’*. Modified from (Seefeldt et al 2007).

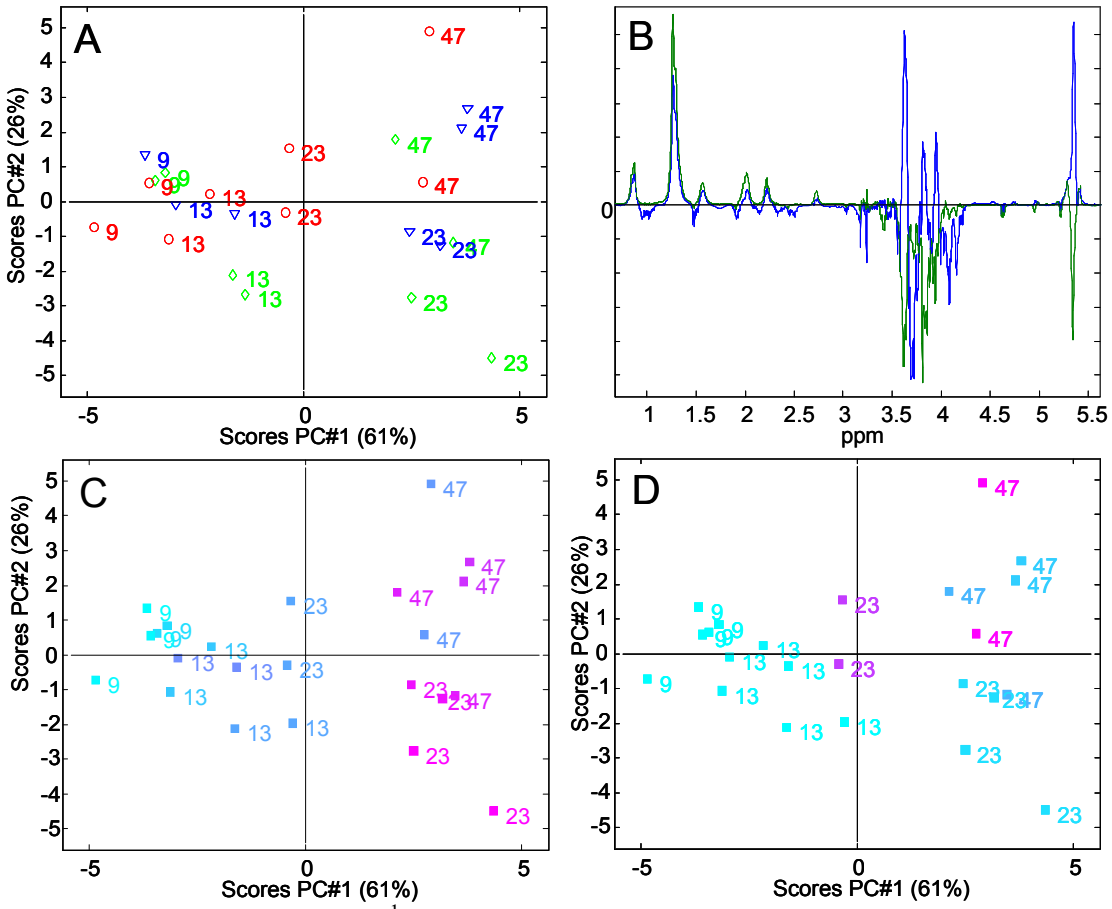

Fig. 3. Score plot of the full ^{1}H HR MAS NMR spectra of barley flour (A) colored according to genotypic location: red circles='*lys5f*', blue rhombs= 'Cork' and green triangles= '*lys3a*'. The corresponding loading plot for first PC, blue line and second PC, green line (B). Score plot of the full ^{1}H HR MAS NMR spectra of barley flour colored according to starch content: light blue equals low levels of starch and cyan the high levels of starch (C). Score plot of the full ^{1}H HR MAS NMR spectra of barley flour colored according to content of β-glucan increasing in content from light blue to cyan (D).

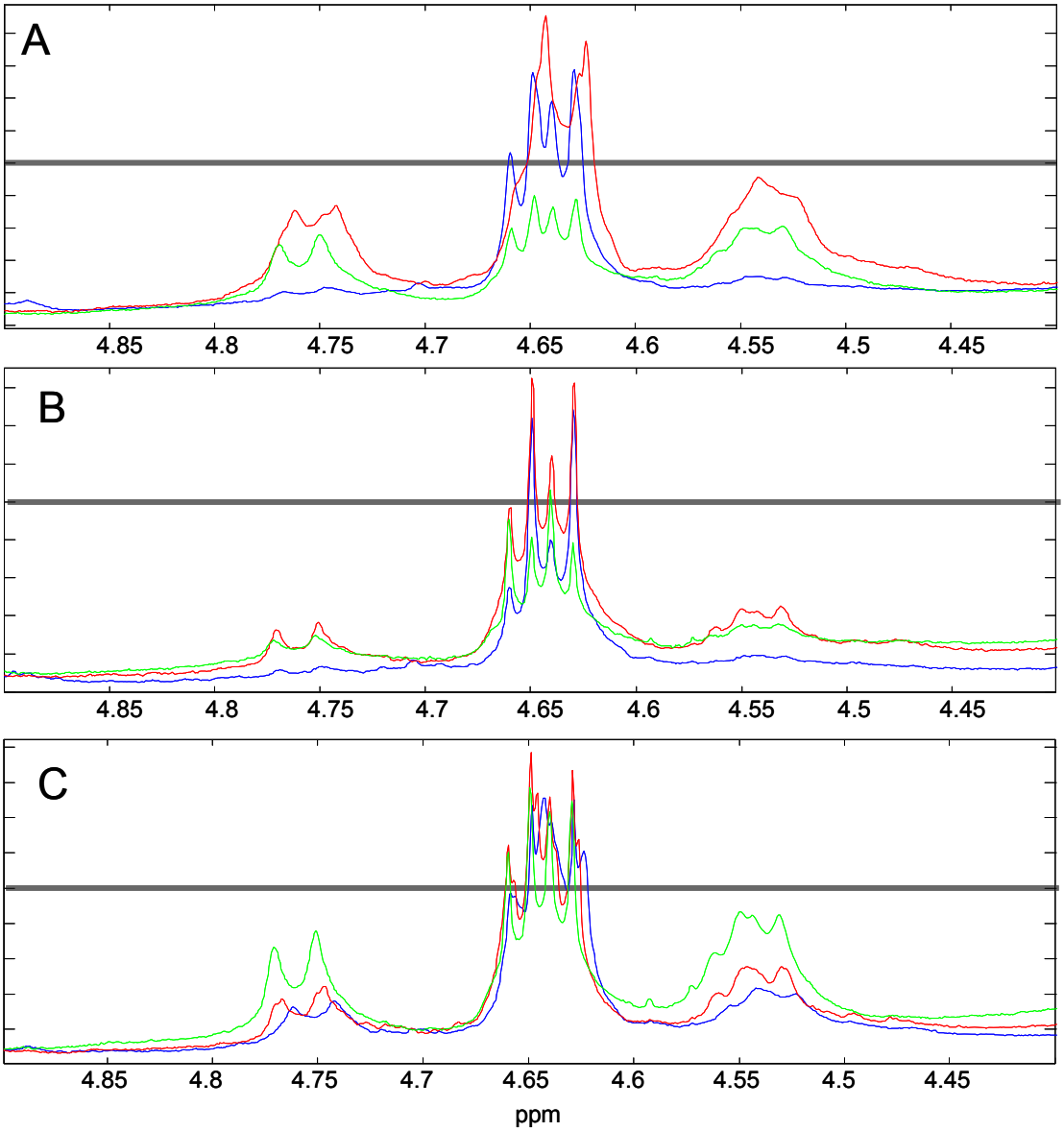

Fig. 4. Three close-ups of the β-glucan region in the NMR spectra at 9 (blue line), 23 (red line) and 47 DAF (green line). The *'lys5f'* mutant (A). The *'lys3a'* mutant (B). The control 'Cork' (C).

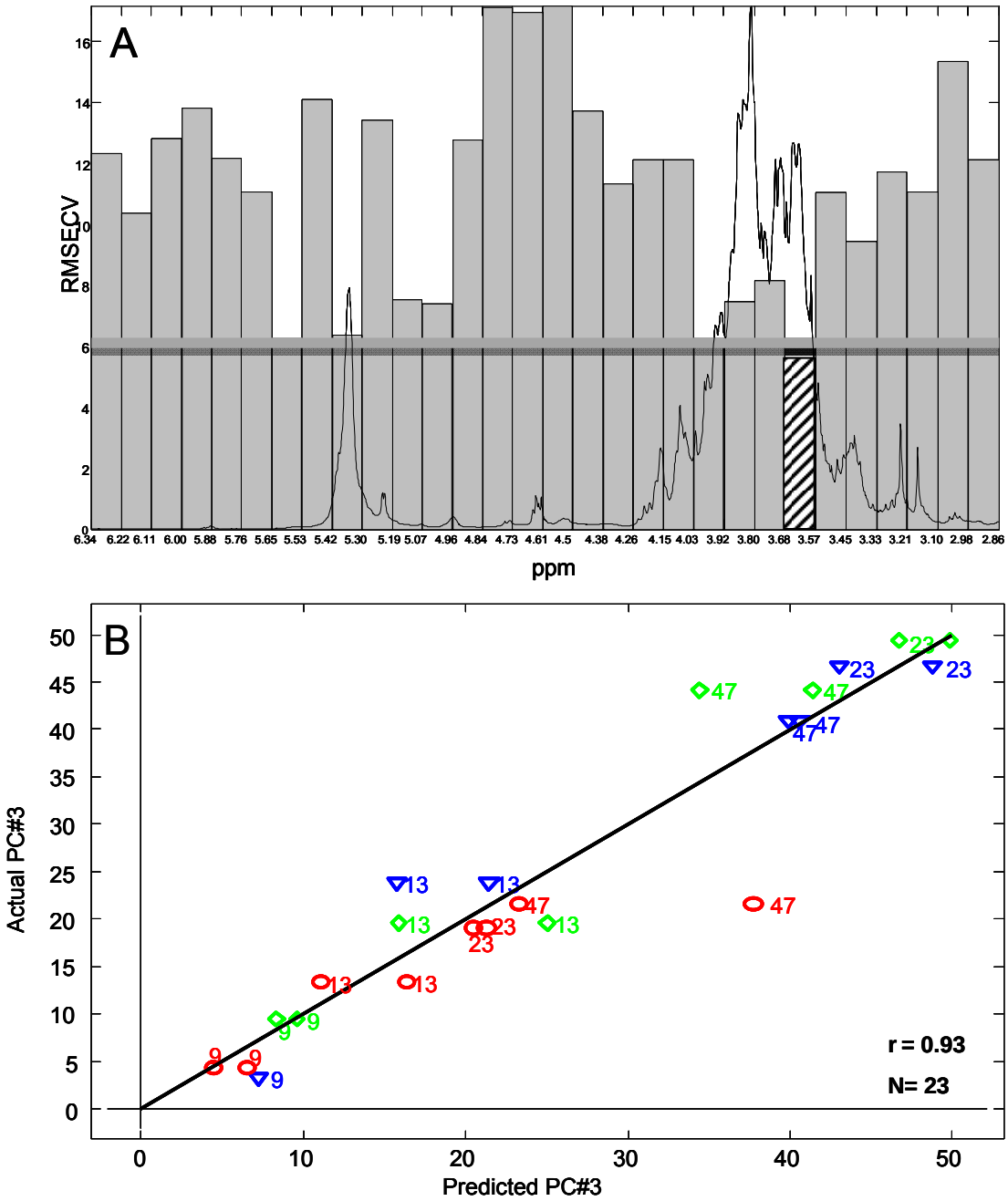

Fig. 5. The iPLS regression (30 intervals) to starch of the full cross validated ^{1}H HR MAS NMR spectra in the region 3-6 ppm for all genotypes and time points, N=23 (A). Two segments perform better than the global model. The squared region: 3.56-3.68 ppm is shown with its regression (B). Rhombs ='Cork', circles='*lys5f*' and triangles='*lys3a*'. The numbers refer to DAF. The grey shaded line is the RMSECV value for 3 PLS components for the global model. Each interval was calculated with 3 PLS components.

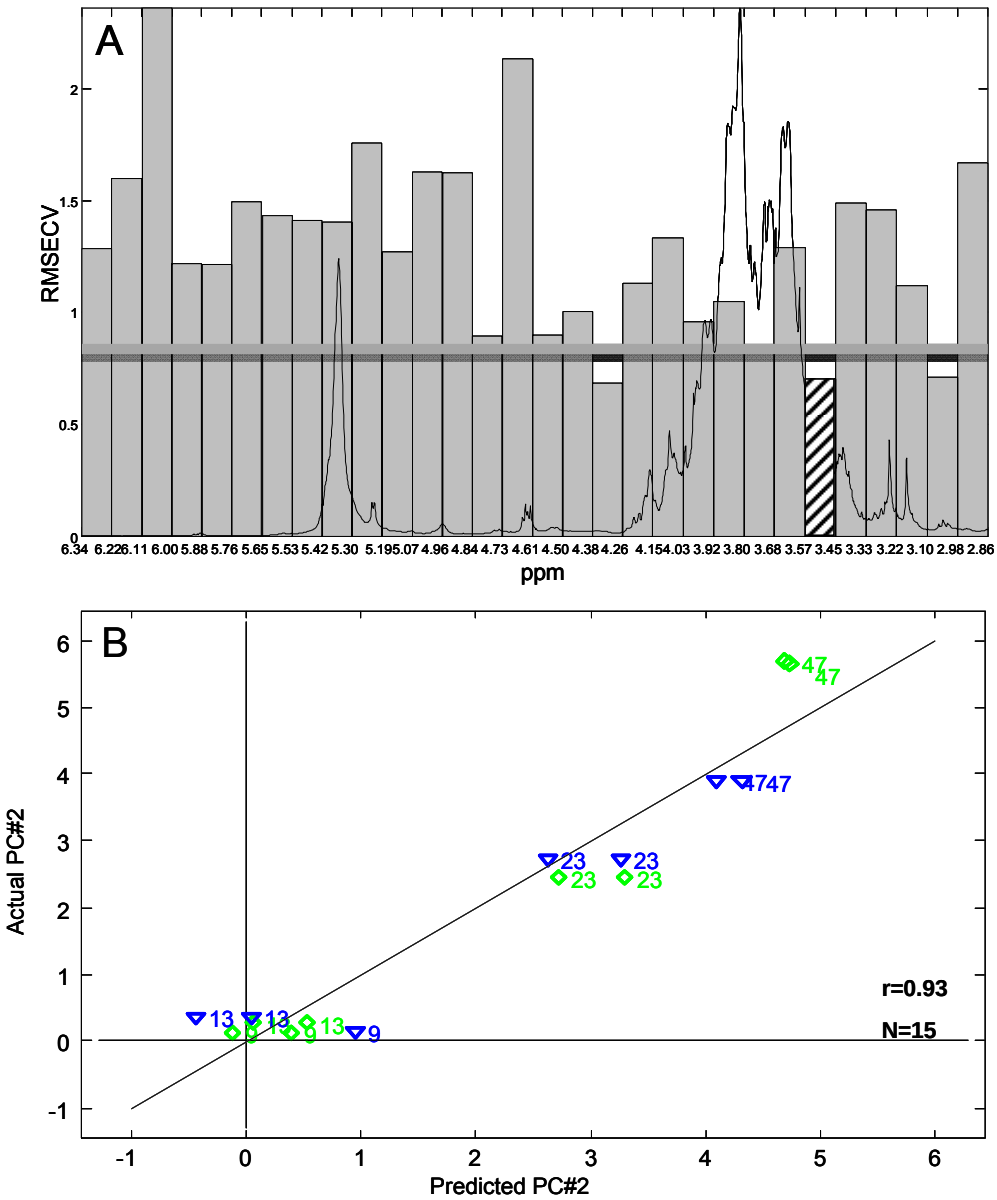

Fig. 6. The iPLS regression (30 intervals) to β -glucan of the full cross validated ^{1}H HR MAS NMR spectra in the region 3-6 ppm for 'Cork' and *'lys3a'*, N=15. Three segments perform better than the global model. The squared region: 3.45-3.57 ppm is shown with red in (A) and in (B) the corresponding regression is seen. 'Cork' is shown with rhombs, and *'lys3a'* with triangles. The numbers refer to DAF. The grey shaded line is the RMSECV value for 2 PLS components for the

PAPER C

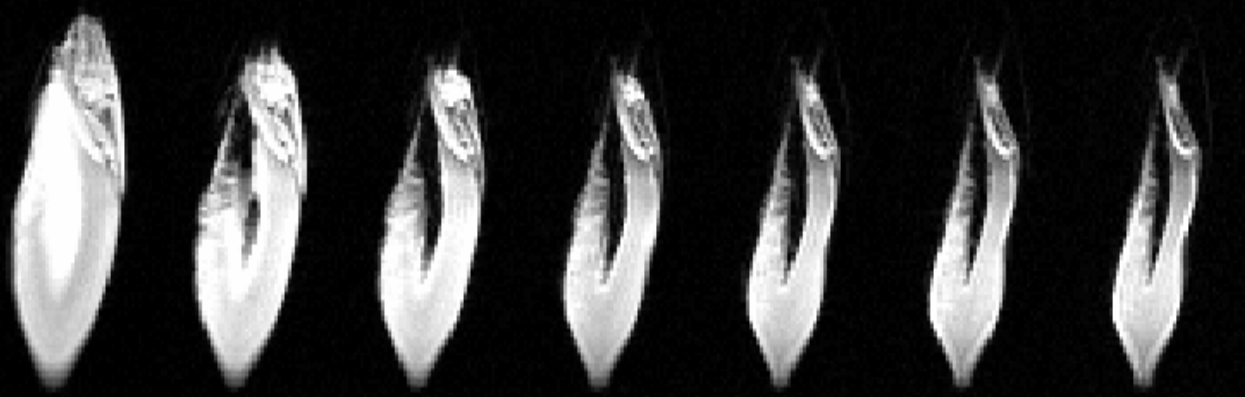

Water mobility in the endosperm of high beta-glucan barley mutants as studied by Nuclear Magnetic Resonance Imaging

Helene Fast Seefeldt, Frans van den Berg, Walter Köckenberger, Bernd Wollenweber, Søren Balling Engelsen

Magnetic Resonance Imaging, **25** (2007), 425-432.

Available online at www.sciencedirect.com
ScienceDirect
Magnetic Resonance Imaging 25 (2007) 425–432
MAGNETIC RESONANCE IMAGING

Water mobility in the endosperm of high beta-glucan barley mutants as studied by nuclear magnetic resonance imaging

Helene Fast Seefeldt[a,*], Frans van den Berg[b], Walter Köckenberger[c], Søren Balling Engelsen[b], Bernd Wollenweber[a]

[a]Department of Genetics and Biotechnology, Danish Institute of Agricultural Sciences, Research Centre Flakkebjerg, DK-4200 Slagelse, Denmark
[b]Department of Food Science, The Royal Veterinary and Agricultural University, 1958 Frederiksberg, Denmark
[c]Sir Peter Mansfield Magnetic Resonance Centre, School of Physics and Astronomy, University of Nottingham, Nottingham NG72RD, UK

Received 28 February 2006; accepted 28 September 2006

Abstract

^{1}H NMR imaging (MRI) was used as a noninvasive technique to study water distribution and mobility in hydrated barley (*Hordeum vulgare* L.) seeds of accessions with varying content of beta glucan (BG), a highly hygroscopic cell wall component. High contents of BG in barley are unfavorable in malting where it leads to clotting of filters and hazing of beer as well as in animal feed where it hinders the rapid uptake of energy. However, a high content of BG has a positive nutritional effect, as it lowers the cholesterol and the glycaemic index. It was studied whether water distribution and mobility were related to content and location of BG. Water mobility was investigated by following the rate and mode of desiccation in hydrated single seeds. In order to determine the different water components, a multispin echo experiment was set up to reveal the T_2 transverse relaxation rates of water within the seeds. A principal component analysis (PCA) discriminated control seeds from the high-BG mutant seeds. MRI proved efficient in tracing the differences in water-holding capacity of contrasting barley seeds. All accessions showed nonuniform distribution of water at full hydration as well as during desiccation. The embryo retained water even after 36 h of drying, whereas the endosperm showed low and heterogeneous mobility of the water after drying. The relaxation time constants indicated that the BG mutants had regions of much higher water mobility around the ventral crease compared to the control. It is concluded that MRI can be applied to investigate temporal and spatial differences in the location of specific chemical compounds in single seeds.

Keywords: ^{1}H NMR imaging; MRI; Beta glucan; Relaxation; Seed hydration; Seed drying; Water mobility

1. Introduction

The composition of carbohydrates in the endosperm of barley varies, depending on genetic constitution [1] as well as on environmental conditions [2]. The barley endosperm cell wall consists of 75% (1–3)(1–4)-D-β-glucan (BG). Beta glucan is unfavourable in malting and beer production due to hazing and clotting during filtration [3]. For human nutrition, BG is considered beneficial due to lowering of serum cholesterol and flattening of the glycaemic response [4,5]. However, high-BG content is unfavourable in barley grown for feed, since it lowers the efficiency of energy consumption in animal husbandry production [6]. Beta glucan is highly hygroscopic; thus, high-level (15–20%) BG mutants should retain more water and show different patterns of water mobility compared to cultivars with normal levels of BG (3–5%). The rate and mode of desiccation reveal information about inhomogeneities in the cereal endosperm since the different structures and compartments show contrasting mobility of water due to their chemical composition. Desiccation studies have revealed that moisture distribution in wheat seeds is not uniformly distributed at an equilibrium [7], since the embryo contained most of the mobile water. The reduction of water was also found to be evacuated nonuniformly from rice during drying [8].

The study of the hydration status of seeds is important for both agronomy and process technology, and NMR has been used to study germination processes in model plant systems such as castor bean [9] and in cowpea [10] in order to identify "water pools" and modes of water uptake. Other

* Corresponding author. Tel.: +45 8999 3537; fax: +45 8999 3501.
E-mail address: helenef.seefeldt@agrsci.dk (H. Fast Seefeldt).

0730-725X/$ – see front matter © 2007 Elsevier Inc. All rights reserved.
doi:10.1016/j.mri.2006.09.030

studies focused on mechanisms for successful germination using various NMR methods in dormant/nondormant wheat seeds [11], in cowpea with different seed coat structure [12] and in barley during storage [13,14]. Water movement during maturation processes in rice, soybean and barley has been studied [15–17] using NMR imaging (MRI). The drying processes during the latter part of maturity have been elucidated in wheat [7] and rice [8]. MRI has mainly been used to visualize the moisture patterns in seeds either as part of germination or maturation, whereas little focus has been given to the structural and chemical composition in the endosperm with regard to water mobility except for a description of water flow in wheat seeds [18,19].

The sensitivity of proton nuclear magnetic resonance (^{1}H NMR) and MRI, the possibility to do in vivo and noninvasive experiments, and the abundance of water in biological systems have made NMR techniques a very promising tool in plant biology [20,21]. MRI uses magnetic field gradients to spatially encode the nuclear magnetic resonance signal [20]. Contrast in MRI can be generated through the spatial dependence of the different relaxation rates. These relaxation rates reveal information about the physico-chemical properties of the spin of interest [22]. Water relaxation is dependent on compartmentalization, size and chemical composition of these compartments, and on the possible exchange of water between them. However, the interpretation of relaxation rates should always be based on well-established knowledge about the system of interest [23]. There are two types of relaxation: the spin-lattice relaxation (T_1), which describes the exchange of energy between spin and system, and the spin–spin relaxation (T_2), which describes the energy exchange between spins. For solids, T_2 values are typically determined by static interactions, e.g., dipolar couplings. T_2 values usually become longer with an increase in mobility of the proton-containing structures [14]. Relaxation studies are abundant, and many authors have correlated relaxation times with water content [24], coat texture [12], viability [11] and chemical stress [25] in seeds. The multi-exponential nature of the T_2-relaxation curves is interpreted in terms of different types of pools of water with different mobility or in terms of proton exchange. The long T_2 values are typical of unbound water and characterize the external or mobile water pool. In contrast to the mobile water, water with hindered mobility is characterized by short T_2 relaxation time constants [23]. Water with short T_2 relaxation time constants is usually associated with macromolecules or solids [11].

The aim of this study was to use spatially resolved relaxation rates from MRI to investigate the moisture distribution patterns in the endosperm of barley accessions contrasting in their BG content. The hypotheses for the hydration and drying experiments are that barley accessions with a high content of BG will contain more water and will lose water more rapidly due to a higher mobility of water. The experiments were designed to determine regions of high water mobility and to identify differences in the spatial distribution of macromolecules interacting with water. The rate and mode of desiccation in the employed contrasting barley accessions were investigated. Methods for analyzing the exponential MRI relaxation data are presented.

2. Material and methods

2.1. Plant material

The barley accessions “Cork” (average BG content 5%, referred to as control in this study), “1201” (average BG 15%) and “1101” (average BG 19%) were grown to maturity. A pot (16.5 cm diameter and 13.0 cm height) experiment was carried out from April to July 2004 in the greenhouse. Each pot was filled with 2 L of fertilised soil mixture of sphagnum and 15% Grodan (Agro Dynamics, Danish Grodan Stonewool, Denmark), and each pot was dressed with a mixture of Perlite (Nordisk Perlite, Hillerød, Denmark) and sphagnum. Five seeds of each accession were sown on 14 April 2004 and thinned to two seedlings per pot on 4 May. All pots were drip watered each day throughout the experiment: pest control was performed against mildew and aphids by routine spraying. Light intensity was 180–200 W m^{-2}, and the temperature was 18°C/16°C on an 18-h day/6-h night basis. Seeds were bulk harvested at the stage of yellow ripeness on 19 July 2004 and stored in a cool and dry place until analysis. The moisture content of untreated seeds was determined after 18 h of oven drying at 80°C.

2.1.1. Hydration experiment

Ten randomly chosen seeds of each accession were weighed, placed in 200 ml distilled water and bubbled with air for a week in darkness at 22°C until full hydration was achieved. Only seeds with chits, but no further sign of germination, were used for investigation. A hydrated barley seed was blotted dry before wrapping in dry cotton wool and paper tissue and placed in a 10-mm imaging probe. A piece of wet cotton was placed in the bottom of the NMR tube to avoid drying out of the seed during data acquisition. A total of 71 seeds were tested (24 of accession 1201 and Cork, and 23 of accession 1101).

2.1.2. Drying experiment

A fully hydrated seed from the hydration experiment was wrapped in cotton wool plus tissue paper and placed above twice its volume of silica gel 60 (Fluka Chemika, St. Gallen, Switzerland) in a 10-mm NMR tube. The silica gel was regenerated at 150°C for 8 h before use. Two or more replicates of each accession were used for analysis.

2.2. MRI measurements

2.2.1. Hydration experiment

A 9.4-T super wide bore magnet equipped with a 400-MHz high-resolution NMR spectrometer (DSX 400, Bruker, Karlsruhe, Germany) and micro-imaging accessory was

used. A conventional multispin echo pulse programme with 40 echoes recorded was used to record a set of 40 T_2-weighted images for further analysis. The field-of-view (FOV) was 15 mm and slice thickness was 1 mm. A 128×128 data matrix was acquired, which resulted in a nominal in-plane resolution of 0.117×0.117 mm. The echo time was 2.47 ms and repetition time was 2000 ms. Acquisition time was approximately 17 min for four averages. Images were acquired of longitudinal cross sections of the seeds.

2.2.2. Drying experiment

Every 2 h for a total of 36 h, a spin-echo scan identical to the previously described conditions was run for each of the seeds tested.

2.3. Data analysis

The image data were analysed using in-house written MATLAB 7.1 routines (The Mathworks Inc., USA) designed to do multi-exponential fitting to describe the relaxation rates based on a Simplex minimization of the nonlinear parameters and a least squares estimation of the linear parameters inside the function evaluation call (http://www.models.kvl.dk/source/lfnmr). Visual inspection of the results showed that the automated procedures functioned satisfactorily for all results presented.

2.3.1. Hydration experiment

The following sequence of operations was performed to distinguish pixel values belonging to the kernels from the background [26]: (1) an image was created by summing the echo vectors; (2) an edge was defined; (3) a closing operation was performed using a disk of 4-pixel radius; (4) an image "hole" filling operation was performed; (5) an image eroding/opening operation using a disk of 3-pixel radius was performed; (6) pixels constituting the biggest separate object were defined as being the seed, all others were categorized as background. Between 1156 and 3371 pixels (out of 128×128=16,384) constituted the effective regions in this experiment. Two recordings were identified as irregular and removed before further analysis, resulting in 69 seed samples.

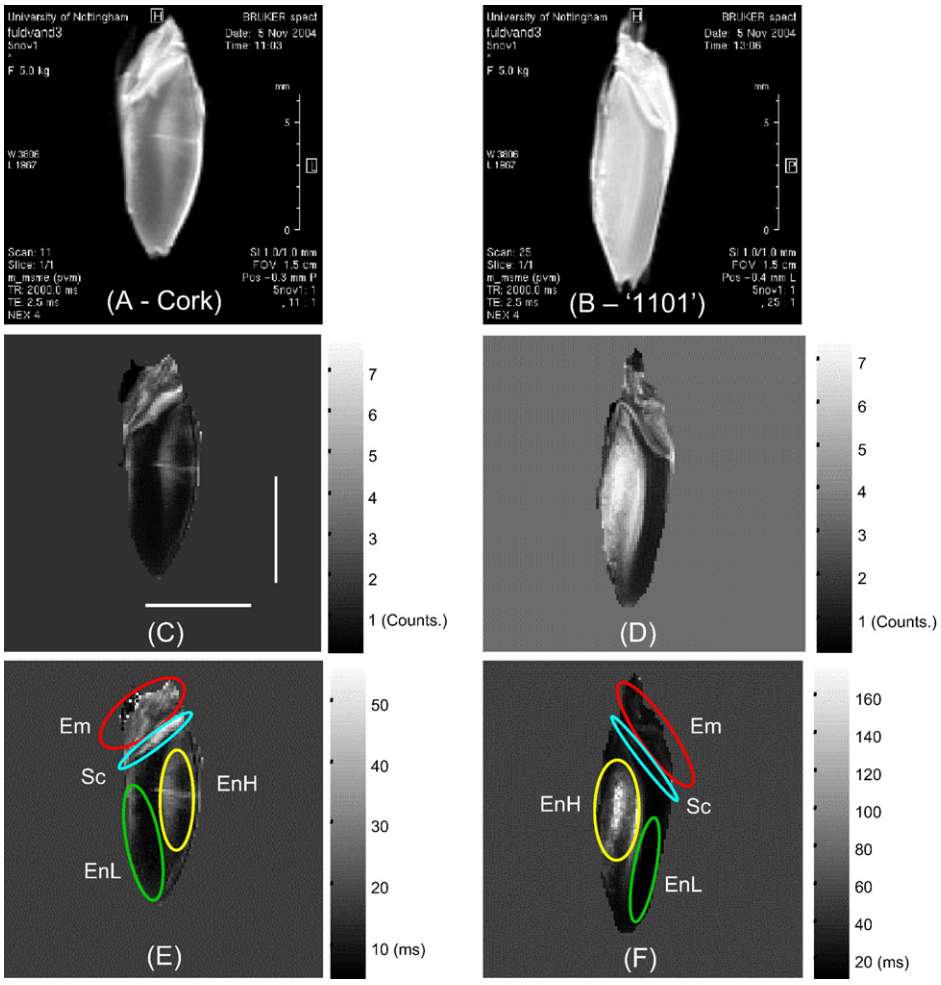

Fig. 1. Intensity images of two barley seeds after 1 week of hydration. (A) Original intensity image of control Cork; (B) original intensity image of high BG mutant 1101; (C) calculated intensity image of Cork (marker lines=5 mm); (D) calculated intensity image of 1101; (E) T_2 value images via Eq. (2) for Cork; (F) 1101 (notice the difference in scales); Em=embryo, Sc=scutellum, EnL=endosperm low intensity, EnH=endosperm high intensity.

2.3.2. Drying experiment

The first (most intense) echo was used in this part of the study. An average value and standard deviation for the background intensity value were established within each recording, based on 2560 values on the edge of the recording. The number of pixels exceeding six times the background standard deviations in intensity was counted as containing water.

3. Results

3.1. Hydration experiment

Fully hydrated seeds show differences in the signal intensity between the accessions as seen from Fig. 1A–D. Although the signal intensities are strongest in the high-BG mutants, one should be careful to equal signal intensity with water content when no internal reference is used. NMR signal intensity is affected by the relaxation rates as well as the moisture diffusion in the tissue. The moisture content of the seeds before hydration was 9%. Water content below 7% indicates structural water and this explains why no signal could be obtained from the endosperm on dry seeds. Seeds were imbibed for 6 days after which no further water was taken up as determined by weighing. After 6 days of water uptake, the high-BG mutant 1201 took up, on average, 33% more water than the control, while the high-BG mutant 1101 took up 42% more water (data not shown). The higher water content fits well with the higher intensity observed for the high-BG mutants compared to the Cork control.

A nonuniform distribution of water was observed in the fully hydrated seeds (Fig. 1A–D). The embryo had by far the highest intensity followed by the scutellum. The nonuniform distribution is also reflected in the relaxation time rates determined for four regions in the seed (Table 1 and Fig. 1A and F), where the dark region of the endosperm showed distinctively less mobile water than the embryo, scutellum and the bright core of the endosperm. Especially in the high-intensity region of the endosperm of the high-BG mutant 1101, the water mobility was very high. The high-intensity region was observed around the ventral crease of each seed, although it was most predominant in the high-BG mutants (Fig. 1).

In order to compute the different relaxation time rates within the seed, the image pixels constituting the seed were identified and separated from the background. A least squares residuals bi-exponential fit was conducted for the pixels matching the seed of the following form:

$$\mathbf{x}(i) = A_{20}(i) + A_{21}(i) \times e^{\frac{-t}{T_{21}}} + A_{22}(i) \times e^{\frac{-t}{T_{22}}} + \mathbf{r}(i) \qquad (1)$$

where **x**, **r** and **t** are vectors containing normalized, individual echo responses, individual fitting residuals and time, respectively. The first three echos (out of 40) were removed because of observed irregular behaviour during estimation. The *A* values are the individual offset and gain fitting parameters, and the *T* values are the exponential decay parameters. The *T* values represent average or combined water physico-chemical behaviour within one kernel. The estimated *T* values for 69 seeds are plotted in Fig. 2. The first observation from this figure is the considerable natural variation found among the three mutant types. Furthermore, an imprecise grouping or clustering is seen between the two high-BG mutants and the control

Table 1
Comparison of relaxation rates of different wet barley seeds

Compartment	Decay rate, ms (S.D.)	
	Cork (Fig. 1A)	1101 (Fig. 1B)
Embryo	22.2 (2.9)	25.8 (6.9)
Scutellum	50.9 (5.4)	28.2 (9.2)
Endosperm low intensity	6.9 (0.8)	9.5 (0.6)
Endosperm high intensity	25.7 (3.8)	152.4 (27.4)

Average decay rate and standard deviation (in parentheses) for the seeds in Fig. 1A and B based on 10 randomly selected pixels in each of the four marked compartments.

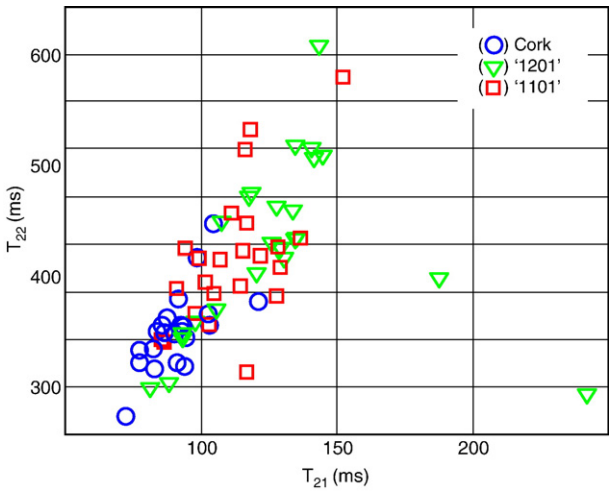

Fig. 2. Score plot of bi-exponential (pixel independent) relaxation times T_{21} and T_{22} estimated from Eq. (1) using all pixels constituting the seed inside the image simultaneously.

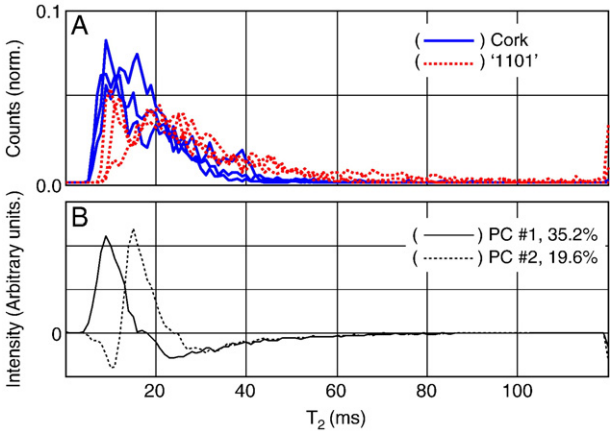

Fig. 3. (A) T_2 mono-exponential estimate [pixel dependent, based on Eq. (2)] normalized histograms for three Cork control seeds and three 1101 high BG seeds; (B) PCA variable-loading profiles for the first two principal components based on Eq. (3).

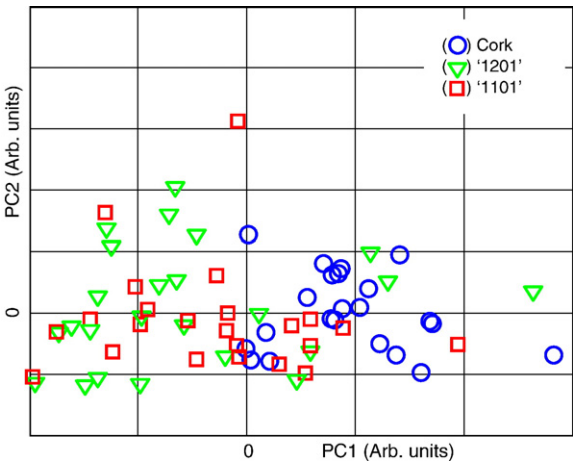

Fig. 4. PCA sample scores for the first two principal components on mono-exponential estimate normalized histograms.

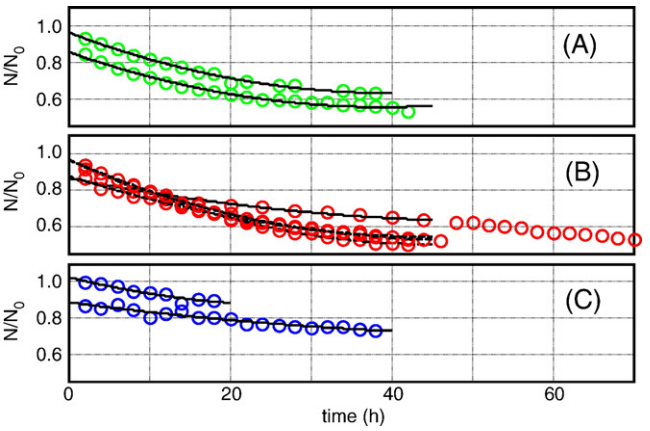

Fig. 6. Plot of the number of pixels identified as containing water (N) as a function of drying hours, the count for time 0 (N_0); (A) two 1201 samples; (B) four 1101 samples; (C) two Cork samples.

barley Cork. It appears that seeds with high values for T_{21} also show high values for T_{22}, which is the more mobile water component.

A second approach to the clustering of different mutants was made based on individual fitting of mono exponentials for each pixel (as compared to an average fitting across all pixels).

$$\mathbf{x}(i) = A_0(i) + A_2(i) \times e^{\frac{-t}{T_2(i)}} + \mathbf{r}(i) \qquad (2)$$

Note that in Eq. (2) each relaxation vector (each pixel) gets its individual time constant. Fig. 1E and F shows a T_2 parameter map derived from the intensity images in Fig. 1A and B, using Eq. (2) for fitting exponential decays. From these maps, it is apparent that high-BG mutants have substantially longer relaxation rates than Cork and the internal water is thus more mobile than observed for Cork. It appears that the mobility of the water is a factor 3 to 6 higher in 1101 than in Cork especially in the high-intensity region (Table 1).

All time constants for the 69 seed images in the hydration experiment are placed in a normalized, equally spaced histogram ranging from 0 to 120 ms. A small number of pixels in the latter sample are classified with a T_2 of >120 ms, but they will be added to the last bin. The histograms form a data table that is decomposed by

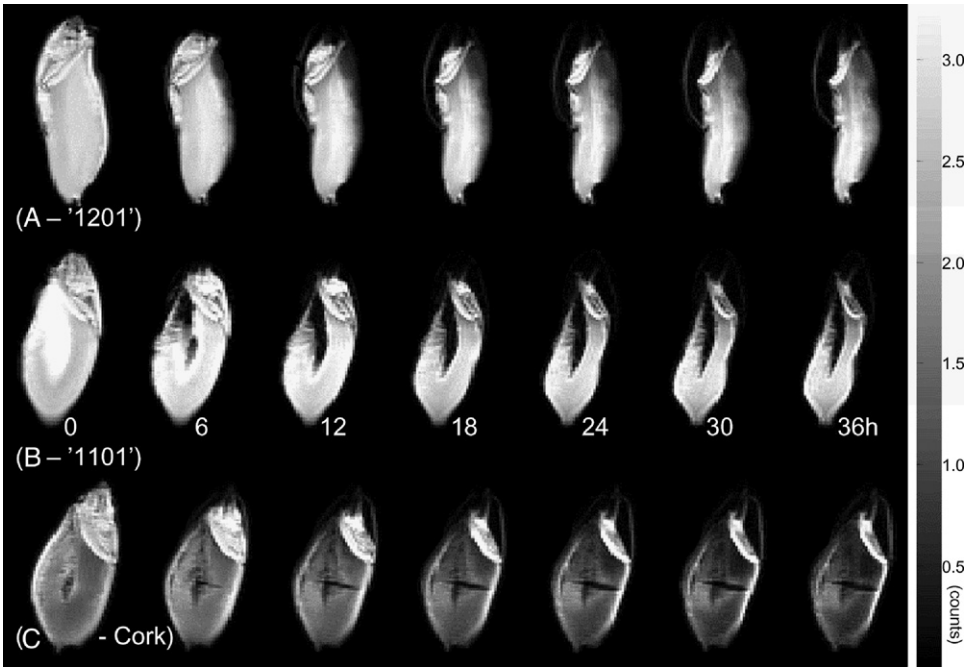

Fig. 5. Seven equidistant intensity snapshots of the same seed during desiccation. A representative sample of each accession used in this study is shown. The first picture is from the fully hydrated seed (time 0). These pictures are used to determine the rate and mode of desiccation presented in Fig. 6; (A) 1201 sample; (B) 1101 sample; (C) Cork sample.

Table 2
The differences in shrinkage between the dried accessions based on the number of pixels with signal; the times (in hours) show when 75% of the initial signal is reached

Accession	$N/N_0=0.75$ in hours of drying time
1201	16.0 and 7.5
1101	11.5, 14.5, 9.5 and 13.0
Cork/control	27.5 and >30.0

principal component analysis (PCA) [27]. Principal component analysis finds the best least squares low-rank approximation of a data matrix **X** (size samples times bins):

$$\mathbf{X} = \mathbf{t}_1\mathbf{p}_1^{\mathrm{T}} + \mathbf{t}_2\mathbf{p}_2^{\mathrm{T}} + \mathbf{E} = \mathbf{T}\mathbf{P}^{\mathrm{T}} + \mathbf{E}$$

$$\text{minimize}\,||\mathbf{X} - \mathbf{T}\mathbf{P}^{\mathrm{T}}||^2 \qquad (3)$$

where the matrix product $\mathbf{T}\cdot\mathbf{P}^{\mathrm{T}}$ is the (in this paper, two principal components) approximation, and **E** is the unmodeled part of **X**. In this work, **X** is assumed column mean-centered before analysis. Furthermore, object scores are selected such that $\mathbf{t}_i\cdot\mathbf{t}_i^{\mathrm{T}}=\lambda_i$, $\lambda_i\geq\lambda_i$ for $i>j$, and $\mathbf{t}_i\cdot\mathbf{t}_j^{\mathrm{T}}=0$, and variable loadings define criteria $\mathbf{p}_i\cdot\mathbf{p}_i^{\mathrm{T}}=1$ and $\mathbf{p}_i\cdot\mathbf{p}_j^{\mathrm{T}}=0$. Hence, the first set of scores and loadings is the best approximation of the original data, and the fraction/percentage explained variance captured from the original data matrix by this first pair expresses how well this approximation succeeded. Similarly, the second orthogonal pair is the next best approximation. The scores can be seen as new pseudo values for the objects; the loadings show the role of the original variables. Fig. 3A shows the histogram for six representative individual fittings. Fig. 3B shows the variable loadings for the first two principal components explaining 35.2% and 19.6% of the total variation in the data table. As seen in Fig. 3A, most T_2 time constants fall in the range 10–20 ms, tailing off up to $T_2\approx 60$ ms. A small residual fraction, as is noticed in Fig. 3A, ends up in the last bin, playing an insignificant role in the PC analysis. Classification based on the first two principal components as shown in Fig. 4 resulted in a reasonable separation between Cork/control and the high-BG mutants, again imbedded in the natural variation between replicates. In conjunction with the variable loadings plotted in Fig. 3B, it is concluded that the discrimination on the first PC axis is established based on a positive score value for Cork samples combined with the positive loading peak slightly below 10 ms and the negative score value for 1201 and 1101 combined with a negative tailing towards 60 ms. This distribution underpins the higher mobility of the water in the high-BG mutants. The second PC, which mimics a derivative of the first loading peak and hence a shift in the histograms, gives no clear interpretation from the samples point of view.

3.2. The drying experiment

Fig. 5 gives seven time snapshots acquired during drying for 36 h for representative seeds from the three barley accessions. It appears that the intensity of the seeds is reduced during time according to the loss of water. The drying process represents a loss of water between 36% and 51% (data not shown). Fig. 6 shows the rates of drying for different mutants. The fitted line for all time series is a second-order polynomial true observations up to 45 h, excluding the first (time 0) observation. Table 2 shows after how many hours the different experiments reach 75% of the initial counts. From Figs. 5 and 6 and Table 2, it appears that Cork has a slower rate of drying, as the water is less mobile when compared to the high-BG mutants. The mode of drying appears to be nonuniform across the seed since the embryo has a high signal even after 36 h of drying. Table 3 verifies that the embryo and scutellum are less affected than the endosperm as seen from relaxation rates determined in four regions of the wet and dry seed, respectively. Especially the high-intensity region in the endosperm around the ventral crease shows a marked decrease in relaxation rate between the wet and dry seed. The mobility of the water in the high-intensity region of the high-BG mutants is decreased more predominantly than in Cork during drying, probably because the water in Cork was much less mobile even in the wet seeds. The endosperm loses water in a nonuniform way from top to bottom instead of from outside in. In the case of Cork (Fig. 5C), some cracking appears, whereas this cracking was absent from the high-BG mutants. The dark area in the seed of 1201 (Fig. 5B) was a feature observed for many of the seeds already before desiccation and is thus not a result of the drying procedure.

4. Discussion

In general, the experiments with the three different seed accessions showed a strong variation of the transverse

Table 3
Average decay rate and standard deviation (in parentheses) for the wet and dry seeds from Fig. 5 based on 10 randomly selected pixels from each of the four marked compartments as indicated in Fig. 1E and F

Seed	Embryo	Scutellum	Endosperm low intensity	Endosperm high intensity
1201 wet (Fig. 5A, 0 h)	23.6 ms (6.8)	32.6 ms (11.7)	20.5 ms (0.9)	82.6 ms (37.7)
1201 dry (Fig. 5A, 36 h)	20.3 ms (4.7)	14.5 ms (4.3)	6.9 ms (1.3)	7.9 ms (1.8)
1101 wet (Fig. 5B, 0 h)	24.5 ms (8.3)	22.5 ms (5.6)	11.1 ms (1.1)	35.5 ms (8.1)
1101 dry (Fig. 5B, 36 h)	17.2 ms (6.4)	23.4 ms (7.1)	7.1 ms (1.3)	6.7 ms (1.0)
Cork wet (Fig. 5C, 0 h)	21.2 ms (5.9)	18.1 ms (1.6)	6.6 ms (1.2)	15.8 ms (1.7)
Cork dry (Fig. 5C, 36 h)	20.1 ms (7.0)	21.1 (2.8)	[a]	5.4 ms (2.7)

[a] Signal strength for this region of the image is insufficient for accurate fitting.

relaxation parameters on a seed-to-seed basis. The variation can be explained by natural variability between individual seeds. We have used a PCA-based approach to analyse the differences between the three different variants.

4.1. Hydration experiment

MRI proved efficient in tracing the differences in water-holding capacity of different barley varieties (Fig. 1) and it was possible to make a reasonable classification based on the T_2 values (Fig. 2) despite a major variation between the seeds. It is well known that seeds vary in size and quality depending on their position on the head [28]. In this study, seeds were randomly chosen from a pool of seeds originating from six plants and thus a variation was expected.

In order to obtain good signals from the endosperm, the seeds were hydrated completely. Sufficient signal strength from dry seeds has only been possible using ^{1}H NMR magic angle spinning (MAS) measurements in which the dipolar–dipolar couplings are removed by spinning the samples at high speed; spinning is not a possibility in MRI based on spatially resolved gradients. Recently, the application of single-point imaging was described to image plant tissue with very low water content and it was possible to record signals in rice seeds between 10% and 40% water [8]. However, this still implies obstacles for studying endosperm features in mature, dry seeds where the water content is often lower.

The moisture distribution was found to be nonuniform throughout the fully hydrated seeds since the embryo and the scutellum region contained the most mobile water (Fig. 1 and Table 1). This could be due to a faster release of hydrolytic enzymes in the embryo and scutellum region leading to a higher mobility of water used in metabolism [29]. The higher content of water surrounding the embryo could partly serve as a reservoir ensuring enough water for radicle growth, but also as a reservoir for further hydrolysis of storage material in the endosperm.

The high-BG mutants had higher signal intensity than the control, reflecting the higher content of water in the endosperm as expected due to a higher content of the hygroscopic material. The relaxation rates also indicate that the mobility of the water in the high-BG mutants was higher than in the control (Figs. 1E and F and 3A). A high-intensity region near the ventral crease is found to be very predominant in the high-BG mutants. The same bright core was observed in maturing barley seeds indicating movement of water [16]. In an X-ray microanalysis of hydration patterns in barley, water moved most quickly along the ventral endosperm, indicating a region of higher water mobility [30]. In an MRI experiment with hydration of barley, the region around the ventral crease was observed to have a markedly higher water transport in the late stage of hydration [29]. Oscarsson et al. [31] stained barley endosperms differing in cell-wall size with *Acid fuchsin* and *Calcoflour white* and found that accessions with high-BG content had thicker cell walls especially around the ventral crease. Beta glucan is a cell-wall polysaccharide in the endosperm, which has a high affinity to water and thus binds more water; it also affects the mobility of the water. This could explain the bright core especially predominant in the high-BG mutants.

4.2. Drying experiment

A change in rate of drying occurs after more than 36 h of drying (Fig. 6, accession 1101). This might reflect that all the more mobile water has evaporated and only structural water remains. The desiccation process appears thus to be a two-step process where most of the water is lost at a fast rate until a certain point at which the water is so immobile that further desiccations occur very slowly (Fig. 6, accession 1101). This is also observed in castor bean [9] and in barley [8]. The rate of desiccation differs according to the structure and chemical composition of the seed. It appears from this dataset that the high-BG mutants show a higher rate of drying (Table 2) as would be expected from the higher mobility of the water found in the relaxation study. The drying process within the seed was found to be nonuniform and it appears that the embryo loses less water than the endosperm (Table 3). Allen et al. [32] tested the hypothesis that barley endosperm functions as a reservoir when imbibed seeds experienced drying using the fluorescent dye trisodium 8-hydroxy-1,3,6-pyrenetrisulfonate. The embryo part hydrated more rapidly, although the endosperm contained nine times more water than the embryo. When imbibed seeds experienced drying, water moved from the endosperm into the embryo and the scutellum, but not vice versa. Thus, the endosperm provides the radicle with water during drying. In the present study, the endosperm lost the most water during desiccation and the water present was much less mobile than in the embryo (Table 3), whereas the embryo showed signal of water even after 36 h of desiccation. This was also found for rice [8]. The mobility of the water in the embryo after drying is two to three times higher than in the endosperm. It is essential for the seed to keep the embryo viable and thus to ensure enough mobile water for metabolic processes. The endosperm lost water from just below the scutellum and toward the distal tip. This probably reflected that the endosperm material just below the scutellum had been mobilized during the hydration and this leads to a higher mobility of water [17].

Seeds experiencing desiccation shrink and in cases of strong desiccation some cracking in the seeds occurs. This was observed only for Cork seeds (Fig. 5C), which in general had less mobile water than the other seeds. Cracking was also observed for high temperatures above 60°C when drying rice using hot air [8]. With regard to drying technology, it is important to know the chemical constitution of seeds in order to direct a proper drying method to avoid cracking, since cracking erodes the quality of seeds.

In conclusion, the use of MRI was shown to be efficient in the study of hydration and drying events in various components of single barley seeds. The results indicated

heterogeneities of water uptake and spatial distribution in the seeds analyzed. The spatial distribution and movement of water within seeds have thus been found to be dependent on the chemical composition of the endosperm. Hence, barley seeds with a high content of BG showed both higher amounts of water and mobility within the seed as compared to the control seeds with normal content of BG. The ventral area of the endosperm showed distinct water mobility compared to the rest of the endosperm during both hydration and drying. The quantitative implications of these findings could be further exploited by other techniques such as high-resolution MAS NMR on single seeds. The results are of interest for both basic and applied research such as process technology. Whether these physiological differences found are based mainly on genetic or environmental factors is an important question that also needs further investigation.

Acknowledgments

The authors are grateful to assistant professor Birthe Møller Jespersen of The Royal Veterinary and Agricultural University, Denmark, for providing the unique seed material and for the support from the project FFS05-9: Build Your Food sponsored by the Ministry of Food, Agriculture and Fisheries. Helene Fast Seefeldt would like to thank the DIAS Competence Fund, Denmark, for financial support, and Betina Sørensen and Ole Bråd Hansen for technical support during the greenhouse experiment, as well as Lise Deleuran, Birte Boelt and Janet F. Bornman for valuable critics and comments to the project. Frans van den Berg would like to thank the Centre for Advanced Food Studies and "Direktoratet for FødevareErhverv"/FSK03-KVL-3, Denmark, for financial support.

References

[1] Munck L, Møller B, Jacobsen S, Søndergaard I. Near infrared spectra indicate specific mutant endosperm genes and reveal a new mechanism for substituting starch with (1-3,1-4) beta-glucan in barley. J Cereal Sci 2004;40(3):213–22.

[2] Savin R, Nicolas ME. Effects of timing of heat stress and drought on growth and quality of barley grains. Aust J Agr Res 1999;50(3): 357–64.

[3] Bamforth CW, Martin HL. The degradation of beta-glucan during malting and mashing: the role of beta-glucanase. J Inst Brew 1983;89:303–7.

[4] McNab JM, Smithard RR. Barley beta-glucan: an antinutritional factor in poultry feeding. Nutr Res Rev 1992;5:45–60.

[5] Kalra S, Joad S. Effect of dietary barley beta-glucan on cholesterol and lipoprotein fractions in rats. J Cereal Sci 2000;31(2):141–5.

[6] Knudsen KEB. The nutritional significance of 'dietary fibre' analysis. Anim Feed Sci Technol 2001;90:3–20.

[7] Gosh PK, Jayas DS, Gruwel MLH, White NDG. Magnetic resonance image analysis to explain moisture movement in wheat drying. ASAE/CSAE Annual Meeting Presentation, Ottawa, Ontario 1–4 August. Paper number 043118, 2004.

[8] Ishida N, Naito S, Kano H. Loss of moisture from harvested rice seeds on MRI. Magn Reson Imaging 2004;22:871–5.

[9] Morris PG, Darceuil HE, Jasinski A, Jha AK, McIntyre DJO, Northcote DH. NMR microscopy of the germinating castor bean. Philos Trans R Soc Lond A 1990;333:487–93.

[10] Brosio E, DiNola IA, Fracassi M, Carnovale E, Marconi E. NMR study of seed hydration: the role of the seed anatomical structures in water uptake of soaked cowpeas. Cell Mol Biol 1992;38(6):693–7.

[11] Krishnan P, Joshi DK, Nagarajan S, Moharir AV. Characterization of germinating and non-germinating wheat seeds by nuclear magnetic resonance (NMR) spectroscopy. Eur Biophys J 2004;33(1):76–82.

[12] Marconi E, Carnovale E, DiNola A, Brosio E. NMR assessment of water uptake in different *Vigna* spp. seeds. Int J Food Sci Technol 1993;28(1):25–33.

[13] Gruwel MLH, Yin XS, Edney MJ, Schroeder SW, MacGregor AW, Abrams S. Barley viability during storage: use of magnetic resonance as a potential tool to study viability loss. J Agric Food Chem 2002;50:667–76.

[14] Ridenour CF, Xiong J, Maciel GE. Investigation of germination and aging in Moravian III barley grain by nuclear magnetic resonance. Biophys J 1996;70:511–31.

[15] Horigane AK, Engelaar WMHG, Yoshida M, Okubo A, Nagata T. Visualisation of moisture distribution during development of rice caryopses (*Oryza sativa* L.) by nuclear magnetic resonance micro-imaging. J Cereal Sci 2001;33:105–14.

[16] Glidewell SM. NMR imaging of developing barley grains. J Cereal Sci 2006;43:70–8.

[17] Kano H, Ishida N, Kobayashi T, Koizumi M. ^{1}H-NMR Imaging analysis of changes of free water distribution in barley and soybean seeds during maturation. Jpn J Crop Sci 1990;59(3):503–9.

[18] Jenner CF, Xia Y, Eccles CD, Callaghan PT. Circulation of water within wheat grain revealed by nuclear magnetic resonance micro-imaging. Nature 1988;336(6197):399–402.

[19] Eccles CD, Callaghan PT, Jenner CF. Measurement of the self-diffusion coefficient of water as a function of position in wheat grain using nuclear magnetic resonance imaging. J Biophys 1988;53:77–81.

[20] Ishida N, Koizumi M, Kano H. The NMR microscope: a unique and promising tool for plant science. Ann Bot (Lond) 2000;86(2):259–78.

[21] Kockenberger W. Nuclear magnetic resonance micro-imaging in the investigation of plant cell metabolism. J Exp Bot 2001;52(356): 641–52.

[22] Ratcliffe RG. *In-Vivo* NMR-studies of higher plants and algae. Adv Bot Res 1994;20:43–123.

[23] Gruwel MLH, Chatson B, Yin XS, Abrams S. A magnetic resonance study of water uptake in whole barley kernels. Int J Food Sci Technol 2001;36:161–8.

[24] DiNola A, Brosio E, Delfini M, Manes F, Quattrocchi S. Hydration mechanism study in lettuce seeds by proton NMR relaxation. Cell Mol Biol 1988;34(6):639–48.

[25] Miedziejko EM. Impact of chemical stimuli and temperature on water transport and mobility in germinating rape seeds by pulsed ^{1}H NMR spectroscopy. Magn Reson Chem 1997;35:S61.

[26] Gonzalez RC, Woods RE, Eddins SL. Digital image processing using Matlab. Englewood Cliffs (NJ): Pearson Prentice Hall; 2004.

[27] Jolliffe IT. Principal component analysis, Springer series in statistics. New York: Springer-Verlag; 2002.

[28] Stoddard FL. Variation in grain mass, grain nitrogen, and starch B-granule content within wheat heads. Cereal Chem 1999;76:139–44.

[29] McEntyre E, Ruan R, Fulcher RG. Comparison of water absorption patterns in two barley cultivars, using magnetic resonance imaging. Cereal Chem 1998;75(6):792–5.

[30] Davies NL. Use of X-ray microanalysis to study hydration patterns in barley. J Cereal Sci 1991;14:85–94.

[31] Oscarsson M, Parkkonen T, Autio K, Aman P. Composition and microstructure of waxy, normal and high amylose barley samples. J Cereal Sci 1997;26(2):259–64.

[32] Allen PS, Thorne ET, Gardner JS, White DB. Is the barley endosperm a water reservoir for the embryo when germinating seeds are dried? Int J Plant Sci 2000;161(2):195–201.